LABORATORY INVESTIGATIONS ON BLACK COTTON SOIL STABILIZED WITH INORGANIC ADDITIVES AND MARGINAL MATERIALS

Thesis

Submitted in partial fulfilment of the requirements for the degree of

DOCTOR OF PHILOSOPHY

by

CHETHAN B A

(187095CV004)

DEPARTMENT OF CIVIL ENGINEERING

NATIONAL INSTITUTE OF TECHNOLOGY KARNATAKA

SURATHKAL, MANGALORE – 575025

JULY, 2021

LABORATORY INVESTIGATIONS ON BLACK COTTON SOIL STABILIZED WITH INORGANIC ADDITIVES AND MARGINAL MATERIALS

Thesis

Submitted in partial fulfilment of the requirements for the degree of

DOCTOR OF PHILOSOPHY

by

CHETHAN B A

(Reg No: 187095CV004)

Under the guidance of

Dr. A. U. RAVI SHANKAR

DEPARTMENT OF CIVIL ENGINEERING

NATIONAL INSTITUTE OF TECHNOLOGY KARNATAKA

SURATHKAL, MANGALORE – 575025

JULY, 2021

D E C L A R A T I O N

by the Ph.D. Research Scholar

I hereby *declare* that the Research Thesis entitled **"Laboratory Investigations on Black Cotton Soil Stabilized with Inorganic Additives and Marginal Materials,"** which is being submitted to the National Institute of Technology Karnataka, Surathkal, in partial fulfilment of the requirements for the award of the Degree of Doctor of Philosophy in Civil Engineering is a *bonafide report of the research work carried out by me*. The material contained in this Research Thesis has not been submitted to any University or Institution for the award of any degree.

Chethan B A
187095CV004
Department of Civil Engineering

Place: NITK-Surathkal
Date: 13-07-2021

C E R T I F I C A T E

This is to *certify* that the Research Thesis entitled **"Laboratory Investigations on Black Cotton Soil Stabilized with Inorganic Additives and Marginal Materials,"** submitted by CHETHAN B A (Register No: 187095CV004) as the record of research work carried out by him, is *accepted as Research Thesis submission* in partial fulfilment of the requirements for the award of degree of Doctor of Philosophy.

Dr. A. U. Ravi Shankar
Research Guide

Chairman – DRPC

Om Saraswati Namastubhyam Varade Kamarupini

Vidyarambham Karishyami Siddirbhwatu Me Sada

ACKNOWLEDGEMENT

Foremost, I will express sincere gratitude to my research supervisor, Prof. A. U. Ravi Shankar, for his continuous support, patience, motivation, enthusiasm, and providing immense knowledge during the research work. His dynamism, vision, sincerity, and motivation have deeply inspired me.

I acknowledge my sincere thanks to Prof. Kulkarni S. M., Dept. of Mechanical Engineering, and Prof. Basavaraj Manu, Dept. of Civil Engineering, for being the Research Progress Assessment Committee members, for giving insightful comments and valuable suggestions at various stages of the work.

I wish to thank the Director NITK Surathkal, Prof. K Uma Maheshwar Rao, for extending all the support from the institute.

I would like to thank former Heads of the Civil Engineering Department Prof. D. Venkat Reddy, Prof. Varghese George, and Prof. K. Swaminathan, for their support, encouragement, and guidance.

I would like to thank Prof. Jayalekshmi B.R., the present Head of the Civil Engineering Department, for her support and encouragement.

The support provided by QIP coordinator Prof. N S V Shet and former QIP coordinators Prof. Arun Mohan Isloor, Dept. of Chemistry, and Prof. M B Saidutta, Dept. of Chemical Engineering, NITK Surathkal, is imperative.

I am grateful to all the teaching faculty and the supporting staff of the Civil Engineering Department.

I sincerely thank laboratory staff, Mr. Chandrashekara Karanth N, Mr. Purushotham, Mr. Yathish S, Mr. Raghurama, Mr. Shashikanth, and Mr. Ravindra K for their help in completing the experimental work on time without any hurdles. I thank Mr. Manohar Shanbhogue for helping me to conduct the chemical analysis of the materials.

I am thankful to my co-research scholars Mr. Sharth, Dr. Avinash H Talkeri, Mr. Raghuram K Chinnabhandar, Dr. L Durga Prashanth, Dr. Amulya S, Mr. Pandith Aradhya, Mr. Kondeti Chiranjeevi, Mr. Doma Hemanthkumar for their support in many possible ways during the work.

I extend my heartfelt thanks to Prof. Babu Narayan S, brother Mr. Manoj A, and Dr. Bhaskar S Malwa for supporting, guiding, and encouraging me during difficult times.

Mr. Harish and Mr. Prashanth, Asst. Engineers, PRED, Chikmagalur District, have supplied the black cotton soil required for the research, which is highly appreciable.

As a faculty, I am grateful to AICTE New Delhi, the Government of Karnataka, and the Department of Technical Education, for providing the opportunity to upgrade my knowledge.

I will fail my duty if I do not thank Dr. Karisiddappa, Vice-chancellor, VTU Belagavi (former Principal), Dr. K. C. Ravishankar, Principal, Government Engineering College, Hassan, for deputing me to the Ph.D. program under QIP. I am always grateful for their encouragement.

Faculty of Civil Engineering Department, Dr. Prashanth S. (HOD), Dr. Vijaykumar H. A., Mr. Amar R, Mr. Harsha H. N., Mr. Devanand R., Mr. Raghu K., Dr. Basavaraja Simpi, and office members of Government Engineering College, Hassan, have supported me for pursuing higher education. I am thankful to them.

I acknowledge the support received from Mrs. Segu Lakshmi Sravani, Ms. Anupama Nag, Mr. Thiyyagura Kiran, Mr. Cittiboina Madhu Kalyan, Mr. Dandakkagari Ramesh Babu, Ms. Poothi Lakshmi Devi, and Mr. Ajith M while conducting the experiments.

I thank Retired Prof. Amarnath M. S., UVCE, Bangalore, for directing and enlightening me with the research spirit.

I am extremely grateful to my parents, family members, and relatives for their love, prayers, caring, and sacrifices to educate and prepare me for my future. I am very much thankful to my wife Shree Priya K and my daughters Achintya and Hima for their love, understanding, prayers, and continuing support to complete this research work.

CHETHAN B A

ABSTRACT

Many roads constructed over the Black Cotton (BC) soil in Chikmagalur district, Karnataka, India, face many problems due to the seasonal variation of the moisture in the subgrade and observed swelling and shrinkage. Therefore, in the present investigation, BC soil obtained from the Chikmagalur district is mixed with different marginal materials, viz, class F fly ash, limestone powder, construction demolition waste (CDW), coconut, and arecanut fibers. These marginal materials used are not capable of improving the strength properties of soil. Therefore, two types of binders, viz, ordinary Portland cement (43 grade) and alkali solution (NaOH solution of 8 molar concentration mixed with Na_2SiO_3 solution to obtain SS/SH (Na_2SiO_3 solution/NaOH solution) ratios of 0.5, 1.0, and 1.5), were used to improve the strength (viz, Unconfined Compressive Strength (UCS), California Bearing Ratio (CBR), flexural strength) and durability properties of the soil.

When durability tests were conducted, the BC soil treated with 3, 6, 8, 10, 12, and 14% cement could not resist the soil loss under Wetting-Drying (WD) and Freezing-Thawing (FT) cycles. If stabilized materials are to be used in pavement, as per IRC 37: 2018, WD and FT durability tests are mandatory. FT test is essential for cold regions like Arunachal Pradesh, Jammu & Kashmir, Ladhak, etc. However, to study the behavior in adverse conditions, both tests were conducted. The soil properties were further improved by adding class F fly ash and cement. The cement dosages of 3, 4, 5, 6, and 7%, along with fly ash dosages of 0 to 32%, improved soil strength but could not control the soil loss within 14% when the durability tests were conducted. The BC soil stabilized again with 8, 10, 12, and 14% cement and fly ash dosage from 10 to 42%. The BC soil stabilized with 8% cement, and a high fly ash dosage of 42% failed in the WD test. At (cement+fly ash) dosages of (10+30), (10+35), (10+40), (12+30), (12+34), (12+38), (14+25), (14+30), and (14+36)% the BC soil exhibited soil loss of <14% after 12 WD and FT cycles. When the UCS test was conducted, there was an improvement in UCS at standard Proctor compaction. The mixes that passed durability tests (both WD and FT) were also evaluated at modified Proctor density and found improvement in UCS values. The stabilized BC soil exhibited higher resistance to weathering actions under FT cycles compared to WD cycles. The soil stabilized with higher cement content

(14%) and fly ash dosage (>30%) exhibited a maximum retained UCS after subjecting to durability tests. At a higher dosage of fly ash (>30%), the mix exhibited low plasticity with uniform distribution of cement cluster formations based on the Scanning Electron Microscopy (SEM) images and led to significant volume stability with improved soaked California Bearing Ratio (CBR(soaked)). The above mixes with high-volume stability are preferred for pavements.

The mixes that passed durability tests were further blended with 0.50% coconut fibers to study the further improvement in strength properties. The inclusion of fibers slightly reduced the density of stabilized soil mixes and thereby a marginal decrease in UCS values; however, the flexural strength of specimens increased. All the mixes exhibited significant improvement in retained UCS after durability tests. Due to the densest compact soil mix, the resistance to penetration has improved and exhibited higher CBR values.

The BC soil is further strengthened by adding an alkali solution. Initially, the BC soil was treated with class F fly ash (<50%) and activated using the alkali solution. There is a marginal improvement in strength due to less dissolution of aluminosilicate materials at a lower SS/SH ratio. The strength gain is more at a high SS/SH ratio of 1.5 due to increased dissolution. To improve the strength further, 5% limestone powder was added with fly ash. However, there is no enhancement in strength. Further to enhance the strength properties, arecanut fibers were added, the stabilized soil resulted in a marginal decrease of UCS values, with improvement in flexural strength. Again when the soil was replaced with CDW (<50%), there was a significant improvement in UCS and CBR(unsoaked) values for all alkali-activated mixes. At the same time, the CBR(soaked) values are in the range of 5–8% for various mixes. All alkali-activated specimens failed during the durability test due to mineral constituent leaching from the set soil. The alkali solution could not retain bonding due to the high moisture affinity of BC soil present in the mix.

SEM images showed formations of cemented intercluster. Hydration products formed resulted in strength improvement, as observed from X-Ray Diffraction (XRD) patterns. As per IRC SP-72: 2015, the only durability passed soil mixes can be used as a modified soil layer or as an improved subgrade. The critical strain values obtained by considering the stabilized soil as subgrade, Cement-Treated Sub-Base (CTSB) for high-volume

pavements were within limits as per the IRC 37: 2018. However, these mixes are generally not preferred as a Cement-Treated Base (CTB) due to the complications involved in mixing, compaction, low interface friction, etc., requiring complete quality control.

Keywords: Black cotton soil, Cement stabilization, Alkali activation, Marginal materials.

CONTENTS

LIST OF TABLES

CHAPTER 5

CHAPTER 6

LIST OF FIGURES

CHAPTER 6

ABBREVIATIONS AND SYMBOLS

BC	Black Cotton
CBR	California Bearing Ratio
CO_2	Carbon Dioxide
CTB	Cement-Treated Base
CTSB	Cement-Treated Sub-Base
CDW	Construction Demolition Waste
CSAL	Cumulative Standard Axle Load
EDAX	Energy Dispersive X-Ray Analysis
FT	Freezing-Thawing
GSB	Granular Sub-Base
IS	Indian Standard
IRC	Indian Roads Congress
MDD	Maximum Dry Density
MH	Highly Compressible Silt
MC	Moisture Content
NH	National Highway
NaOH or SH	Sodium Hydroxide
Na_2SiO_3 or SS	Sodium Silicate
OMC	Optimum Moisture Content
OPC	Ordinary Portland Cement
SEM	Scanning Electron Microscopy
SH	State Highway
SC-SM	Silty Sand-Clayey Sand
SM	Silty Sand
SS/SH	Na_2SiO_3 solution/NaOH solution
UCS	Unconfined Compressive Strength
USCS	Unified Soil Classification System
WBM	Water Bound Macadam
WD	Wetting-Drying
WMM	Wet Mix Macadam
XRD	X-Ray Diffraction

CHAPTER 1
INTRODUCTION

1.1 GENERAL

A widespread, properly connected all-weather road network that gives maximum service to the end-users is essential for the nation's overall progress. India has the second-largest road network (6,215,797 km) in the world. It includes 151,000 km of national highways (NH)/ expressways, 186,528 km of state highways (SH), and 6,064,797 km of other roads (MoRT&H: 2021). A good road network connects remote areas and acts as a feeder system to different modes of transportation. At present, pavements are subjected to excessive stresses due to overladen freight traffic. Premature failure of pavements was observed due to extreme wheel loads and improper construction practices. The road construction industry predominantly uses in-situ soil, locally available materials like kankar, moorum, aggregates, industrial byproducts like fly ash, steel slag, blast furnace slag, natural and processed fibers, cement, bitumen, etc., and combinations thereof. These materials are suitably used in different pavement layers depending on their engineering properties, traffic load repetitions, prevailing weather conditions, and type of pavement.

The design and construction of pavements is a dynamic process. As and when technology improves or updates based on the research findings, the pavements are to be designed. In the recent past, due to the depletion of natural resources, there has been a scarcity of aggregates and good soil. Researchers started using marginal materials produced from many industries as an alternate material for pavement construction. Marginal materials can be defined as materials that do not in their present form possess quality levels as defined by current highway standards sufficient for their use as various pavement structural components, including surfaces, bases, and subbases (Robnett 1980). Marginal materials are obtained from the industry as a byproduct while processing the naturally available materials like crude oil or burning coal in thermal power stations etc. It is the waste material for that industry and may be useful for road construction or stabilizing soil, replacing cement and aggregates. For example, fly ash is a byproduct of thermal power stations, and it may be useful for stabilizing soil, construction of embankment, replacing cement, depending on the quality. The technology used for improving the engineering properties of marginal materials should be cost-effective, and the stabilized material should be durable and available.

1.2 SOIL STABILIZATION AND ITS NEED

The concept of soil stabilization was developed 5000 years back (Firoozi et al. 2017). In ancient Egypt and Mesopotamia, roads were constructed using stabilized soil; lime was used as a stabilizer by Greeks and Romans (McDowell 1959). In general, stabilization is used to improve the engineering properties of soil by mixing with other materials. The improvement in density, strength, bearing capacity, volume stability (i.e., resistance to volume change with moisture content variation), and reduction in moisture susceptibility of weak soil is intended by stabilization. Such improved soil can be used for various construction purposes, viz, pavement subgrade, sub-base, base course (IRC SP-72: 2015, IRC 37:2018), the foundation for building, hydraulic structures (Bergado et al. 1996), etc., depending on their suitability as per the recommendations of relevant codes.

Stabilization can be done by mechanical and chemical methods.

1. Mechanical stabilization: It is the process of improving the properties of soil by changing its gradation. This process includes soil compaction, densification by using mechanical equipment like rollers, compactors, and tampers.
2. Chemical stabilization: In this method, the additives such as cement, lime, and bitumen are mixed with soil. The effectiveness of stabilization depends on the dosage of additives, nature of the soil, moisture content, curing period, and dry density achieved from the compaction. Also, the liquid chemicals obtained from calcium chloride, sodium chloride and sodium silicate, etc., react with source materials and alter their chemical properties.

Road infrastructure demands a massive quantity of good quality soil as subgrade material. Due to the non-availability of good quality earth, the construction industry aims to improve the poor quality soil by proper in situ stabilization techniques. Stabilization can solidify soft materials like clay to change their physical state. Stabilized soils can be recommended only after confirming the enhancement in the strength and durability characteristics. It is a widely used technique for improving the engineering characteristics of road embankments and subgrades. Ultimate support to the pavement structure is provided by the subgrade soil, resting on the natural embankment. Therefore, the subgrade becomes an integral part of the pavement structure; it should perform well during all weather conditions. Properties of subgrade are also essential for designing pavements. The soil subgrade should be stable, incompressible to avoid differential settlement. Various types of weak soil subjected to proper treatments are often used even in base and sub-base layers.

1.3 PROBLEMS OF BLACK COTTON (BC) SOIL

Construction of pavement layers with weak soil constituting clay or silt particles is a difficult task. BC soil is one among these, which exhibits low strength and drastic volume changes with moisture imbalance. BC soils are characterized by high shrinkage and swelling properties. These soils are very hard when dry but lose their strength completely in wet conditions. A pavement structure constructed on this soil without improving its strength and other engineering properties may fail by sinking, upheaval due to moisture absorption and increase in swell pressure, rut formations, cracks in the bituminous surface, pothole formations, mud pumping, and edge failure due to insufficient support in rigid pavements. There will be a functional failure of the pavement due to the wide shrinkage cracks developed in BC soil due to moisture loss during the summer season that may propagate to other layers. The rectification of such pavements is a difficult task. Therefore, wherever BC soil is encountered, proper treatment should be given to improve the engineering properties before construction. Either these soils are entirely replaced with better soil, or in-situ improvements are undertaken based on laboratory investigation.

1.4 MARGINAL MATERIALS

The depletion of natural resources has put enormous thrust on the road industry to use alternative materials. Mining restrictions and environmental concerns promote the utilization of marginal materials. The processing of various raw materials produces many industrial byproducts, which are dumped in open fields. These byproducts are called marginal materials and can be partially or fully replaced as pavement material depending on strength and other properties specified for pavement materials. Some of the marginal materials may require a process to bring them to the required gradation. The segregation and processing of marginal materials may be manually difficult and require proper machinery to do this task. Many times, the byproducts do not fulfill the required standards. Therefore, processing or modification of marginal materials finds importance. The IRC codes for low and high-volume roads suggest the usage of marginal materials, if abundantly available. Fly ash, slags, broken bricks, construction demolition waste (CDW), etc., can be used in different pavement layers. Few industrial wastes with proper stabilizers can suitably transform the weak soil into reasonably good soil.

1.5 FLEXIBLE PAVEMENTS

The construction cost of flexible pavement is approximately half that of rigid pavement. Also, the repair of flexible pavement is relatively easier (Taher et al. 2020). Flexible pavements are generally provided with a bituminous surface. The unsurfaced roads are not preferred even for low-volume traffic where the intensity of rainfall is more than 500 mm/year. The bituminous surface should be rough and impermeable to prevent the ingress of water into the lower layers during the monsoon. The strong base course supporting the bituminous layers will help to distribute the wheel load stresses to a broader area. A granular sub-base layer constructed below base layers will help in draining off the water from the pavement layers. The subgrade constructed at the bottom supports the pavement. Provisions are given in IRC SP-72: 2015 and IRC 37: 2018 for the economical use of locally available marginal, modified materials in these various layers.

As per IRC SP-72: 2015, the pavements carrying < 2 msa cumulative standard axle load (CSAL) applications during the design life are categorized as low-volume roads. As per IRC 37: 2018, the roads are considered high-volume if the design traffic is 5–50 msa. The design life of the flexible pavement is usually 15-20 years. Flexible pavement is composed of various layers, viz, surface (bituminous), Base (Water-Bound Macadam (WBM), Wet Mix Macadam (WMM), Cement-Treated Base (CTB)), Sub-Base (Granular Sub-Base (GSB), Cement-Treated Sub-Base (CTSB), the subgrade (borrowed soil, stabilized soil), over an embankment or on natural ground. The stresses due to wheel load are transferred to a broader area below. The surface layer is subjected to the highest stress, and hence, it must be constructed with high-quality materials. For the better performance of pavement, the tensile strain at the bottom of bituminous and

CTB layers and compressive stress at the top of the subgrade should be within limits specified by IRC 37: 2018.

1.6 RESEARCH OBJECTIVES

In the present investigation, the BC soil is mixed with fly ash, coconut fibers and then bonded with cement. Also, to check the suitability of the alkali activation method, the BC soil is mixed with marginal materials like fly ash, CDW, limestone powder, arecanut fibers and then bonded with alkali solution. The effect of cement and alkali solution along with marginal materials are tested with the objectives of

1. Characterization of materials, finding the strength of stabilized mixes by conducting Unconfined Compressive Strength (UCS), California Bearing Ratio (CBR), flexure tests.
2. Evaluating the durability/ sustainability of stabilized soil under wetting-drying and freezing-thawing tests.
3. Analyzing the fatigue behaviour of stabilized mixes at different stress levels.
4. Analysis of the structural changes of stabilized mixes through Scanning Electron Microscopy (SEM) and X-Ray Diffraction (XRD) tests.
5. Developing pavement design charts for low and high-volume roads.

1.7 SCOPE OF THE INVESTIGATION

The BC soil used in the present investigation exhibits poor engineering properties with variation in moisture content. To use it as a pavement layer, it is necessary to alter the properties of the soil. The scope of the research work includes evaluating the effectiveness of BC soil stabilization using two binders, viz, cement and alkali solution, after mixing with marginal materials.

Initially, BC soil is mixed with fly ash and bonded with a conventional binder, Ordinary Portland cement (OPC). To improve flexural strength and control the propagation of drying shrinkage cracks, soil-cement mixes were blended with coconut fibers. In the second stage, the BC soil mixed with marginal materials like fly ash, CDW, limestone powder, and arecanut fibers and bonded using an alkali solution. This alkali solution was prepared by using NaOH flakes, Na_2SiO_3 solution, and water. The strength of stabilized soil was evaluated by conducting UCS, CBR, flexural, fatigue, and durability tests at both the standard and modified Proctor densities. The stabilized mixes are further analyzed by conducting SEM and XRD tests to evaluate morphological changes. The revised guidelines of IRC SP-72: 2015 and IRC 37: 2018 suggest using cement-treated/chemical-treated mixes for pavement layers, which satisfy the strength and durability criteria. As per these guidelines, the properties of improved/ stabilized BC soil were used to design the low and high-volume pavements, and analysis was carried out by using IITPAVE software.

1.8 THESIS ORGANIZATION

CHAPTER 1 gives a brief introduction to soil stabilization and its necessity. It also includes the scope and objectives of the investigation.

CHAPTER 2 gives information about the history of soil stabilization pertinent to the selected materials. The improvement in stabilized soil properties relevant to pavement or field application is highlighted. It also describes the methodology followed for the investigation.

CHAPTER 3 description of materials along with their physical and chemical characteristics.

CHAPTER 4 provides a detailed description of experimental outcomes of the cement-treated BC soil along with marginal materials (viz, class F fly ash, coconut fibers).

CHAPTER 5 provides a detailed description of experimental outcomes of the alkali-activated BC soil along with marginal materials (viz, class F fly ash, limestone powder, arecanut fibers, CDW).

CHAPTER 6 provides details of pavement composition for low and high-volume pavements for durability tests passed BC soil stabilized with cement, fly ash, and fibers. The pavement analysis results, cost of treated materials are discussed in detail.

CHAPTER 7 gives concluding remarks on cement and alkali stabilization methods used for BC soil.

CHAPTER 2

LITERATURE REVIEW

2.1 GENERAL

This chapter provides a comprehensive review of research works carried out by various researchers to rectify problems related to BC soil in road construction. Chemical stabilization was commonly used for improving the properties of BC soils. The improvement in soil properties was observed using different additives and different marginal materials based on availability in their location.

2.2 BLACK COTTON SOIL

Black soil is formed from volcanic rocks and lava. It is named ‘regur’ from the Telugu word ‘reguda,’ and due to its suitability for growing cotton crops, it is called ‘Black Cotton soil.’ Calcium carbonate, lime, potash, and magnesium carbonates are rich in this soil (https://www.mapsofindia.com 2020). BC soil is found in south Asia, middle Africa, and some tropical areas (Patel and Shahu 2015). Expansive soil covers around 20% of Indian land (i.e., Parts of Deccan Plateau, western Madhya Pradesh, Rajasthan, Bundelkhand in Uttar Pradesh, Karnataka, and Andhra Pradesh), as depicted in Figure 2.1. These soils can undergo volume changes, which is considered detrimental to residential buildings, pavements, linings, etc. (McKeen 1988; Nevels James B 2001; Walsh et al. 1993). The seasonal variation resulted in extreme swell-shrink of the BC soils in Kenya (Ola 1978). Soil containing common minerals of smectite group absorbs water and exhibits high expansion (Ackroyd and Husain 1986; Ola 1978). High plasticity clay can exhibit volume expansion of 150–300% (Gadre and Chandrasekaran 1994). On expansion, this soil can build a swell pressure of 8–10 kg/cm^2 (Mehta et al. 2014). The swell-shrink behaviour of soil is considered as a severe problem (Chen 2012). BC soils are inferior and problematic if used in road construction due to their low strength and considerable expansion in a moist condition (Etim et al. 2017). Bowles 1992 stated that the soil with a CBR value of < 2% is weak for subgrade.

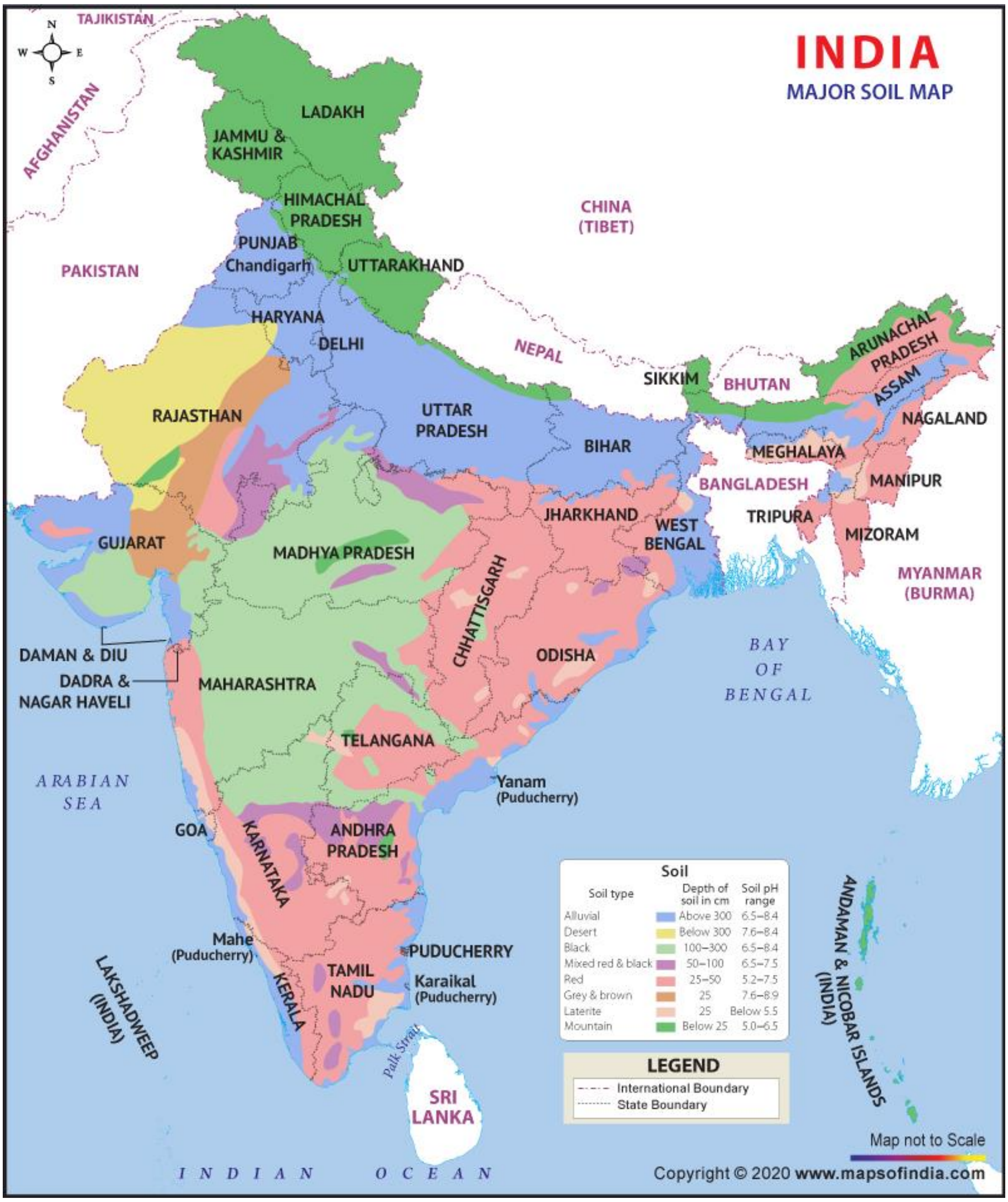

Figure 2. 1 Geographical distribution of Indian soils

(https://www.mapsofindia.com 2020)

2.3 CEMENT STABILIZATION

Generally, additives are classified as non-cementitious (reclaimed aggregates, stone dust, rock powder, etc.), supplementary cementitious (lime kiln dust, silica fume, lime, fly ash, etc.), and chemical (KCl, NaCl, $MgCl_2$, etc.) (Reddy et al. 2015). Lime and cement are common additives used to enhance the BC or weak soil properties from ancient times (Lemaire et al. 2013; Maubec et al. 2017; Osinubi et al. 2011; Oza and

Gundaliya 2013). Here, the ionic substitution of Na^{+} and Ca^{2+} ions and cementitious matrix precipitation promotes the agglomeration and flocculation of soil particles leading to stabilization (Scheuermann Filho et al. 2021). To strengthen BC soil, additives like cement kiln dust, lime, fly ash, and their combinations are used, but the type of cementitious compound formation was not analyzed (Maneli et al. 2016; Salahudeen et al. 2014). For various infrastructural applications, unsuitable soft soil properties were improved using compacted soil-cement mixtures for decades (Bergado et al. 1996). The cement-metakaolin admixtures formed hydration products and strengthened the compacted weak soil (Wu et al. 2016).

Compacting soil-cement mixture to a target density substantially improves its shear strength and durability. Also, a cement dosage of >3% by weight of soil effectively enhances the cohesion of silty sand (Yang et al. 2020). SC-SM soil treated with 8.6% cement by weight of soil and compacted to standard Proctor density achieved significant improvement in UCS with curing and hence recommended for embankment fills (Wu et al. 2017). Clay soil stabilized with 20–30% cement exhibited a significant improvement in UCS of >3.5 MPa on 7 days, and it is found that strength improvement is a function of hydration of cement which depends on curing time (Estabragh et al. 2016). By improving cement dosage, stabilized soil behaviour changes from ductile to brittle (Bahar et al. 2004; Tang et al. 2007). For diminishing expansive soil's swell potential, a cement dosage of 2–6% is found sufficient (Chen 2012). A Portland cement dosage of 10–16% is suggested to improve BC soil strength (PCA 1979). A cement-treated soil can gain strength due to the reformation of soil structure by pore space reduction and intercluster cementation bonding (Horpibulsuk et al. 2010). For cement stabilized low plasticity clay (CL), the failure strength and brittleness of specimens were increased with the increase in cement percentage (Estabragh et al. 2012, 2016). Also, the specimen's moisture content has exhibited a profound effect on the failure strain and strength. A cement (9%) and sludge ash (0–30%) stabilized silt of low compressibility (ML) at 20% ash content exhibited 26% improvement in UCS compared to cement stabilized soil without sludge ash (Durante Ingunza et al. 2015). Therefore, suitable cement dosage and availability of enough moisture content at the time of curing can contribute to the strength development of soil-cement mixes due to proper hydration.

2.3.1 Cemented Soil Modification Mechanism

The mechanism of soil-cement modification is explained by Jerod and Wayne 2020, and is depicted in Figure 2.2.

Cation Exchange: Plastic soils have a high Plasticity Index (PI) and tend to be comprised of clay, which is primarily composed of aluminum silicates. The clay particles sustain net negative charges on their surfaces that are balanced by exchangeable positively charged ions (cations) held together by electrostatic attraction. Some cations are capable of only forming a single, or monovalent, bond.

The plasticity of a soil is determined by the amount of expansive clay (e.g., montmorillonite) present. The clay mineral forms a bonded crystal structure through the stacking of silica and alumina layers. Because of the negative charge on this crystal structure, cations and water molecules are attracted to its negatively charged surfaces in an attempt to neutralize the charge deficiency. This results in a separation of the charged surfaces, forming a diffuse double layer. The thicker this double layer, the more plastic the soil.

If the cation responsible for the neutralization is monovalent, such as sodium, the soil becomes plastic. In order to reduce the soil's plasticity, the monovalent cations present in the clay surface must be exchanged so that the thickness of the double layer is reduced. Fortunately, the monovalent cations within the double layer can be easily exchanged for other cations. Cement, a good calcium-based soil modifier, can provide sufficient calcium ions to replace the monovalent cations on the surfaces of the clay particles. This ion exchange process occurs within hours, shrinking the layer of water between the clay particles and reducing the plasticity of the soil.

Particle Restructuring: Typically, clay soils are lightweight, have high void ratios, and are difficult to manipulate. The addition of cement results in soil restructuring. The restructuring of modified soil particles, known as flocculation and agglomeration, changes the texture of the material from that of a plastic, fine-grained material to one more resembling a friable, granular soil (Halsted et al. 2008).

Flocculation is defined as the process by which clay particles form clot-like masses as a result of a chemical reaction between clay and another substance, in this case, cement. In the context of soil modification, agglomeration refers to the weak bonding at the edge surface interfaces of the clay particles, which, as a result, forms larger aggregate-like particles from finely divided clay particles and further improves the texture of the soil (Halsted et al. 2008).

Before soil undergoes flocculation and agglomeration, the clay particles are naturally aligned parallel to each other in layers due to their chemical composition. After undergoing flocculation and agglomeration, the clay particles are aligned randomly in an edge-to-face orientation, which gives the soil a granular-like texture. The high electrolyte content and high pH of the treated soil, and the reduction in the thickness of the double layer are all attributed to dispersion.

Cementitious Hydration: Cementitious hydration is a process that is unique to cement and produces products referred to in cement chemistry as Calcium-Silicate-Hydrate (CSH) and Calcium-Aluminate-Hydrate (CAH). CSH and CAH act as the "glue" that provides structure in a cement-modified soil by stabilizing flocculated clay particles through the formation of cement-clay bonds. This bonding between the hydrating cement and the clay particles improves the gradation of the modified clay by forming larger aggregate-like particles from fine-grained particles. The majority of this reaction occurs within the first 30 days after the cement is added to the soil.

Pozzolanic Reactions: While cementitious hydration is the primary reaction between cement and water, secondary reactions, known as pozzolanic reactions, also occur. These reactions are created from the combination of calcium ions, silica, and alumina. Although pozzolanic reactions occur via a through-solution process, it has been claimed that they are direct reactions between calcium hydroxide ($Ca(OH)_2$) and adjacent clay surfaces, with the pozzolanic products formed as precipitates (Prusinski and Bhattacharja 1999).

Calcium hydroxide results from hydration, which furthers the cementing action. The process takes calcium ions (from cement) and combines them with silica and alumina (from clay) to form additional aluminates and silicates. Although pozzolanic reactions occur to a much lesser degree than cementitious hydration, they add further strength and durability to the soil and can continue for several months or years.

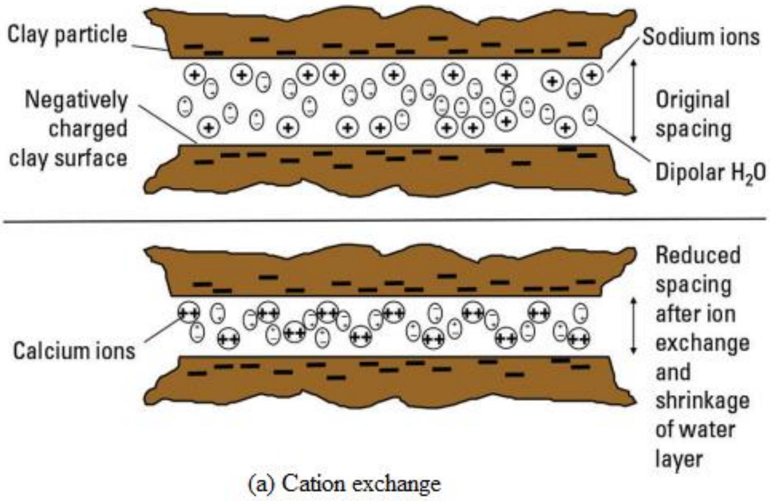

(a) Cation exchange

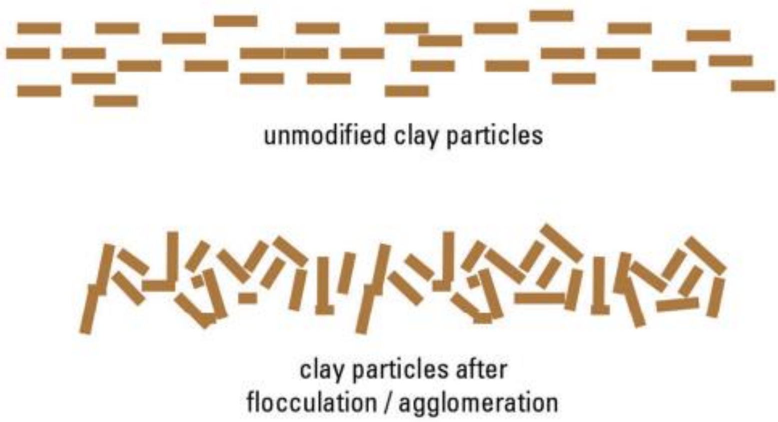

(b) Particle restructuring

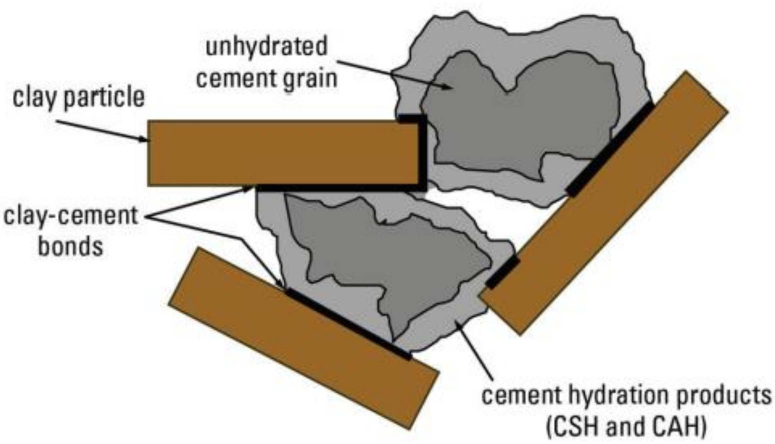

(c) Cementitious hydration

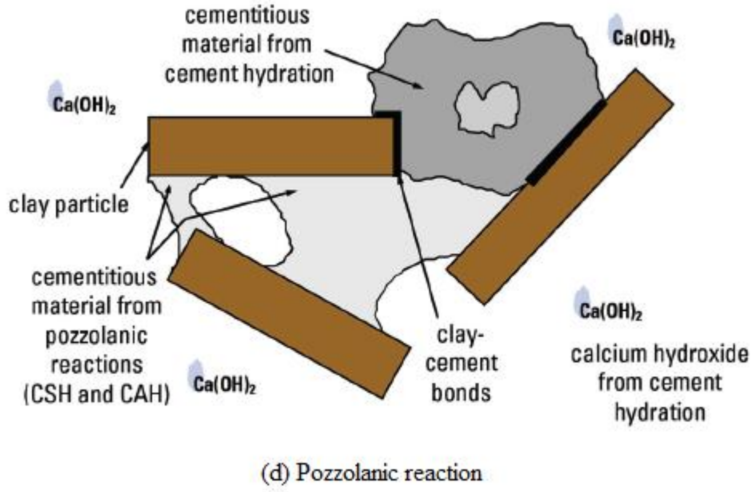

Figure 2. 2 Modification mechanism of cemented soil

(Halsted et al. 2008; Jerod and Wayne 2020)

2.3.2 Cement Production and Environmental Concern

The construction industry of the world is mainly dependent on cement. World statistics indicate that cement production has increased from 3310 to 4100 million metric tons per year from 2010 to 2015 (Verdolotti et al. 2008). The quantity of cement produced in the year 2021 is 4100 million metric tons (https://www.statista.com/ 2021). The cement production begins with massive mining of raw materials and processing with high energy consumption, emitting 5–8% CO_2 in global scenarios with a substantial environmental impact footprint (Oh et al. 2014; Scrivener and Kirkpatrick 2008; Shi et al. 2012). Approximately 1 ton of CO_2 is released to produce 1 ton of cement (Provis and Van Deventer 2013; Scrivener and Kirkpatrick 2008). In addition to CO_2, other key polluting substances emitted to air by the cement industry include dust, other carbon oxides such as carbon monoxide (CO), nitrogen oxides (NO_xs), sulphur oxides (SO_xs), polychlorinated dibenzo-*p*-dioxins, dibenzofurans, total organic carbon, metals, hydrogen chloride, and hydrogen fluoride, which are serious health-hazardous substances such as toxicological and cancer risks and some are hilariously odorous (Schuhmacher et al. 2004). However, cement is an essential material for human survival nowadays. As such, there is no suitable alternative that can be used for mass construction activities to give high strength and easy working, but the production of cement is essential. At present, to protect the environment, the Government and other organizations insist to utilize the waste material produced from various industries to effectively use in roads and other constructions to avoid landfills and other environmental hazards.

2.4 FLY ASH AS A MARGINAL MATERIAL IN SOIL STABILIZATION

Thermal power plants use pulverized coal as fuel, which produces a vast quantity of fly ash. This ash consists of hollow, spherical particles of silicon, aluminum, iron oxides, and unoxidized carbon. As per USCS, it is classified as non-plastic fine silt. Characteristics of the power plant and the nature of the coal used govern fly ash composition (Cabrera and Woolley 1994; Rollings 1996). The burning of bituminous or anthracitic coal produces class F fly ash. Burning of sub-bituminous coal and lignite produces class C fly ash. Both are defined as siliceous or siliceous and aluminous materials, which are said to be pozzolans (Dwivedi and Jain 2014). The total production of fly ash in India in the year 2018–2019 is 217.04 million tons, with a safe and productive utilization of 168.40 million tons (Yousuf et al. 2020). Class F fly ash lacks self-cementitious characteristics and requires an activator like cement. At present, only 32% of fly ash is used in construction. Massive utilization of this waste material is challenging for the construction industries, leading to dumping and environmental problems (Martin et al. 1990; Misra et al. 2005).

Numerous industrial waste materials like pond ash, fly ash may improve the engineering properties and reduce the swell-shrink characteristics of highly expansive soils (Khattab et al. 2007; Kumar et al. 2007; Kumar and Singh 2008; Sivakumar Babu et al. 2008). Fly ash possesses a nonplastic nature; hence, its amendment can control expansive soil's plasticity characteristics (Sukmak et al. 2013). Expansive soil treated with fly ash exhibited increased density and decreased OMC up to 20% dosage, and the plasticity characteristics were substantially controlled (Phani Kumar and Sharma 2004). When class F fly ash is replaced in the BC soil, the soil friction is enhanced (Pandian and Krishna 2003). Bulk construction activities like road works and soil stabilization can use these materials in huge quantities and can be admixed with other cementitious materials (Pandian 2013).

A study conducted on marine clay in Singapore suggested that 20% of fly ash with 30% of cement enhances the undrained shear strength by 75 times that of untreated clay (7.23 kPa), and it was suggested to increase the fly ash content for improvising pozzolanic activities (Show et al. 2003). BC soil stabilized with 18 and 37% class F fly ash with

3% cement has resulted in a significant improvement in soaked CBR values of 28 and 58%, respectively, after 28 days curing when compared to 1% soaked CBR of untreated soil, but the durability and volume stability tests were not conducted (Leelavathamma et al. 2005).

A 5–20% cement content is considered a low stabilizer dosage for marine clay mixed with 5–20% fly ash (Xiao et al. 2017). Soil treated with bottom ash and cement was found to improve its strength characteristics, depending on the hydration process, which is greatly controlled by proper curing (Cai et al. 2006b; Chauhan et al. 2008; Jafar et al. 1996; Kumar and Gupta 2016; Lekha et al. 2015; Moghal et al. 2018; Sahu et al. 2017).

2.5 INCLUSION OF FIBERS

Chemical stabilization can make the soil stronger to sustain higher compressive loads but contribute less to tensile strength improvement (Sobhan 2008). The problem of tensile cracking due to shrinkage aggravates during the summer when the soil moisture reduces, thereby depleting tensile strength. A suitable reinforcement technique can enhance tensile strength and reduce the deformation of soil. Natural fibers like jute, sisal, coconut, arecanut, etc., and artificial/ synthetic fibers like polypropylene, polyvinyl alcohol, etc., can impart tensile strength to soil based on the dosage and are utilized for soft ground improvement. Like industrial wastes, there are various agricultural byproducts like rice husk ash, coconut fiber, arecanut fibers, etc., which are considered to be waste. Many investigations were carried out using these byproducts in geotechnical constructions (Balan 1995; Jayasree et al. 2014; Payá et al. 2001; Priyadarshee et al. 2015; Sivakumar Babu et al. 2008).

Vidal 1969 has postulated the ground improvement techniques by utilizing tensile reinforcement. Various shapes and sizes of reinforcement like metallic strips, sheets, geosynthetic grids, tyre waste, short or long fibers formed from natural or synthetic sources are available for construction (Cabalar et al. 2014; Cabalar and Karabash 2014). Natural or synthetic fibers are extensible type reinforcement (McGown et al. 1978). As per Tang et al. 2016, the interfacial strength developed by bridging the soil particles and randomly mixed synthetic fibers crosses the tensile failure plane; it is a viable option for improving soil tensile strength. Osinubi 2000 suggested that a pavement subgrade should exhibit a minimum tensile strength of 469 kPa. Many studies were conducted on various soils using natural or synthetic fibers with stabilizers for use in pavement layers. The UCS, shear strength, and axial strain were increased for the cemented and uncemented clayey soils when reinforced with fibers (Tang et al. 2007). The higher fiber content in the soil increased peak axial stress, flexibility, and post-peak strength. Friction at the interface and bond strength due to the cementation magnify the benefits of soil reinforcement. The mechanical behaviour of clayey soil reinforced with fibers is governed by the interaction occurring at the fiber surface and clay particles.

Marandi et al. 2008 strengthened soil with the natural palm fibers from 0.25–2.5% by varying lengths of 20–40 mm, the stress-strain behavior markedly improved. The inclusion of palm fibers made the soil specimens more ductile. The peak strength and the residual strength of palm fiber included soil were more (Marandi et al. 2008). The fiber inclusion increased the UCS and reduced swell pressure and volumetric shrinkage of the expansive clays when studies were conducted to analyze reinforcement effectiveness. The inclusion of fiber increased the soil's free swell potential (Puppala and Musenda 2000). Cai et al. 2006a tested six different soils treated with lime and fibers and observed that an increased dosage of fibers increases compressive strength. The inclusion of both fiber and lime has a magnified effect on the strength improvement compared to the usage of lime or fiber alone, which is due to the combined effect of reinforcement and bonding. The inclusion of lime into the soil improves UCS and reduces the swelling-shrinkage potential of soil.

The CBR of high plasticity clay (CH) reinforced with soft textured multifilament polypropylene fibers was higher than that with rough-textured fibrillated polypropylene fibers. CBR value was found to decrease beyond a 0.5% dosage of both fibers (Şenol 2012). The soaked CBR value of soil reinforced with 20 mm length polypropylene fiber has increased 3 times that of unreinforced soil at a dosage of 0.8% by weight of soil (Pradhan et al. 2012). The fiber length and concentration significantly influence the CBR value, with long fibers (higher slenderness ratio) imparting more improvement in CBR (Moghal et al. 2018). Coir fiber-reinforced subgrade soil with fly ash exhibited good resilient responses to the repeated loading due to their higher frictional resistance (Chauhan et al. 2008). Clay soil's strength and compaction parameters were studied by adding rice husk ash, pond ash, and cement with fibers. Fiber quantity has shown a profound effect on strength behaviour and ductility or brittleness of the specimen. As the dosage of fibrillated polypropylene fibers has increased from 0.5 to 1.5%, a significant improvement in UCS was observed due to increased contact area and improved friction between soil and fibers (Kumar and Gupta 2016).

The stabilization soil with natural and synthetic fibers is found to be more economical because of its abundance. Also, along with cementitious compound, i.e., cement, fiber has a profound effect on fatigue life improvement of soils (Cai et al. 2006b; Chauhan et al. 2008; Kumar and Gupta 2016; Lekha et al. 2015; Moghal et al. 2018). It is found that the strength improvement of soil depends on various factors like cement or lime content, fiber content, fiber length, and curing period. Arecanut fiber-reinforced lateritic soils have improved their engineering properties when used with the cement and could be effectively utilized as subgrade for or low-volume roads (Lekha et al. 2015). The improvement in the tensile property of soil is generally due to the interlinking property of added fiber (Kumar and Gupta 2016; Sahu et al. 2017).

A silty soil of high compressibility (MH) treated with 30% bottom ash, 3% cement, and 1.5% areca fibers showed CBR improvement from 2 to 39% and 1 to 30% under unsoaked and soaked conditions, respectively (Sudhakaran et al. 2018); similar trends were observed from previous studies (Sahu et al. 2017). Coir reinforcement up to 1% has improved soil strength, but further addition has decreased strength (Ravishankar and Raghavan 2004). Randomly distributed fibers could reduce the base course thickness (Gosavi and Patil 2004). Longer date palm fibers improve the CBR value of reinforced soil than shorter ones (Sarbaz et al. 2014). A stabilized mix gains strength due to CSH called tobermorite (Solanki and Zaman 2012). The addition of cement to the bottom ash can enhance hydration products like tobermorite, CSH, and other hydrates (Mohamed 2002). The interfacial interaction of soil grains induced can be enhanced due to the rough texture of arecanut fibers. Hence, the interfacial interaction can enhance the strength of bottom ash stabilized silty soil of high compressibility (MH). Further, the higher resistance between fiber and hydration products resulted from the denser microstructure formation of the cementitious compounds on curing (Li et al. 2014; Sudhakaran et al. 2018). As per Dang et al. 2016, the frictional resistance to the shrinkage was offered due to soil fiber interaction and interlocking mechanism.

2.6 ALKALI-ACTIVATED SOILS

The efficacy of traditional binders like cement and lime in improving the mechanical properties of weak soils is well accepted (Boardman et al. 2001; Guidobaldi et al. 2018;

Miura et al. 2001; Uddin et al. 1997; Vitale et al. 2019a). Alkali-activated marginal materials can reduce greenhouse gas emissions by >80% (Duxson et al. 2007c). The utilization of industrial byproducts can effectively reduce novel binders production, minimize waste generation, and is economically viable (Cristelo et al. 2012, 2013; Rao and Acharya 2013; Sukmak et al. 2014; Vitale et al. 2019b). The reduction of CO_2 emissions into the atmosphere is possible by using alkali-activated artificial pozzolans in place of novel and efficient binders (viz, cement, lime, etc.) to improve the engineering properties of weak soil (Coudert et al. 2019; Cristelo et al. 2015, 2017; Davidovits 2002; Provis 2014; Provis and Van Deventer 2013; Rios et al. 2018; Vitale et al. 2017; Wilkinson et al. 2010).

A combination of hydroxyl (e.g., NaOH, KOH) and a glassy silicate (e.g., Na_2SiO_3, K_2SiO_3) are used in the production of alkaline activators due to easy availability and low cost (Barbosa and MacKenzie 2003; Davidovits 1991; Duxson et al. 2007a; Hardjito et al. 2004; Palomo et al. 1999; Xu and Van Deventer 2000). The precursor materials (artificial pozzolans) like fly ash, blast furnace slag, silica fume, steel sludge, or natural pozzolans, which are the source of aluminosilicate materials, are activated by alkaline solutions of NaOH and Na_2SiO_3 (Buchwald et al. 2003). As an alternative to the cement, alkali-activated fly ash and GGBFS with Na_2SiO_3 and NaOH solutions were subjected to extensive research at present (Phummiphan et al. 2016; Rios et al. 2019; Sargent et al. 2016; Sharma and Sivapullaiah 2016; Singhi et al. 2016). Alkali activation results in a more robust material with superior mechanical properties than Portland cement stabilization. Most of the alkali activation studies were conducted using fly ash (Cristelo et al. 2012; Rios et al. 2015; Sargent et al. 2013; Silva et al. 2013; Singhi et al. 2016; Sukmak et al. 2014; Wilkinson et al. 2010; Zhang et al. 2013).

Alkali activation improves the properties of materials mixed with low calcium products. The reaction occurs between aluminosilicate materials and alkali or alkali-based substances (ROH, $Ca(OH)_2$, R_2CO_3, R_2S, Na_2SO_4, $CaSO_4 \cdot 2H_2O$, $R_2 \cdot (n)SiO_2$, where, R is alkaline ions of Na, K or Ca) (Davidovits 1991). The alkali reaction promotes the aluminosilicate materials dissolution that condenses into an alkali aluminosilicate phase 3D network due to precipitation (Duxson et al. 2007a; Provis and Van Deventer 2013). The Si to Al ratio governs the exact type of aluminosilicate phase formed in the reactions, depending on the material composition (Duxson et al. 2007b; Weng and

Sagoe-Crentsil 2007). The amorphous gel phase developed gives the mix good strength, durability, and desired properties (Liew et al. 2016). Crystalline form products like zeolite are also sometimes formed (Criado et al. 2007). Lower Si to Al ratio develops crystalline products, whereas higher Si to Al ratio is more likely to develop a geopolymer phase (Buchwald et al. 2003; Duxson et al. 2005).

The hydration mechanism of alkali-activated materials is quite different from ordinary Portland cement (Almakhadmeh and Soliman 2021). The diffused double layer surrounding soil particles reduces due to the exchange of Ca^{2+} ions in the alkali-activated mix with other metal ions like Na^{+} and Al^{3+}, thus increasing the flocculation and shear strength. The calcium oxide dissolution in water increases pH, leading to the rapid dissolution of SiO_2 and Al_2O_3 forms CSH and CAH gels (Ho et al. 2020).

Soils with unsuitable properties are termed as construction wastes (Llatas 2011). Soil is an abundantly available natural resource at a low cost that can be potentially alkali-activated to improve geotechnical properties (Diop and Grutzeck 2008). As a low-cost replacement, bottom ash is used in place of costly sand to produce concrete blocks and road bases (Ghafoori and Cai 1998). BC soil mixed with fly ash and stabilized with an alkali solution made up of 5 molar NaOH solution and Na_2SiO_3 solution with different SS/SH ratios (0.5–2.0) has shown improvement in strength. It was suggested not to use an SS/SH ratio of >1.5 due to a decrease in the strength of mixes (Murmu et al. 2019). The alkali solution prepared using NaOH and Na_2SiO_3 solutions has suitably improved the strength and durability of GGBS admixed lithomargic clay (Amulya et al. 2020). The alkali (NaOH) activated class C fly ash with higher CaO content has contributed more strength to the stabilized soft soil than with class F fly ash (Cristelo et al. 2012).

The extent of aluminosilicate dissolution in concentrated alkali solution governs the extent of alkali aluminosilicate phase formation (Xu and Van Deventer 2000). The alkali activation process begins with SiO_2 and Al_2O_3 dissolution in a high pH liquid. Due to polymerization, large molecules are formed by clumping particles, which precipitate into a gel. The industrial wastes in an amorphous state produced due to the thermal treatment are rich in SiO_2 and Al_2O_3. They can be effectively subjected to chemical reactions to produce a better-organized material as they are less stable. Depending on the type of activator used, the dissolution rate of alkali-activated fly ash depends on the mixture's alkalinity level (Fernández-Jiménez et al. 2005;

Fernández-Jiménez and Palomo 2005). Clay soil mainly contains minerals like kaolinite, montmorillonite, and illite, with less common allophane and halloysite (Reeves et al. 2006). Clay is the most soluble component than common aluminosilicate phases of soil like quartz (Autef et al. 2012; Tchakoute et al. 2015) and muscovite (Zografou 2015). Calcined clay is more reactive, but the cost and energy involved are more (MacKenzie 2009).

Alkali-activated low expansion precursor replaced in highly expansive clay can improve strength and durability. Soils may contain minor quantities of non-reactive clay mineral quartz and other minerals (Dixon et al. 1990). Investigations were carried out on the behaviour of alkali-activated clay minerals like kaolinite (Liew et al. 2016), montmorillonite (Belviso et al. 2017; Seiffarth et al. 2013), and illite (El Hafid and Hajjaji 2015; Seiffarth et al. 2013; Sperberga et al. 2011). Where in previous studies, montmorillonite and illite were calcined before alkali activation. However, calcined non-kaolinitic clays were used as supplementary cementitious materials with Portland cement blends (Hollanders et al. 2016; Snellings et al. 2012; Tironi et al. 2013). High calcium environments confirm CSH phases, but there is a limited knowledge of low calcium environments where it is an objective to form NASH geopolymer. The studies on kaolinite soil, natural soil, and blends of uncalcined soil, metakaolin are popular, but lower attention has been given to the studies of activation of individual clay and controlled clay mixtures (Lemougna et al. 2014; Liew et al. 2016; Sore et al. 2018). Around the world, soils may contain different clay amounts (Abe et al. 2006; Nickovic et al. 2012) with other minor quantities of minerals. Therefore, it is necessary to understand the fundamentals of clay soils and their behaviour under the activated conditions as a reliable construction material. The binary, ternary mixtures of kaolinite, montmorillonite, and illite, which were activated using aqueous NaOH solution formed a combination of products like sodalite, cancrinite, and nepheline (Richardson et al. 1986). But, XRD characterization was used without mentioning geopolymerization or formation of amorphous phases. The aluminum and silicon solutions were favorable for geopolymerization when Si:Al ratio is >1.5 with coexisting geopolymer and zeolites in some systems (Buchwald et al. 2011).

Laboratory investigations were conducted on alkali-activated clayey soil, sandy clay, and silty sand (Cristelo et al. 2011; Rios et al. 2015; Sargent et al. 2013; Singhi et al.

2016; Wilkinson et al. 2010; Zhang et al. 2013). The alkali activation has much potential for soft soil stabilization at high depth, shallow depth, or rammed earth construction (Cristelo et al. 2011; Silva et al. 2013; Zhang et al. 2013).

Attempts were made to geopolymerize BC soil in India (Bagewadi and Rakaraddi 2015). Stabilization and shrinkage control of BC soil treated with $Ca(OH)_2$ and KOH was observed due to new mineral phases formation with zeolite structure by irreversible chemical bonding (Miao et al. 2017). Based on characteristics of raw materials, curing, alkali concentration, alkali activator type, alkali cations, a variety of cementitious compounds with varying compressive strength, fire resistance, and low thermal conductivity are formed (Duxson et al. 2007a). Specimens prepared with 10 molar NaOH solution, cured at 65°C for 48 h, exhibited high compressive strength up to 20 MPa (Kim et al. 2016). The addition of Ca-rich components with a suitable alkali activator resulted in stable binder phase formations with C–A–S–H and N–A–S–H gels (Bernal et al. 2011; Garcia-Lodeiro et al. 2011).

2.7 STUDIES ON VOLUME STABILITY

Primarily, expansive soils are known to be a significant problem in geotechnical engineering. Swelling is defined as unsaturated clay soils taking water inside their body by interacting with water (i.e., diffused double layer of water) and increasing volume depending on this process. Previous literature demonstrates profound experiences belong to damage formed by expansive soils (Nelson and Miller 1997; Steinberg 1998; Türköz and Tosun 2011). The economic losses occurring due to buildings constructed on expansive soil, or built with expansive soil, are more than the losses due to earthquakes, floods, and storms (Nelson and Miller 1997; Zumrawi et al. 2017). The damage occurring due to swelling soil in the USA is billions of dollars annually (Steinberg 1998).

Expansive soil is a special unsaturated soil that is fractured and has significant swell shrink characteristics and over-consolidation (Shi et al. 2014). Many factors govern the expansive behaviour of soils. The initial factors are the availability of moisture and the percentage of clay particles in the soil. Other factors affecting the expansive behavior include the type of soil, soil condition in terms of dry density and the moisture content, the magnitude of the surcharge pressure, and the amount of non-expansive material (Estabragh et al. 2013). Expansive soil reinforced with geo-fibers showed that discrete and randomly distributed fibers help to restrain the swelling tendency (Viswanadham et al. 2009). Injection of 6% cement grout into the soil decreased swelling considerably (>90%) and resulted in 2.2 times compressive strength improvement (Daraei et al. 2018).

Class-C fly ash can effectively reduce the swell potential of highly plastic clays (Nalbantoğlu 2004). Efforts were made to improve soft subgrade soil's strength and swelling properties by sewage sludge ash and hydrated lime (Lin et al. 2007). An equation developed between swell percent and liquidity index is applied well with acceptable accuracy for percent swell estimation (Yilmaz 2009). For cement/ fly ash–treated soils, the skeleton structure is likely to form because of the generation of cementing agents CSH, which leads to the formation of coarser particles and restrains the swelling potential of stabilized soils (Osula 1996). Swell pressure of 48 kPa or less is considered a nonproblematic condition for the structures constructed on soil with a fly ash content of 10.2% (Chen 2012; Nelson and Miller 1997).

2.8 USE OF CONSTRUCTION DEMOLITION WASTE

During the renovation of megacities, the demolition of existing structures becomes inevitable. The generation of enormous construction waste is a serious issue from the disposal point of view. The proper reuse of construction waste is essential for sustainable construction to save waste disposal costs (Sivakumar et al. 2004). With the depleting natural (nonrenewable) resources due to continuous usage in construction, the employment of CDW from various resources is helpful from environmental concerns (Akhtar and Sarmah 2018). Investigations were undertaken to understand the feasibility of using CDW for various construction works. Many researchers appreciated the strength and durability improvements of concrete prepared with CDW (Collivignarelli et al. 2021; Reis et al. 2021).

In India, the estimated annual generation of CDW in 2019 is 3000 million tonnes (Jain et al. 2020). Various recycled aggregates such as crushed concrete, brick metal, concrete fines, etc., obtained from CDW were found suitable for pavement sub-base (Arulrajah et al. 2013). The recycled material obtained from collected CDW should be separated, cleaned, and crushed to obtain coarse and fine fractions. The cement mortar waste quantifies up to 25–30% from crushed concrete (Kien et al. 2013). Due to the massive quantity of CDW production, most of it is used for low or medium traffic volume road subgrade, and embankment works as a sustainable solution (Ossa et al. 2016). The use of fine CDW (<2 mm size) is effective in reducing the swelling of clays (Sekkel et al. 2020). The non-plastic nature of CDW is found advantageous for controlling the expansion and improving the bearing capacity of the soil (Jiménez et al. 2012). Larger fragments of non-moisture susceptible CDW used in the base layer enhanced UCS, CBR, stiffness, and resistance to FT cycles (Blankenagel and Guthrie 2006). The fine concrete fractions (<190μm) stabilized with 10 molar NaOH solution and Na_2SiO_3 solution resulted in compressive strength of 13 MPa on 7 days curing; further curing was not effective (Komnitsas et al. 2015). As per Komnitsas et al. 2015 and Yunsheng et al. 2007, the unreacted grains of CDW contribute to low polymerization product formations, thus resulting in low UCS values. Fine particles of set mortar were reactivated, but the involvement of inert sand particles is less in hydration.

2.9 DURABILITY

Durability is defined as the long-term capability of a material to resist varying climatic conditions by maintaining its integrity and stability (Dempsey and Thompson 1967). The durability of cement stabilized soils is an essential concern for pavement application. For instance, it is well-known that two-clayey soils with the same index properties subjected to moisture changes may exhibit different volumetric responses due to differences in clay mineralogy (Puppala et al. 2016). Therefore, strength loss and weathering are major problems associated with geotechnical structure when exposed to alternate wetting-drying (WD) or freezing-thawing (FT). The WD and FT tests are used to determine the stability of pavement material during different weather conditions. The CBR of a compacted soil depends predominantly on its compacted dry density, the suction of water, and the hysteretic nature of the soil-water characteristic curve and wetting-drying characteristics of subgrade material (Mirzaii and Negahban 2016).

The hydration reaction plays a crucial role in governing the durability of a stabilized material in the field (Kogbara 2014). The subfreezing temperature leads to the formation and accumulation of ice crystals in the various pavement layers. The succeeding warm season melts ice crystals and thaws pavement (Saberian and Li 2020). If an embankment constructed during the winter is frozen, the critical failure will begin when the ice melts and the soil thaws (De Guzman et al. 2018). FT cycles showed a detrimental effect on the stability of aggregate mixed Norway soils (Kværnø and Øygarden 2006). Stabilizing agents can improve the shear strength of frozen soil due to the absorption of water generated during ice melting (Fatehi et al. 2018; Ren and Hu 2014). For class F amended SM-cement and SM-lime mixes, strength gain was predominantly based on curing time, compaction energy, cement dosage, and water contents. The lime treatment could not provide the required strength for pavement bases; also, FT cycles are not detrimental to these cemented mixes (Arora and Aydilek 2005).

The shape of stress-strain curves of Tibet clay was not affected by the FT test, but the resilient modulus and failure strength were highly affected (Wang et al. 2007). In a previous study of the strength and permeability of landfill liner and cover systems prepared using silica fume, the effective resistance to the FT cycles was observed (Kalkan 2009). The expansive soil stabilized with 4 and 6% lime has improved durability to WD cycles (Ibrahaim et al. 2011). UCS of fiber-reinforced soils subjected to FT cycles increased with fiber content (Zaimoglu 2010). As cement and recycled gypsum content increased, stabilized soil durability has improved when tested for WD and FT cycles (Ahmed and Ugai 2011). The aging effect due to FT and water immersion can reduce the strength of stabilized soil. But, the type and dosage of a binder can significantly change the behaviour of stabilized soil. Small dosage class F fly ash is incapable of improving resistance to FT and water immersion. Cement behaves better than lime in improving UCS, but its strength loss coefficient is more than lime treatment after durability tests (Wang et al. 2018). A series of durability tests conducted on BC soil with CKD and quarry fines shows that a higher dosage of these stabilizers satisfies the durability criteria (Amadi 2014). Fine concrete waste geopolymer has retained low strength after 2 months of FT and immersion tests (Komnitsas et al. 2015). Also, depolymerization of the aluminosilicate matrix results in strength loss of stabilized material in extreme temperatures or due to water absorption on soaking (Komnitsas et al. 2015). Alkali-activated materials release water during curing enhances strength, whereas, water presence or absorption could induce strength loss (Rios et al. 2019; Xu and Van Deventer 2000).

2.10 SUMMARY OF LITERATURE

BC soil is a natural soil available in most of the regions on a larger area. The improvement of BC soil helps in enhancing the load-carrying capacity of a structure/ pavement. To reduce the carbon footprint, large-scale dumping problems, and construction cost, the partial replacement of industrial waste class F fly ash is inevitable. Only 32% of the fly ash is used for construction purposes, and the remaining quantity ends up in landfills. The dumping of fly ash pollutes the precious land and environment. Whereas, replacement of fly ash can control the swell-shrink of BC soil and reduce pollution. When fly ash is added more than 15 or 20%, it was found the swelling of BC soil is controlled.

Literature review reveals the use of OPC for soft soil stabilization to improve strength and control swell. A cement dosage of 10 to 16% was suggested as effective in enhancing the strength of BC soil. But, the suitable combinations of OPC and fly ash, the minimum required strength, and durability needs to be evaluated for use in pavement layers such as improved subgrade, CTSB, and CTB layers. Again natural coconut and arecanut fibers are abundantly available in coastal areas of the Konkan belt. It was revealed that various types of fibers with different optimum dosages can effectively control the crack propagation of stabilized soil.

Alkali activation of soil is a recent technology, which converts aluminosilicate-rich industrial wastes into binders. Many recent investigations showed excellent strength improvement of alkali-activated soil with industrial wastes such as low calcium fly ash, ground granulated blast furnace slag, etc. It is found that the optimum dosage of marginal materials may vary with the concentration of alkali solution. An 8 molar NaOH solution mixed with Na_2SiO_3 solution was found effective for strength improvement and is economically viable. Also, for soil stabilization, SS/SH ratios of 0.5 to 1.5 are found to be suitable. Studies conducted using various marginal materials like class F fly ash, coconut fibers, lime, and CDW resulted in improved engineering properties when blended with different binders.

As per IRC SP 72-2015, IRC 37-2018, the stabilized materials are recommended for use in improved/ modified subgrade, CTSB, and CTB layers of pavement. The stabilized material should attain minimum UCS, flexural strength, durability criteria along with fatigue life improvement for this purpose. This investigation was performed since limited studies were conducted on BC soil with marginal materials and binders for use in pavements.

CHAPTER 3

MATERIALS AND METHODS

3.1 WORK SCHEDULE

Research work includes details of the mix prepared, tests, and the use of selected mixes for pavements. The flow chart of scheduled work is depicted in Figure 3.1.

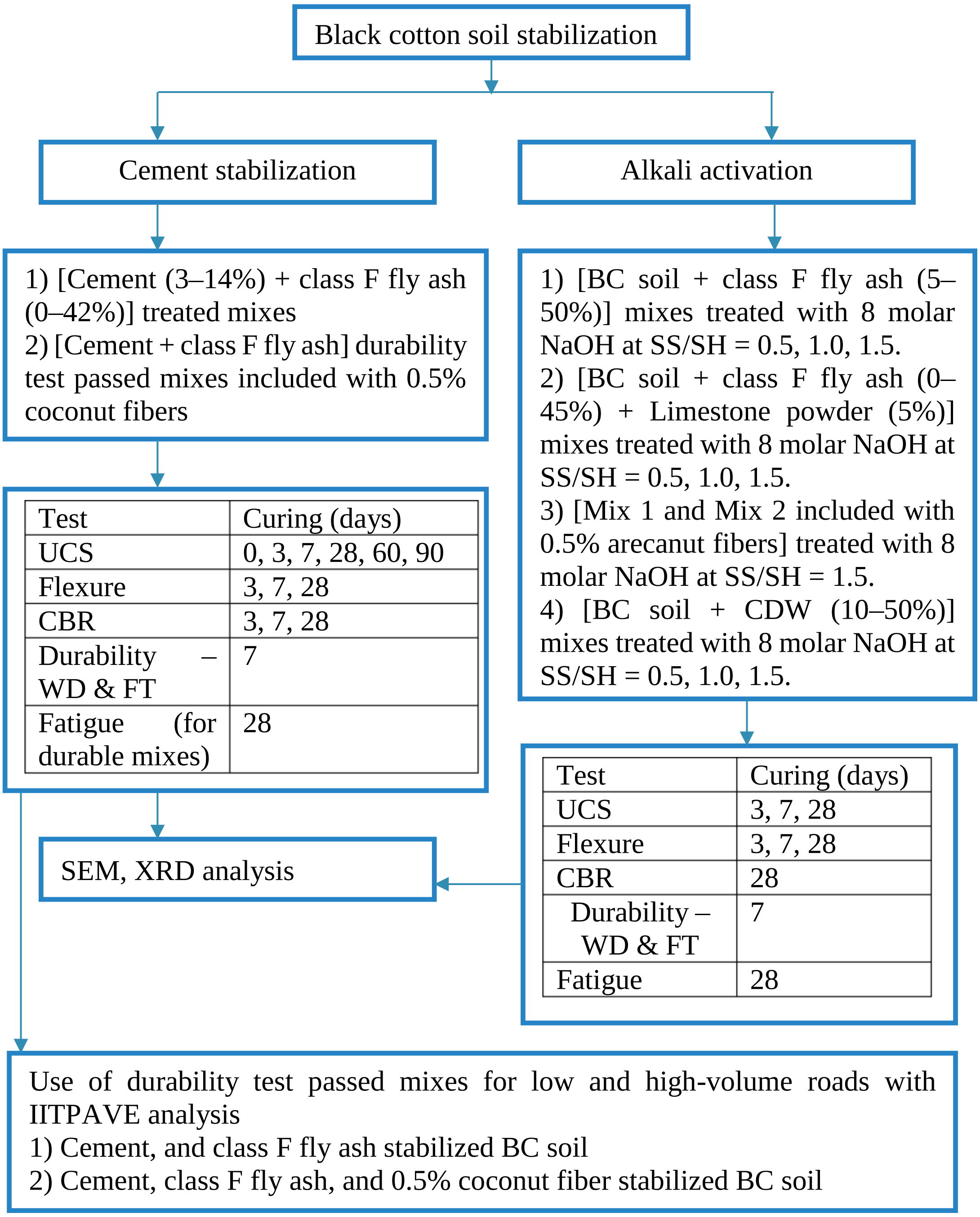

Figure 3. 1 Flow chart of experimental investigation

3.2 PRELIMINARY INVESTIGATION OF MATERIALS

This chapter describes details of experimental works carried in the laboratory. Preliminary investigations on constituent materials, mix preparation, synthesis of alkali solution, specimen preparation, and curing methods are discussed in detail. The materials such as Class F fly ash, limestone powder, CDW, coconut fibers, and arecanut fibers were used for stabilizing BC soil. Ordinary Portland cement (43 grade) and alkali solution (synthesized using NaOH and Na_2SiO_3) are used as binders.

3.2.1 Black Cotton Soil

Few roads in Chikmagalur district, Karnataka, India, built over BC soil, are having structural and functional problems due to seasonal variation of moisture in the subgrade, and hence, this soil was selected for the present investigation. A significant portion of this soil falls within the 75–2µm range. Therefore, it is classified as the silty soil of high compressibility (MH) as per IS 1498: 2016. The chemical properties of all the materials used in the investigation were identified as per the procedure given in the IS 2720 Part-25: 1982, by using titration methods. The physical and chemical properties of soil are tabulated in Tables 3.1 and 3.2, respectively. The grain size distribution was determined by mechanical wet sieving and hydrometer sedimentation analysis, and the results are depicted in Figure 3.2.

Table 3. 1 Index properties of BC soil

Properties	Test method	Average value
Specific gravity, G_s	(IS 2720-Part 3/Section-1: 2016)	2.56
Standard Proctor compaction MDD (g/cc) OMC (%)	(IS 2720-Part 7: 2016)	 1.64 22.2
Modified Proctor compaction MDD (g/cc) OMC (%)	(IS 2720-Part 8: 2015)	 1.85 16.0
Liquid limit (%)	(IS 2720-Part 5: 2015)	60
Plastic limit (%)		33
Plasticity index (%)		27
Shrinkage limit (%)	(IS 2720-Part 6: 2016)	23
Gravel (%)	(IS 2720-Part 4: 2015)	2
Sand (%)		26
Silt (%)		68
Clay (%)		4

Properties	Test method	Average value	
Free swell index (%)	(IS 2720-Part 40: 2016)	58	
Organic content (%)	(IS 1498: 2016)	2.25	
Indian standard soil classification		MH	
UCS (MPa) at Standard Proctor density Modified Proctor density	(IS 2720-Part 10: 2015)	 0.4 1.1	
CBR (%) at Standard Proctor density Modified Proctor density	(IS 2720-Part 16: 2016)	Unsoaked 8 12	Soaked 2 2

Table 3. 2 Chemical properties of BC soil

Properties	pH	SiO_2 (%)	Al_2O_3 (%)	Fe_2O_3 (%)	CaO (%)	SO_3 (%)	LOI (%)
Value	8.24	75.4	7.06	2.64	0.007	0.16	2.3

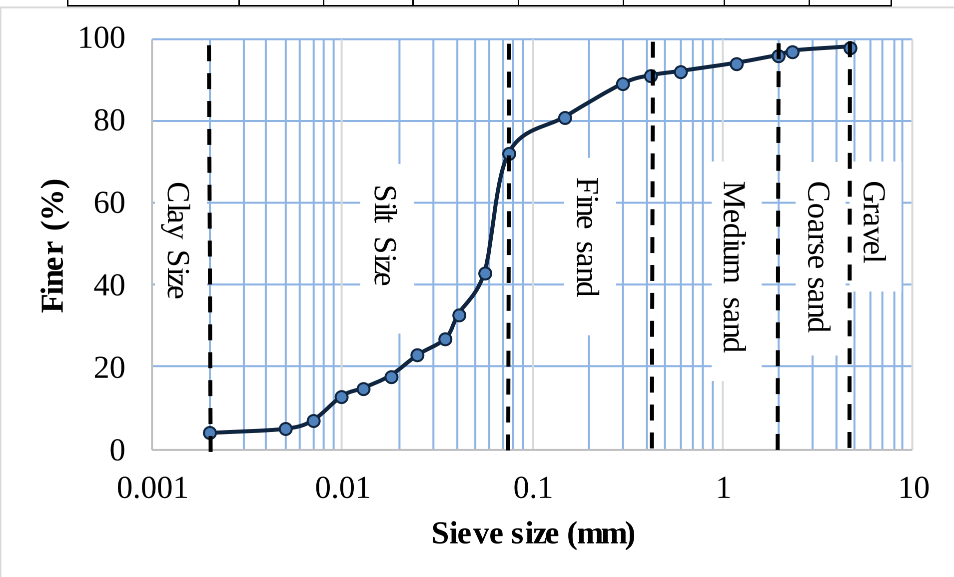

Figure 3. 2 Grain size distribution curve for BC soil

Figure 3.3 depicts the microstructure of the BC soil, which mainly consists of montmorillonite clay minerals. Undisturbed soil exhibits a flocculated structure due to clay mineral orientation by attractive forces. When compacted with water, face-to-edge orientation clay minerals change to face-to-face orientation, resulting in a dispersed structure.

Figure 3.4 depicts the diffractogram of the untreated BC soil. Peaks of silica are prominent in BC soil. Traces of titanium oxide impart black colour to the soil. Many peaks of montmorillonite are present, which strongly supports the water affinity of this soil. The crystalline minerals of BC soil also contain illite clay minerals at several d spacing's. These minerals indicate the susceptibility for the swell shrink behavior of soil. This soil consists of the major minerals such as [Q] Quartz (SiO_2), [H] Halite ($NaCl$), [K] Kuzminite (Hg_2Br_2), [C] Carlinite (Tl_2S), [M] Montmorillonite ($Na_{0.3}(Al, Mg)_2Si_4O_{10}(OH)_2{\cdot}8H_2O$), [I] Illite ($(K, H_3O)Al_2Si_3AlO_{10}(OH)_2$) with many other minerals in minor quantities.

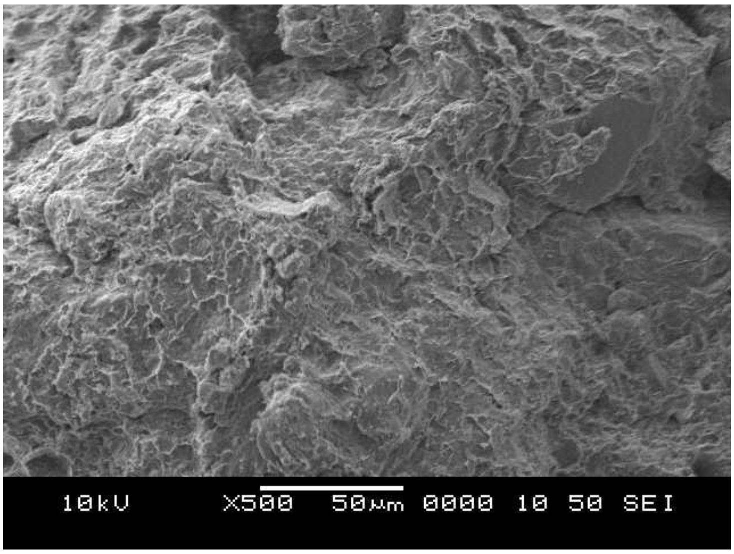

Figure 3. 3 SEM image of BC soil

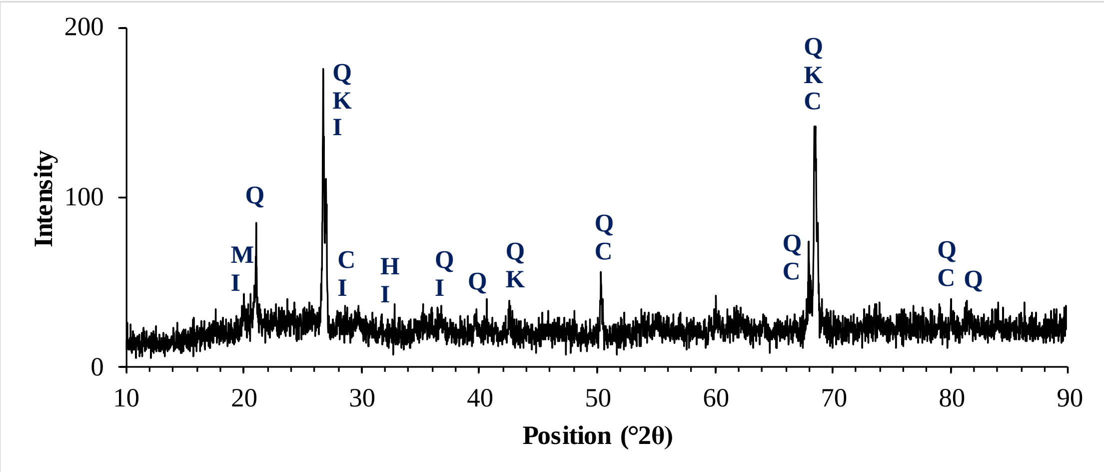

Figure 3. 4 XRD diffractogram of BC soil

Note:- For example, [Q] Quartz (SiO_2), where, [Q] is the symbol used for representation, Quartz is the compound name, and SiO_2 is the chemical formula.

3.2.2 Ordinary Portland Cement

Ordinary Portland cement (43 grade) confirming to IS 269: 2020 was used as a binder for the present investigation. The chemical properties of cement are tabulated in

Table 3.3. It has a specific gravity of 3.15. Initial and final setting times were 50 and 540 min, respectively. It is mainly composed of calcium silicate.

Table 3. 3 Chemical properties of ordinary Portland cement

Properties	pH	SiO_2 (%)	Al_2O_3 (%)	Fe_2O_3 (%)	CaO (%)	SO_3 (%)	LOI (%)
Value	11.8	20.27	5.32	3.56	60.41	0.2	1.5

Figure 3.5 depicts the presence of crystalline particles of cement. OPC consists of the following major minerals as depicted in Figure 3.6, [Q] Quartz, low (SiO_2), [G] Graphite (C), [T] Tellurobismuthite (Bi_2Te_3), [B] Bismuth Tellurium Oxide (Bi_2TeO_5), [C] Carlinite (Tl_2S), [Ca] Calcite ($CaCO_3$), [P] Potassium Magnesium Aluminum Silicate Hydroxide ($KMg_3(Si_3Al)O_{10}(OH)_2$), etc.

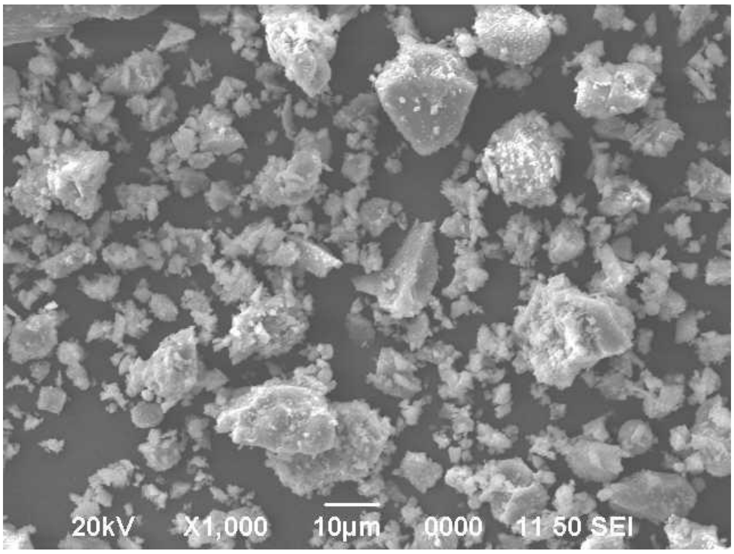

Figure 3. 5 SEM image of ordinary Portland cement

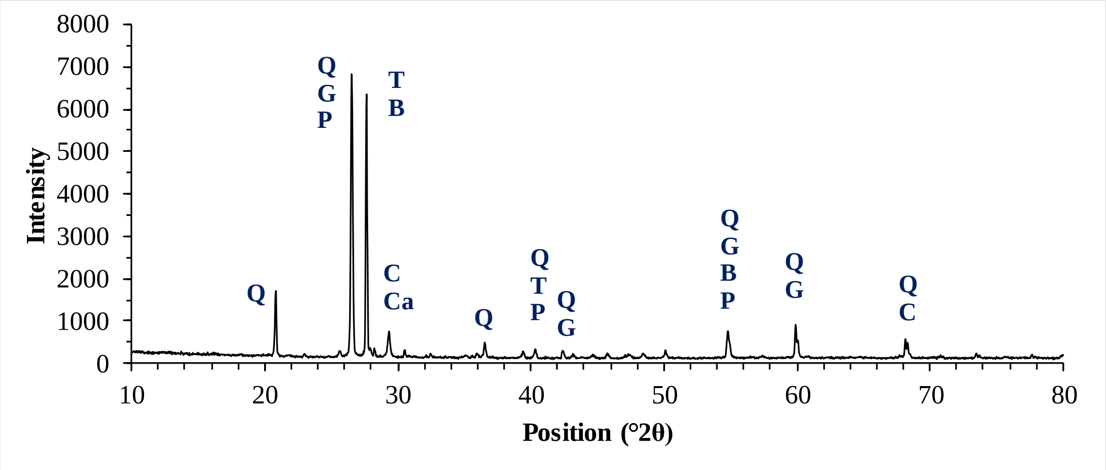

Figure 3. 6 XRD diffractogram of ordinary Portland cement

3.2.3 Class F Fly ash

M/s Udupi Thermal Corporation Ltd., Karnataka, India, uses coal to produce electricity. During this process, a substantial quantity of fly ash is produced. The major constituents of fly ash are ($SiO_2 + Al_2O_3 + Fe_2O_3$) >70%, as provided in Table 3.4. A negligible amount of CaO, i.e., 0.003% < 18%, is present in the fly ash. The material passing through 45µm IS sieve is 92%, which is >66%. It has a specific gravity of 2.25. According to ASTM C618-19: 2019, it satisfies Class F fly ash requirements. Globules of various sizes are present in the fly ash, as depicted in Figure 3.7. Oxides of various minerals are found in fly ash and are depicted in Figure 3.8. If properly activated, this material can be used for soil treatment (Yousuf et al. 2020), thereby reducing the disposal problem.

Table 3. 4 Chemical properties of class F fly ash

Properties	pH	SiO_2 (%)	Al_2O_3 (%)	Fe_2O_3 (%)	CaO (%)	SO_3 (%)	LOI (%)
Value	10.7	70.5	10.98	1.84	0.003	0.15	1.7

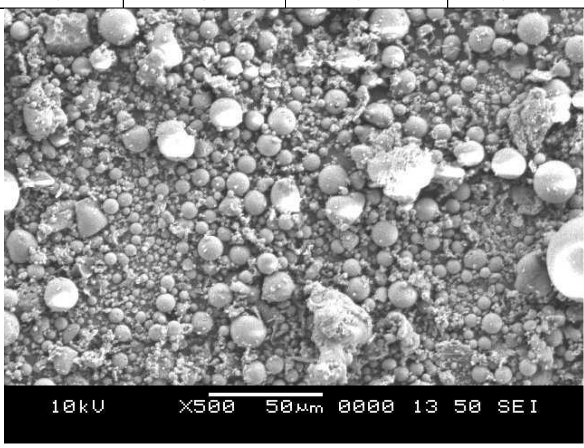

Figure 3. 7 SEM image of class F fly ash

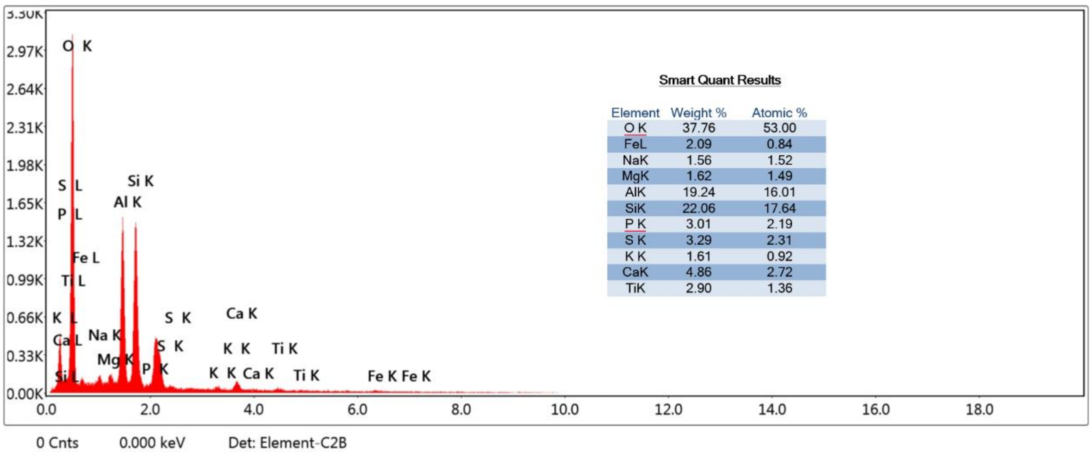

Figure 3. 8 EDAX plot of class F fly ash

3.2.4 Limestone Powder

To increase the calcium content in the mix, crystalline whitish limestone powder was used. Limestone powder is available as quicklime (CaO), hydrated lime ($Ca(OH)_2$), and calcite ($CaCO_3$) in the market. The collected limestone powder is mainly composed of $CaCO_3$ (93%). It has a specific gravity of 2.72, and its melting point is 1339 °C. It is denser than $Ca(OH)_2$ and lighter than CaO. By reacting with water, it dissociates into Ca^{2+} and CO_3^{2-} ions. It is commonly used in Portland cement production. This inorganic compound finds application in soil stabilization. It was stored in airtight plastic bags. Other minerals like silica, aluminium, iron, magnesium, etc., are also present. The collected limestone powder has rich calcium content, which may help develop calcium-based hydration products in an alkaline environment. The chemical properties of limestone powder are tabulated in Table 3.5.

Table 3. 5 Chemical properties of limestone powder

Properties	pH	SiO_2 (%)	Al_2O_3 (%)	Fe_2O_3 (%)	CaO (%)	MgO (%)	LOI (%)
Value	10	5.90	1.1	0.15	72.10	0.84	39.5

Limestone powder is available in very fine powder form with >90% passing 45μm IS sieve. The flocculated particle structure with several small-size pore spaces is observed as depicted in Figure 3.9. Common mineral phases found in limestone powder as depicted in Figure 3.10 are, [C] Calcite ($CaCO_3$), [Q] Quartz, low (SiO_2), [Ca] Carlinite (Tl_2S), [F] Iron (Fe), [I] Inyoite ($CaB_3O_3(OH)_5\cdot 4H_2O$), [N] Nitratine ($NaNO_3$), [G] Graphite (C), etc.

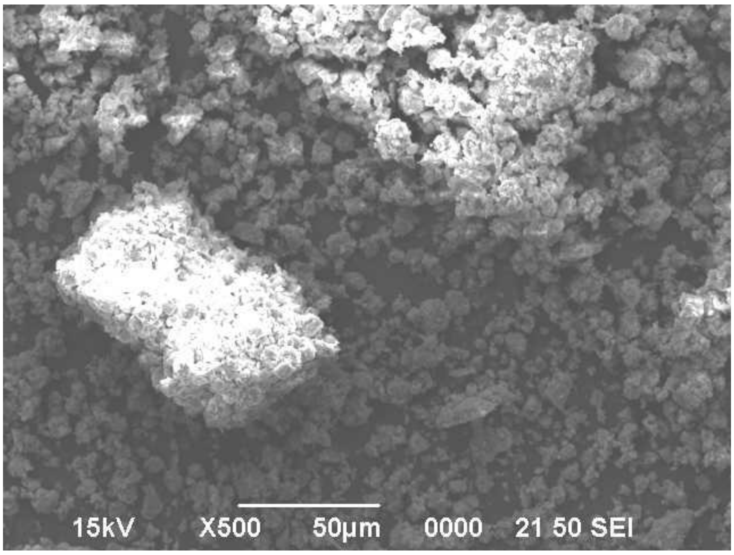

Figure 3. 9 SEM image of limestone powder

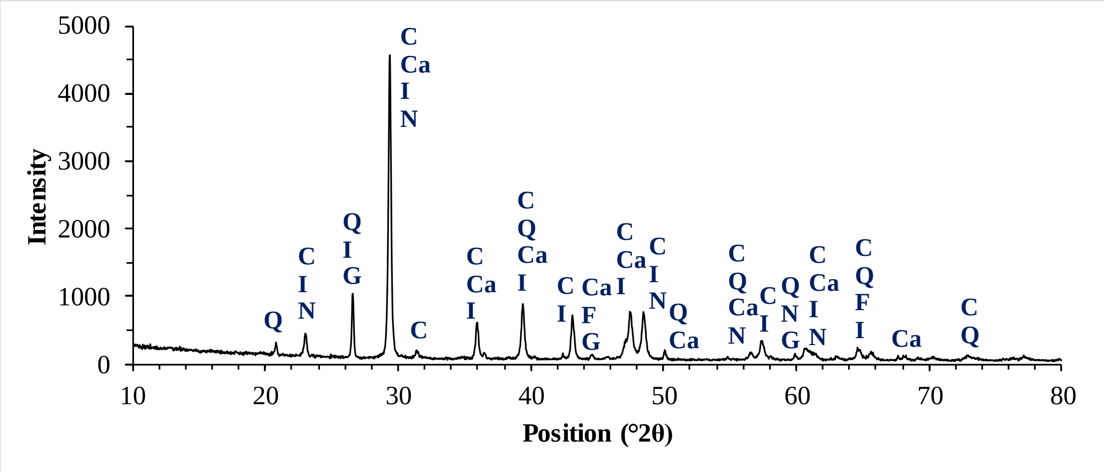

Figure 3. 10 XRD diffractogram of limestone powder

3.2.5 Construction Demolition Waste

The CDW was collected from a local building construction site located at NITK, Surathkal. Around 300 kg of material was collected for the study. It consists of mortar waste accumulated from excessive cutoffs, and broken pieces originating from plastering. All other waste types, such as concrete, masonry, polymers, glass, wood, etc., were removed manually to obtain a unique material. Mortar waste consists of a mixture of sand and cement used for plastering. It has a specific gravity of 2.45. Cemented lumps of this material were crushed before using for experiments. It satisfies the Zone II specifications of fine aggregates as per IS 383: 2016, and the results are tabulated in Table 3.6. Its grain size distribution curve is depicted in Figure 3.11. It is mainly composed of silica and small quantities of alumina and iron oxide. The demolished waste has a CaO content of 8.92%. The chemical properties of CDW are tabulated in Table 3.7.

Table 3. 6 Particle size distribution of CDW

Sieve size (mm)	Finer (%)	Grading specifications as per IS 383: 2016 for Zone II
10	100	100
4.75	92.5	90–100
2.36	77.5	75–100
1.18	56.5	55–90
0.6	38.7	35–59
0.3	26.8	8–30
0.15	9.8	0–10

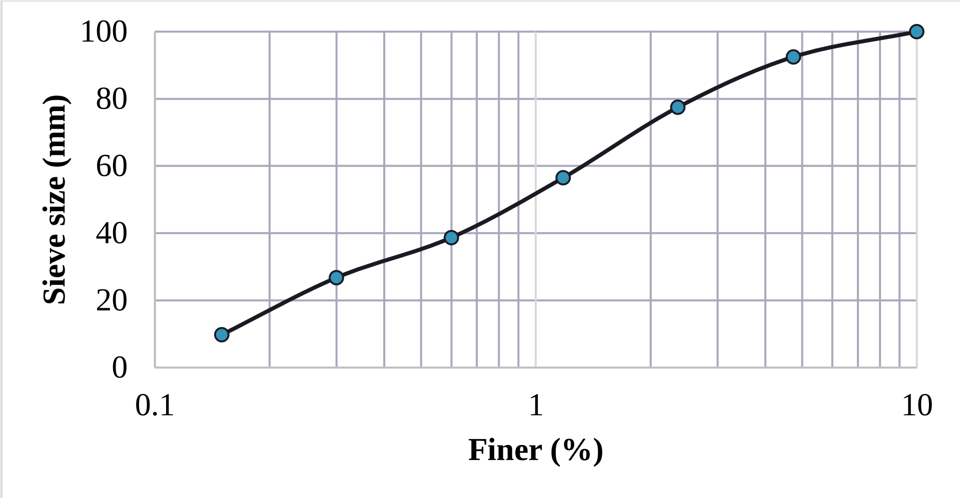

Figure 3. 11 Particle size distribution curve for CDW

Table 3. 7 Chemical properties of CDW

Properties		pH	SiO_2 (%)	Al_2O_3 (%)	Fe_2O_3 (%)	CaO (%)
Value		9.5	81.65	3.87	2.54	8.92
SO_3 (%)	Na_2O (%)	MnO (%)	MgO (%)	K_2O (%)	TiO_2 (%)	LOI (%)
0.54	0.17	0.14	0.69	0.32	0.45	2.38

The CDW precursor shows the hydration products formed due to the cement setting when used for plastering. Aggregation of particles due to the hydration process resulted in a crystalline structure, as depicted in Figure 3.12a. An enlarged SEM image of the CDW cluster shows the deposition of hydration products on the sand particle, as depicted in Figure 3.12b.

a)

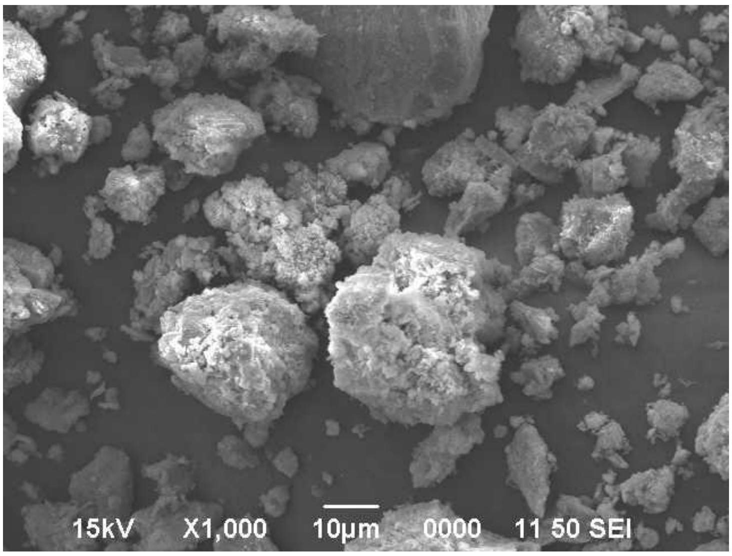

b) 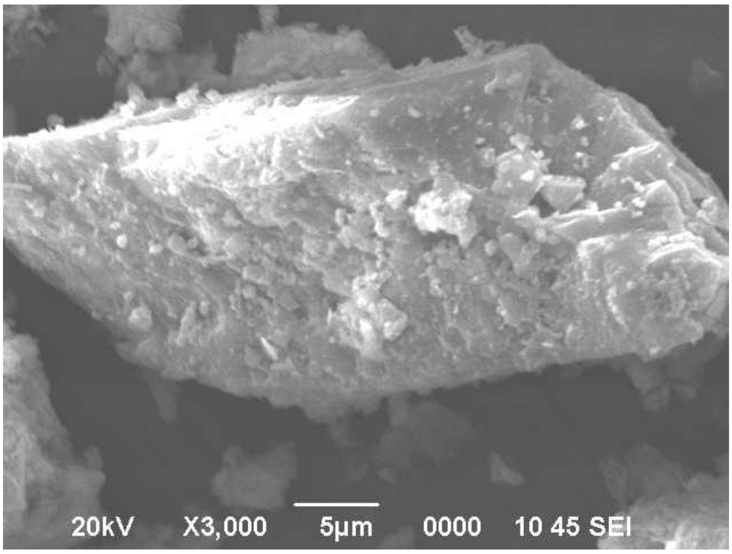

Figure 3. 12 SEM images of a) CDW particles b) Enlarged view of CDW particles showing hydration products

Common mineral phases found in CDW include hydration products and minerals as depicted in Figure 3.13 are, [C] Calcite ($CaCO_3$), [CS] Calcium Silicate (Ca_2SiO_4), [I] Iron Nickel Cobalt Arsenide ((Fe, Ni, Co)As), [L] Larnite (Ca_2SiO_4), [M] Manganese Sulfide ($Mn_{+2}S$), [P] Potassium Copper Chloride Sulfate ($K_2CuSO_4Cl_2$), [T] Thallium Sulfide (Tl_2S), etc.

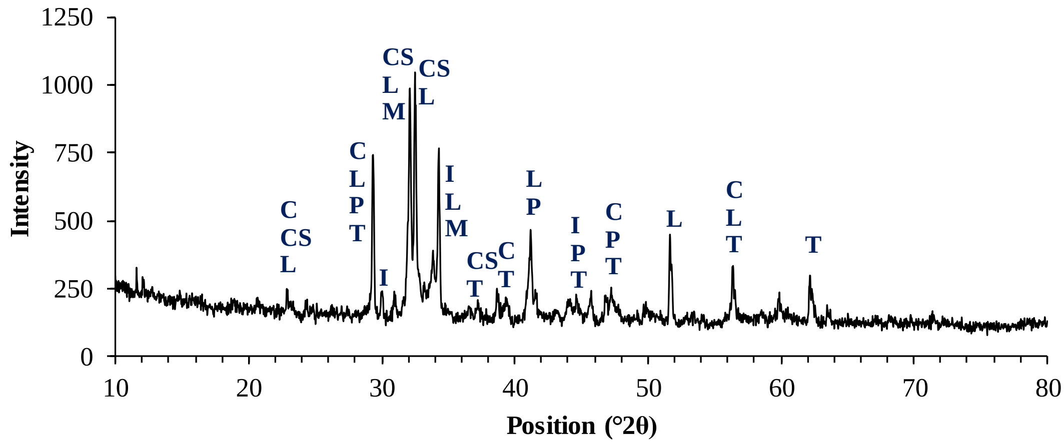

Figure 3. 13 XRD diffractogram of CDW

3.2.6 Coconut Fiber

Coconut fiber is natural and organic (Figure 3.14). It is extracted from coconut husk available in all parts of southern Indian states. Fibers of average diameter 0.45 mm were cut to 25 mm length to obtain an aspect ratio of 55. The typical properties of coconut fiber obtained from the same source are presented in Table 3.8. Coir fibers have competitive advantages over other natural fibers, such as low cost, low density, higher elongation at break, and lower elastic modulus. Wet coconut fiber exhibit better tensile strength with high breaking stress compared to other natural fibers. A high lignin content reduces its degradation rate.

Figure 3. 14 Coconut fibers

Table 3. 8 Physical and chemical properties of coconut fibers (Sudhakaran Pillai and Vasudev 2001)

Length (mm)	Diameter (mm)	Density (g/cc)	Lignin (%)	Cellulose (%)	Breaking elongation (%)	Tensile strength (N/mm^2)
100–300	0.25–0.65	1.4	45	43.5	32	60–130

3.2.7 Arecanut Fiber

The dry shells of mature arecanut were collected from Puttur, Dakshina Kannada, India (Figure 3.15). It belongs to the species Areca catechu linnaeus under the family palmecea, which originated in the Malaya peninsula, East India. Arecanut trees yield commercially important products like nuts, fiber, and oil. The arecanut husk is a hard, fibrous material covering the endosperm, and it constitutes about 60–80% of the total weight and volume of the areca fruit. The dry arecanut shell has a brown colour. Manually extracted arecanut fibers of average diameter 0.35 mm were cut to 25 mm length to obtain an aspect ratio of 70. These fibers have a specific gravity of 0.67. The properties of arecanut fiber used from the same source by Lekha et al. 2015 are tabulated in Tables 3.9 and 3.10. The arecanut fiber has better tensile strength, which can restrict the crack development in soil. Also, its degradation rate is low due to its high lignin content.

Figure 3. 15 Arecanut fibers

Table 3. 9 Physical properties of arecanut fiber (Lekha et al. 2015)

Diameter (mm)	Length (mm)	Density (g/cc)	Young's modulus (kN/m^2)	Tensile strength (kN/m^2)
0.35	50	1.09	27×10^6	2.2

Table 3. 10 Chemical properties of arecanut fiber (Lekha et al. 2015)

Cellulose (%)	Hemicellulose (%)	Lignin (%)	Ash (%)	Pectin (%)	Wax (%)
Nil	35–64.8	13–24.8	4.4	Nil	Nil

3.2.8 Linseed Oil

Commercially available linseed oil was used for the pretreatment of coconut and arecanut fibers. During the solvent extraction process, from the dried seeds of the flax plant, a colorless to yellowish liquid, i.e., linseed oil, is obtained. It is commonly used as a varnish for woods due to its polymer-forming properties. After drying this oil, a hydrophobic (water repellent) hydrocarbon-based material is formed. It is used for coating wood, cricket bats, etc., to enhance lifespan.

3.2.9 Sodium Hydroxide

Sodium hydroxide (or caustic soda) is available in the flakes form. It is a white crystalline odorless solid with 97% purity, and it is corrosive. On exposure to the air moisture, these flakes react; hence, they are stored in airtight containers. Its molecular weight is 39.997 g/mol.

3.2.10 Sodium Silicate

Sodium silicate is available in a viscous liquid form. It is composed of 55.9% water, 29.4% SiO_2, and 14.70% Na_2O.

3.3 METHODOLOGY OF INVESTIGATION

3.3.1 Mix Preparation

Air dehydrated BC soil was oven-dried at 105–115 °C for 24 h and cooled to room temperature. Soil lumps were broken using a rubber mallet. It contains a significant amount of sand, silt, and clay particles (i.e.,> 98%); hence, the soil passing through a 4.75 mm IS sieve was used for sample preparation. Precalculated quantity of materials like cement and fly ash or fly ash and limestone powder was blended properly on a weight basis. These mixes were properly blended with powdered dry BC soil. Potable water or alkali solution of quantity equivalent to OMC was added to this dry mix and blended until a homogeneous mixture was obtained. The prepared mixes were immediately moulded for different tests as per requirement and as suggested by various IS codes.

3.3.2 Alkali Solution Preparation

The desired concentration of 8 molar NaOH solution was initially prepared by dissolving 320 g of NaOH pellets in 1 liter of distilled water. The exothermic reaction of NaOH flakes liberates enormous heat when reacted with water, and hence, proper care has to be taken to handle it. It is allowed to cool down before mixing with Na_2SiO_3 solution. The alkali solution was prepared by mixing NaOH and Na_2SiO_3 solutions of calculated quantities to achieve SS/SH ratios of 0.5, 1.0, and 1.5.

A maximum SS/SH ratio of 1.5 was suggested by Murmu et al. 2019 based on strength gain and economy. Therefore, for the complete investigation, a ratio beyond 1.5 was not considered. Based on Rios et al. 2019, the integrated analysis of the mixture with a 7.5 molar concentration gives better strength at less cost. Whereas the lower concentration of 5 molar gives poor strength, and the higher concentrations of 10 and 12.5 molar increase the cost. A concentration >10 molar produces high pH, which delays polymerization and reduces initial strength.

The procedure for calculating NaOH and Na_2SiO_3 contents required to prepare the alkali solution is as follows:

Consider an 8 molar NaOH solution with an SS/SH ratio of 1.5.

SS/SH = 1.5 => SS = 1.5SH

Alkali solution = Quantity equl to OMC = SS+SH = 30g

30 = 1.5SH+SH => SH =30/2.5 => SH = 12g

SS = 30-12 = 18g

Molarity = Number of moles of solute per liter solution

Molecular weight of NaOH = 40 g/mol

Molarity = (NaOH flakes/molecular weight of NaOH)

For 1 liter of 8 molar solution, the weight of NaOH pellets required = 8×40 = 320g

Therefore, for 12g NaOH solution, weight of NaOH pellets required = (12×320)/1000 = 3.84g

Therefore, 3.84g of NaOH flakes dissolved in distilled water makes 12g of 8 molar NaOH solution and mixed with 18g of Na_2SiO_3 solution to prepare 30g of alkali solution.

3.3.3 Fiber Pretreatment with Linseed Oil

Initially, the arecanut shells were immersed in water for 15 days. Only coarser fibers were extracted from the shells. The pretreatment of coconut and arecanut fibers was done to minimize the decomposition under seasonal variations when stabilized with soil. Linseed oil of quantity equal to 0.6 times the dry weight of fibers was added and mixed homogeneously. It was allowed to dry for 30 min at room temperature of 29±1 °C. Then fibers were oven-dried for 2 h at 120 °C. As per Tan et al. 2019, this process gives a rougher morphology to the fiber surface, which improves the interaction between the fiber surface and treated soil.

3.3.4 Compaction Test

Standard and modified Proctor compaction tests were conducted following the procedure given in IS codes to determine the maximum dry density (MDD) and optimum moisture content (OMC) of soil with different stabilizer dosages. For the standard Proctor test, soil mix is compacted in 3 layers by giving 25 blow/ layer with a rammer of weight 2.5 kg. Whereas, for modified Proctor, the compaction is done in 5 layers by giving 25 blow/ layer with a rammer of weight 4.89 kg. The compaction test was done immediately after mix preparation.

3.3.5 Unconfined Compressive Strength Test

UCS specimens of stabilized mixes were prepared in a steel mould of 38 mm diameter and 76 mm height using a static compaction method to attain MDD values obtained from compaction. A compressive load is applied slowly using a hydraulic plunger and retained for 1 minute to ensure the compact packing of particles. Then the specimens were extracted using a hydraulic plunger. Cement-treated specimens were kept in a desiccator for curing. After 0, 3, 7, 28, 60, and 90 days of curing, the specimens were taken out from the desiccator, the weight and dimensions were measured to monitor changes in MDD. Whereas, the alkali-activated specimens cured at ambient (room) temperature were tested after 3, 7, and 28 days. Compressive loading is applied to evaluate UCS as depicted in Figure 3.16. The failure pattern of the specimens was visually observed.

Figure 3. 16 UCS test

3.3.6 Flexure Test

The flexure test is performed by following ASTM D1635/D1635M-19: 2012. Beams of dimension (breadth×depth×length) 76×76×290 mm were prepared at MDD. The third point loading method was used for determining the flexure strength of specimens. Bearing blocks shall ensure that forces applied to the beam will be vertical only without any eccentricity. While testing, the specimens were turned on their side, considering their moulded position, and centered on the lower half-round steel supports, which were placed apart at a distance of three times the beam depth. Stabilized beam specimens were tested after 3, 7, and 28 days of curing. The flexure test setup is depicted in Figure 3.17.

Figure 3. 17 Flexure test

Flexural strength is calculated as follows:-

If the fracture occurs in the middle third of span length

$$R = \frac{l \times (P + 0.75W)}{b \times d^2} \qquad \text{................ (3.1)}$$

If the fracture occurs outside of the middle span, not more than 5% of the span length

$$R = \frac{3 \times P \times a}{b \times d^2} \qquad \text{..................... (3.2)}$$

where,

R = flexural strength (modulus of rupture) in kg/cm^2

l = length of span in cm

W = weight of the beam after curing in kg

P = maximum applied load in kg

b = width of the beam in cm

d = depth of the beam in cm

a = distance between the line of fracture and nearest support measured along the centerline of the bottom surface of beams in cm

3.3.7 CBR test

CBR specimens cured at room temperature for 28 days were tested for plunger penetration resistance. Further, on 4 days of soaking, CBR depletion was evaluated. Alkali activated samples were cured at room temperature (35–40 °C). Whereas, cement-treated samples were covered with a moist cloth to favour hydration. A strain rate of 1.2 mm/min was adopted for the test. After the specified curing period, the change in weight and dimensions was noted to evaluate the achieved density and visually inspected for the signs of shrinkage cracks.

Figure 3. 18 CBR test

The average CBR of specimens is calculated as,

$$\text{CBR} = \frac{\text{Load sustained by stabilized soil at 2.5 mm penetration}}{\text{Load sustained by standard aggregates at 2.5 mm penetration}} \quad \ldots\ldots\ldots (3.3)$$

3.3.8 Fatigue Test

Fatigue life is defined as the number of repetitions a stabilized material can withstand at the specified load stress. Due to the repeated application of wheel loads, the pavement layers will be continuously stressed. The repetition will also accumulate the strain in the pavement layer, and eventually, its lifespan is reduced. After a certain number of repeated load applications, the pavement layer may develop microcracks. These cracks will develop in length and width and convert into macrocracks. Such a cracked pavement layer will undergo catastrophic failure. To evaluate this behaviour, repeated loads were applied using a fatigue machine. At a frequency of 1 Hz and a rest period of 0.1 seconds, a constant load less than UCS was applied to the UCS specimen cured for 28 days. The fraction of load was calculated as the ratio between applied load to the UCS of the specimen. Fraction of load of 0.5, 0.35, and 0.2 are considered for the study. Testing is continued until the failure of the specimen. The type of failure, such as plastic, brittle, or due to the debonding of fibers, is noted. The fatigue loading test setup is depicted in Figure 3.18.

Figure 3. 19 Fatigue test setup

Fatigue machine consists following units:-

a) A loading frame to place the UCS specimen,

b) Load cell to apply the required repeated load,

c) LVDT's to measure the accumulated deformation,

d) A control unit with dedicated software to control the repeated loading operation by inputting the necessary information such as frequency of loading, rest period, waveform type, etc. It records the fatigue data output.

3.3.9 Durability Tests

For durability tests, 7 days cured UCS specimens were used. Each specimen's diameter, height, and weight were recorded after curing and after the completion of each durability cycle. The retained UCS and corresponding moisture content of durability-test passed samples were evaluated at the end.

3.3.9.1 Wetting-Drying and Freezing-Thawing Tests

In the wetting-drying test (ASTM D559/D559M-15: 2015), the specimens were immersed in water for 5 h to complete the first wetting cycle. Then, they were dried in a temperature-controlled oven at 71 ± 3 °C for 42 h to complete the first drying cycle.

In the freezing-thawing test (ASTM D560/D560M-16: 2016), the specimens were covered in water-saturated felt pads and frozen at < -23 °C for 24 h to complete the first freezing cycle. Then, they were thawed at 23 ± 2 °C for 23 h to complete the first thawing cycle. One set of specimens was brushed after the completion of drying and thawing cycles. Another set of unbrushed specimens acts as control samples. The testing was continued until failure or completion of 12 cycles. The weight, diameter, and height were recorded after each cycle to calculate water content variation, volume expansion or shrinkage, and soil loss.

a) Soaking of specimens in water

b) Drying of specimens in oven

c) Frozen specimens

d) Thawed specimens

e) Brushing of specimen

Figure 3. 20 WD and FT test

3.3.10 Microstructural Analysis

3.3.10.1 SEM Analysis

Hitachi S-520 Scanning Electron Microscope (SEM), with a voltage of 20 kV applied across the tungsten filament electron gun, was used to examine the textural characteristics or morphological changes of various materials. A thin layer of gold coating was applied to the powdered sample and held in position by a brass sample holder, and tested.

3.3.10.2 XRD Analysis

Bruker D8 advance X-Ray Powder Diffractometer with CuKα radiation, with a 2θ configuration, was used to examine the X-ray Diffraction (XRD) of powder samples of various materials. XRD analysis was carried out to find the composition of raw and stabilized materials. At a step size of 0.02°/s, angular scans ranging from 10–90° were performed at a laboratory temperature of 20 °C. The patterns obtained were analyzed using International Centre for Diffraction Data Powder Diffraction File (ICDD PDF).

3.4 PAVEMENT ANALYSIS

A typical flexible pavement is composed of numerous layers. Each layer is assumed to be homogeneous, isotropic, and continuous. The lowest layer extends semi-infinitely in the vertical direction. During wheel load application, all the layers will be subjected to stresses and strains. The bottom of the lower bituminous layer will be subjected to the highest tensile strain. Whereas, the highest compressive strain will occur at the top of the subgrade. Also, if a cement-treated base is used, it is to be analyzed for critical tensile strain at the bottommost fiber. These critical stresses and strains were calculated exactly below wheel load application. Manually it is a time-consuming process to evaluate these values. A modified version of FPAVE software (1997) was developed by IIT Kharagpur for pavement analysis (Das and Pandey 1999). IRC 37: 2018 has developed IITPAVE software for the design of flexible pavements. For different traffic categories 10–50 msa catered during the lifespan of the pavement, this program can be used to analyze the stresses and strains. Inputs, such as the number of layers, layer thickness, Poisson's ratio, resilient modulus, wheel load, tyre pressure, type of wheel assembly, are fed in the software to get the output.

3.5 SUMMARY

In this chapter, the properties of the materials like BC soil, class F fly ash, OPC, limestone powder, CDW, coconut fibers, arecanut fibers, NaOH, and Na_2SiO_3 are discussed. The methodology adopted for various tests is discussed in detail. The UCS, flexural strength, CBR, fatigue, durability tests, and microstructural analysis for stabilized soil are discussed in detail. The alkali solution dosage calculation and preparation procedure are also discussed.

CHAPTER 4
CEMENT STABILIZED BLACK COTTON SOIL WITH MARGINAL MATERIALS

4.1 GENERAL

In this chapter, laboratory evaluation of BC soil stabilized with ordinary Portland cement (43 grade), class F fly ash, and coconut fibers are discussed in detail. The cement dosage varied from 3 to 14%. For cement-fly ash (class F) combined mixes, the cement from 3 to 14% and fly ash from 5 to 42 % were added. Standard Proctor compaction tests were conducted on all combinations of mixes. The strength of stabilized mixes was evaluated by performing UCS tests on 0, 3, 7, 28, 60, and 90 days curing. Further, mix combinations were selected for pavement layers based on durability test results. The specimens that exhibited weight loss less than equal to 14% as recommended by IRC SP-72: 2015, IRC 37: 2018, ASTM D 559: 2015, and ASTM D 560: 2016 under both WD and FT tests are considered for pavement applications. In the second phase, only on the durability test passed mixes, tests were conducted for modified Proctor, CBR, flexural strength, and fatigue. These mixes are further strengthened by adding coconut fibers. Again on these samples, Proctor, CBR, flexure, and fatigue tests were conducted to find the enhanced properties in terms of strength.

4.2 BC SOIL STABILIZATION WITH CEMENT AND CLASS F FLY ASH

4.2.1 Compaction

Cement-treated mixes at standard Proctor:- In low-volume roads, the subgrade is compacted to standard Proctor density as per the rural road manual IRC SP-72: 2015 when standard axle load repetitions are < 2 msa. The soil is replaced with 3 to 14% cement, and the Proctor compaction test was conducted. At 10% cement replacement, the mix obtained a maximum density of 1.69 g/cc with 17.6% OMC. Further, with an increase in cement content, the MDD values started reducing. Up to 10% cement, there is flocculation of silt and clay particles and beyond lower packing of particles with less dispersed structure. The BC soil and cement absorb more water, and hence the OMC increases. The test results are depicted in Figure 4.1. As per Yang et al. 2020, in cement-treated silty sand, the moisture consumption by the hydration process depends on cement percentage. The higher cement content yields to increase in OMC.

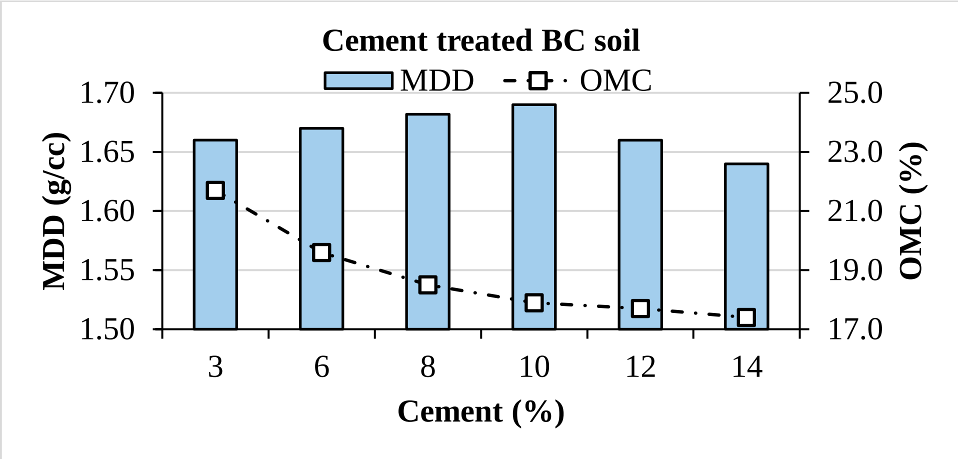

Figure 4. 1 Standard Proctor test results for cement-treated BC soil

Cement and fly ash treated soil at standard Proctor:- Standard Proctor tests were conducted on mixes with 3 to 7% cement, at a combined dosage of cement and fly ash ≤35%, and on the mixes with 8 to 14% cement, at a combined dosage of cement and fly ash up to 50%. In these mixes, as the percentage of cement and fly ash increases, the density decreases. This is quite obvious due to the replacement more quantity of lighter material fly ash. The maximum MDD of 1.73g/cc with 18.3% OMC was obtained for the mix with 4% fly ash and 6% cement, as depicted in Figure 4.2(a–i). According to Durante Ingunza et al. 2015, the usage of sludge ash with cement for low compressible silt reduced MDD. Due to the hydrophilic nature of cement, the increased dosage caused a marginal increase in OMC. Therefore, the OMC of soil-cement mixes depends on the properties of soil and the cement content. For soil-cement-fly ash mixes, OMC variations followed the concave trend.

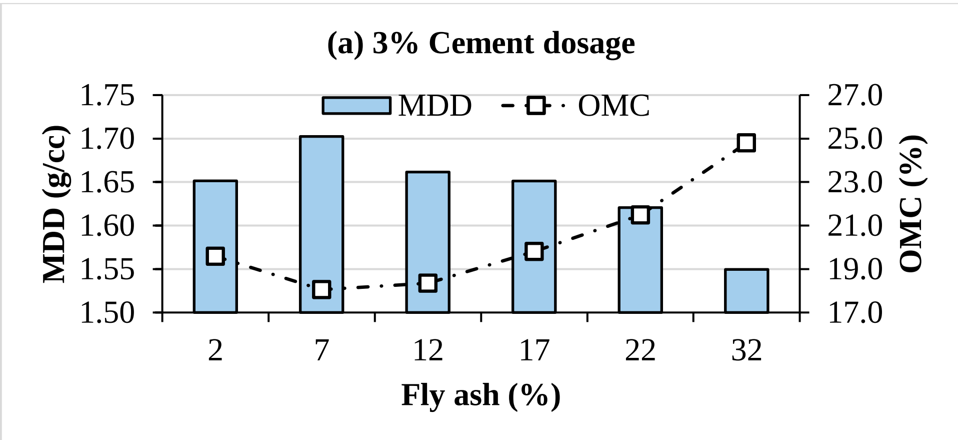

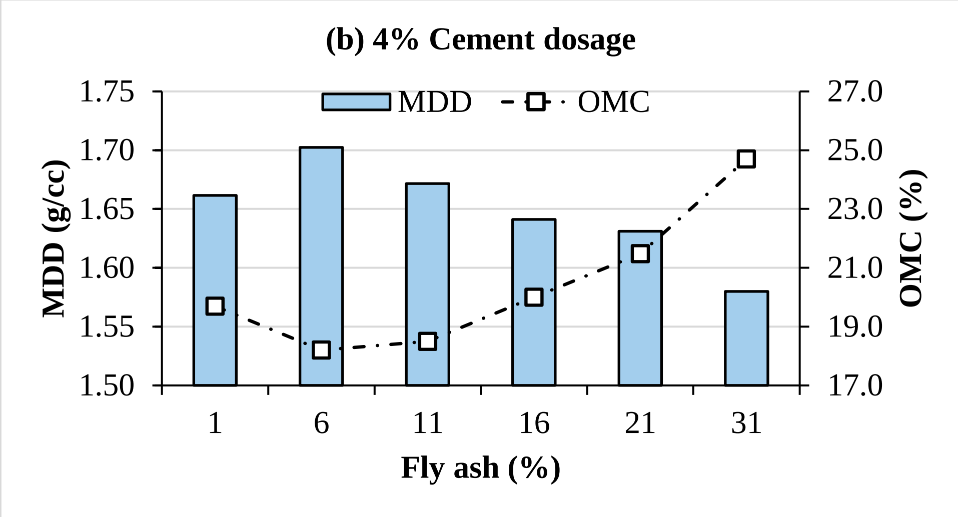
(b) 4% Cement dosage
MDD
OMC
MDD (g/cc)
1.75
1.70
1.65
1.60
1.55
1.50
OMC (%)
27.0
25.0
23.0
21.0
19.0
17.0
1
6
11
16
21
31
Fly ash (%)

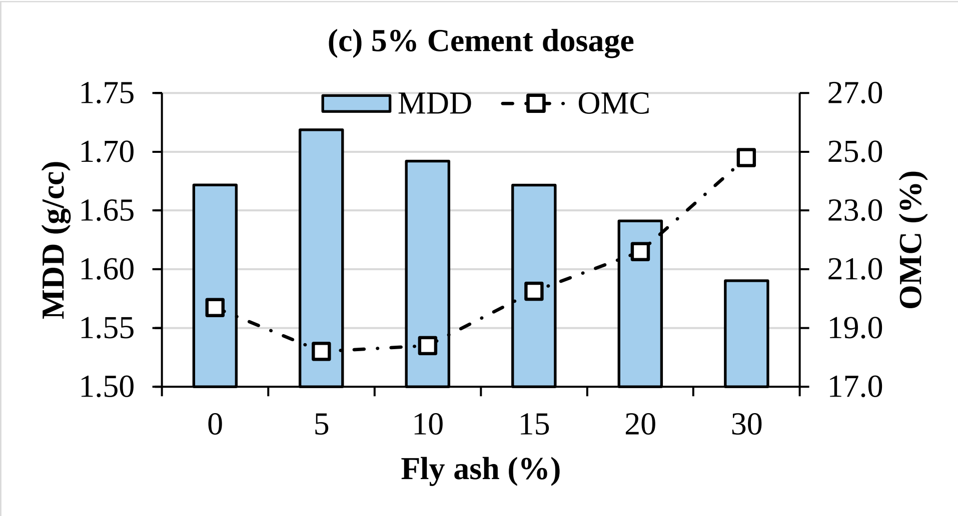
(c) 5% Cement dosage
MDD
OMC
MDD (g/cc)
1.75
1.70
1.65
1.60
1.55
1.50
OMC (%)
27.0
25.0
23.0
21.0
19.0
17.0
0
5
10
15
20
30
Fly ash (%)

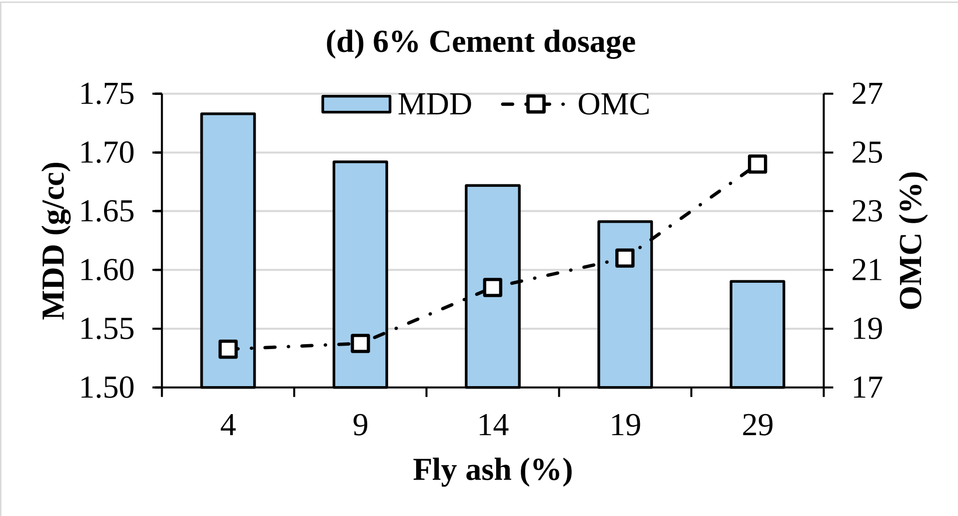
(d) 6% Cement dosage
MDD
OMC
MDD (g/cc)
1.75
1.70
1.65
1.60
1.55
1.50
OMC (%)
27
25
23
21
19
17
4
9
14
19
29
Fly ash (%)

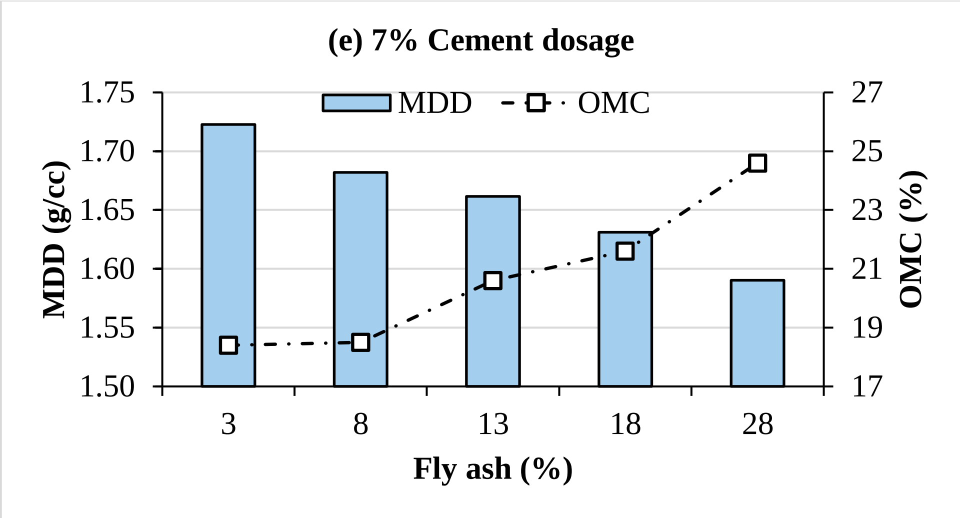
(e) 7% Cement dosage
MDD
OMC
1.75
1.70
1.65
1.60
1.55
1.50
27
25
23
21
19
17
MDD (g/cc)
OMC (%)
3
8
13
18
28
Fly ash (%)

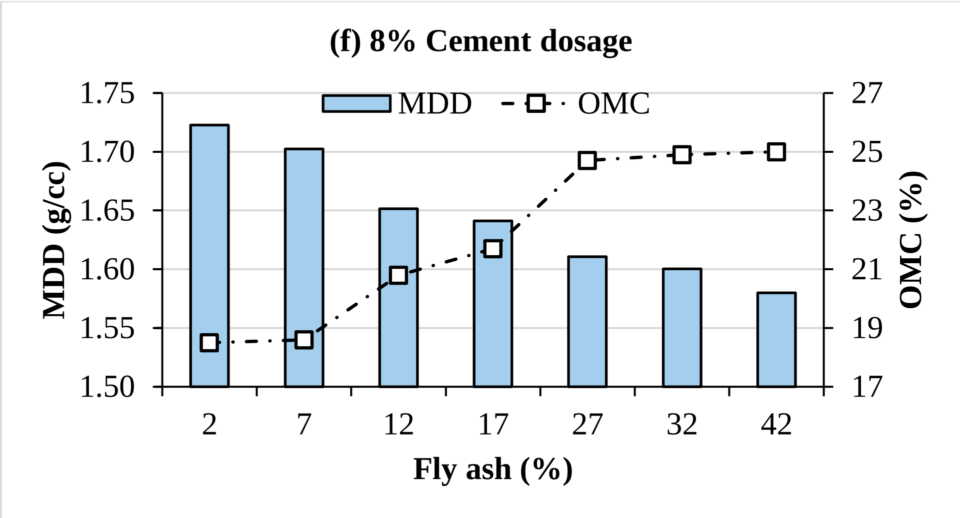
(f) 8% Cement dosage
MDD
OMC
1.75
1.70
1.65
1.60
1.55
1.50
27
25
23
21
19
17
MDD (g/cc)
OMC (%)
2
7
12
17
27
32
42
Fly ash (%)

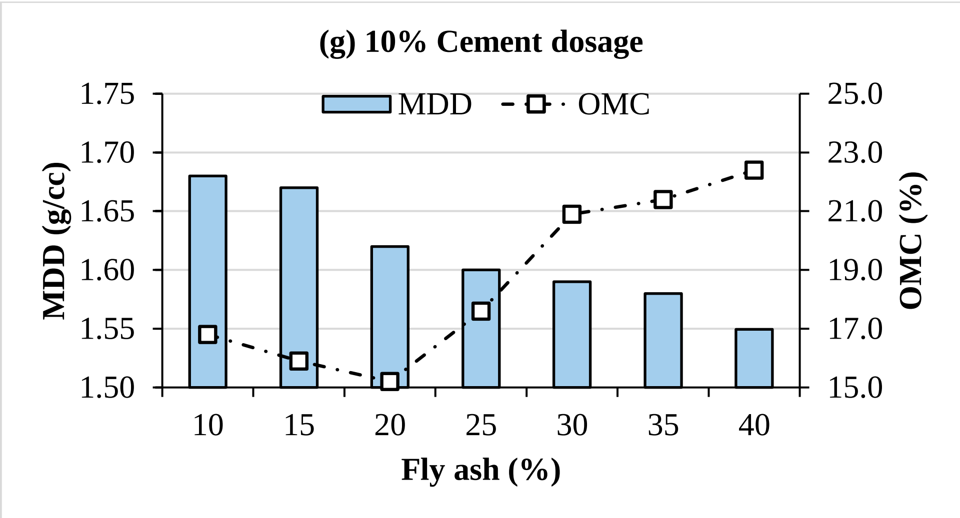
(g) 10% Cement dosage
MDD
OMC
1.75
1.70
1.65
1.60
1.55
1.50
25.0
23.0
21.0
19.0
17.0
15.0
MDD (g/cc)
OMC (%)
10
15
20
25
30
35
40
Fly ash (%)

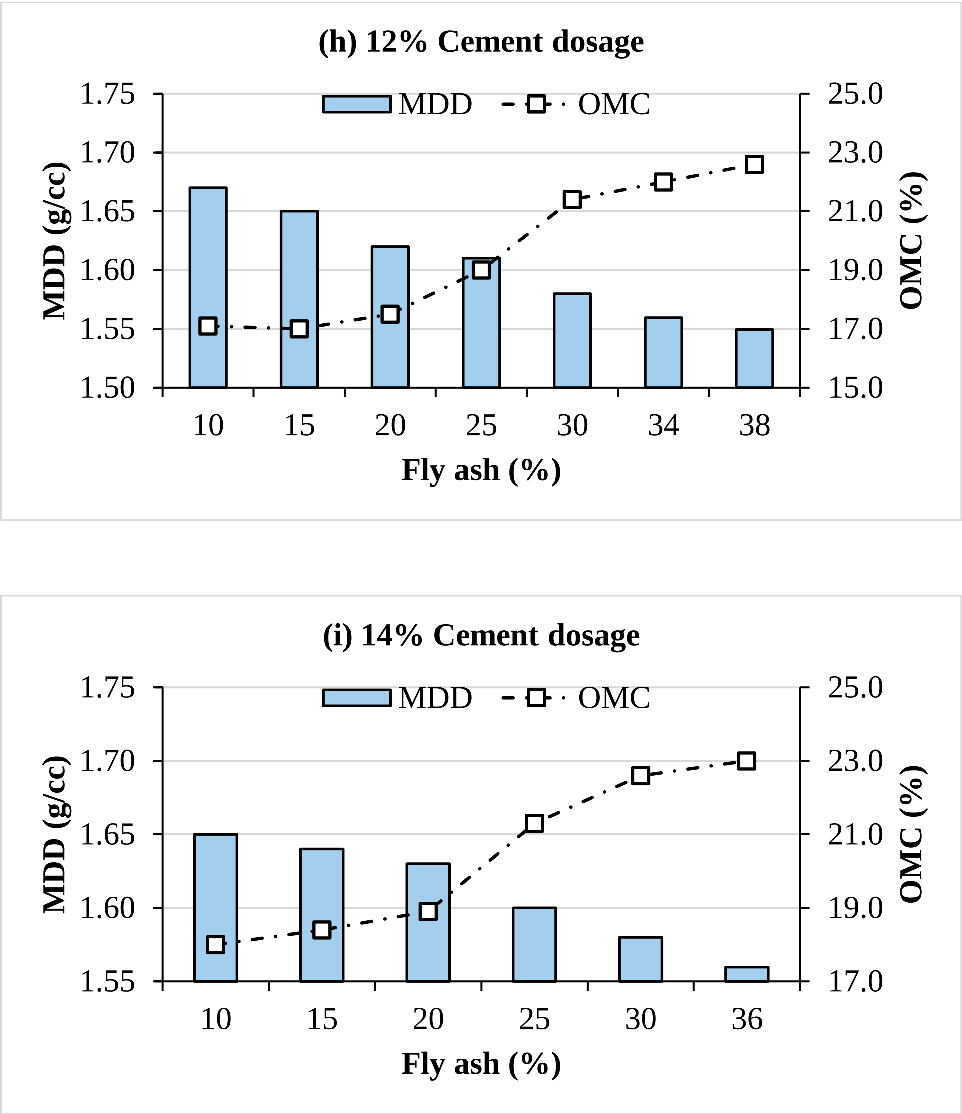

Figure 4. 2 Standard Proctor test results for (a) 3, (b) 4, (c) 5, (d) 6, (e) 7, (f) 8, (g) 10, (h) 12, and (i) 14% cement-treated BC soil with fly ash dosages

Cement and fly ash treated soil at modified Proctor test:- The samples passed durability tests in the standard Proctor test only considered for modified compaction. The standard compaction results are useful for low-volume roads. Whereas, for high-volume roads, all layers are compacted to the modified Proctor density. The following mix combinations satisfy the durability tests and hence, are considered for modified Proctor tests. Modified Proctor tests were conducted on mixes with 10 to 12% cement, at a combined dosage of cement and fly ash ≥30%, and on the mixes with 14% cement, at a combined dosage of cement and fly ash ≥25%. The compaction test results are depicted in Figure 4.3.

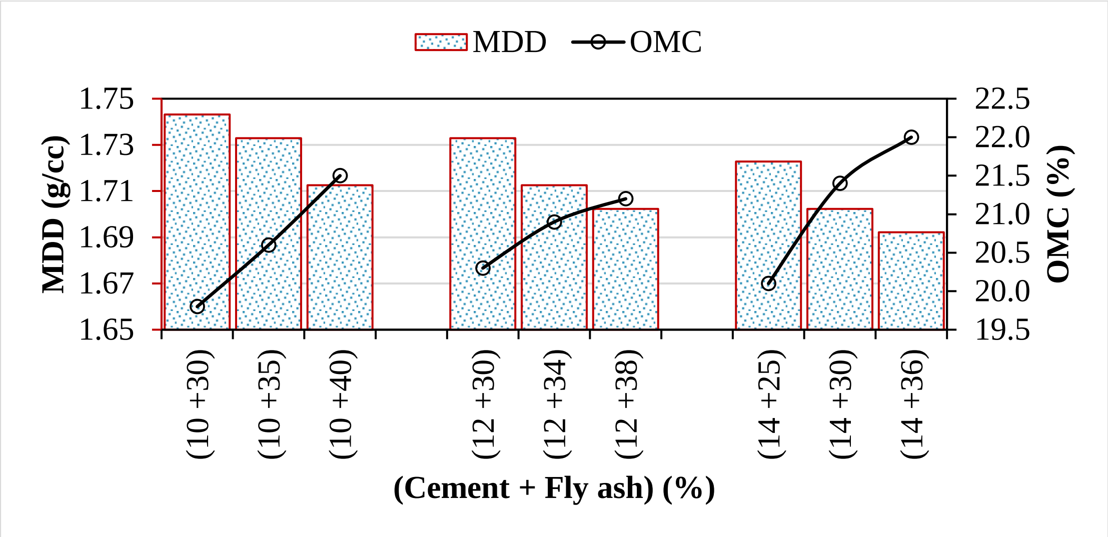

Figure 4. 3 Modified Proctor test results for durability test passed cement-treated BC soil with fly ash dosages

4.2.2 Unconfined Compressive Strength

The UCS tests were conducted to evaluate the suitability of stabilized soil for low and high-volume roads. BC soil specimens with a UCS of 0.40 MPa at standard Proctor density and 1.1 MPa at modified Proctor density exhibited semi-plastic or plastic failure. At higher cement and fly ash percentages, the improvement in UCS values is significant with curing, as depicted in Figures 4.4 and 4.5(a–i). All stabilized samples with an increase in cement, cement–fly ash content, and curing period exhibited brittle failure.

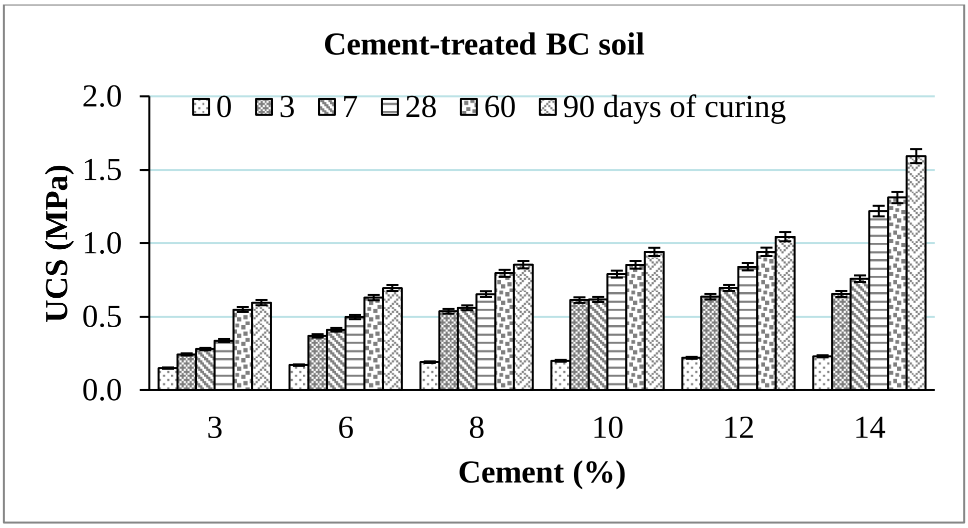

Figure 4. 4 UCS of cement stabilized BC soil at standard Proctor density

When curing the specimens with high cement content (≥10%), it absorbs moisture for hydration and reduces the water content in samples. Few specimens that absorbed free moisture from the desiccator showed an increase in moisture content, which may be due to water demand by both cement and hydrophilic montmorillonite clay mineral present in the soil.

BC soil with 14% cement and 30% fly ash achieved the maximum UCS of 6.9 MPa on 90 days of curing under standard Proctor density. For 14% cement and 36% fly ash contents at standard and modified compaction, the UCS values of 7.2 and 7.3 MPa are obtained after 90 days of curing. The UCS at modified Proctor density is depicted in Figure 4.7. The higher compaction energy has resulted in a marginal improvement of UCS due to the improved compactness of mixes. ASTM D4609-08: 2008 recommended a UCS increase of 0.345 MPa for stabilized soils. Most of the specimens did not exhibit this UCS improvement at low stabilizer dosages and curing periods of 3 and 7 days and due to less formation cement hydration product. Cement stabilized specimens did not exhibit significant improvement in strength with curing. However, most of the cement-fly ash-treated specimens cured for more than 7 days exhibited significant improvement in UCS.

During the initial hydration of cement, the calcium ions released from the cement will take part in the cation exchange process. These calcium cations attract on the surface of fine soil particles, thereby reducing the soil's plasticity. Reactive silica and alumina will take part in hydration reactions to produce cementitious compounds, bond the soil particles, and make them immobile. As per Estabragh et al. 2016, this strong bonding forms a honeycomb structure, leading to strength improvement.

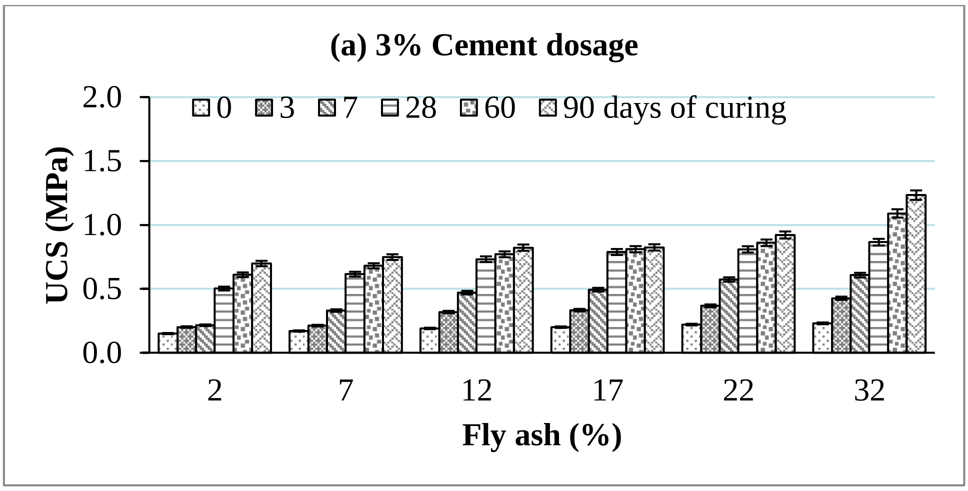

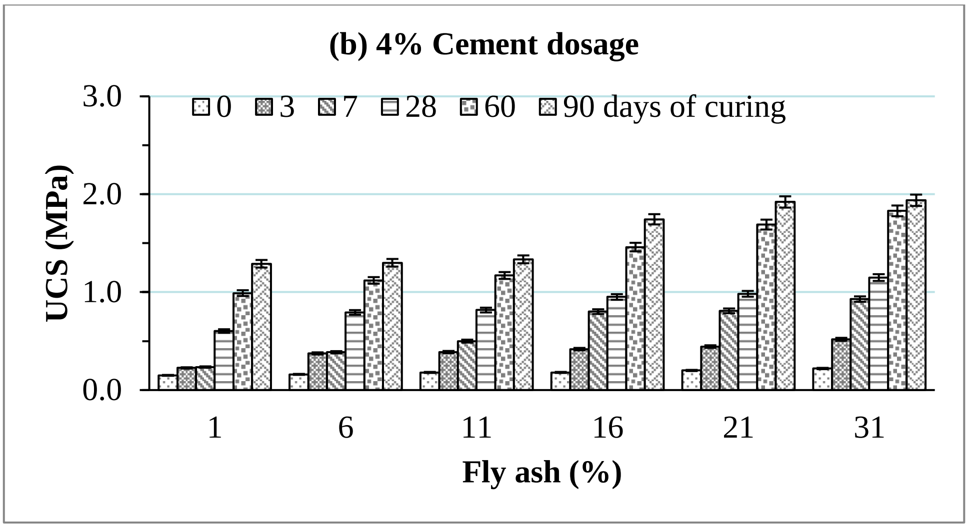
(b) 4% Cement dosage
0 3 7 28 60 90 days of curing
UCS (MPa)
3.0
2.0
1.0
0.0
1 6 11 16 21 31
Fly ash (%)

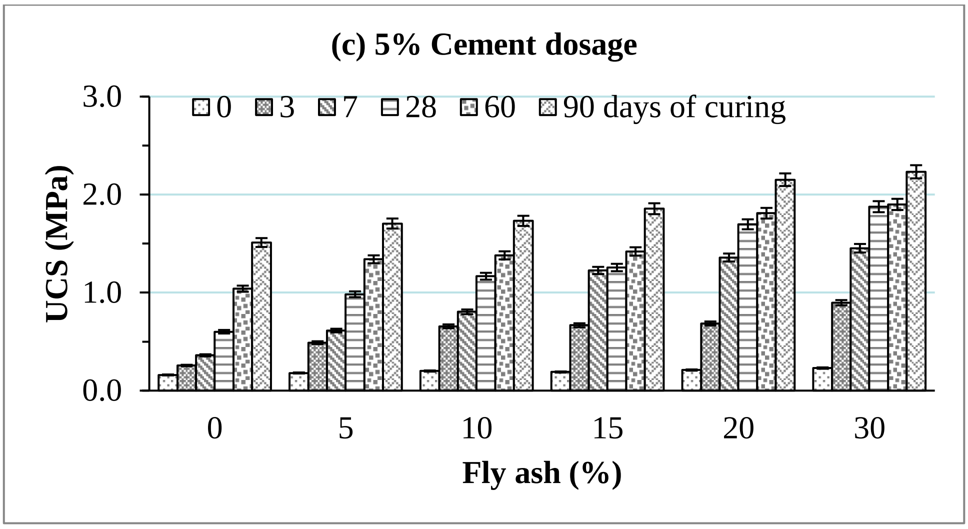
(c) 5% Cement dosage
0 3 7 28 60 90 days of curing
UCS (MPa)
3.0
2.0
1.0
0.0
0 5 10 15 20 30
Fly ash (%)

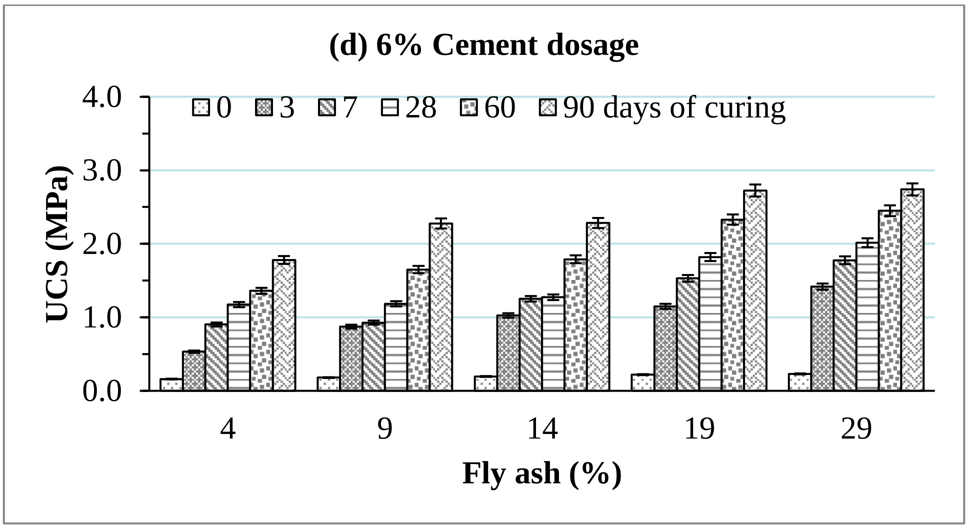
(d) 6% Cement dosage
0 3 7 28 60 90 days of curing
UCS (MPa)
4.0
3.0
2.0
1.0
0.0
4 9 14 19 29
Fly ash (%)

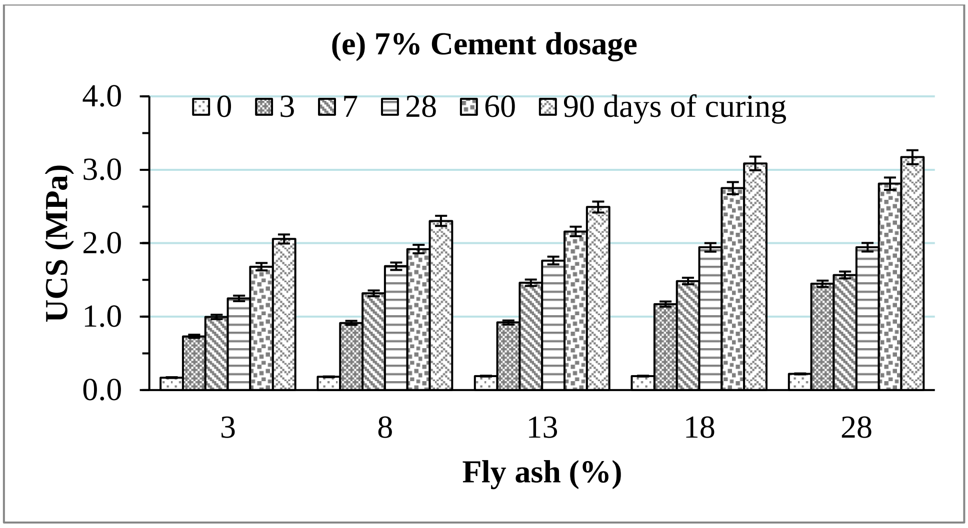
(e) 7% Cement dosage
0 3 7 28 60 90 days of curing
UCS (MPa)
4.0
3.0
2.0
1.0
0.0
3
8
13
18
28
Fly ash (%)

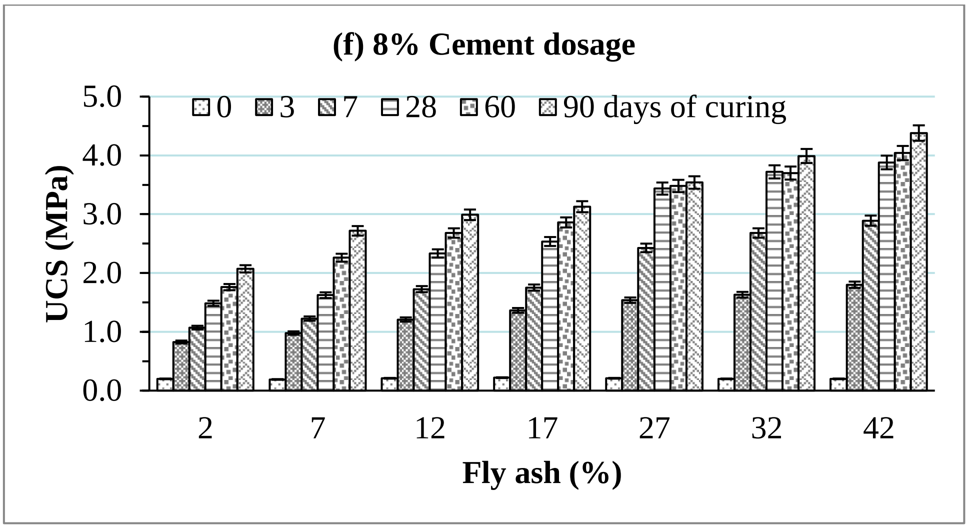
(f) 8% Cement dosage
0 3 7 28 60 90 days of curing
UCS (MPa)
5.0
4.0
3.0
2.0
1.0
0.0
2
7
12
17
27
32
42
Fly ash (%)

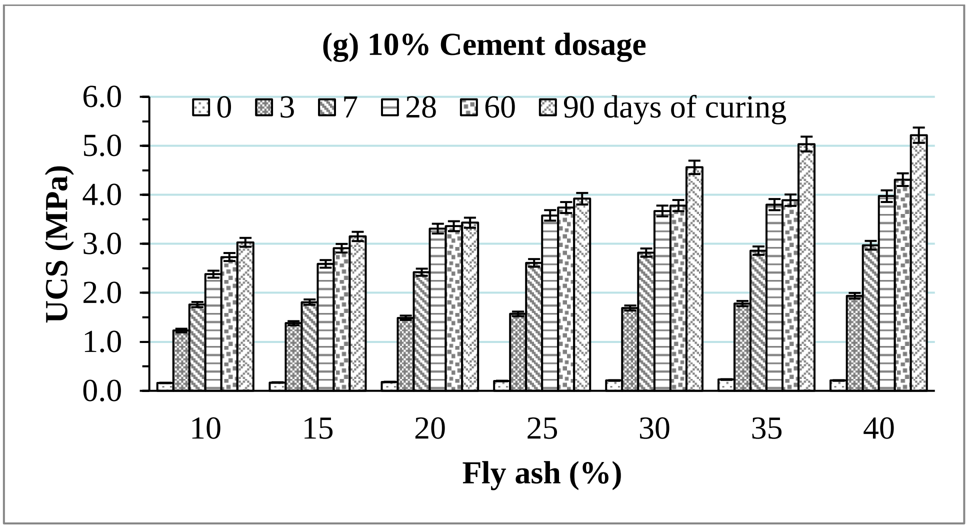
(g) 10% Cement dosage
0 3 7 28 60 90 days of curing
UCS (MPa)
6.0
5.0
4.0
3.0
2.0
1.0
0.0
10
15
20
25
30
35
40
Fly ash (%)

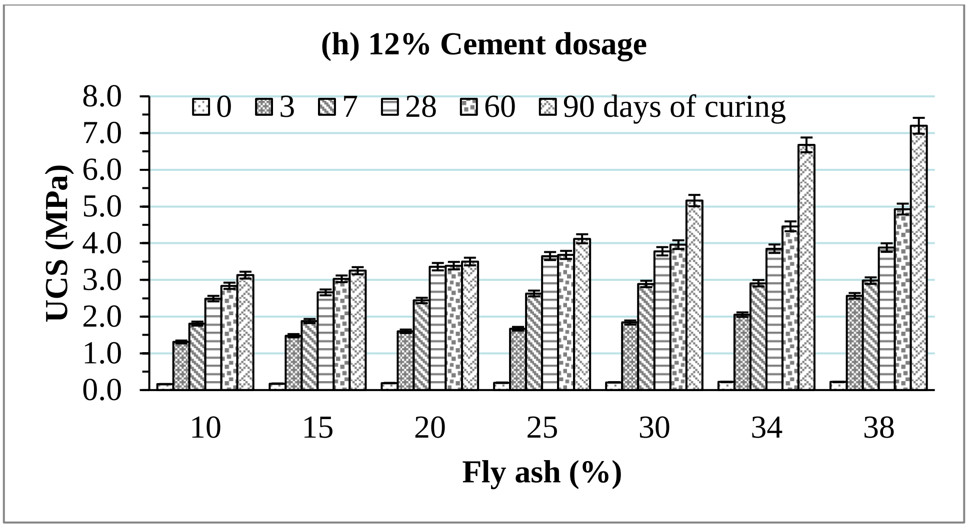

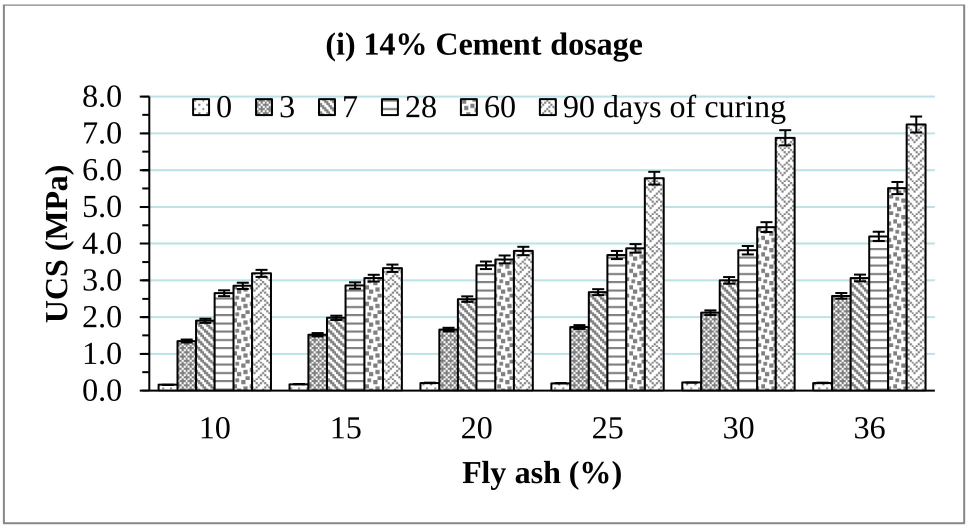

Figure 4. 5 UCS of (a) 3, (b) 4, (c) 5, (d) 6, (e) 7, (f) 8, (g) 10, (h) 12, and (i) 14% cement stabilized BC soil with various fly ash dosages at standard Proctor density

ANOVA:- Univariate analysis of variance performed indicates that the UCS values are significantly (i.e., $p<0.05$) influenced by the dosage of cement, dosage of fly ash, and curing period. $R^2 = 0.822$ indicates that 82.2% of the variance in UCS values can be explained by the dosage of cement, dosage of fly ash, and curing period. The ANOVA results are tabulated in Table 4.1.

Table 4. 1 ANOVA of UCS with the dosage of cement, dosage of fly ash, and curing period at standard Proctor density

Tests of Between-Subjects Effects					
Dependent Variable: UCS (MPa)					
Source	Type III Sum of Squares	df	Mean Square	F	Sig.
Corrected Model	577.280[a]	46	12.550	31.987	.000
Intercept	679.301	1	679.301	1731.433	.000
Curing	270.278	5	54.056	137.779	.000
Cement	46.259	6	7.710	19.651	.000
Fly ash	120.515	33	3.652	9.308	.000
Error	125.155	319	.392		
Total	1714.440	366			
Corrected Total	702.435	365			
a. R^2= .822 (Adjusted R^2= .796)					

E values at standard Proctor density:- E values obtained for different mix combinations are plotted against respective UCS values. Linear relationships were established between UCS and E values, as depicted in Figure 4.6.

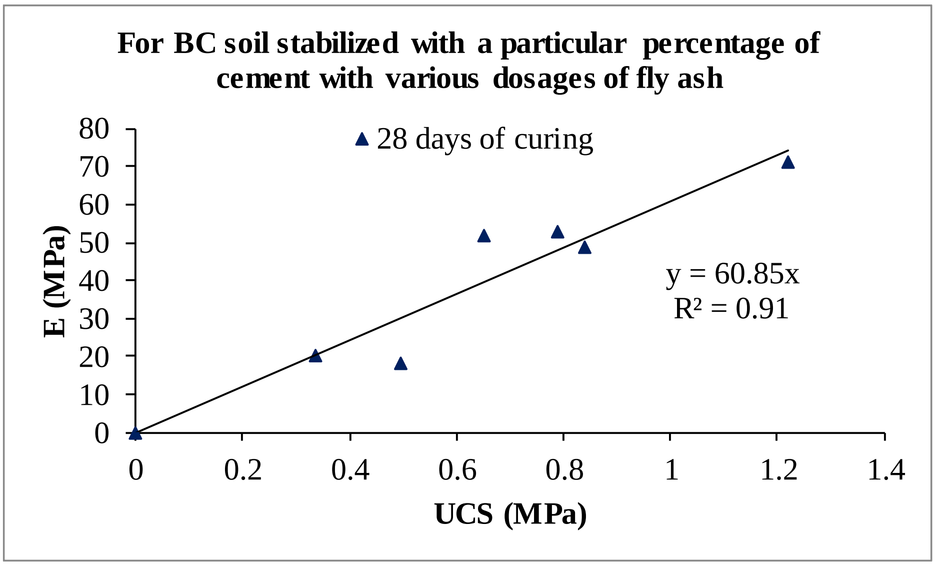

Figure 4. 6 Typical UCS versus E graph

$$E = m \times UCS \quad \ldots\ldots\ldots\ldots\ldots\ldots (4.1)$$

where, E = Youngs modulus

UCS = Unconfined compressive strength

m = Slope of stress-strain curve

The graph is plotted for different combinations of cement and fly ash dosages for different curing periods. The results are depicted in Figure 4.7.

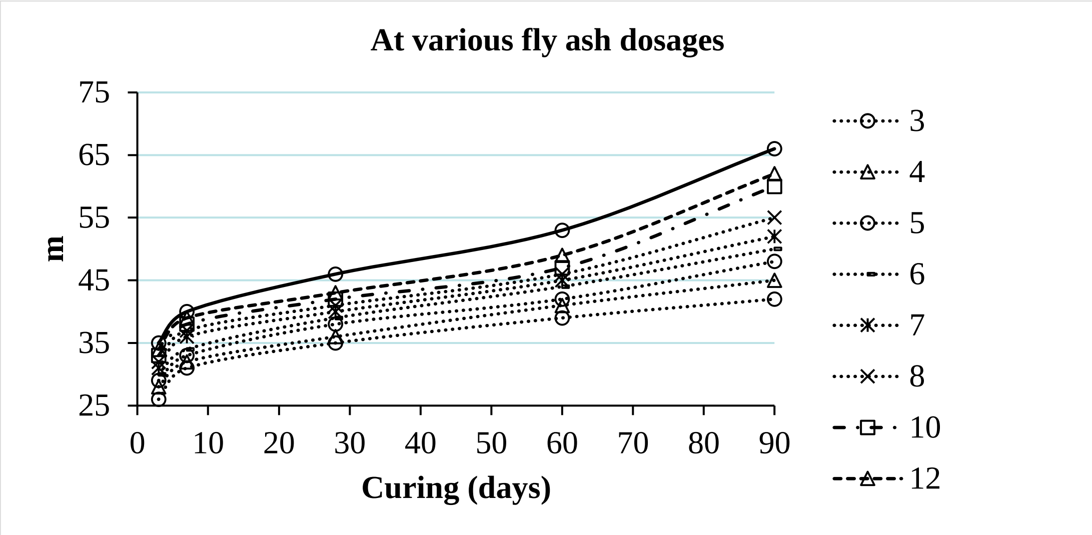

Figure 4. 7 'm' values for cement stabilized BC soil with various fly ash dosages at standard Proctor density

The higher values of 'm' were obtained for higher cement dosages and curing periods. The samples with higher dosages and cured for 90 days exhibited higher E values. This is evident from Table 4.2 for all the mixes.

Table 4. 2 'E' values for cement stabilized BC soil with various fly ash dosages at standard Proctor density

Cement + (Fly ash) (%)	Curing (days)	UCS (MPa)	m	E (MPa)
3 + (2–32)	3	0.2–0.4	26	5–10
	7	0.2–0.6	31	6–19
	28	0.5–0.9	35	18–32
	60	0.6–1.1	39	23–43
	90	0.7–1.2	42	29–50
4 + (1–31)	3	0.2–0.5	28	6–14
	7	0.2–0.9	32	6–29
	28	0.6–1.1	36	22–40
	60	1.0–1.8	41	41–74
	90	1.3–1.9	45	59–86
5 + (0–30)	3	0.3–0.9	29	9–26
	7	0.4–1.5	33	13–50
	28	0.6–1.9	38	23–72
	60	1.0–1.9	42	42–80
	90	1.5–2.2	48	72–106
6 + (4–29)	3	0.5–1.4	30	15–42
	7	0.9–1.8	34	31–61
	28	1.2–2.0	39	47–78
	60	1.4–2.5	44	62–110
	90	1.8–2.7	50	90–135

Cement + (Fly ash) (%)	Curing (days)	UCS (MPa)	m	E (MPa)
7 + (3–28)	3	0.7–1.4	31	22–43
	7	1.0–1.6	36	36–58
	28	1.2–1.9	40	48–76
	60	1.7–2.8	45	77–126
	90	2.1–3.2	52	109–166
8 + (2–42)	3	0.8–1.8	32	26–58
	7	1.1–2.9	37	41–107
	28	1.5–3.9	41	62–160
	60	1.8–4.0	46	83–184
	90	2.1–4.4	55	116–242
10 + (10–40)	3	1.2–1.9	33	40–63
	7	1.8–3.0	38	68–114
	28	2.4–4.0	42	101–168
	60	2.7–4.3	47	127–202
	90	3.0–5.2	60	180–312
12 + (10–38)	3	1.3–2.6	34	44–88
	7	1.8–3.0	39	70–117
	28	2.5–3.9	43	108–168
	60	2.8–4.9	49	137–240
	90	3.1–7.2	62	192–446
14 + (10–36)	3	1.4–2.6	35	49–91
	7	1.9–3.1	40	76–124
	28	2.7–4.2	46	124–193
	60	2.9–5.5	53	154–292
	90	3.2–7.2	66	211–475

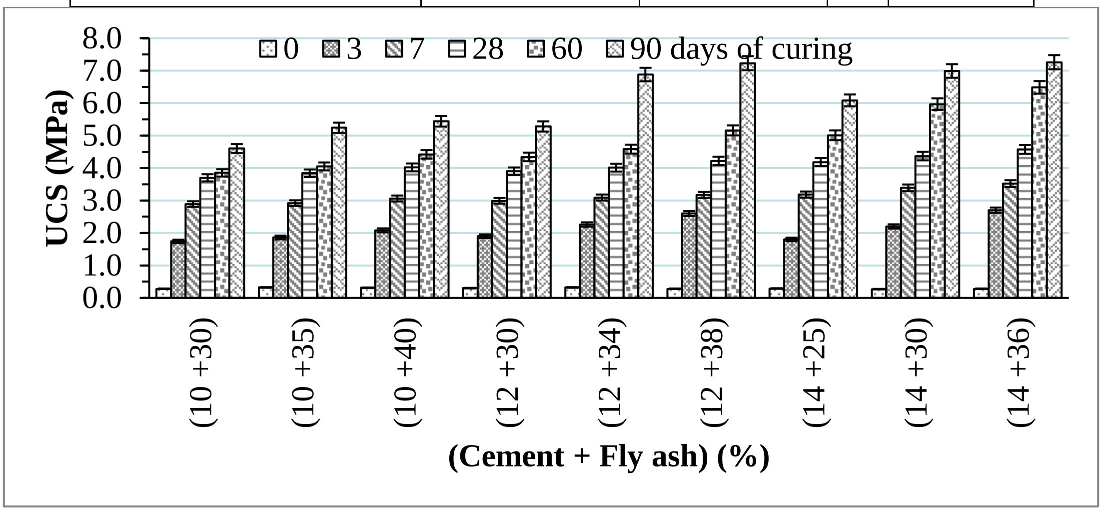

Figure 4. 8 UCS of durability test passed cement stabilized BC soil with various fly ash dosages at modified Proctor density

ANOVA: Univariate analysis of variance performed indicates that the UCS values are significantly (i.e., $p<0.05$) influenced by the dosage of cement, dosage of fly ash, and curing period. R^2 = 0.964 indicates that 96.4% of the variance in UCS values can be explained by the dosage of cement, dosage of fly ash, and curing period. The ANOVA results are tabulated in Table 4.3.

Table 4. 3 ANOVA of UCS with the dosage of cement, dosage of fly ash, and curing period at modified Proctor density

Tests of Between-Subjects Effects					
Dependent Variable: UCS (MPa)					
Source	Type III Sum of Squares	df	Mean Square	F	Sig.
Corrected Model	200.754[a]	13	15.443	82.154	.000
Intercept	565.567	1	565.567	3008.782	.000
Curing	191.784	5	38.357	204.056	.000
Cement	3.453	2	1.727	9.186	.001
Fly ash	3.339	6	.556	2.960	.017
Error	7.519	40	.188		
Total	848.940	54			
Corrected Total	208.273	53			
a. R^2 = .964 (Adjusted R^2= .952)					

E values at modified Proctor density:- The more compact packing of mixes under modified Proctor compaction has resulted in higher 'm' values as depicted in Figure 4.9, and higher E values for different mixes as tabulated in Table 4.4.

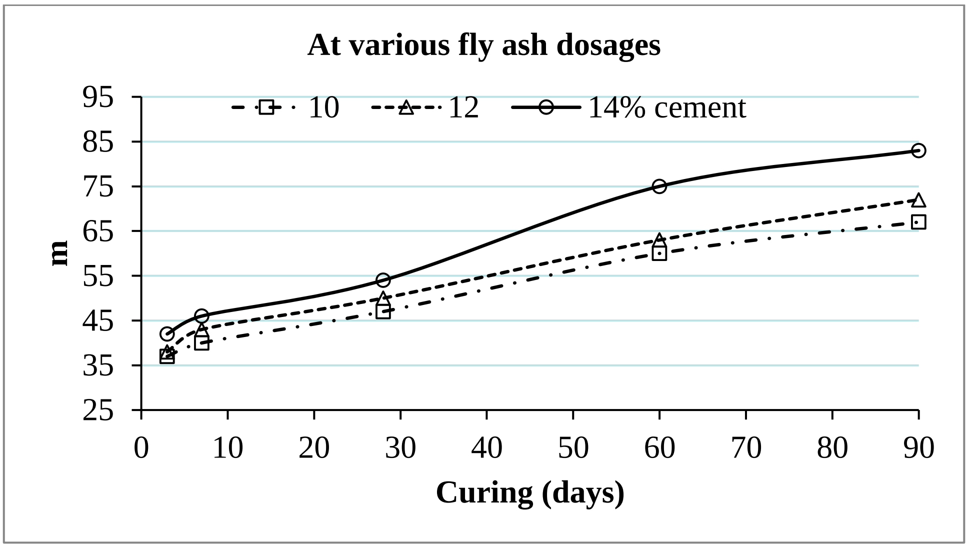

Figure 4. 9 'm' values for cement stabilized BC soil with various fly ash dosages at modified Proctor density

Table 4. 4 'E' values for cement stabilized BC soil with various fly ash dosages at modified Proctor density

Cement + (Fly ash) (%)	Curing (days)	UCS (MPa)	m	E (MPa)
10 + (30–40)	3	1.7–2.1	37	63–78
	7	2.9–3.1	40	116–124
	28	3.7–4.0	47	174–188
	60	3.9–4.4	60	234–264
	90	4.6–5.4	67	308–362
12 + (30–38)	3	1.9–2.6	38	72–99
	7	3.0–3.2	43	129–138
	28	3.9–4.2	50	195–210
	60	4.3–5.2	63	271–328
	90	5.3–7.2	72	382–518
14 + (25–36)	3	1.8–2.7	42	76–113
	7	3.2–3.5	46	147–161
	28	4.2–4.6	54	227–248
	60	5.0–6.5	75	375–488
	90	6.1–7.3	83	506–606

4.2.3 Flexural Strength

The durability passed specimens at standard Proctor and modified Proctor density are only considered for flexure test.

The stabilized mixes exhibited improved flexural strength with a higher dosage of cement and fly ash, with curing as depicted in Figures 4.10 (a, b). Whereas, at low dosages, few shrinkage cracks were developed on the surface of the prism. The shrinkage cracks (micro) were reduced when treated with higher dosages. While testing, the width, and length of these cracks were increased, thereby leading to quick failure. As the samples failed suddenly, the progress of crack length and width could not be measured. Maximum flexural strength of 0.68 and 0.81 MPa was observed for 14% cement and 36% fly ash stabilized soil after 28 days curing at standard and modified Proctor density, respectively.

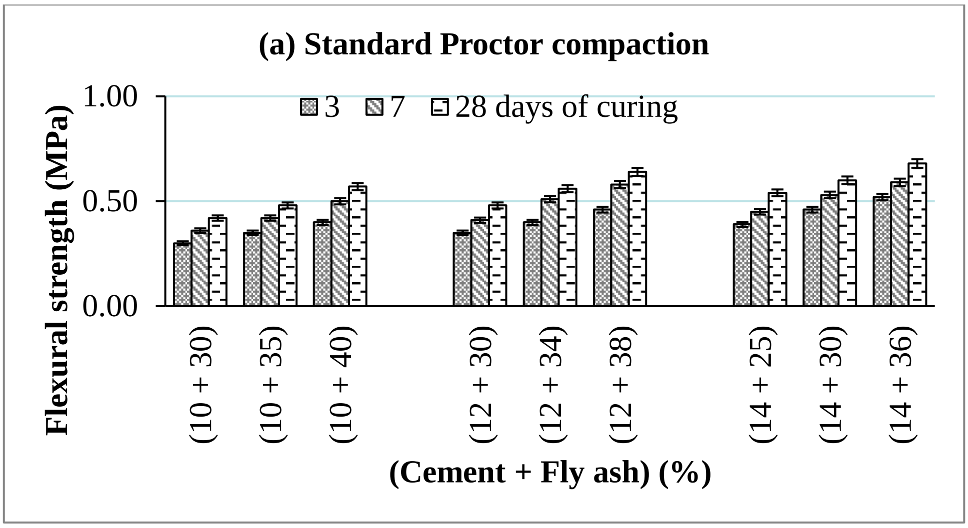

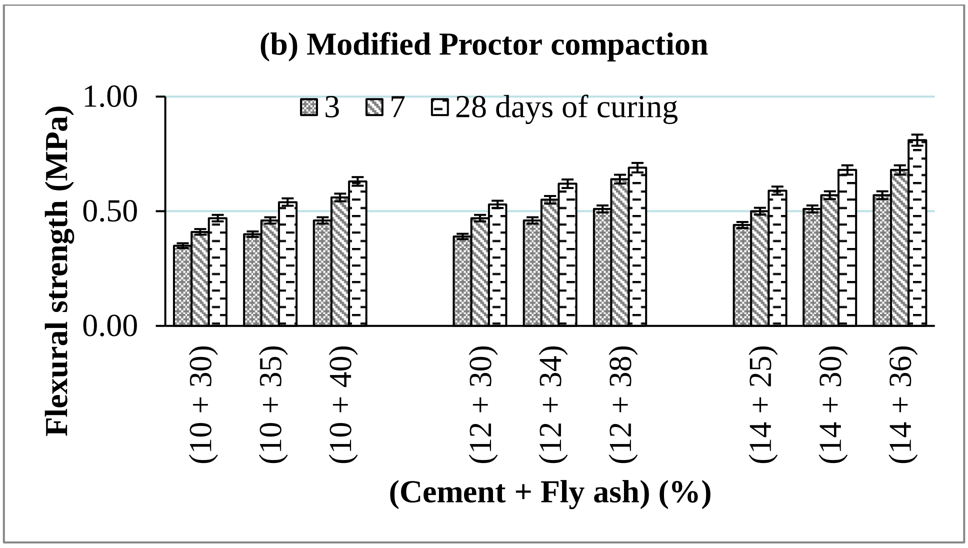

Figure 4. 10 Flexural strength of cement and fly ash stabilized BC soil at (a) standard, (b) modified Proctor density

ANOVA: Univariate analysis of variance performed indicates that the flexural strength values are significantly (i.e., $p<0.05$) influenced by the dosage of cement, dosage of fly ash, and curing period. R^2 = 0.987 and 0.978 indicates that 98.7% and 97.8% of the variance in flexural strength values can be explained by the dosage of cement, dosage of fly ash, and curing period at standard and modified Proctor density, respectively. The ANOVA results at the standard and modified Proctor density are tabulated in Tables 4.5 and 4.6, respectively.

Table 4. 5 ANOVA of UCS with the dosage of cement, dosage of fly ash, and curing period at standard Proctor density

Tests of Between-Subjects Effects					
Dependent Variable: Flexural strength (MPa)					
Source	Type III Sum of Squares	df	Mean Square	F	Sig.
Corrected Model	.238[a]	10	.024	124.389	.000
Intercept	5.631	1	5.631	29449.040	.000
Curing	.100	2	.050	261.346	.000
Cement	.045	2	.023	118.605	.000
Fly ash	.086	6	.014	74.789	.000
Error	.003	16	.000		
Total	6.452	27			
Corrected Total	.241	26			
a. R^2= .987 (Adjusted R^2= .979)					

Table 4. 6 ANOVA of UCS with the dosage of cement, dosage of fly ash, and curing period at modified Proctor density

Tests of Between-Subjects Effects					
Dependent Variable: Flexural strength (MPa)					
Source	Type III Sum of Squares	df	Mean Square	F	Sig.
Corrected Model	.294[a]	10	.029	69.972	.000
Intercept	7.046	1	7.046	16741.832	.000
Curing	.120	2	.060	142.653	.000
Cement	.049	2	.025	58.535	.000
Fly ash	.111	6	.018	43.820	.000
Error	.007	16	.000		
Total	8.078	27			
Corrected Total	.301	26			
a. R^2 = .978 (Adjusted R^2= .964)					

Regression: Regression analysis is performed between UCS and flexural strength, and the results are tabulated in Table 4.7. A correlation of 0.768 at standard Proctor density and 0.811 at modified Proctor density ($p<0.0005$) confirms a strong positive relationship between UCS and flexural strength. R^2 = 0.590 and 0.657 indicate that 59.0% and 65.7% of the variance in flexural strength can be explained by UCS at standard and modified Proctor density, respectively. From ANOVA, it can be concluded that the model is statistically significant ($p<0.0005$). From the coefficient table, for every 1 MPa increase in UCS, the model predicted an increase of 0.093 MPa and 0.102 MPa flexural strength at standard and modified Proctor density, respectively. Also, the t-test confirms the statistical significance of the model.

Table 4. 7 Regression analysis of UCS and flexural strength for BC soil stabilized with cement and fly ash at standard Proctor density

Correlations

		Flexural strength (MPa)	UCS (MPa)
Pearson Correlation	Flexural strength (MPa)	1.000	.768
	UCS (MPa)	.768	1.000
Sig. (1-tailed)	Flexural strength (MPa)	.	.000
	UCS (MPa)	.000	.
N	Flexural strength (MPa)	27	27
	UCS (MPa)	27	27

Model Summary[b]

Model	R	R Square	Adjusted R Square	Std. Error of the Estimate
1	.768[a]	.590	.573	.06288

a. Predictors: (Constant), UCS (MPa)

b. Dependent Variable: Flexural strength (MPa)

ANOVA[a]

Model		Sum of Squares	df	Mean Square	F	Sig.
1	Regression	.142	1	.142	35.927	.000[b]
	Residual	.099	25	.004		
	Total	.241	26			

a. Dependent Variable: Flexural strength (MPa)

b. Predictors: (Constant), UCS (MPa)

Coefficients[a]

Model		Unstandardized Coefficients		Standardized Coefficients	t	Sig.	95.0% Confidence Interval for B	
		B	Std. Error	Beta			Lower Bound	Upper Bound
1	(Constant)	.206	.047		4.373	.000	.109	.303
	UCS (MPa)	.093	.016	.768	5.994	.000	.061	.125

a. Dependent Variable: Flexural strength (MPa)

Table 4. 8 Regression analysis of UCS and flexural strength for BC soil stabilized with cement and fly ash at modified Proctor density

Correlations

		Flexural strength (MPa)	UCS (MPa)
Pearson Correlation	Flexural strength (MPa)	1.000	.811
	UCS (MPa)	.811	1.000

Sig. (1-tailed)	Flexural strength (MPa)	.	.000
	UCS (MPa)	.000	.
N	Flexural strength (MPa)	27	27
	UCS (MPa)	27	27

Model Summary[b]

Model	R	R Square	Adjusted R Square	Std. Error of the Estimate
1	.811[a]	.657	.644	.06426

a. Predictors: (Constant), UCS (MPa)

b. Dependent Variable: Flexural strength (MPa)

ANOVA[a]

Model		Sum of Squares	df	Mean Square	F	Sig.
1	Regression	.198	1	.198	47.950	.000[b]
	Residual	.103	25	.004		
	Total	.301	26			

a. Dependent Variable: Flexural strength (MPa)

b. Predictors: (Constant), UCS (MPa)

Coefficients[a]

Model		Unstandardized Coefficients		Standardized Coefficients	t	Sig.	95.0% Confidence Interval for B	
		B	Std. Error	Beta			Lower Bound	Upper Bound
1	(Constant)	.220	.047		4.633	.000	.122	.317
	UCS (MPa)	.102	.015	.811	6.925	.000	.071	.132

a. Dependent Variable: Flexural strength (MPa)

4.2.4 California Bearing Ratio

As per IRC, when the annual rainfall is more than 500 mm, the pavement has to be designed for soaked CBR only. In the present investigation, all the samples were tested in soaked condition. The BC soil exhibited a CBR value of 2% at standard and modified Proctor density. Therefore, untreated BC soil requires stabilization to bring it to the desired strength (CBR = 5%). The samples were prepared at both standard and modified Proctor density, tested for CBR after 3, 7, and 28 days of curing. All samples exhibited significant improvement in CBR, and test results are depicted in Figure 4.11(a–c), with negligible swelling (< 2%), which indicates excellent volume stability (Table 4.9). At modified Proctor, the CBR values were improved further, and test results are depicted in Figure 4.12(a–c). The samples absorbed less moisture at higher cement and fly ash dosages due to the formation of stronger bonding. Therefore, these stabilized mixes can resist higher loads under severe weather conditions. During the monsoon, the pavement is surrounded by water; in such cases, there is a possible increase in the CBR value of stabilized soil with time due to the formation of more hydration products. But, in the case of untreated soil, the CBR reduces due to submergence.

As per Amadi 2014, for the black cotton soil having high swell potential, with the addition of 16% cement kiln dust along with 10% quarry fines, the soaked CBR has increased from 8 to 36%, along with a considerable decrease in swell potential. According to Estabragh et al. 2016, it is found that increase in strength of a soil-cement mix is due to the hydration of cement and production of cementing materials.

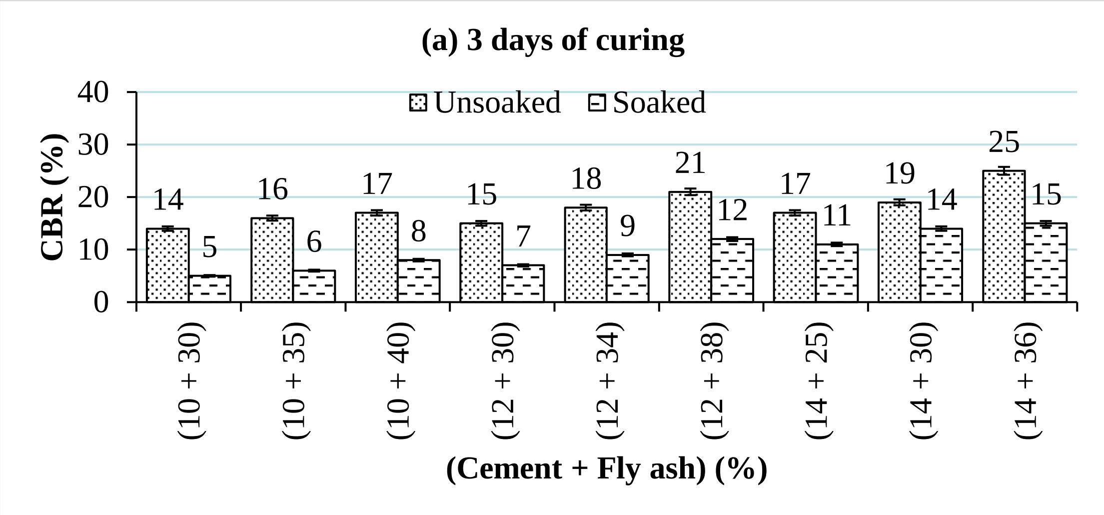

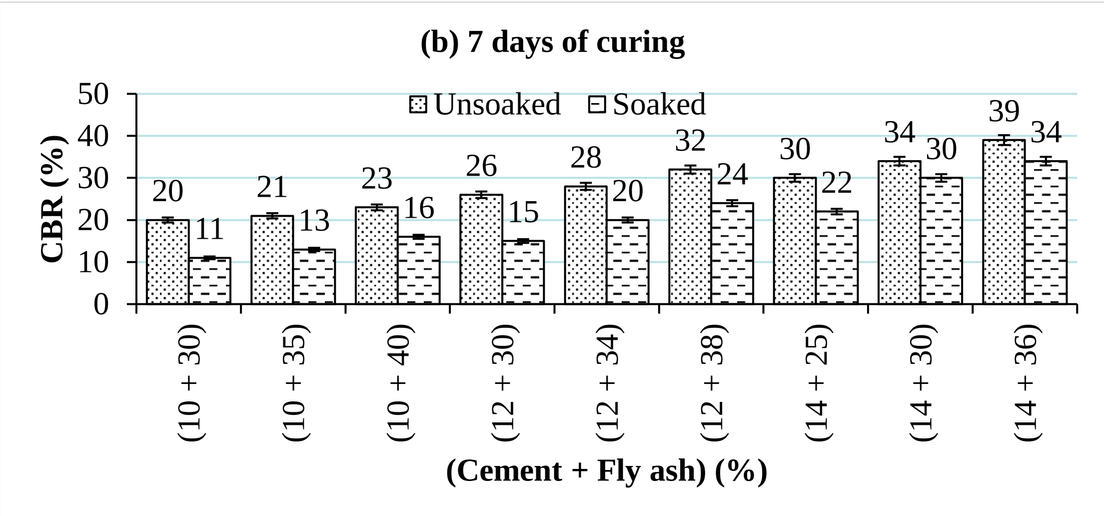

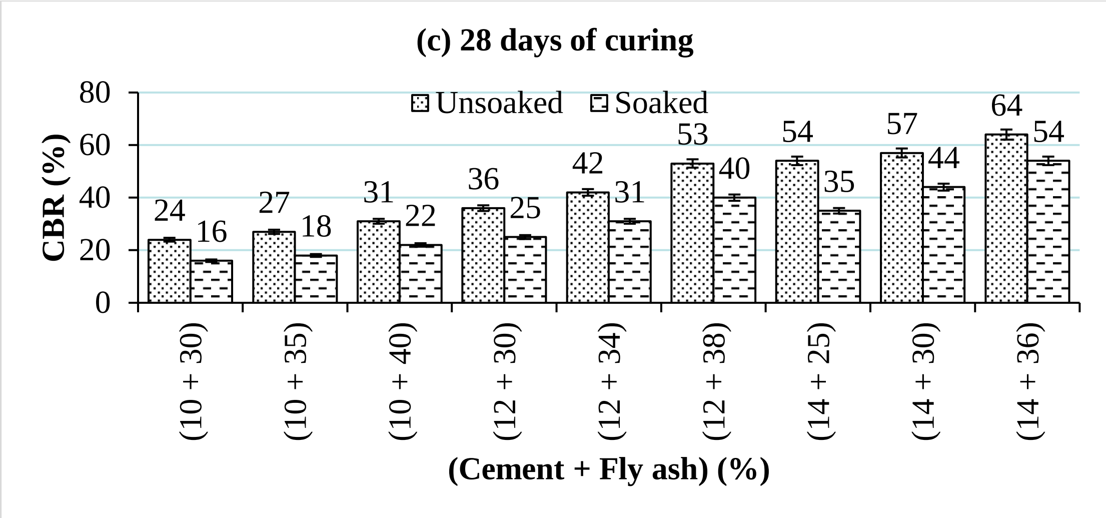

Figure 4. 11 CBR of cement and fly ash stabilized BC soil cured for (a) 3, (b) 7, and (c) 28 days at standard Proctor density

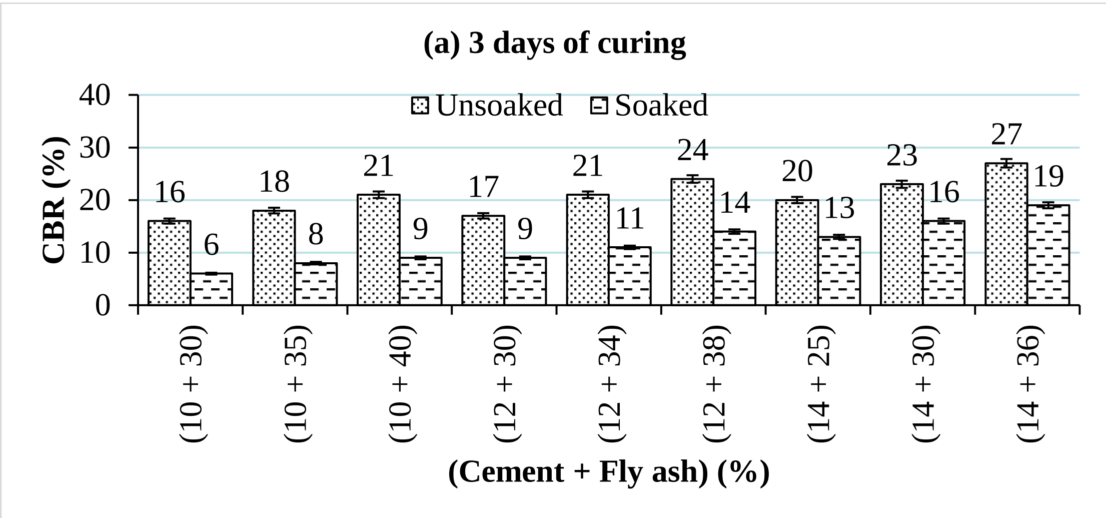

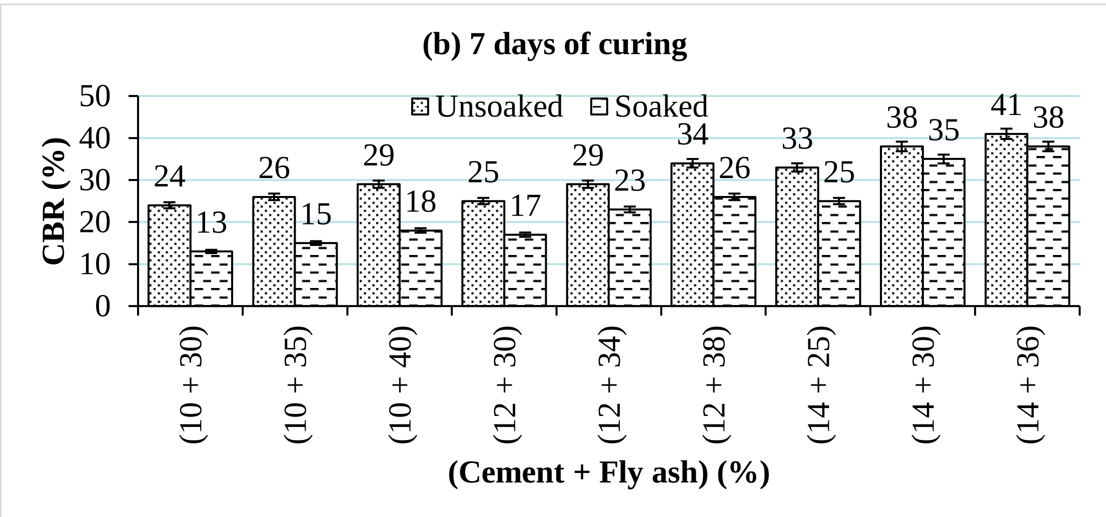

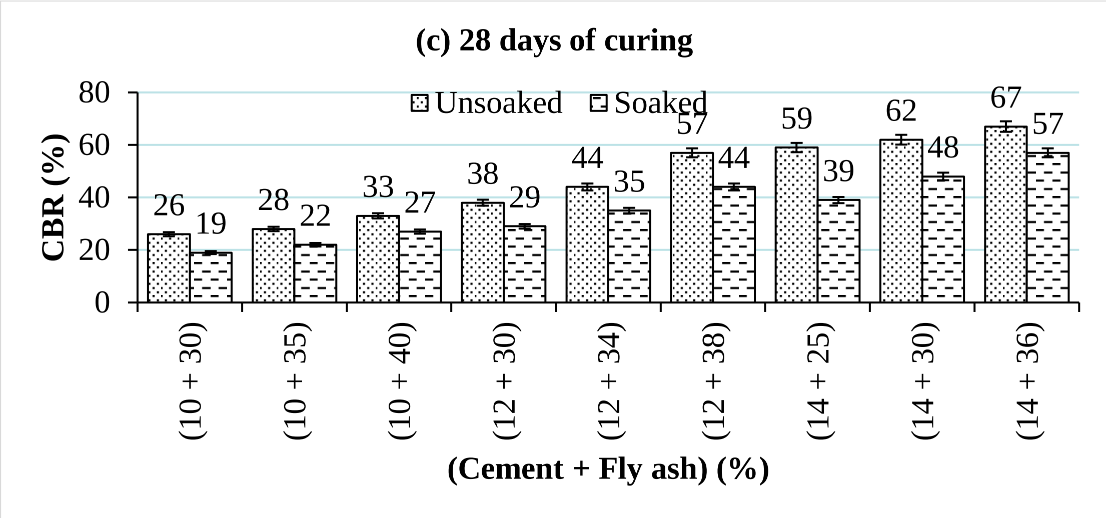

Figure 4. 12 CBR of cement and fly ash stabilized BC soil cured for (a) 3, (b) 7, and (c) 28 days at modified Proctor density

Table 4. 9 Swelling values of cement-fly ash stabilized BC soil after soaking

Cement (%)	Fly ash (%)	Swelling (%)
10	30	2.00
10	35	0.70
10	40	0.30
12	30	1.25
12	34	0.50
12	38	0.20
14	25	1.18
14	30	0.20
14	36	0.10

4.2.5 Durability

During the monsoon, the soil moisture content increases and vice versa during summer. Dropdown in temperature during winter crystallizes the soil water in regions where the soil temperature goes below zero degrees, and a rise in temperature in summer leads to ice melting. BC soils spread in various regions of the world subjected to such seasonal variations in moisture and temperature may cause distress in pavements. For evaluating the sustainability of stabilized soil under these long-term weathering conditions, WD and FT durability tests were necessary, and as per code, it is mandatory. If the stabilized soil exhibits a weight loss of ≤14% after 12 weathering cycles, it can be considered as a pavement layer (for the base, sub-base, or subgrade) as per IRC SP-72: 2015 and IRC 37: 2018.

4.2.5.1 Wetting-Drying

The samples considered for wetting and drying followed two methods. In the first method, samples were not brushed after drying. In the second method, samples were brushed after each cycle. Brushing of samples is performed to remove loosened particles during repeated durability test cycles. The particles will be detached from stabilized soil due to stresses developed as a result of changes in moisture content, temperature.

The specimens with 3, 6% cement, and 10% cement with 20% fly ash failed after the second cycle. After the first drying cycle, these specimens could retain moisture contents of 4.5, 3.2, and 0.7%, respectively. During the second cycle, due to a drastic increase in moisture contents (>25%), and low bonding, these mixes could not resist the soil loss. However, few specimens were failed during the successive cycles, as depicted in Figure 4.13(a–e). The soil with 8% cement exhibited a weight loss of 13.5% after the fourth drying cycle and failed during the next cycle. The mixes with 14, 15%, and 14, 20% cement, fly ash exhibited low resistance with soil loss of 4.9, 5.6%, respectively, after four WD cycles before failure.

At the low dosage of cement and fly ash, the samples could not withstand WD cycles. The cementation at low dosages cannot resist the expansion and crack of soil during the WD test. At low fly ash dosage, the expansive behaviour of soil is not controlled; therefore, the stabilized samples were quickly failed with high soil loss. As the fly ash content increased, the specimens exhibited more resistance to the WD cycles. Only the mixes with 10% cement along with 30, 35, and 40% fly ash, 12% cement along with 30, 34, and 38% fly ash, and 14% cement along with 25, 30, and 36% fly ash, could resist the test with soil loss <14% (brushed and unbrushed).

The soil loss trend of brushed and unbrushed specimens did not follow a particular pattern. The specimens could withstand the test in general at higher cement and fly ash percentages (cement >10%, fly ash >25%). The brushing of specimens has a significant effect, leading to higher soil loss. The water affinity of clay minerals present in the mix governed the soil loss.

The mixes at higher cement and fly ash content could control volume change during the first wetting cycle, indicating excellent volume stability on saturation after 7 days of curing. After the first drying cycle, these samples could retain 0.7–4.5% moisture, with a shrinkage of 0.0–3.2%, respectively (Table 4.10). The shrinkage is inversely proportional to the strength (UCS) of the mixes. These durable mixes can be used at different pavement layers depending on UCS and flexural strength.

Table 4. 10 Shrinkage values of cement-fly ash stabilized BC soil after drying

Cement (%)	Fly ash (%)	Shrinkage (%)
3	2–32	3.20–1.78
4	1–31	2.88–1.46
5	0–30	2.46–1.04
6	4–29	1.90–0.87
7	3–28	1.24–0.56
8	2–42	0.80–0.18
10	10–40	0.46–0.00
12	10–38	0.36–0.00
14	10–36	0.30–0.00

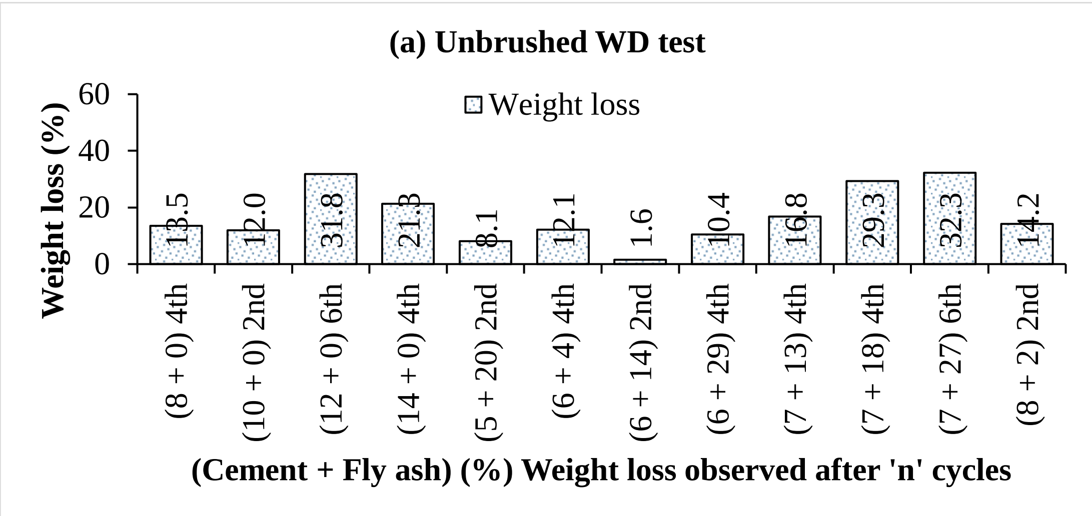

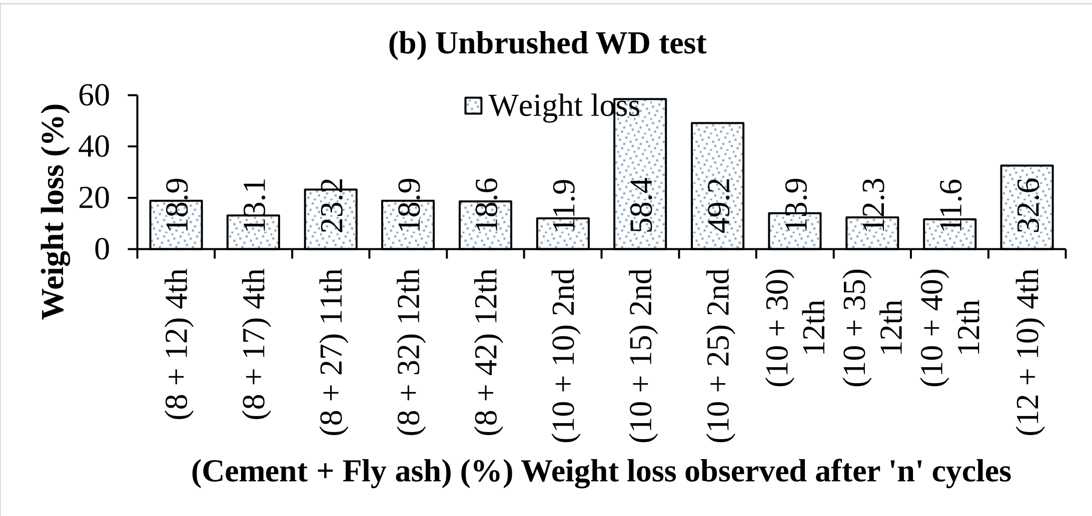

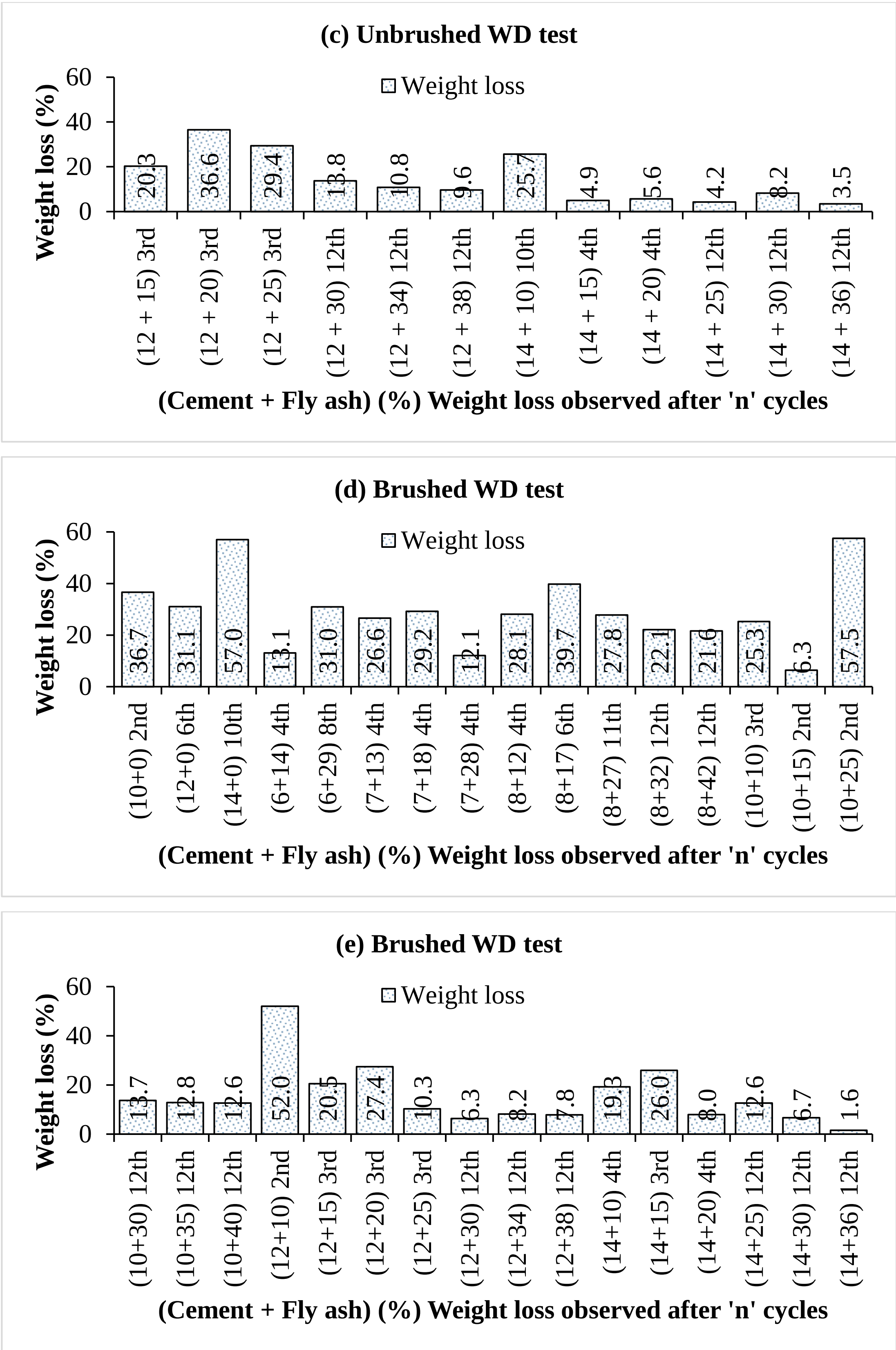

Figure 4. 13 Weight loss of cement stabilized BC soil with various fly ash dosages under (a), (b), (c) unbrushed and (d), (e) brushed wetting-drying test

4.2.5.2 Freezing-Thawing

The specimens exhibited excellent resistance to the FT cycles when compared to the WD test. Unbrushed FT specimens exhibited weight gain due to the absorption of water during thawing cycles, which is available from moist felt fads covered around the specimen. The moisture contents of all the specimens were increased by approximately 5% due to thawing. The maximum weight gain of 18.3% for the unbrushed FT sample with 10% cement, 20% fly ash was observed after the complete test (12 cycles) and effectively resisted soil loss even during brushing due to stronger cemented matrix formation. The weight loss of 13.1, 14.2% were observed with 3% cement for the unbrushed, brushed FT samples at the end of the test, which could not resist the soil loss due to low cementation. The samples with a higher percentage of cement and fly ash could sustain the test (weight loss <14%). The brushed sample with 14% cement and 36% fly ash has exhibited only 0.3% weight loss after 12 FT cycles due to strong bonding developed by cement hydration.

The weight gain or weight loss can be calculated as a ratio of decrease or increase in the weight of the specimen corresponding to the cured weight of the specimen and is represented in percentage. In Figure 4.14(a–h), positive values indicate soil loss, and the negative values depict weight gain due to water absorption. Due to good bonding, the specimens exhibited resistance to crack propagation on freezing. There was no sign of expansion for all dosages of cement and fly ash. After the first freezing cycle, these samples showed a volume shrinkage of 0.0–1.91% (Table 4.11). The volume shrinkage during FT cycles is inversely proportional to the strength (UCS) of the mixes.

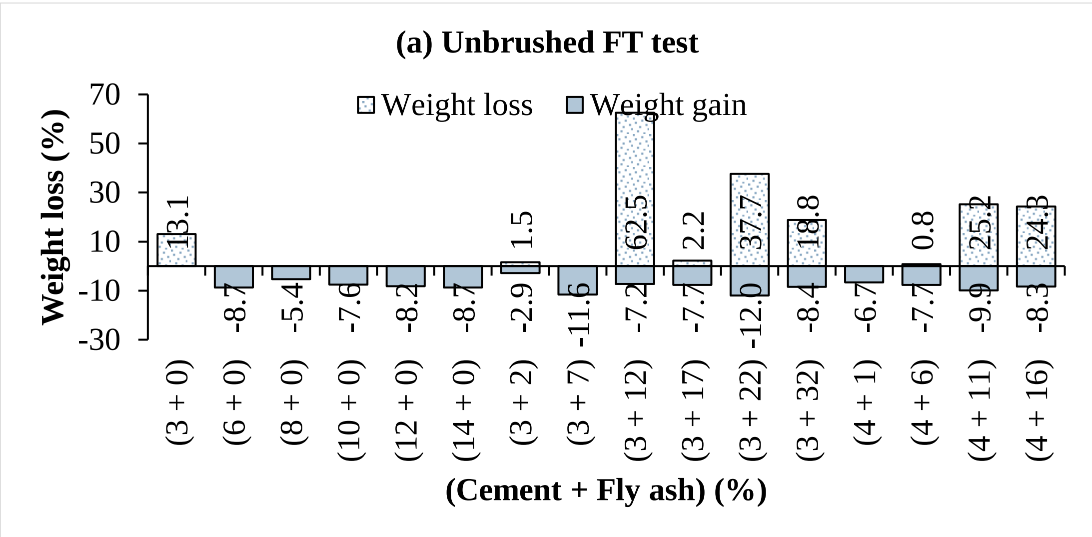

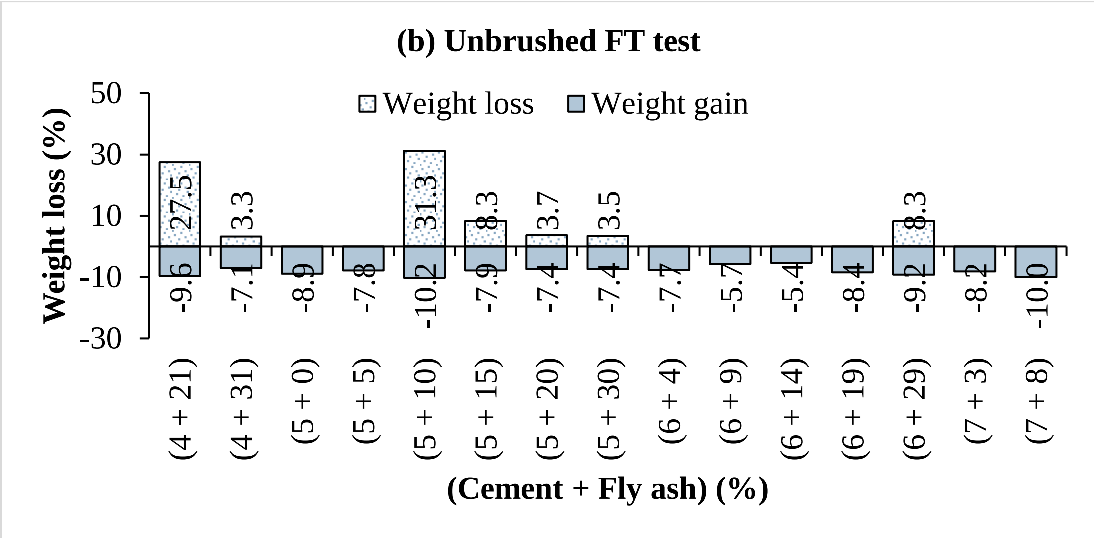
(b) Unbrushed FT test
Weight loss
Weight gain
Weight loss (%)
50
30
10
-10
-30
27.5
3.3
31.3
8.3
3.7
3.5
8.3
-9.6
-7.1
-8.9
-7.8
-10.2
-7.9
-7.4
-7.4
-7.7
-5.7
-5.4
-8.4
-9.2
-8.2
-10.0
(4 + 21)
(4 + 31)
(5 + 0)
(5 + 5)
(5 + 10)
(5 + 15)
(5 + 20)
(5 + 30)
(6 + 4)
(6 + 9)
(6 + 14)
(6 + 19)
(6 + 29)
(7 + 3)
(7 + 8)
(Cement + Fly ash) (%)

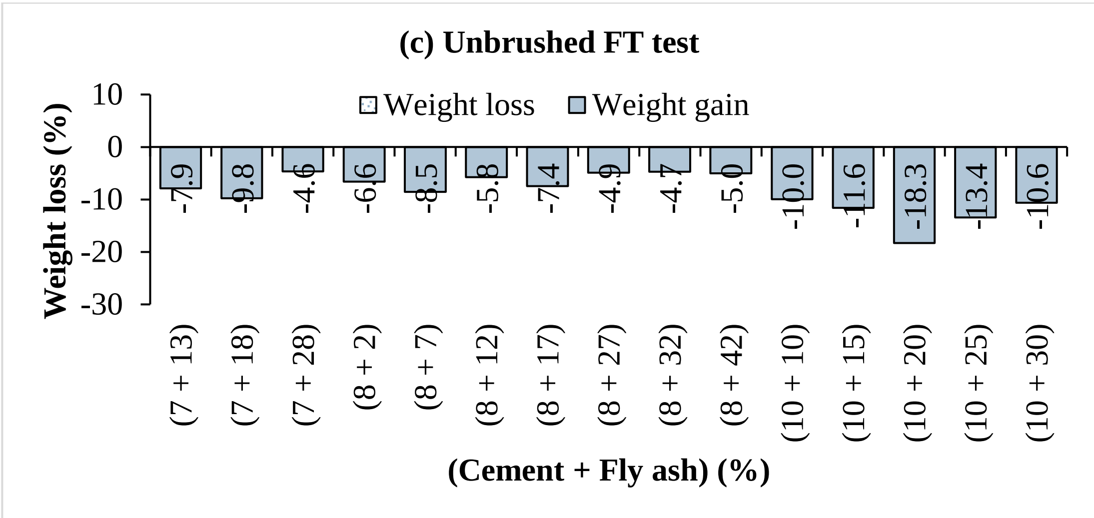
(c) Unbrushed FT test
Weight loss
Weight gain
Weight loss (%)
10
0
-10
-20
-30
-7.9
-9.8
-4.6
-6.6
-8.5
-5.8
-7.4
-4.9
-4.7
-5.0
-10.0
-11.6
-18.3
-13.4
-10.6
(7 + 13)
(7 + 18)
(7 + 28)
(8 + 2)
(8 + 7)
(8 + 12)
(8 + 17)
(8 + 27)
(8 + 32)
(8 + 42)
(10 + 10)
(10 + 15)
(10 + 20)
(10 + 25)
(10 + 30)
(Cement + Fly ash) (%)

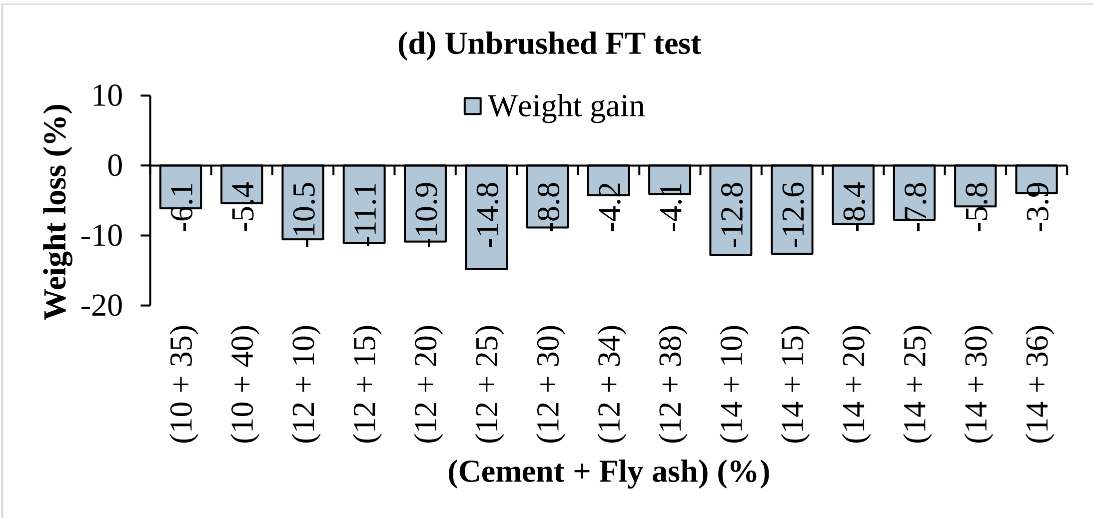
(d) Unbrushed FT test
Weight gain
Weight loss (%)
10
0
-10
-20
-6.1
-5.4
-10.5
-11.1
-10.9
-14.8
-8.8
-4.2
-4.1
-12.8
-12.6
-8.4
-7.8
-5.8
-3.9
(10 + 35)
(10 + 40)
(12 + 10)
(12 + 15)
(12 + 20)
(12 + 25)
(12 + 30)
(12 + 34)
(12 + 38)
(14 + 10)
(14 + 15)
(14 + 20)
(14 + 25)
(14 + 30)
(14 + 36)
(Cement + Fly ash) (%)

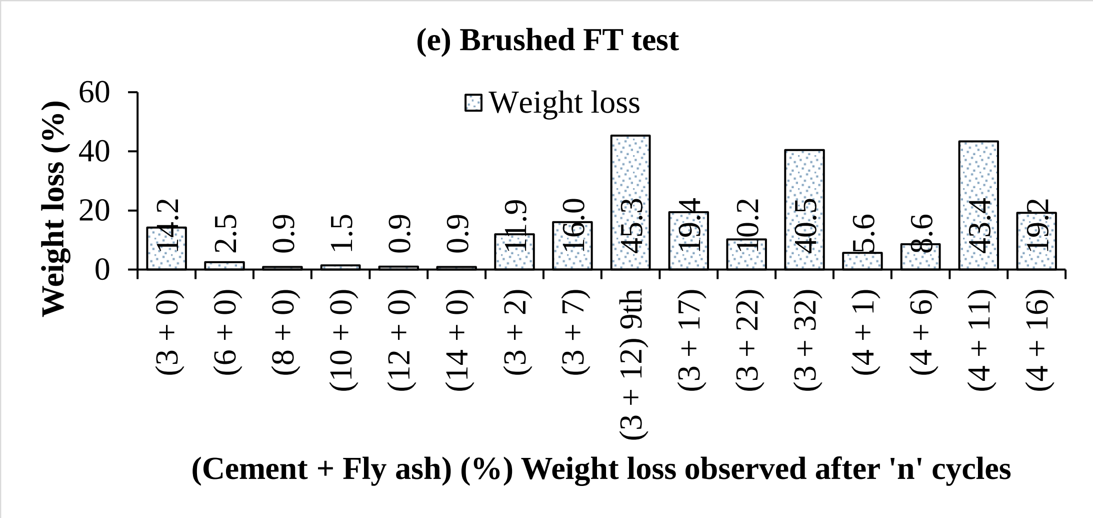
(e) Brushed FT test
Weight loss
Weight loss (%)
60
40
20
0
14.2
2.5
0.9
1.5
0.9
0.9
11.9
16.0
45.3
19.4
10.2
40.5
5.6
8.6
43.4
19.2
(3 + 0)
(6 + 0)
(8 + 0)
(10 + 0)
(12 + 0)
(14 + 0)
(3 + 2)
(3 + 7)
(3 + 12) 9th
(3 + 17)
(3 + 22)
(3 + 32)
(4 + 1)
(4 + 6)
(4 + 11)
(4 + 16)
(Cement + Fly ash) (%) Weight loss observed after 'n' cycles

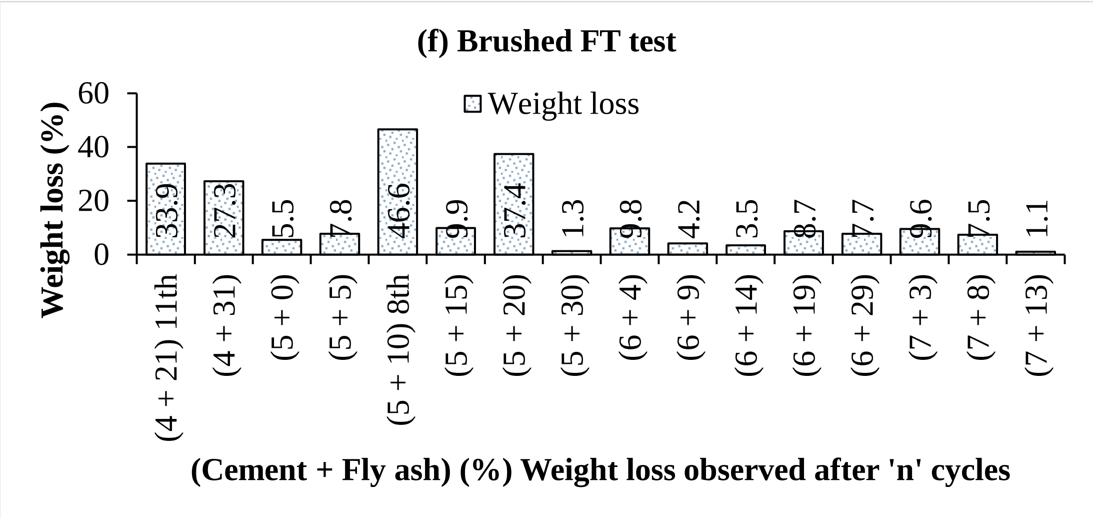
(f) Brushed FT test
Weight loss
Weight loss (%)
60
40
20
0
33.9
27.3
5.5
7.8
46.6
9.9
37.4
1.3
9.8
4.2
3.5
8.7
7.7
9.6
7.5
1.1
(4 + 21) 11th
(4 + 31)
(5 + 0)
(5 + 5)
(5 + 10) 8th
(5 + 15)
(5 + 20)
(5 + 30)
(6 + 4)
(6 + 9)
(6 + 14)
(6 + 19)
(6 + 29)
(7 + 3)
(7 + 8)
(7 + 13)
(Cement + Fly ash) (%) Weight loss observed after 'n' cycles

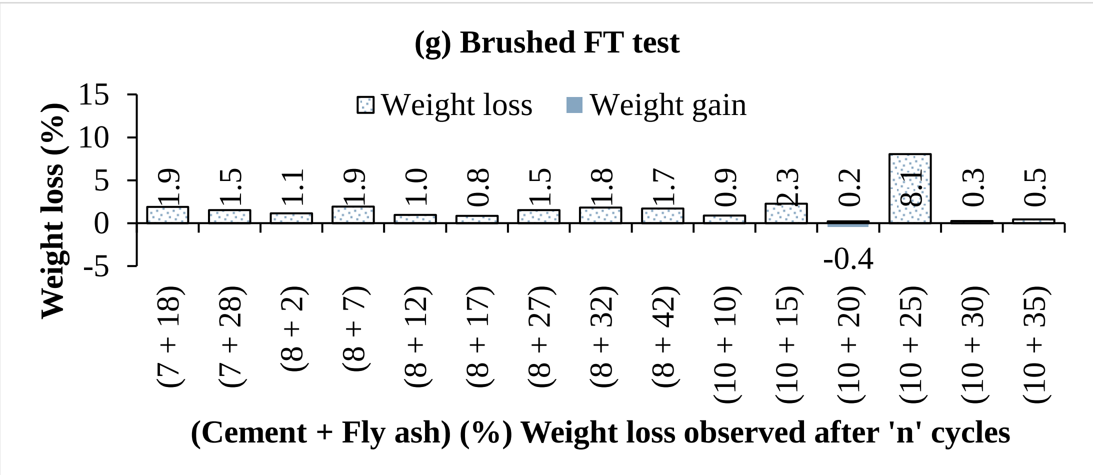
(g) Brushed FT test
Weight loss
Weight gain
Weight loss (%)
15
10
5
0
-5
1.9
1.5
1.1
1.9
1.0
0.8
1.5
1.8
1.7
0.9
2.3
0.2
-0.4
8.1
0.3
0.5
(7 + 18)
(7 + 28)
(8 + 2)
(8 + 7)
(8 + 12)
(8 + 17)
(8 + 27)
(8 + 32)
(8 + 42)
(10 + 10)
(10 + 15)
(10 + 20)
(10 + 25)
(10 + 30)
(10 + 35)
(Cement + Fly ash) (%) Weight loss observed after 'n' cycles

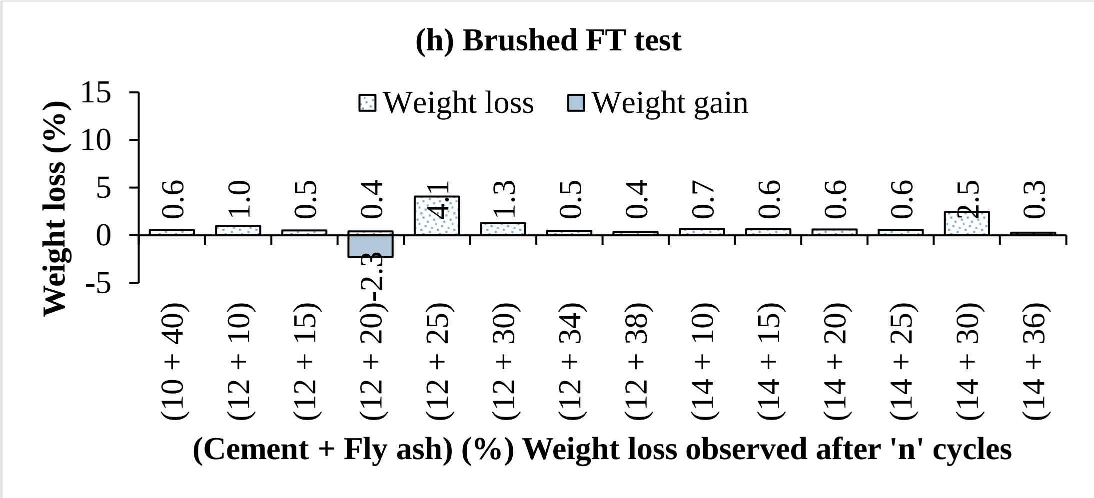

Figure 4. 14 Weight loss of cement stabilized BC soil with various fly ash dosages under (a), (b), (c), (d) unbrushed and (e), (f), (g), (h) brushed freeze-thaw durability test

Note:- In figures, weight loss of specimens is after 12 WD/FT cycles if not mentioned.

Table 4. 11 Shrinkage values of cement-fly ash stabilized BC soil after freezing

Cement (%)	Fly ash (%)	Shrinkage (%)
3	2–32	1.91–0.60
4	1–31	1.58–0.48
5	0–30	1.20–0.37
6	4–29	0.70–0.21
7	3–28	0.45–0.10
8	2–42	0.20–0.10
10	10–40	0.10–0.00
12	10–38	0.10–0.00
14	10–36	0.10–0.00

4.2.6 Retained UCS

After WD test:- Retained UCS values are very significant to assess the strength of the soil sample after vigorous WD and FT tests. This indicates the sustainability of the material in adverse environmental conditions. Stabilized specimens subjected to different durability cycles were tested for retained UCS. Generally, the specimens with higher cement, fly ash percentages showed good resistance to soil loss and retained higher UCS. The results are depicted in Figure 4.15(a–j). Most of the specimens retained a moisture content of less than 5% after the WD test. There was 4.2% weight loss for the unbrushed specimen with 14% cement and 25% fly ash after the dry test, and its retained UCS value 3.6 MPa at 2.9% moisture content. The same sample, when cured for 28 days and tested, its UCS value was 2.80 MPa. The moisture content at the time of the UCS test was around 25%. After wet and dry cycles, the moisture in the sample was reduced to 5%. Due to this variation in moisture, the retained UCS values are marginally higher. The moisture plays a significant role in retained UCS. A uniform mix with proper distribution of cement and fly ash particles, sufficient moisture availability for hydration, higher mix density, and adequately formed cement clusters leads to low soil loss and higher retained strength. The effect of brushing cannot be perfectly correlated to the soil loss and retained UCS values.

After FT test:- The specimen with 3% cement failed after 12 cycles due to more moisture absorption. As the cement content increased, the retained UCS values increased due to improved cement cluster formation. The specimen with 14% cement at unbrushed condition attained UCS of 1.6 MPa, which is the highest. Most of the specimens retained a moisture content >20% after the test. When tested at unbrushed conditions, the specimen with 14% cement and 30% fly ash could get a retained UCS of 2.6 MPa with 23.3% moisture. The sample with 12% cement and 38% fly ash could get a higher retained UCS of 3.4 MPa at 25.7% moisture. The brushed sample with 14% cement and 36% fly ash could get a higher UCS of 4.1 MPa at 25% moisture. The sample with 12% cement and 38% fly ash could get a retained UCS of 2.2 MPa at 26.8% moisture.

But, a brushed sample with 12% cement and 25% fly ash could get a low UCS value of 0.01 MPa at 29% moisture content. Therefore, even when the cement and fly ash contents are more, the specimen absorbs more moisture at every cycle and develops more void spaces, thereby expanding volume. Low retained UCS values are obtained even though there is adequate cement available for hydration due to expansion. Therefore, in FT specimens, the increase in moisture and volume expansion are governing factors for the retained UCS.

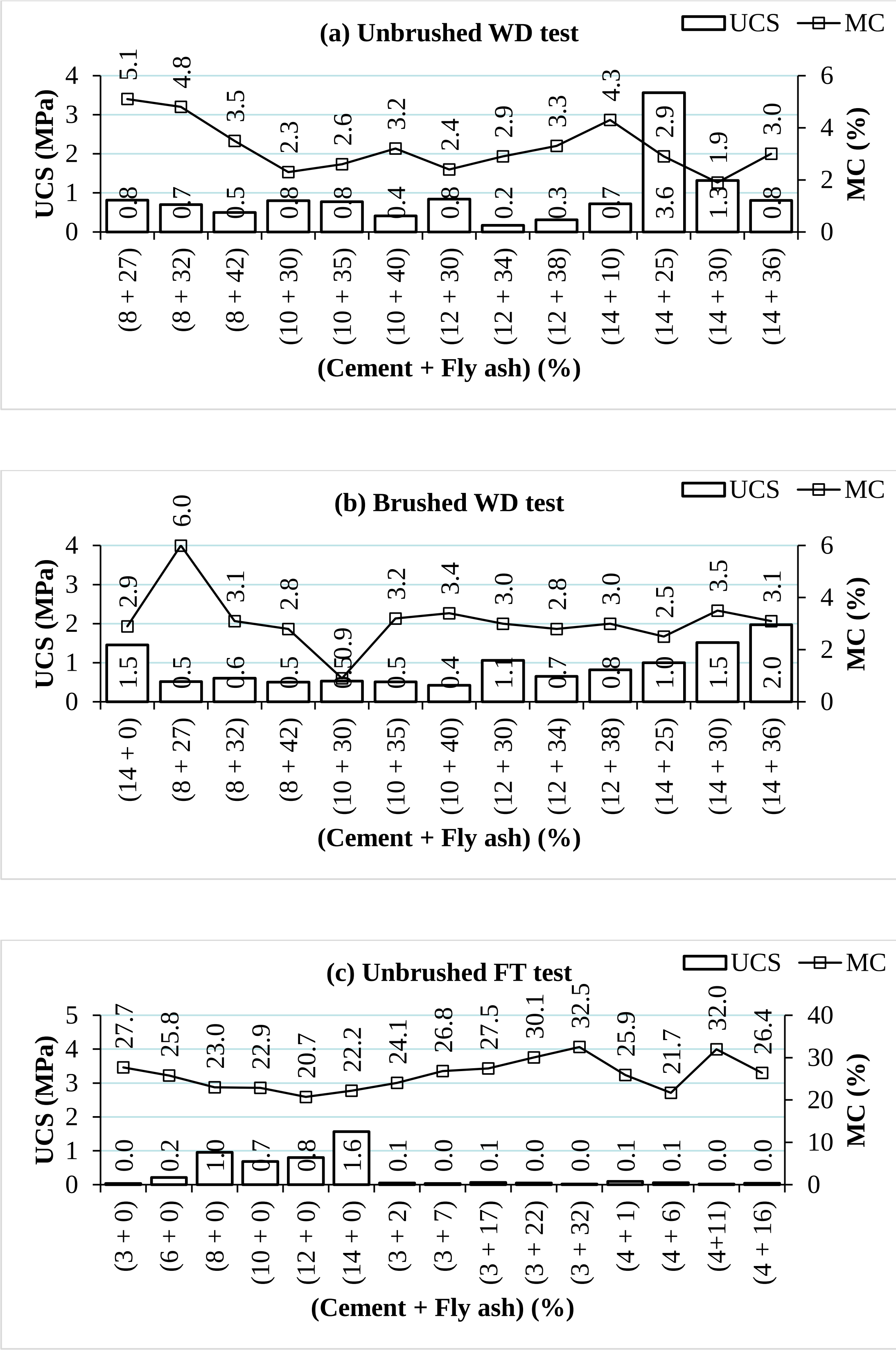
(a) Unbrushed WD test
UCS
MC
UCS (MPa)
MC (%)
5.1 4.8 3.5 2.3 2.6 3.2 2.4 2.9 3.3 4.3 2.9 1.9 3.0
0.8 0.7 0.5 0.8 0.8 0.4 0.8 0.2 0.3 0.7 3.6 1.3 0.8
(8 + 27) (8 + 32) (8 + 42) (10 + 30) (10 + 35) (10 + 40) (12 + 30) (12 + 34) (12 + 38) (14 + 10) (14 + 25) (14 + 30) (14 + 36)
(Cement + Fly ash) (%)
(b) Brushed WD test
UCS
MC
UCS (MPa)
MC (%)
2.9 6.0 3.1 2.8 0.9 3.2 3.4 3.0 2.8 3.0 2.5 3.5 3.1
1.5 0.5 0.6 0.5 0.5 0.5 0.4 1.1 0.7 0.8 1.0 1.5 2.0
(14 + 0) (8 + 27) (8 + 32) (8 + 42) (10 + 30) (10 + 35) (10 + 40) (12 + 30) (12 + 34) (12 + 38) (14 + 25) (14 + 30) (14 + 36)
(Cement + Fly ash) (%)
(c) Unbrushed FT test
UCS
MC
UCS (MPa)
MC (%)
27.7 25.8 23.0 22.9 20.7 22.2 24.1 26.8 27.5 30.1 32.5 25.9 21.7 32.0 26.4
0.0 0.2 1.0 0.7 0.8 1.6 0.1 0.0 0.1 0.0 0.0 0.1 0.1 0.0 0.0
(3 + 0) (6 + 0) (8 + 0) (10 + 0) (12 + 0) (14 + 0) (3 + 2) (3 + 7) (3 + 17) (3 + 22) (3 + 32) (4 + 1) (4 + 6) (4+11) (4 + 16)
(Cement + Fly ash) (%)

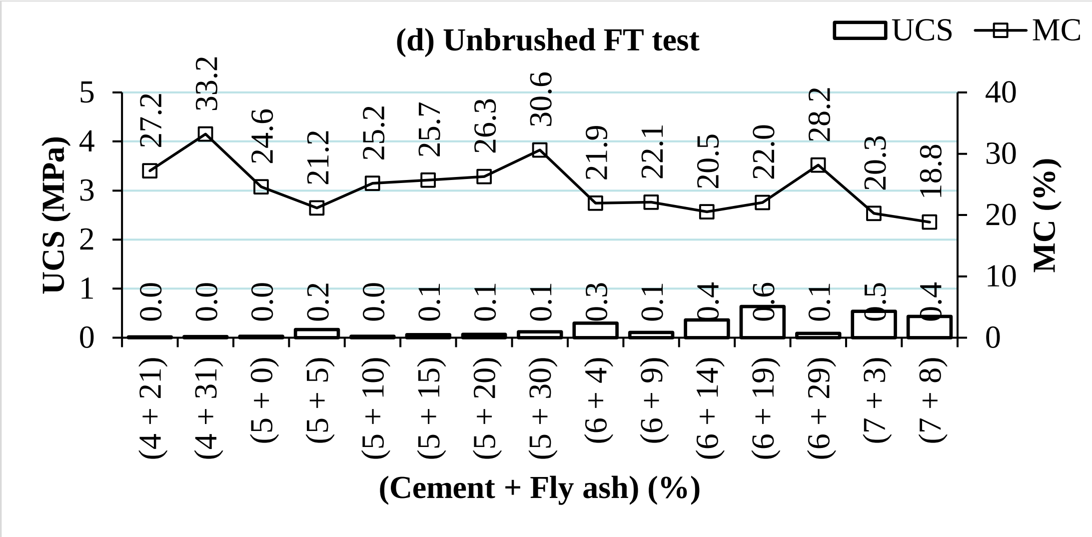

(d) Unbrushed FT test
UCS
MC
UCS (MPa)
MC (%)
(Cement + Fly ash) (%)
(4 + 21)
(4 + 31)
(5 + 0)
(5 + 5)
(5 + 10)
(5 + 15)
(5 + 20)
(5 + 30)
(6 + 4)
(6 + 9)
(6 + 14)
(6 + 19)
(6 + 29)
(7 + 3)
(7 + 8)

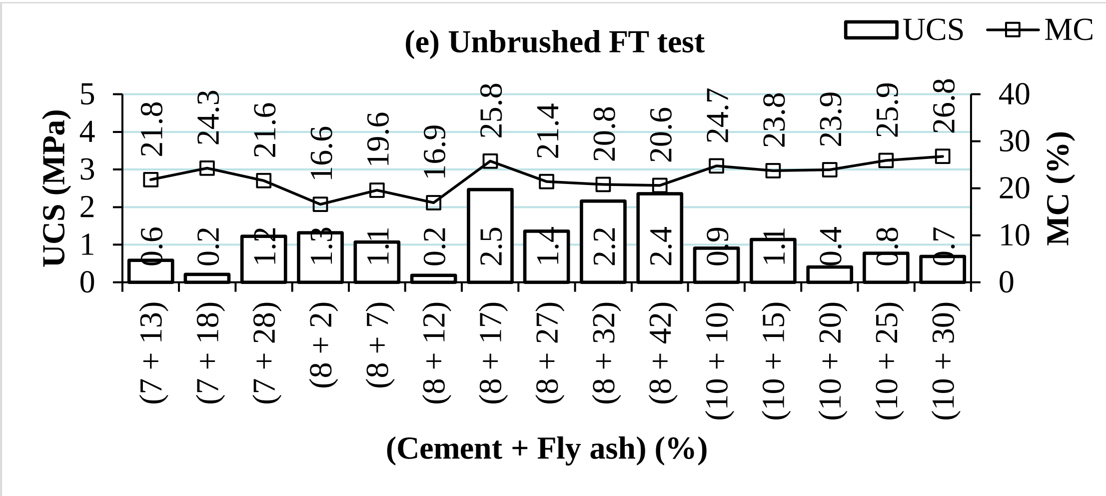

(e) Unbrushed FT test
UCS
MC
UCS (MPa)
MC (%)
(Cement + Fly ash) (%)
(7 + 13)
(7 + 18)
(7 + 28)
(8 + 2)
(8 + 7)
(8 + 12)
(8 + 17)
(8 + 27)
(8 + 32)
(8 + 42)
(10 + 10)
(10 + 15)
(10 + 20)
(10 + 25)
(10 + 30)

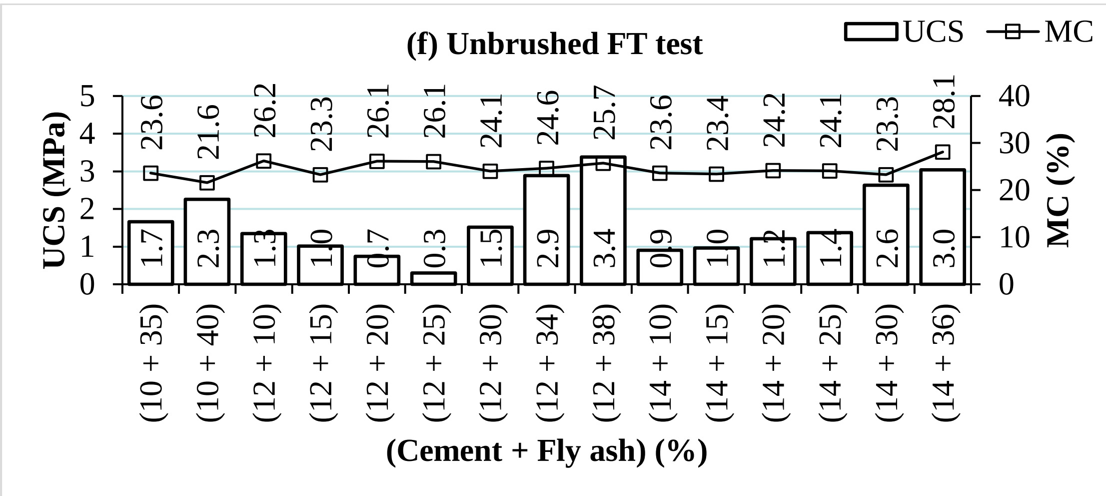

(f) Unbrushed FT test
UCS
MC
UCS (MPa)
MC (%)
(Cement + Fly ash) (%)
(10 + 35)
(10 + 40)
(12 + 10)
(12 + 15)
(12 + 20)
(12 + 25)
(12 + 30)
(12 + 34)
(12 + 38)
(14 + 10)
(14 + 15)
(14 + 20)
(14 + 25)
(14 + 30)
(14 + 36)

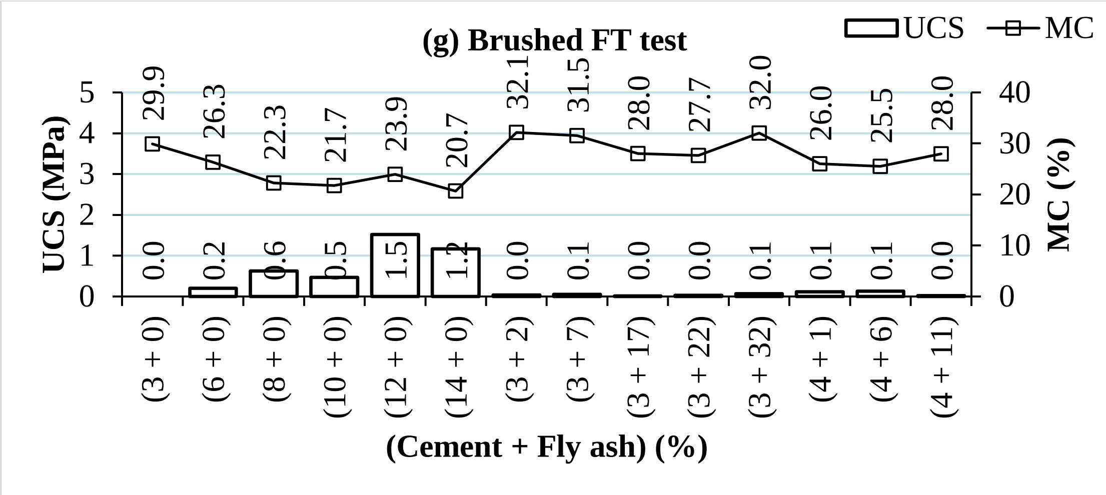
(g) Brushed FT test
UCS
MC
UCS (MPa)
MC (%)
29.9 26.3 22.3 21.7 23.9 20.7 32.1 31.5 28.0 27.7 32.0 26.0 25.5 28.0
0.0 0.2 0.6 0.5 1.5 1.2 0.0 0.1 0.0 0.0 0.1 0.1 0.1 0.0
(3 + 0) (6 + 0) (8 + 0) (10 + 0) (12 + 0) (14 + 0) (3 + 2) (3 + 7) (3 + 17) (3 + 22) (3 + 32) (4 + 1) (4 + 6) (4 + 11)
(Cement + Fly ash) (%)

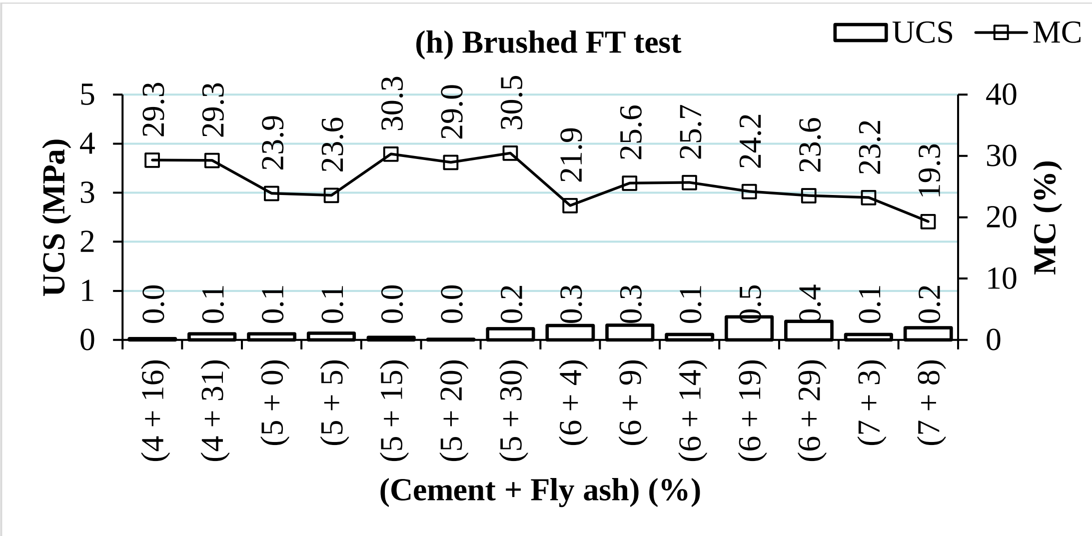
(h) Brushed FT test
UCS
MC
UCS (MPa)
MC (%)
29.3 29.3 23.9 23.6 30.3 29.0 30.5 21.9 25.6 25.7 24.2 23.6 23.2 19.3
0.0 0.1 0.1 0.1 0.0 0.0 0.2 0.3 0.3 0.1 0.5 0.4 0.1 0.2
(4 + 16) (4 + 31) (5 + 0) (5 + 5) (5 + 15) (5 + 20) (5 + 30) (6 + 4) (6 + 9) (6 + 14) (6 + 19) (6 + 29) (7 + 3) (7 + 8)
(Cement + Fly ash) (%)

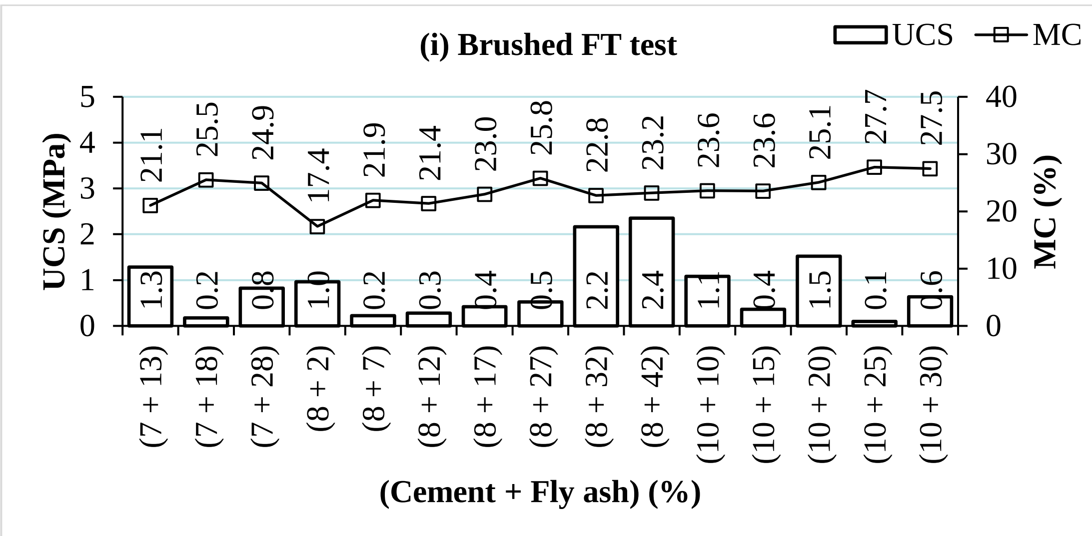
(i) Brushed FT test
UCS
MC
UCS (MPa)
MC (%)
21.1 25.5 24.9 17.4 21.9 21.4 23.0 25.8 22.8 23.2 23.6 23.6 25.1 27.7 27.5
1.3 0.2 0.8 1.0 0.2 0.3 0.4 0.5 2.2 2.4 1.1 0.4 1.5 0.1 0.6
(7 + 13) (7 + 18) (7 + 28) (8 + 2) (8 + 7) (8 + 12) (8 + 17) (8 + 27) (8 + 32) (8 + 42) (10 + 10) (10 + 15) (10 + 20) (10 + 25) (10 + 30)
(Cement + Fly ash) (%)

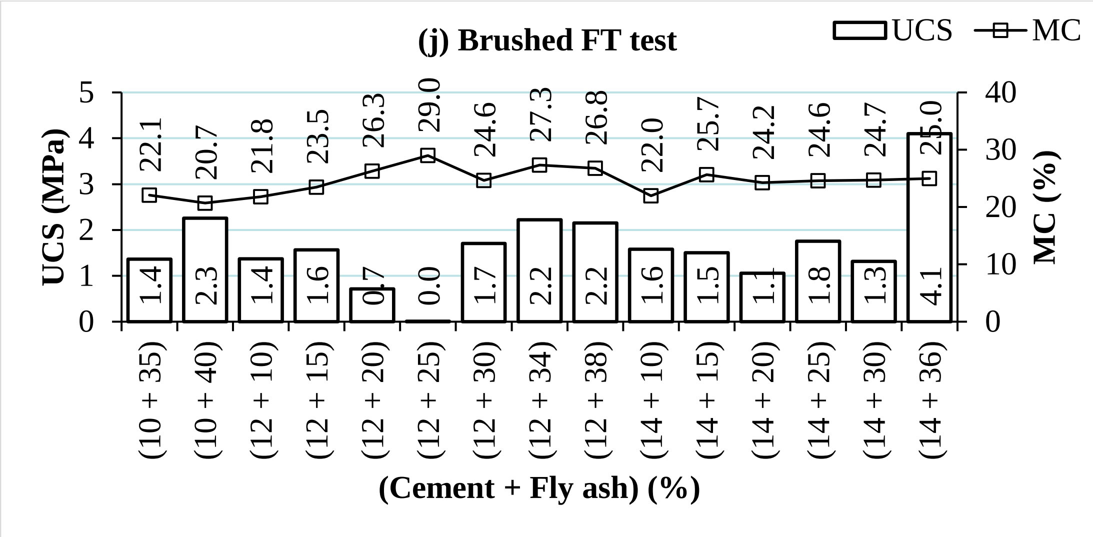

Figure 4. 15 Retained UCS of cement stabilized BC soil with various fly ash dosages under (a) unbrushed WD, (b) brushed WD, (c), (d), (e), (f) unbrushed FT, and (g), (h), (i), (j) brushed FT tests

4.3 BC SOIL STABILIZATION WITH CEMENT, CLASS F FLY ASH, AND COCONUT FIBERS

4.3.1 Compaction

Coconut fibers are added to the durability test passed soil samples consisting of cement and fly ash to enhance its fatigue life and flexural strength. A preliminary investigation was carried out with coconut fibers having the length of 25 mm for different dosages ranging from 0.25, 0.5, 0.75, and 1.0%. If the fibers are added beyond 0.5%, the balling effect is taking place and found difficult to distribute fibers uniformly in the mix. Therefore, in the present investigation, only 0.5% of fibers are fixed for all cement and fly ash combinations. The MDD values of fiber stabilized soil were marginally reduced due to lighter material and are depicted in Figures 4.16 and 4.17. The mix with 10% cement and 30% fly ash along with fibers achieved the MDD of 1.69 g/cc at 20.2% moisture for the modified Proctor test. It was observed that at higher content of cement, fly ash, the MDD reduces and OMC increases, and it is quite obvious when lighter materials are replaced with soil.

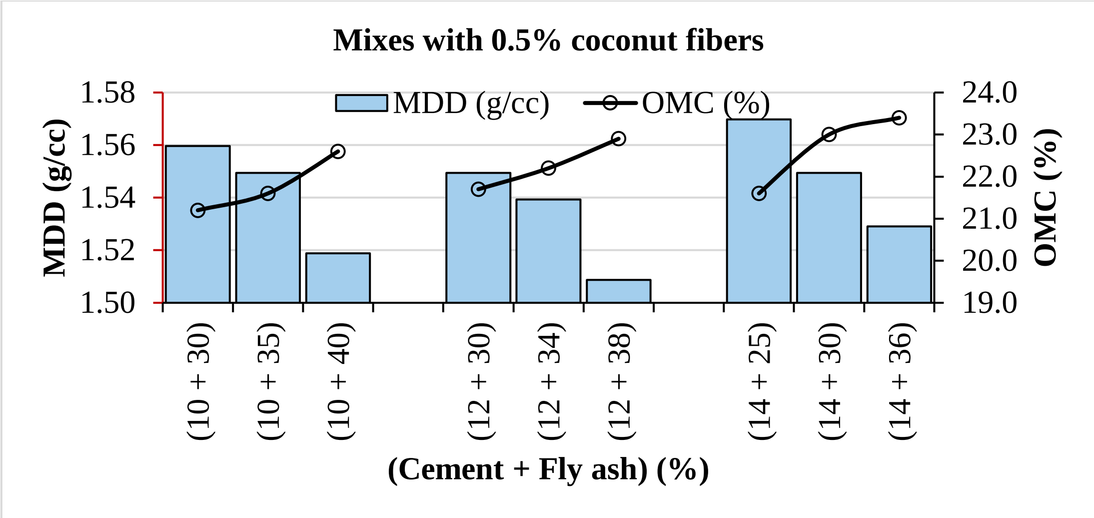

Figure 4. 16 Standard Proctor test results for cement, fly ash, and 0.5% coconut fiber treated BC soil

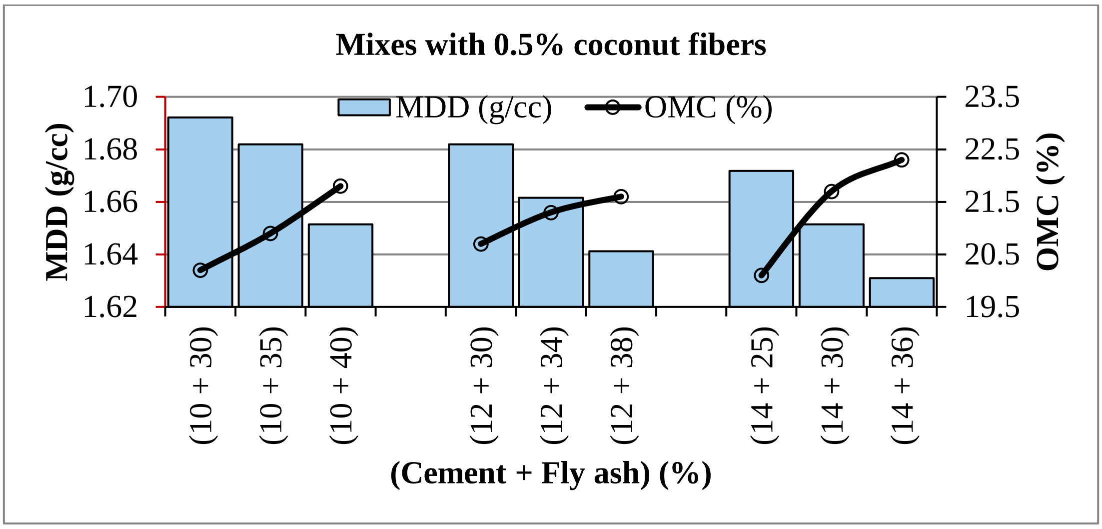

Figure 4. 17 Modified Proctor test results for cement, fly ash, and 0.5% coconut fiber treated BC soil

4.3.2 Unconfined Compressive Strength

There is an improvement in the UCS values of cement, fly ash, and fiber-treated samples, as depicted in Figures 4.18 and 4.20. All the mixes exhibited a marginal decrease in UCS values due to a marginal reduction in density. The specimen with 14% cement, 36% fly ash, and 0.50% fibers could achieve the UCS value of 6.1 MPa at modified Proctor density. The fiber inclusion exhibited good interlocking of bonded soil particles. The fibers have good strength to resist the failure of the specimen in bending. When the load was applied to specimens with coconut fibers, the sample was separated at the fiber interface. Based on the dimension of the specimen and aspect ratio of fiber, the strength varies. In smaller UCS specimens, due to overlapping of fibers, quick crack development was observed. Since the specimen is unconfined and hence, the crack propagation was unrestricted. However, the effect of fibers was significant in flexure and fatigue tests.

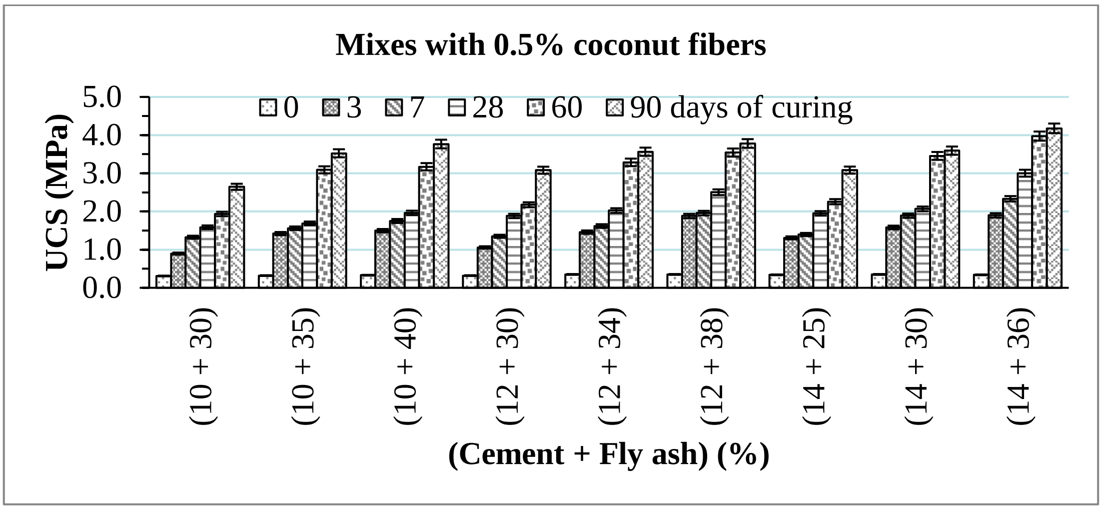

Figure 4. 18 UCS of BC soil stabilized with cement, fly ash, and 0.5% coconut fibers at standard Proctor density

ANOVA: Univariate analysis of variance performed indicates that the UCS values are significantly (i.e., $p<0.05$) influenced by the dosage of cement, dosage of fly ash, and curing period. $R^2 = 0.938$ indicates that 93.8% of the variance in UCS values can be explained by the dosage of cement, dosage of fly ash, and curing period. However, the same dosage of coconut fiber of 0.5% added in all stabilized mixes has the same effect on strength. The ANOVA results are tabulated in Table 4.12.

Table 4. 12 ANOVA of UCS with the dosage of cement, dosage of fly ash, 0.5% coconut fibers, and curing period at standard Proctor density

Tests of Between-Subjects Effects					
Dependent Variable: UCS (MPa)					
Source	Type III Sum of Squares	df	Mean Square	F	Sig.
Corrected Model	48.973[a]	13	3.767	46.508	.000
Intercept	113.707	1	113.707	1403.792	.000
Cement	1.121	2	.561	6.920	.003
Fly ash	3.207	6	.534	6.598	.000
Curing	44.953	5	8.991	110.996	.000
Coconut fiber	.000	0	.	.	.
Error	3.240	40	.081		

Total	175.520	54			
Corrected Total	52.213	53			
a. R^2= .938 (Adjusted R^2= .918)					

E values at standard and modified Proctor density:- The 'm' values calculated for different cement and fly ash combinations along with fibers are depicted in Figures 4.19 and 4.21. The variation of UCS versus E for different curing periods for different mixes is tabulated in Tables 4.13 and 4.15. The modulus of elasticity of fiber stabilized soils exhibited slightly lower values due to lighter material as shown in Tables 4.16 and 4.17.

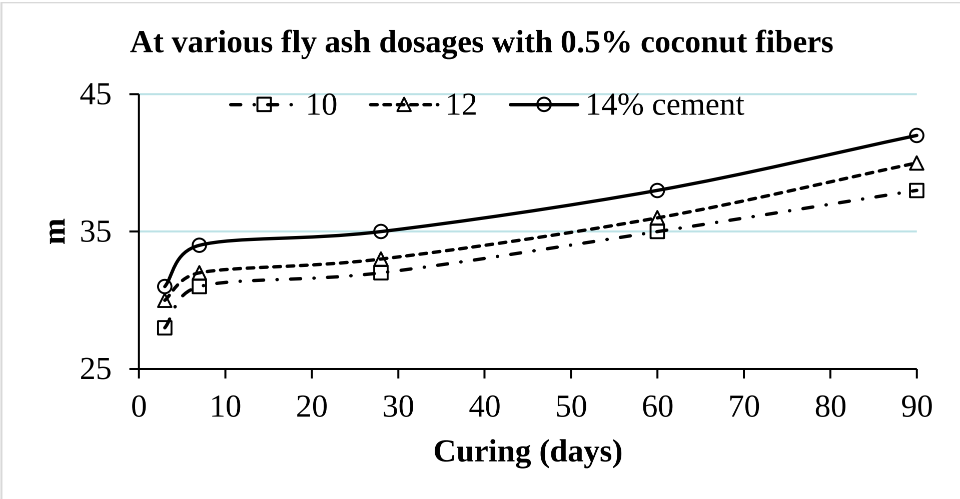

Figure 4. 19 'm' values for cement, fly ash, and 0.5% coconut fiber stabilized BC soil at standard Proctor density

Table 4. 13 'E' values for cement, fly ash, and 0.5% coconut fiber stabilized BC soil at standard Proctor density

Cement + (Fly ash) (%)	Curing (days)	UCS (MPa)	m	E (MPa)
10 + (30–40)	3	0.9–1.5	28	25–42
	7	1.3–1.8	31	40–56
	28	1.6–2.0	32	51–64
	60	1.9–3.2	35	67–112
	90	2.6–3.8	38	99–144
12 + (30–38)	3	1.1–1.9	30	33–57
	7	1.3–2.0	32	42–64
	28	1.9–2.5	33	63–83
	60	2.2–3.5	36	79–126
	90	3.1–3.8	40	124–152
14 + (25–36)	3	1.3–1.9	31	40–59
	7	1.4–2.3	34	48–78
	28	2.0–3.0	35	70–105
	60	2.3–4.0	38	87–152
	90	3.1–4.2	42	130–176

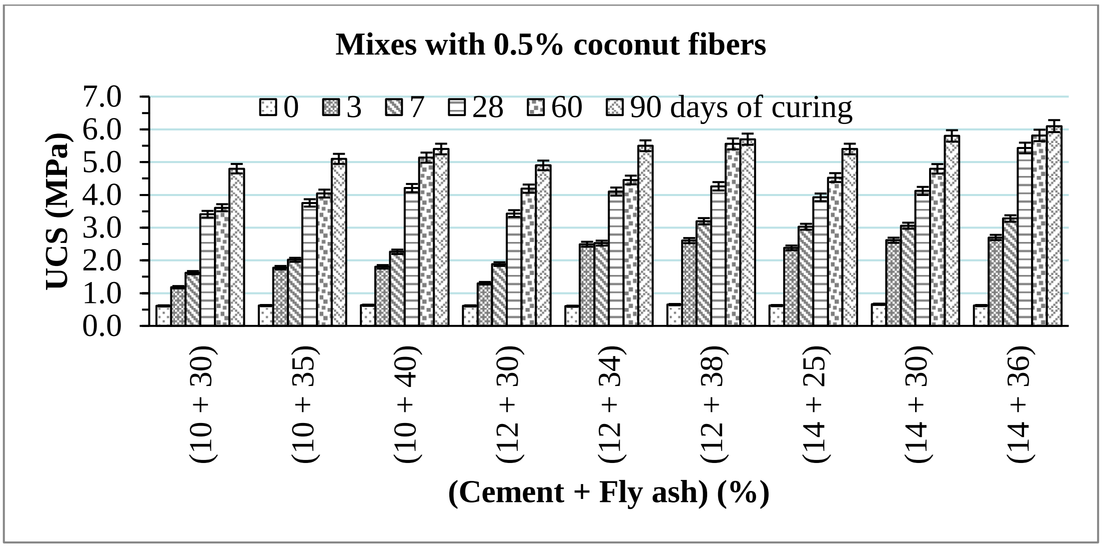

Figure 4. 20 UCS of BC soil stabilized with cement, fly ash, and 0.5% coconut fibers at modified Proctor density

ANOVA: Univariate analysis of variance performed indicates that the UCS values are significantly (i.e., $p<0.05$) influenced by the dosage of cement, dosage of fly ash, and curing period. $R^2 = 0.975$ indicates that 97.5% of the variance in UCS values can be explained by the dosage of cement, dosage of fly ash, and curing period. However, the same dosage of coconut fiber of 0.5% added in all stabilized mixes has the same effect on strength. The ANOVA results are tabulated in Table 4.14.

Table 4. 14 ANOVA of UCS with the dosage of cement, dosage of fly ash, 0.5% coconut fibers, and curing period at modified Proctor density

Tests of Between-Subjects Effects					
Dependent Variable: UCS (MPa)					
Source	Type III Sum of Squares	df	Mean Square	F	Sig.
Corrected Model	155.293[a]	13	11.946	117.895	.000
Intercept	513.826	1	513.826	5071.119	.000
Curing	144.904	5	28.981	286.020	.000
Cement	3.281	2	1.641	16.191	.000
Fly ash	5.764	6	.961	9.482	.000
Coconut fiber	.000	0	.	.	.
Error	4.053	40	.101		
Total	725.180	54			
Corrected Total	159.346	53			
a. R^2= .975 (Adjusted R^2= .966)					

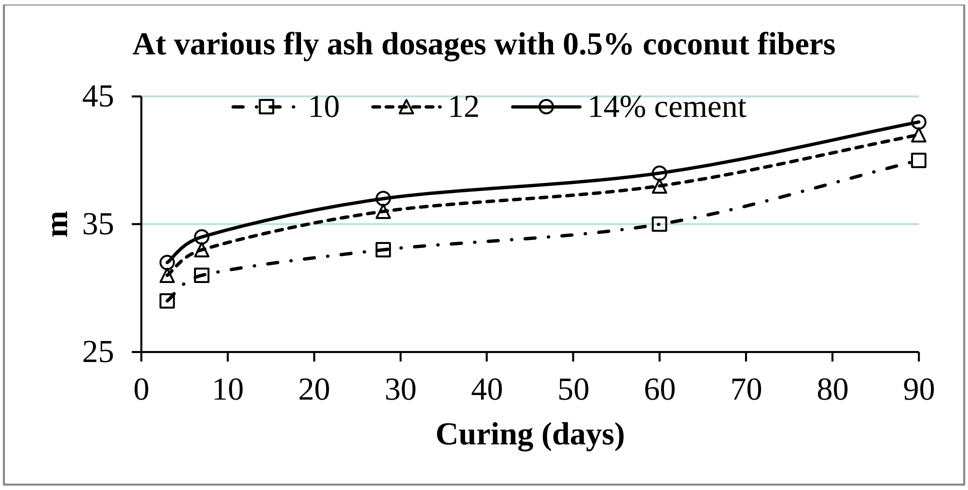

Figure 4. 21 'm' values for cement, fly ash, and 0.5% coconut fiber stabilized BC soil at modified Proctor density

Table 4. 15 'E' values for cement, fly ash, and 0.5% coconut fiber stabilized BC soil at modified Proctor density

Cement + (Fly ash) (%)	Curing (days)	UCS (MPa)	m	E (MPa)
10 + (30–40)	3	1.2–1.8	29	35–52
	7	1.6–2.3	31	50–71
	28	3.4–4.2	33	112–139
	60	3.6–5.1	35	126–179
	90	4.8–5.4	40	192–216
12 + (30–38)	3	1.3–2.6	31	40–81
	7	1.9–3.2	33	63–106
	28	3.4–4.3	36	122–155
	60	4.2–5.6	38	160–213
	90	4.9–5.7	42	206–239
14 + (25–36)	3	2.4–2.7	32	77–86
	7	3.0–3.3	34	102–112
	28	3.9–5.4	37	144–200
	60	4.5–5.8	39	176–226
	90	5.4–6.1	43	232–262

Table 4. 16 Comparision of 'E' values for cement, fly ash, stabilized BC soil with and without coconut fiber at standard Proctor density

Cement + (Fly ash) (%)	Curing (Days)	Without coconut fiber			With 0.5% coconut fiber		
		UCS (MPa)	m	E (MPa)	UCS (MPa)	m	E (MPa)
10+ (30–40)	3	1.7–1.9	33	56–63	0.9–1.5	28	25–42
	7	2.8–3.0	38	106–114	1.3–1.8	31	40–56
	28	3.7–4.0	42	155–168	1.6–2.0	32	51–64
	60	3.8–4.3	47	179–202	1.9–3.2	35	67–112
	90	4.6–5.2	60	276–312	2.6–3.8	38	99–144

12+ (30–38)	3	1.9–2.6	34	65–88	1.1–1.9	30	33–57
	7	2.8–3.0	39	109–117	1.3–2.0	32	42–64
	28	3.8–3.9	43	163–168	1.9–2.5	33	63–83
	60	4.0–4.9	49	196–240	2.2–3.5	36	79–126
	90	5.2–7.2	62	322–446	3.1–3.8	40	124–152
14+ (25–36)	3	1.7–2.6	35	60–91	1.3–1.9	31	40–59
	7	2.7–3.1	40	108–124	1.4–2.3	34	48–78
	28	3.7–4.2	46	170–193	2.0–3.0	35	70–105
	60	3.9–5.5	53	207–292	2.3–4.0	38	87–152
	90	5.8–7.2	66	383–475	3.1–4.2	42	130–176

Table 4. 17 Comparision of 'E' values for cement, fly ash, stabilized BC soil with and without coconut fiber at modified Proctor density

Cement + (Fly ash) (%)	Curing (Days)	Without coconut fiber			With 0.5% coconut fiber		
		UCS (MPa)	m	E (MPa)	UCS (MPa)	m	E (MPa)
10+ (30–40)	3	1.7–2.1	37	63–78	1.2–1.8	29	35–52
	7	2.9–3.1	40	116–124	1.6–2.3	31	50–71
	28	3.7–4.0	47	174–188	3.4–4.2	33	112–139
	60	3.9–4.4	60	234–264	3.6–5.1	35	126–179
	90	4.6–5.4	67	308–362	4.8–5.4	40	192–216
12+ (30–38)	3	1.9–2.6	38	72–99	1.3–2.6	31	40–81
	7	3.0–3.2	43	129–138	1.9–3.2	33	63–106
	28	3.9–4.2	50	195–210	3.4–4.3	36	122–155
	60	4.3–5.2	63	271–328	4.2–5.6	38	160–213
	90	5.3–7.2	72	382–518	4.9–5.7	42	206–239
14+ (25–36)	3	1.8–2.7	42	76–113	2.4–2.7	32	77–86
	7	3.2–3.5	46	147–161	3.0–3.3	34	102–112
	28	4.2–4.6	54	227–248	3.9–5.4	37	144–200
	60	5.0–6.5	75	375–488	4.5–5.8	39	176–226
	90	6.1–7.3	83	506–606	5.4–6.1	43	232–262

4.3.3 Flexural Strength

The inclusion of fibers in cement-fly ash stabilized soil significantly contributes to flexural strength, as depicted in Figure 4.23(a, b). The shrinkage cracks were disappeared with the addition of fibers (Figure 4.22). The specimen developed cracks in the flexure test under two-point loading, and fibers restricted the crack propagation. While observing crack propagation, the fibers were pulled out of soil-cement clods. The failure strains were significantly increased, and the specimens were found to be more flexible. Maximum flexural strength of 1.98 MPa was observed for BC soil treated with 14% cement and 36% fly ash at modified compaction after 28 days of curing.

Figure 4. 22 Beam specimen of BC soil stabilized with Cement, fly ash, and 0.5% coconut fiber without cracks

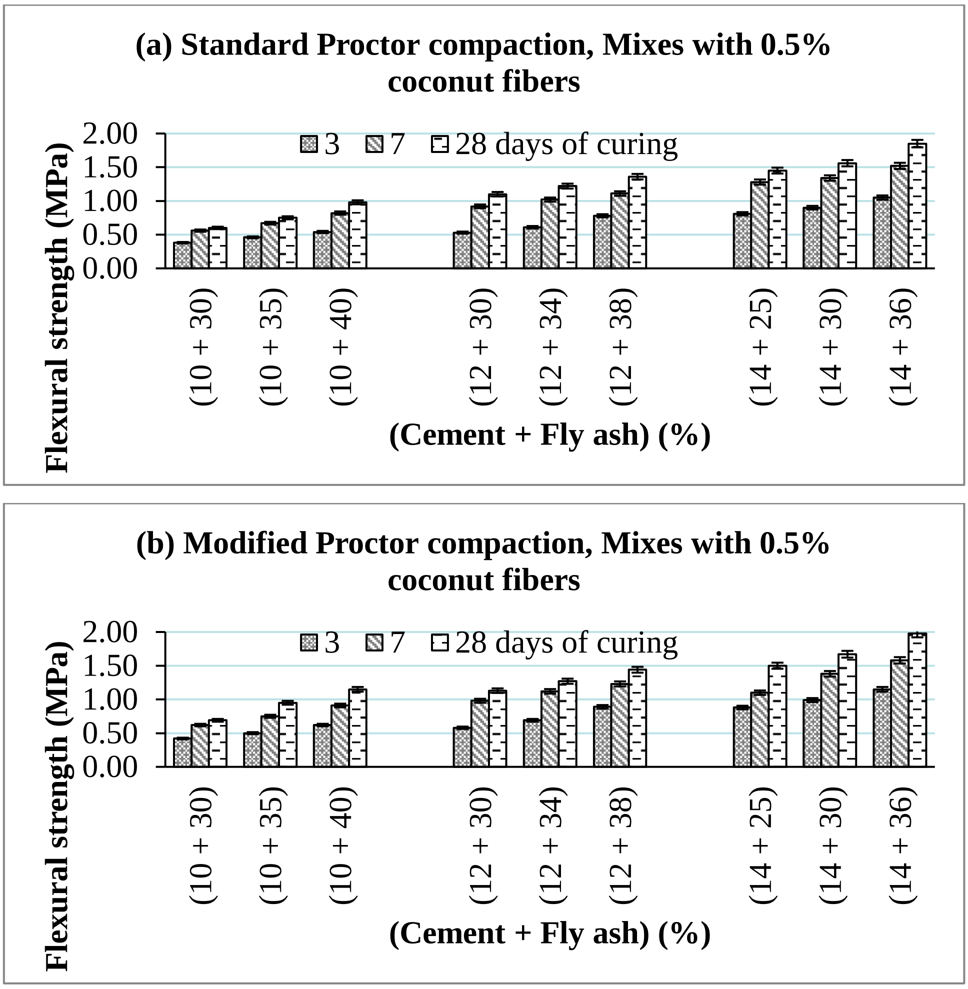

Figure 4. 23 Flexural strength of BC soil stabilized with cement, fly ash, and 0.5% coconut fibers at (a) standard, (b) modified Proctor density

ANOVA: Univariate analysis of variance performed indicates that the flexural strength values are significantly (i.e., $p<0.05$) influenced by the dosage of cement, dosage of fly ash, and curing period. R^2 = 0.962, 0.969 indicates that 96.2% and 96.9% of the variance in flexural strength values can be explained by the dosage of cement, dosage of fly ash, and curing period, at standard and modified Proctor compaction, respectively. However, the same dosage of coconut fiber of 0.5% added in all stabilized mixes has the same effect on strength. The ANOVA results are tabulated in Tables 4.18 and 4.19.

Table 4. 18 ANOVA of UCS with the dosage of cement, dosage of fly ash, 0.5% coconut fibers, and curing period at standard Proctor density

Tests of Between-Subjects Effects					
Dependent Variable: Flexural strength (MPa)					
Source	Type III Sum of Squares	df	Mean Square	F	Sig.
Corrected Model	3.657[a]	10	.366	40.884	.000
Intercept	23.012	1	23.012	2572.904	.000
Cement	.854	2	.427	47.768	.000
Fly ash	.326	6	.054	6.074	.002
Curing	1.330	2	.665	74.342	.000
Coconut fiber	.000	0	.	.	.
Error	.143	16	.009		
Total	29.165	27			
Corrected Total	3.800	26			
a. R^2= .962 (Adjusted R^2 = .939)					

Table 4. 19 ANOVA of UCS with the dosage of cement, dosage of fly ash, 0.5% coconut fibers, and curing period at modified Proctor density

Tests of Between-Subjects Effects					
Dependent Variable: Flexural strength (MPa)					
Source	Type III Sum of Squares	df	Mean Square	F	Sig.
Corrected Model	3.721[a]	10	.372	50.288	.000
Intercept	26.716	1	26.716	3610.926	.000
Curing	1.435	2	.718	97.011	.000
Cement	.898	2	.449	60.674	.000
Fly ash	.530	6	.088	11.936	.000
Coconut fiber	.000	0	.	.	.
Error	.118	16	.007		
Total	33.230	27			
Corrected Total	3.839	26			
a. R^2= .969 (Adjusted R^2= .950)					

Regression: Regression analysis is performed between UCS and flexural strength at standard and modified Proctor density, and the results are tabulated in Table 4.20 and

4.21, respectively. A correlation of 0.737 at standard Proctor density and 0.840 at modified Proctor density ($p<0.0005$) confirms a strong positive relationship between UCS and flexural strength. $R^2 = 0.543$ and 0.706 indicate that 54.3% and 70.6% of the variance in flexural strength can be explained by UCS at standard and modified Proctor density, respectively. From ANOVA, it can be concluded that the model is statistically significant ($p<0.0005$). From the coefficient table, for every 1 MPa increase in UCS, the model predicted an increase of 0.427 MPa and 0.312 MPa flexural strength at standard and modified Proctor density, respectively. Also, the t-test confirms the statistical significance of the model.

Table 4. 20 Regression analysis of UCS and flexural strength for BC soil stabilized with cement, fly ash, and 0.5% coconut fibers at standard Proctor density

Correlations

		Flexural strength (MPa)	UCS (MPa)
Pearson Correlation	Flexural strength (MPa)	1.000	.737
	UCS (MPa)	.737	1.000
Sig. (1-tailed)	Flexural strength (MPa)	.	.000
	UCS (MPa)	.000	.
N	Flexural strength (MPa)	27	27
	UCS (MPa)	27	27

Model Summary[b]

Model	R	R Square	Adjusted R Square	Std. Error of the Estimate
1	.737[a]	.543	.524	.26370

a. Predictors: (Constant), UCS (MPa)

b. Dependent Variable: Flexural strength (MPa)

ANOVA[a]

Model		Sum of Squares	df	Mean Square	F	Sig.
1	Regression	2.061	1	2.061	29.645	.000[b]
	Residual	1.738	25	.070		
	Total	3.800	26			

a. Dependent Variable: Flexural strength (MPa)

b. Predictors: (Constant), UCS (MPa)

Coefficients[a]

Model		Unstandardized Coefficients		Standardized Coefficients	t	Sig.	95.0% Confidence Interval for B	
		B	Std. Error	Beta			Lower Bound	Upper Bound
1	(Constant)	.474	.104		4.547	.000	.259	.688

	UCS (MPa)	.427	.078	.737	5.445	.000	.266	.589
a. Dependent Variable: Flexural strength (MPa)								

Table 4. 21 Regression analysis of UCS and flexural strength for BC soil stabilized with cement, fly ash, and 0.5% coconut fibers at modified Proctor density

Correlations			
		Flexural strength (MPa)	UCS (MPa)
Pearson Correlation	Flexural strength (MPa)	1.000	.840
	UCS (MPa)	.840	1.000
Sig. (1-tailed)	Flexural strength (MPa)	.	.000
	UCS (MPa)	.000	.
N	Flexural strength (MPa)	27	27
	UCS (MPa)	27	27

Model Summary[b]				
Model	R	R Square	Adjusted R Square	Std. Error of the Estimate
1	.840[a]	.706	.694	.21246
a. Predictors: (Constant), UCS (MPa)				
b. Dependent Variable: Flexural strength (MPa)				

ANOVA[a]						
Model		Sum of Squares	df	Mean Square	F	Sig.
1	Regression	2.711	1	2.711	60.047	.000[b]
	Residual	1.128	25	.045		
	Total	3.839	26			
a. Dependent Variable: Flexural strength (MPa)						
b. Predictors: (Constant), UCS (MPa)						

Coefficients[a]								
Model		Unstandardized Coefficients		Standardized Coefficients	t	Sig.	95.0% Confidence Interval for B	
		B	Std. Error	Beta			Lower Bound	Upper Bound
1	(Constant)	.138	.124		1.119	.274	-.116	.393
	UCS (MPa)	.312	.040	.840	7.749	.000	.229	.394
a. Dependent Variable: Flexural strength (MPa)								

4.3.4 California Bearing Ratio

The inclusion of fibers improved the CBR values of stabilized soil, and it is depicted in Figures 4.24(a–c) and 4.25(a–c). An excellent improvement in soaked CBR value with the curing period was observed. The bonded soil particles were firmly held within the fiber matrix, which provided strong resistance to the plunger penetration. The confinement of soil in the mould played a major role, leading to the low deformation with strongly bonded soil. Due to confinement, the larger diameter of the specimen, and the strong bonding of fibers in the cemented mix, crack propagation was restricted. There was no volume change on soaking. Many of the stabilized mixes exhibited soaked CBR values of >100%. The stabilized BC soil with fibers exhibits the advantages of higher confined strength, no swelling, with no cracks on the surface during testing. This soil structure may prevent crack propagation if used in pavement construction.

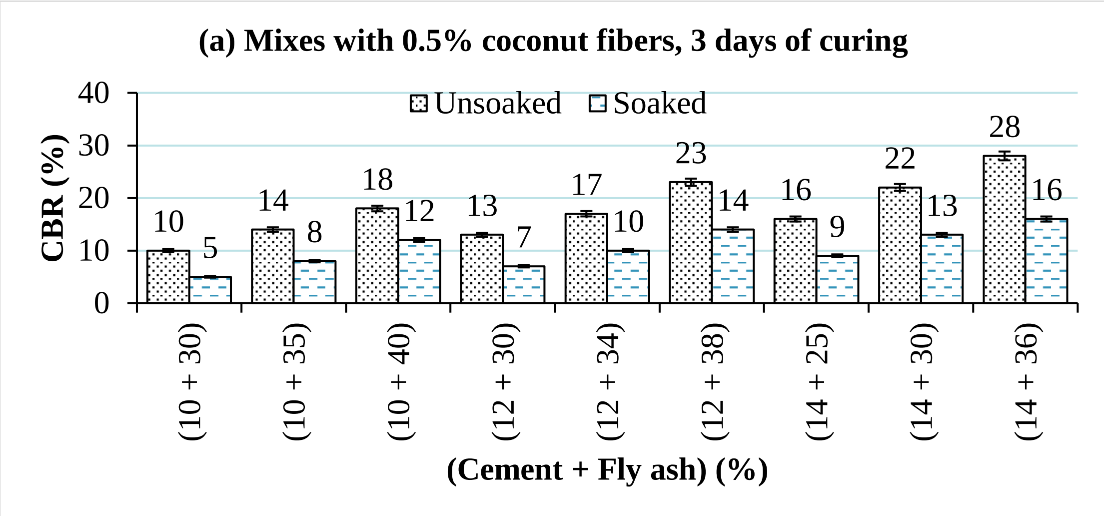

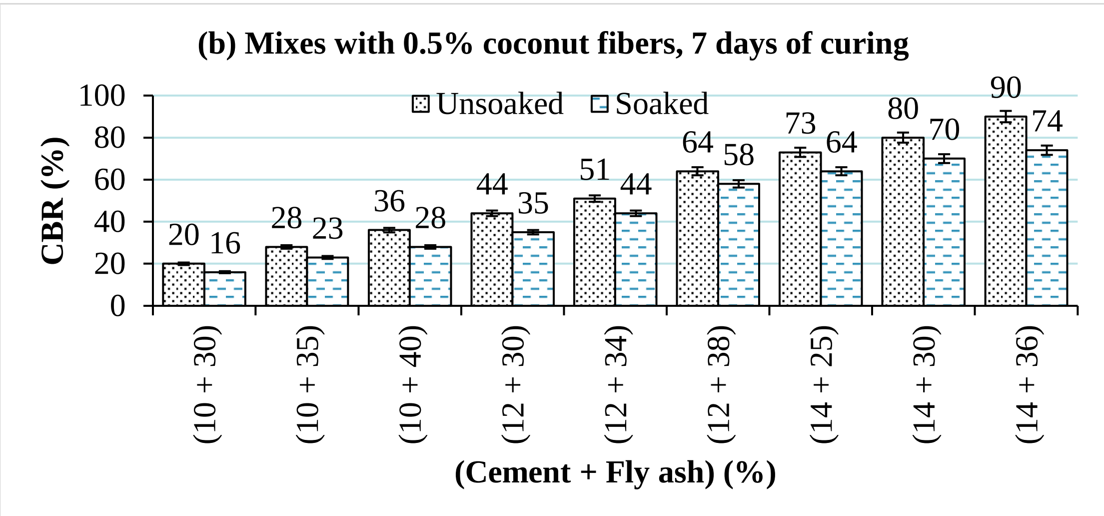

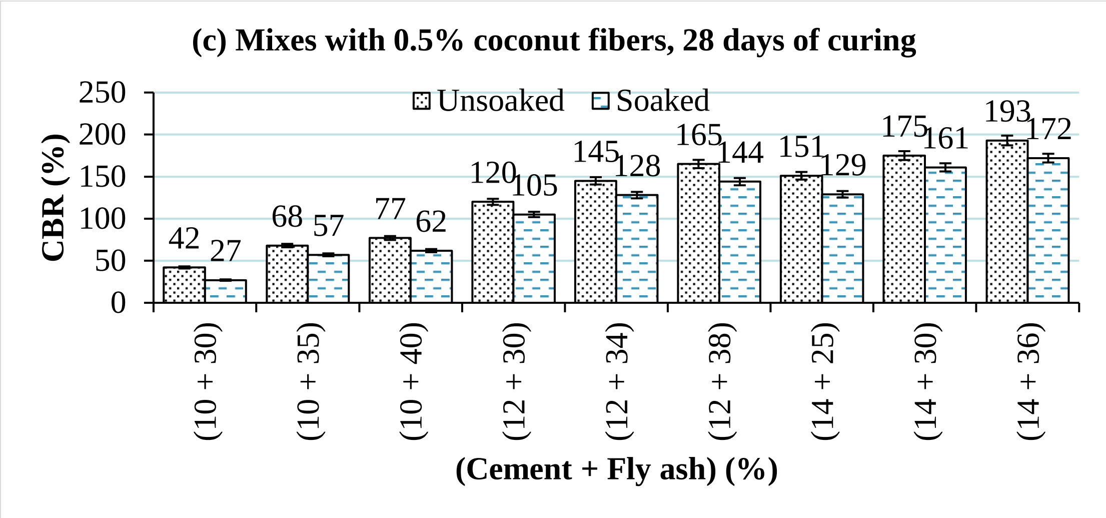

Figure 4. 24 CBR of BC soil stabilized with cement, fly ash, and 0.5% coconut fibers at standard Proctor density after (a) 3, (b) 7, and (c) 28 days of curing

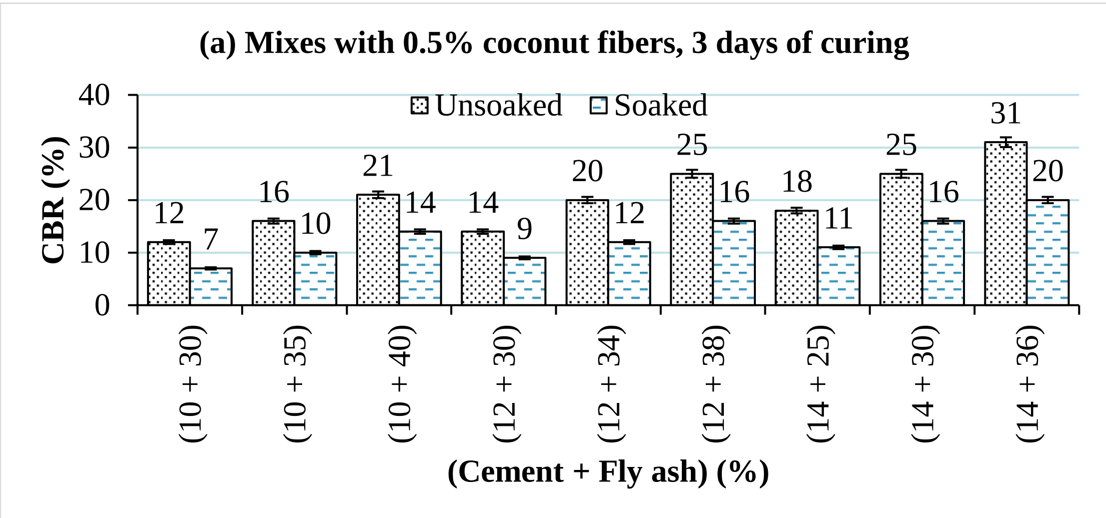

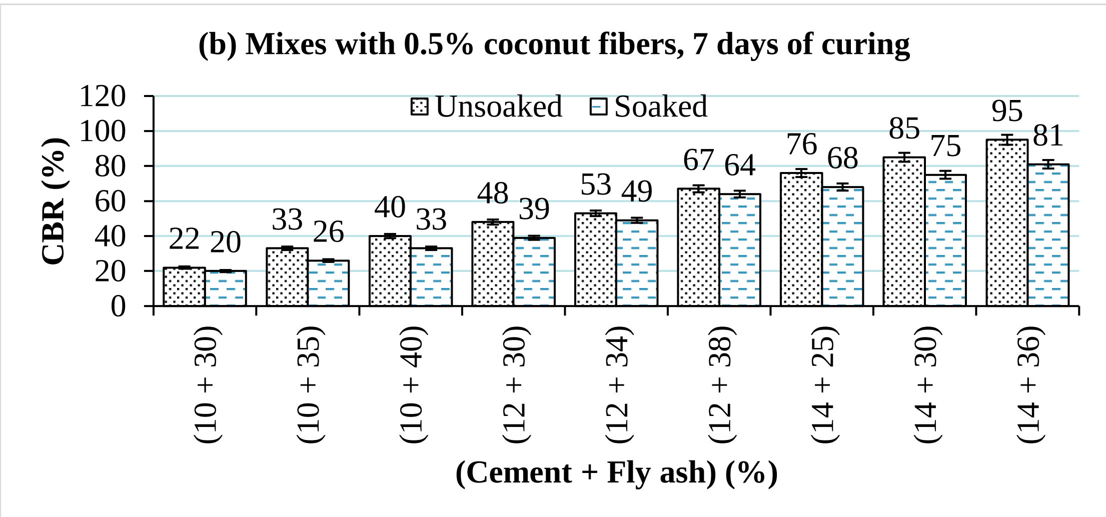

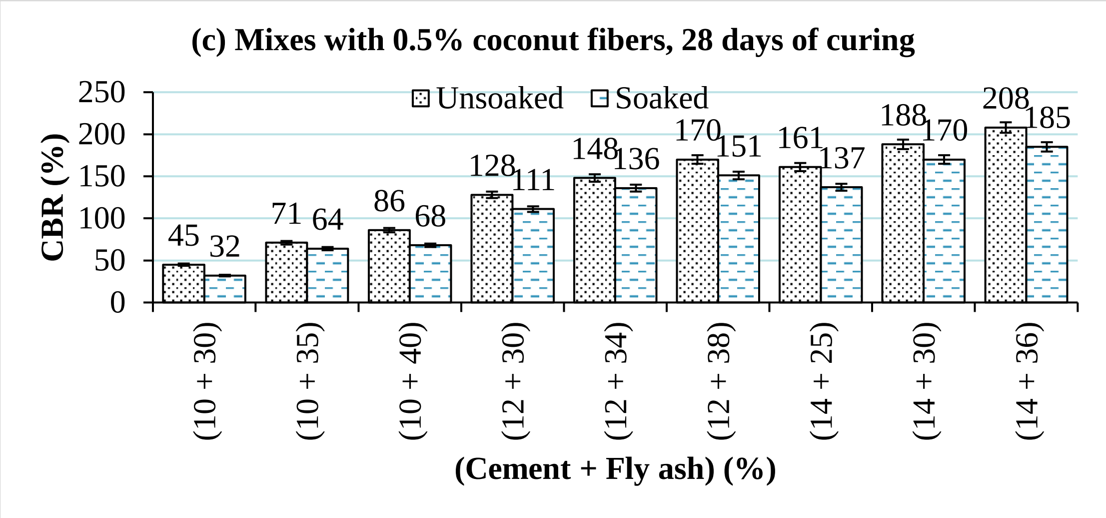

Figure 4. 25 CBR of BC soil stabilized with cement, fly ash, and 0.5% coconut fibers at modified Proctor density after (a) 3, (b) 7, and (c) 28 days of curing

4.3.5 Durability

4.3.5.1 Wetting-Drying

The durability test results of BC soil stabilized with cement, fly ash, and fibers are depicted in Figure 4.26(a, b). It was observed that the fibers were effective in holding the bonded soil matrix together without swelling and shrinkage. The fibers held the specimens intact to withstand the damage due to brushing, temperature, and moisture changes during alternate WD cycles. The loss of soil of these specimens is relatively less than the stabilized cement and fly ash stabilized soil. All the specimens passed the durability test, and hence, they can be considered for pavement construction.

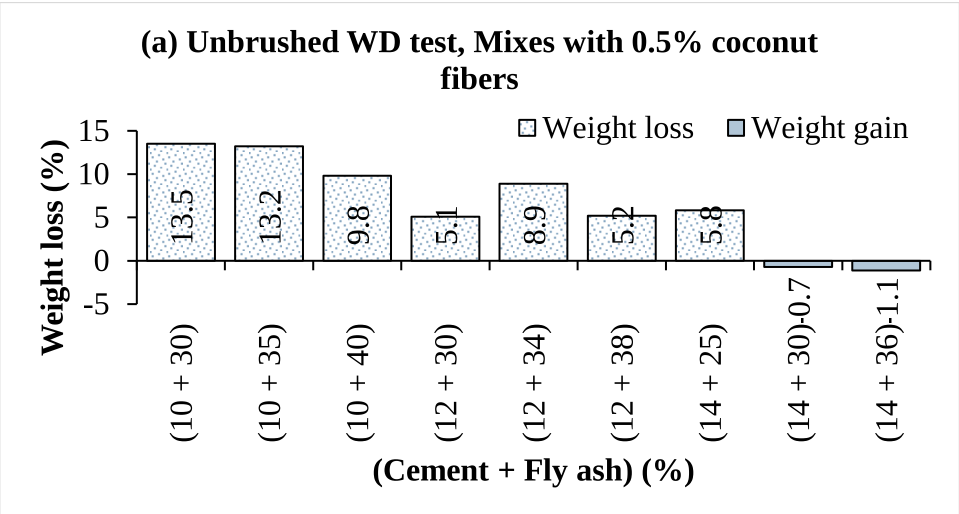

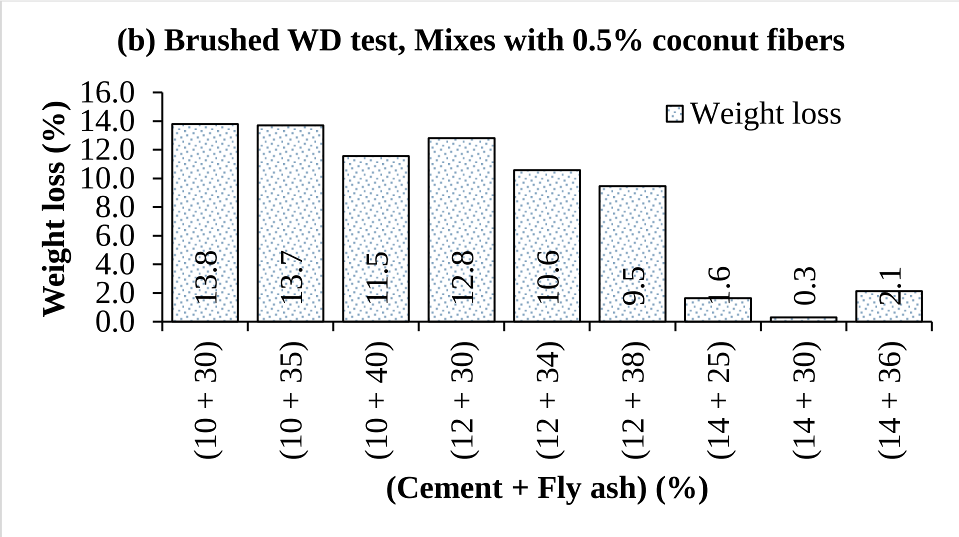

Figure 4. 26 Weight loss of BC soil stabilized with cement, fly ash, and 0.5% coconut fibers under (a) unbrushed (b) brushed WD durability tests

4.3.5.2 Freezing-Thawing

During the FT test, the unbrushed specimens exhibited weight gain with cycles, and it is depicted in Figure 4.27(a, b). The strong soil-cement fiber matrix controlled the moisture absorption; hence, the formation of ice crystals was restricted. No cracks were observed due to the freezing of samples. The excellent volume stability (no swelling and no shrinkage) of specimens was observed due to the effect of fibers. The brushed specimens exhibited minimal soil loss after 12 FT cycles. Therefore, the mixes with fibers can withstand weather changes.

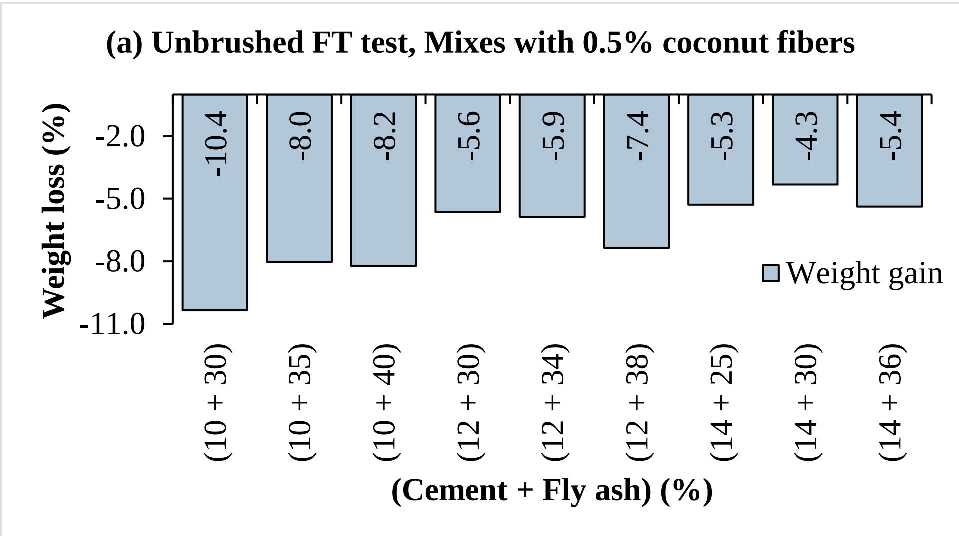

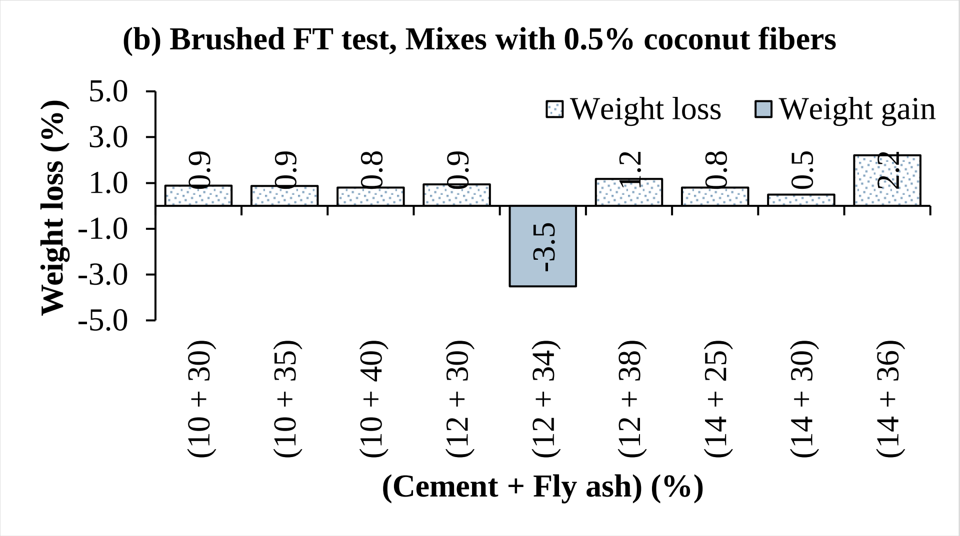

Figure 4. 27 Weight loss of BC soil stabilized with cement, fly ash, and 0.5% coconut fibers under (a) unbrushed (b) brushed FT durability tests

(a) Soaked BC soil specimen

(b) Soaked BC soil specimen with coconut fibers

(c) Stabilized BC soil with low cement and fly ash dosage

(d) Cement-fly ash stabilized soil specimen without soil loss

(e) Cement-fly ash stabilized soil specimen subjected to FT test

f) Cement-fly ash stabilized WD specimen with coconut fibers

Figure 4. 28 Durability tested samples

4.3.6 Retained UCS

After the durability test, these samples were again tested for UCS and found a marginal increase. These results are depicted in Figure 4.29(a–d). However, the retained UCS value depends on soil loss, crack development, moisture content, bonding, and fiber content. In general, soil blended with a high percentage of cement and fly ash exhibits better strength. The specimens without any cracks exhibited high strength. The unbrushed and brushed samples with 14% cement and 30% fly ash exhibited retained UCS values of 5.0, 5.2 MPa at 2.5, 2.9 % moisture content, respectively, after the WD test, similarly, after FT test exhibited 2.2, 3.3 MPa at 22.5, 19.5% moisture content, respectively.

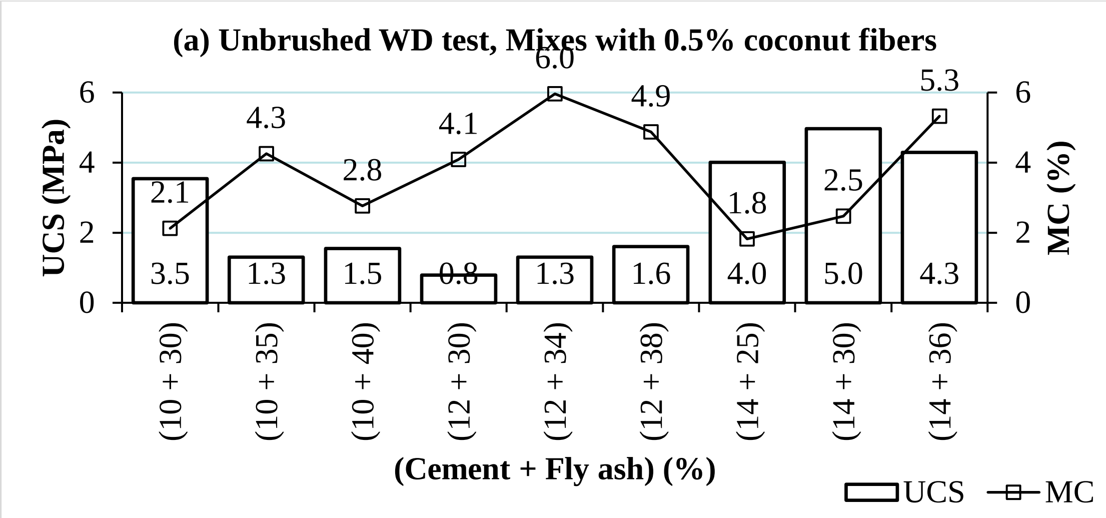
(a) Unbrushed WD test, Mixes with 0.5% coconut fibers
UCS (MPa)
MC (%)
0
2
4
6
3.5
1.3
1.5
0.8
1.3
1.6
4.0
5.0
4.3
2.1
4.3
2.8
4.1
6.0
4.9
1.8
2.5
5.3
(10 + 30)
(10 + 35)
(10 + 40)
(12 + 30)
(12 + 34)
(12 + 38)
(14 + 25)
(14 + 30)
(14 + 36)
(Cement + Fly ash) (%)
UCS
MC

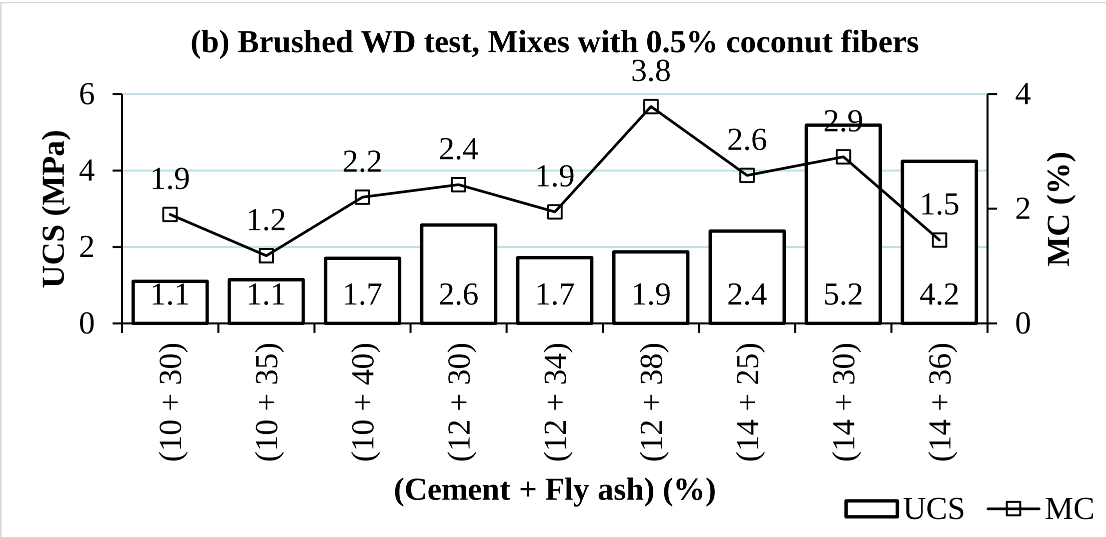
(b) Brushed WD test, Mixes with 0.5% coconut fibers
UCS (MPa)
MC (%)
0
2
4
6
1.1
1.1
1.7
2.6
1.7
1.9
2.4
5.2
4.2
1.9
1.2
2.2
2.4
1.9
3.8
2.6
2.9
1.5
(10 + 30)
(10 + 35)
(10 + 40)
(12 + 30)
(12 + 34)
(12 + 38)
(14 + 25)
(14 + 30)
(14 + 36)
(Cement + Fly ash) (%)
UCS
MC

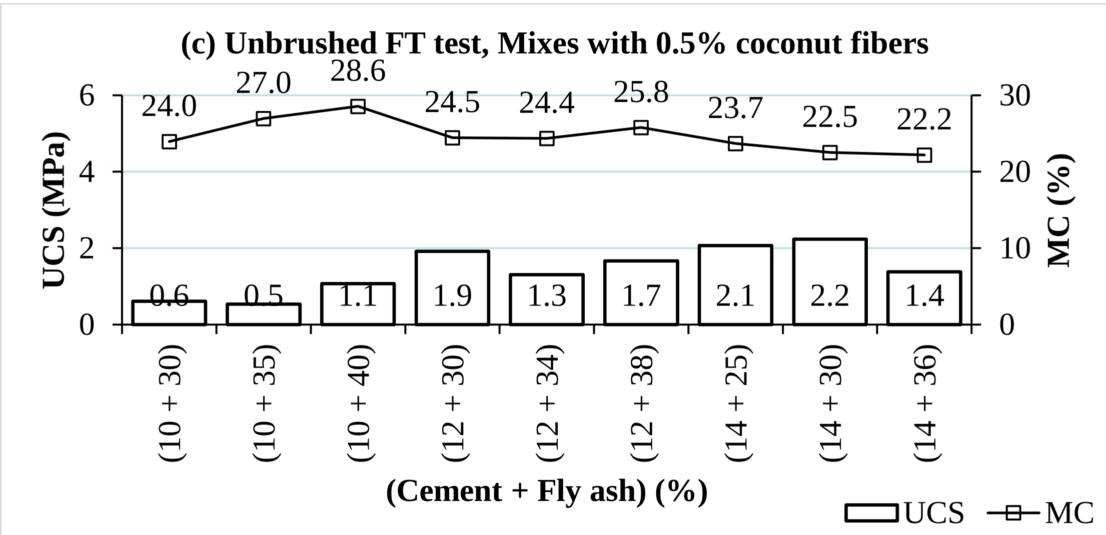
(c) Unbrushed FT test, Mixes with 0.5% coconut fibers
UCS (MPa)
MC (%)
0
2
4
6
10
20
30
0.6
0.5
1.1
1.9
1.3
1.7
2.1
2.2
1.4
24.0
27.0
28.6
24.5
24.4
25.8
23.7
22.5
22.2
(10 + 30)
(10 + 35)
(10 + 40)
(12 + 30)
(12 + 34)
(12 + 38)
(14 + 25)
(14 + 30)
(14 + 36)
(Cement + Fly ash) (%)
UCS
MC

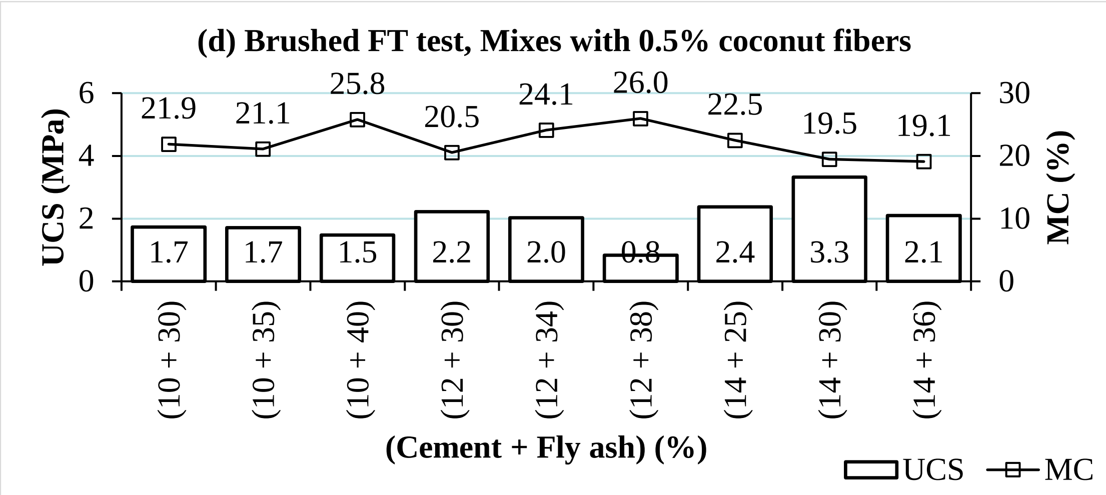

Figure 4. 29 Retained UCS of BC soil stabilized with cement, fly ash, and 0.5% coconut fibers under (a) unbrushed WD, (b) brushed WD, (c) unbrushed FT, (c) brushed FT durability tests

4.4 FATIGUE PERFORMANCE

The UCS samples cured for 28 days were subjected to repeated loading. Samples were subjected to a repeated applied load of 0.65, 0.5, 0.35, and 0.2 times load corresponding to UCS. For testing, minimum UCS at a particular cement dosage is considered at the standard or modified Proctor density. For example, in the case of standard Proctor S-C-Fa mixes, loads are calculated corresponding to UCS of 3.7 MPa. As the applied load was decreased, the fatigue life of the samples increased. The test results are tabulated in Table 4.22. These samples exhibited higher fatigue life (N) due to good bonding developed at the cemented soil-fiber interface. Due to close packing, the samples compacted at higher density sustained slightly higher load repetitions. The samples at an applied load of 0.2 times UCS exhibited more than $2X10^5$ repetitions without failure.

Table 4. 22 Fatigue life of BC soil stabilized with cement-fly ash and cement-fly ash-0.5% coconut fiber (durable mixes)

Mix ID	Ingredient (%)	28 days UCS (MPa)	Stress level					
			0.65		0.5		0.35	
			Load (N)	N	Load (N)	N	Load (N)	N
Standard Proctor, S-C-Fa	60-10-30	3.7	2705	721	2081	6927	1457	54198
	60-10-40	4.0		1878		16860		68707
	58-12-30	3.8		1056		10713		59048

Mix ID	Ingredient (%)	28 days UCS (MPa)	Stress level					
			0.65		0.5		0.35	
			Load (N)	N	Load (N)	N	Load (N)	N
	50-12-38	3.9		1789		15821		66008
	61-14-25	3.7		681		9089		55337
	50-14-36	4.2		2980		16975		77875
Modified Proctor, S-C-Fa	60-10-30	3.7	2728	444	2098	6810	1469	55396
	60-10-40	4.0		1567		17561		68282
	58-12-30	3.9		987		13873		64015
	50-12-38	4.2		1670		26395		81756
	61-14-25	4.2		322		22520		75026
	50-14-36	4.6		9258		39704		93222
Standard Proctor, S-C-Fa-Cf	60-10-30-0.5	1.6	1170	638	900	7627	630	56210
	60-10-40-0.5	1.6		5441		35438		93036
	58-12-30-0.5	1.9		1475		27909		85152
	50-12-38-0.5	2.5		34424		73564		129786
	61-14-25-0.5	2.0		3679		33094		91563
	50-14-36-0.5	3.0		63734		103514		155072
Modified Proctor, S-C-Fa-Cf	60-10-30-0.5	3.4	2513	818	1933	8383	1353	56007
	60-10-40-0.5	4.2		5402		37050		95818
	58-12-30-0.5	3.4		650		9621		58595
	50-12-38-0.5	4.3		8835		40870		97371
	61-14-25-0.5	3.9		2229		27060		79702
	50-14-36-0.5	5.4		39448		80383		136131

Note:- S = BC soil, C = ordinary Portland cement (43 grade), Fa = class F fly ash, Cf = Coconut fibers

4.5 MICROSTRUCTURAL ANALYSIS

4.5.1 SEM Image Analysis

When the anionic or negatively charged surface of clay particles come in contact with water, it attracts free cations and positively charged ends of water dipoles. As a result, a thin film of adsorbed (diffused double layer) water forms surrounding the soil particles. Strength improvement of stabilized soil depends on cement and fly ash percentage, curing time, water content, etc. Water addition to a dry soil-cement-fly ash mix initiates the rapid hydration process to form hydrated lime. Hydrated cementitious products reduce the plasticity of the soil. The reaction of the atmospheric CO_2 with soil water and air forms carbonic acid to alter soil acidity. Subsequently, lime dissociates into Ca^{+2} and OH^{-1}. These ions take part in the cation exchange process to form a flocculated soil structure. The active SiO_2 and Al_2O_3 present in the soil react with the $Ca(OH)_2$ present in soil water to form the pozzolanic compounds. The dissolved silica and alumina react with the calcium ions to form calcium silicate hydrate (CSH) and calcium aluminate hydrate (CAH) gels. These gels strongly bond the soil particles and avoid the relative sliding of particles. Generally, cement's pozzolanic reaction occurs at a slower rate, which is further slowed down by the CSH gel shell formed around the fly ash particles. The rate of hydration and strength gain is directly proportional to $Ca(OH)_2$ consumption. As per Kang et al. 2016, the curing of hydration products forms cementing crust around the soil particle; its thickness increases with curing time.

Figure 4.30a shows a mix of 90% soil and 10% fly ash, indicating the uniform dispersion of fly ash particles in the soil mass, which resulted in the plasticity reduction. Figure 4.30b shows the microstructure of 6% cement-treated soil. The geometrical arrangements of stabilized soil were changed due to cement hydration and the mechanical moulding process. CSH formed a bond between the soil particles. By linking soil particles together, stabilized soil attained a lamellar shape; Estabragh et al. 2016 found a similar microstructure when contaminated CL soil was treated with 30% cement.

Higher stabilizer dosages resulted in a more compact microstructure. In a study conducted by Iyengar et al. 2013, the cement-treated mixture of gravel, sand, silt, and clay showed compact structures. A porous structure was observed in the stabilized mix, which may be due to air voids present, and low density resulting from soil expansion. Due to the active participation of fly ash globules and reactive soil particles in the hydration process, reaction products were formed on the surface of the soil and fly ash when the soil is treated with 10% cement and 10% fly ash, and it is depicted in Figure 4.30c. More compact morphology was found at high cement and fly ash contents due to higher hydration rates and is justified by the higher strength. Compact morphology resulted in low discontinuity of bonded soil particles. The addition of fly ash contributed to the formation of a denser and homogeneous distribution of hydration products. Cement hydration caused a reduction in space between clay particles, thereby reduced the possibilities of volume expansion on immersion in water. Even though BC soil exhibits expansive properties, only a few microcracks and void spaces were observed after stabilization.

(a) Mix with 90% BC soil and 10% fly ash

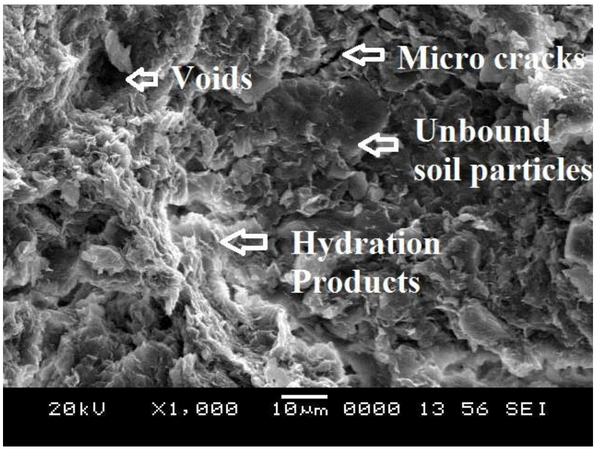

(b) BC soil stabilized with 6% cement

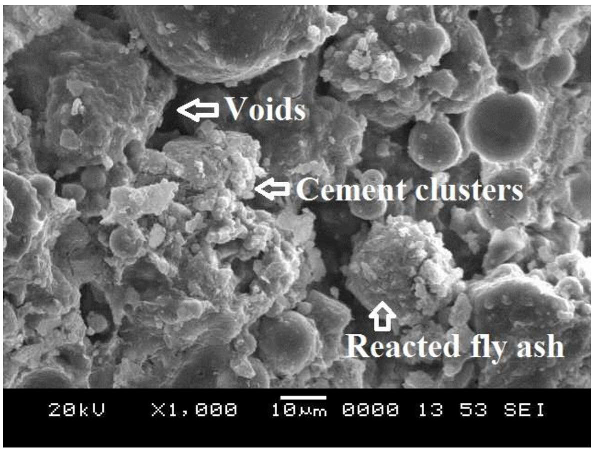

(c) BC soil stabilized with 10% cement and 10% fly ash

Figure 4. 30 SEM images of BC soil stabilized with (a) 10% fly ash, (b) 6% cement, (c) 10% cement and 10% fly ash

4.5.2 XRD Analysis

Figure 4.31b depicts the chemical changes of 10% cement, 10% fly ash treated BC soil after 90 days of curing. The diffractograms of cement-fly ash-treated BC soil depict various crystalline peaks due to the formation of hydration products, which resulted in strength development. At each peak, various cementitious compounds found are: [Ma] Periclas (MgO), [C] Calcite ($CaCO_3$), [La] Laumontite ($CaAl_2Si_4O_{12}·4H_2O$), [CSH] Calcium silicate hydrate ($Ca_2SiO_4·H_2O$), [G] Gibbsite ($Al(OH)_3$), [M] Magnesite ($MgCO_3$), [Cr] Cristobalite (SiO_2), [Ss] Sodium sulphate (Na_2SO_4), [Cs] Calcium sulphate ($CaSO_4$), [No] Nordstrandite ($Al(OH)_3$), [Mi] Millosevichite (($Al_2(SO_4)_3$), [Ci] Calcium iron oxide ($Ca_4Fe_{14}O_{25}$), [Pl] Stratlingite ($Ca_2Al_2SiO_7·8H_2O$), [Co] Cowlesite ($CaAl_2Si_3O_{10}·6H_2O$), [Fo] Foshagite ($Ca_4(SiO_3)_3$ $(OH)_2$), [CSHO] Calcium silicate hydroxide ($Ca_4Si_5O_{13.5}$ $(OH)_2$), [Pi] Piemontite (Ca_2Al_2Mn $(SiO_4)(Si_2O_7)(O,OH)_2$), [Ar] Arcanite (K_2SO_4), [Gi] Gismondine ($CaAl_2Si_2O_8·4H_2O$), [Gy] Gypsum ($CaSO_4·2H_2O$).

The observed crystalline peak intensity was slightly higher in BC soil treated with cement alone, as depicted in Figure 4.31a. The number of cementitious products formed was increased when fly ash was added along with cement for BC soil stabilization. A higher dosage of cement has led to the formation of a stronger soil matrix with more crystalline peaks of much higher intensity, as depicted in Figure 4.31c.

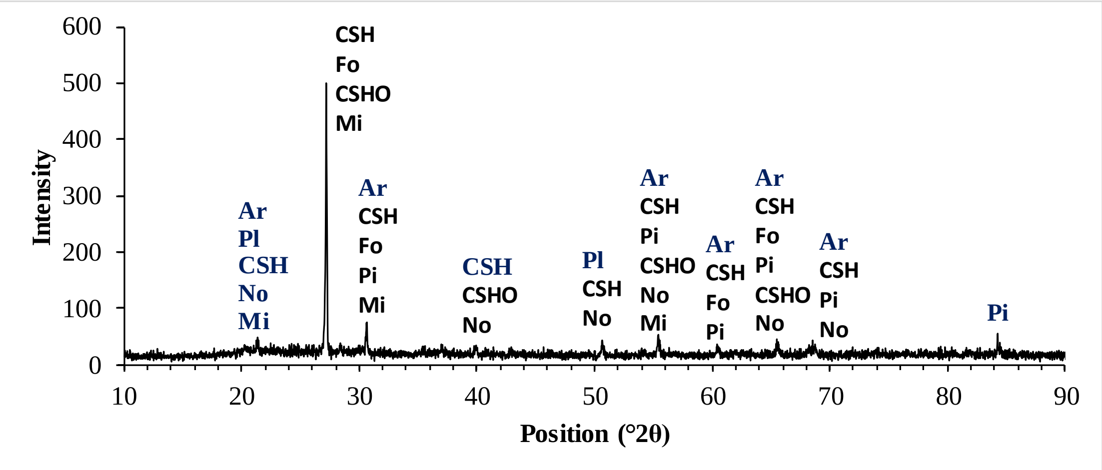

(a) Stabilized BC soil with 5% OPC

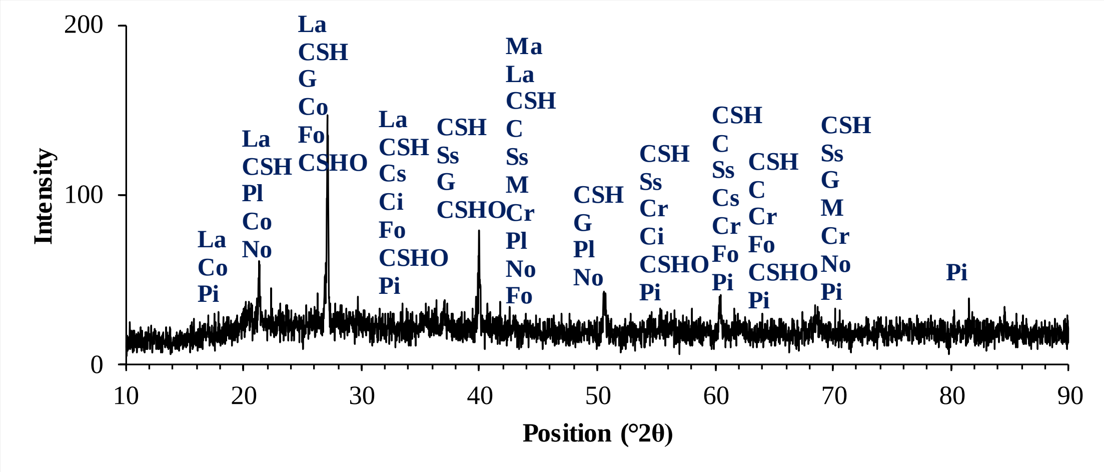

(b) Stabilized BC soil with 10% OPC and 10% class F fly ash

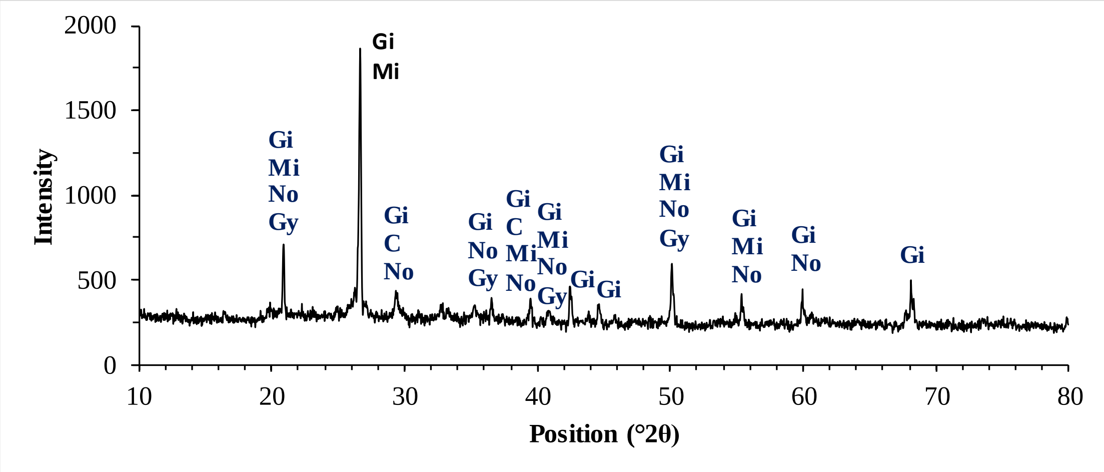

(c) Stabilized BC soil with 14% OPC and 36% class F fly ash

Figure 4. 31 XRD diffractograms of BC soil stabilized with (a) 5% OPC, (b) 10% OPC and 10% class F fly ash, (c) 14% OPC and 36% class F fly ash

4.6 SUMMARY

The higher dosage of OPC (>10%) and fly ash (>25%) has significantly improved the UCS of the stabilized soil. Also, specimens at these dosages passed both WD and FT durability tests. Significant improvement in CBR and flexural strengths were observed with the inclusion of coconut fibers. Also, the stabilized mixes have exhibited improved fatigue life. The stronger cementitious bonds resisted the volume instability of mixes.

CHAPTER 5

ALKALI-ACTIVATED BLACK COTTON SOIL WITH MARGINAL MATERIALS

5.1 GENERAL

This chapter deals with laboratory evaluation of BC soil stabilized with alkali solution, class F fly ash, limestone powder, construction demolition waste, and arecanut fibers. Alkali solutions prepared by mixing NaOH solution of 8 molar concentration and Na_2SiO_3 solution at SS/SH ratios of 0.5, 1.0, and 1.5 were used to activate the precursor or marginal materials in various mixes discussed in later sections of this chapter. Initially, BC soil was blended with marginal materials before adding the alkali solution. To use for high-volume roads, only modified Proctor compaction tests were conducted on all mix combinations. The strength of stabilized BC soil mixes was evaluated by performing UCS tests after 3, 7, and 28 days of curing. The CBR, flexural strength, and fatigue life of selected mixes were evaluated. Further, mixes were tested for WD and FT tests to check their suitability under adverse weather conditions. To enhance the flexural strength and fatigue life, arecanut fibers were added to the stabilized soil.

5.2 ALKALI-ACTIVATED BC SOIL WITH CLASS F FLY ASH

5.2.1 Compaction

The modified Proctor tests were conducted on BC soil replaced with class F fly ash (<50%) mixes.

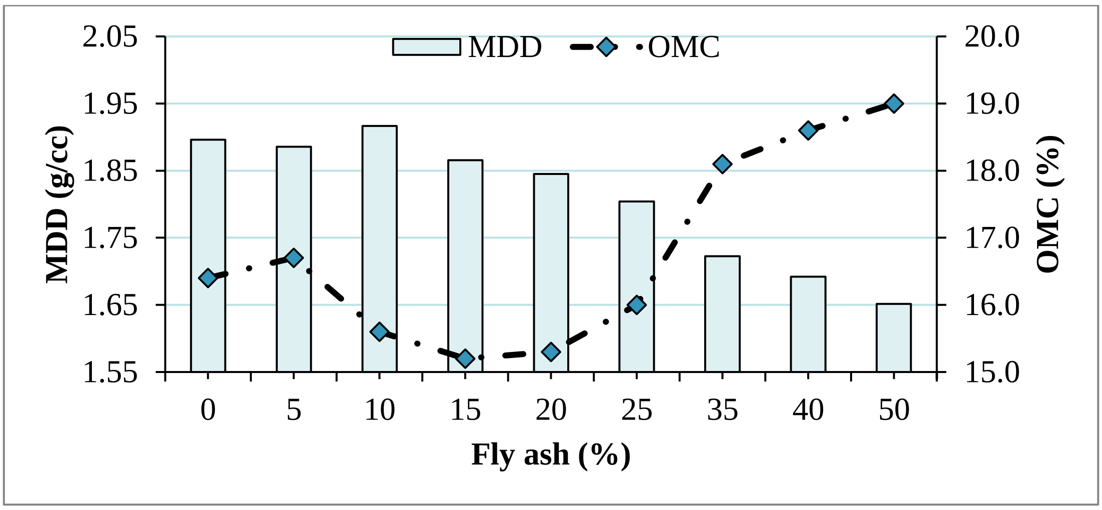

Figure 5. 1 Modified Proctor results for 0–50% fly ash treated BC soil

At 10 % replacement of soil with fly ash, the MDD of 1.92 g/cc at 15.6% OMC was obtained, and with further replacement of fly ash, MDD was reduced. The test results are depicted in Figure 5.1. As fly ash content increases, the MDD decreases, and OMC increases due to the higher specific surface area of fly ash. An increase in the dosage of fly ash and due to its low specific gravity resulted in the decrease of MDD of the mixes. Also, more water is required to moisten the particles to favour the compaction; therefore, an increase in OMC was observed.

5.2.2 Unconfined Compressive Strength

The UCS tests were conducted on 3, 7, and 28 days curing at ambient (room) temperature. The specimens were prepared using alkali solution at the SS/SH ratios of 0.5, 1.0, and 1.5. The SS/SH ratio of 0.5 is ineffective for improving the UCS of stabilized soil due to the lower dissolution of precursor material. SS/SH ratio of 1.5 is highly significant in strength improvement. The trial mixes were prepared with 2.0 and 2.5 SS/SH ratios could not contribute to the hike in strength, hence avoided further. An increase in the fly ash dosage has resulted in a significant improvement in the strength values. After 7 days of curing, the specimens achieved quite substantial strength; on further curing till 28 days, improvement was marginal. The sample with 50% fly ash achieved a UCS value of 9.7 MPa at SS/SH ratio of 1.5 after curing for 28 days, whereas at SS/SH ratio of 0.5, it achieved 3.8 MPa, as depicted in Figure 5.2(a–c). The higher amount of fly ash has formed more reaction products resulting in higher strength. Shrinkage cracks were noticed on the surface of BC soil specimens, and when activated with fly ash, there were no cracks.

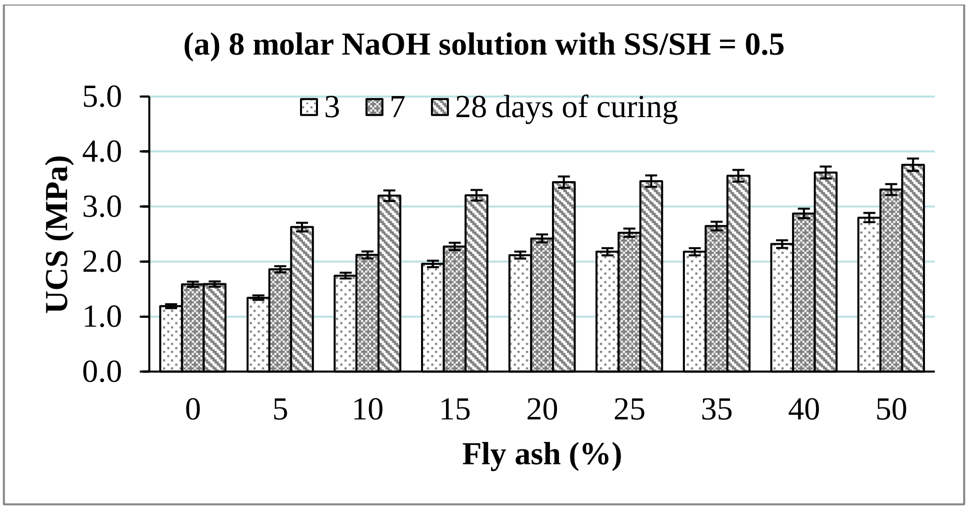

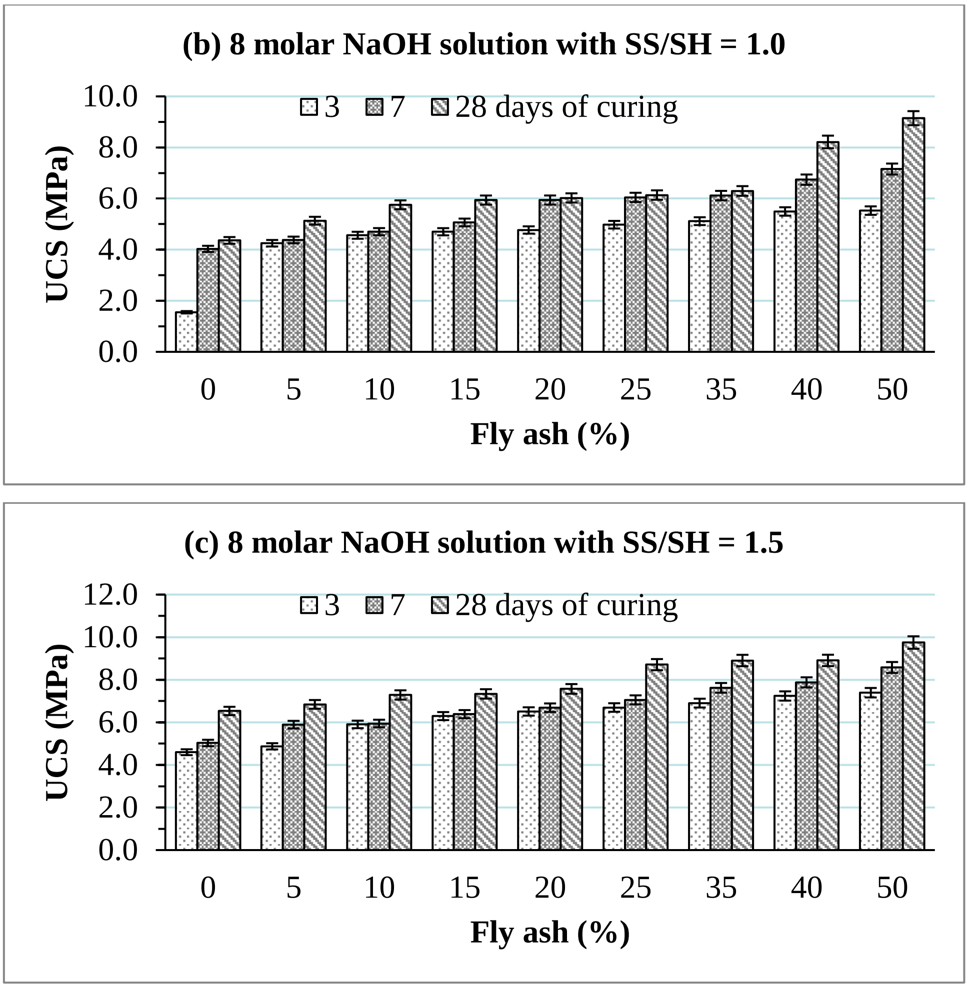

Figure 5. 2 UCS of alkali-activated BC soil with 0–50% fly ash at (a) 0.5, (b) 1.0, and (c) 1.5 SS/SH ratios

ANOVA: Univariate analysis of variance performed indicates that the UCS values are significantly (i.e., $p<0.05$) influenced by the dosage of fly ash, SS/SH ratio, and curing period. R^2= 0.961 indicates that 96.1% of the variance in UCS values can be explained by the dosage of fly ash, SS/SH ratio, and curing period. The ANOVA results are tabulated in Table 5.1.

Table 5. 1 ANOVA of UCS of alkali-activated BC soil with the dosage of fly ash, SS/SH ratio, and curing period at modified Proctor density

Tests of Between-Subjects Effects					
Dependent Variable: UCS (MPa)					
Source	Type III Sum of Squares	df	Mean Square	F	Sig.
Corrected Model	374.513[a]	12	31.209	139.462	.000
Intercept	2026.000	1	2026.000	9053.390	.000
Curing	32.788	2	16.394	73.259	.000
Ratio	281.817	2	140.908	629.663	.000

Fly ash	59.908	8	7.488	33.463	.000
Error	15.217	68	.224		
Total	2415.730	81			
Corrected Total	389.730	80			
a R^2= .961 (Adjusted R^2= .954)					

E values:- The 'm' values for various fly ash replacements are depicted in Figure 5.3.

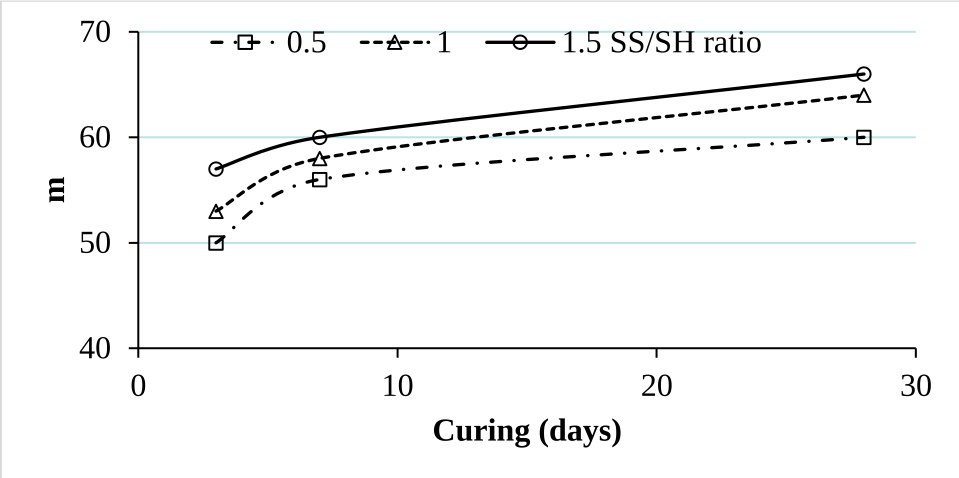

Figure 5. 3 'm' values for alkali-activated BC soil with 0–50% fly ash at modified Proctor density

The variation of UCS versus E for different curing periods for different mixes is tabulated in Table 5.2. Due to the higher dissolution of aluminosilicate materials, the specimens at the SS/SH ratio of 1.5 resulted in higher E values.

Table 5. 2 'E' values for alkali-activated BC soil with 0–50% fly ash at modified Proctor density

SS/SH ratio	Curing (days)	UCS (MPa)	m	E (MPa)
0.5	3	1.2–2.8	50	60–140
	7	1.6–3.3	56	90–185
	28	1.6–3.8	60	96–228
1.0	3	1.5–5.5	53	80–292
	7	4.0–7.2	58	232–418
	28	4.4–9.1	64	282–582
1.5	3	4.6–7.4	57	262–422
	7	5.0–8.6	60	300–516
	28	6.5–9.7	66	429–640

5.2.3 Flexural Strength

The flexural strength of alkali-activated mixes with fly ash has improved with the increase in the fly ash dosages. The maximum flexural strength of 1.2 MPa was obtained on 28 days for 50% fly ash replacement, and it is depicted in Figure 5.4. Also, the continued dissolution of precursor with the increase in curing time has a significant effect on strength.

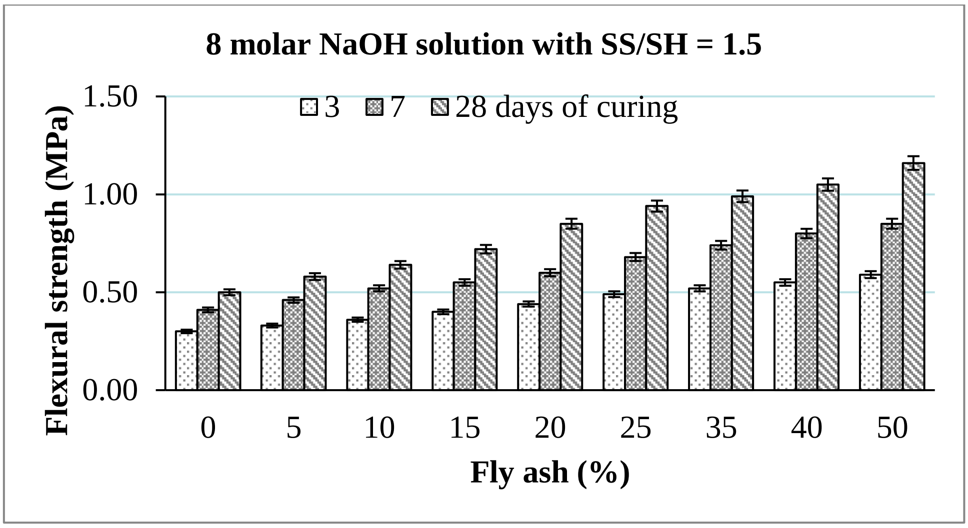

Figure 5. 4 Flexural strength of alkali-activated BC soil with 0–50% fly ash at 1.5 SS/SH ratio

ANOVA: Univariate analysis of variance performed indicates that the flexural strength values are significantly (i.e., $p<0.05$) influenced by the dosage of fly ash, SS/SH ratio, and curing period. $R^2 = 0.951$ indicates that 95.1% of the variance in flexural strength values can be explained by the dosage of fly ash, SS/SH ratio, and curing period. The ratio of SS/SH considered is 1.5 for all the mixes. The ANOVA results are tabulated in Table 5.3.

Table 5. 3 ANOVA of flexural strength of alkali-activated BC soil with the dosage of fly ash, SS/SH ratio, and curing period at modified Proctor density

Tests of Between-Subjects Effects					
Dependent Variable: Flexural strength (MPa)					
Source	Type III Sum of Squares	df	Mean Square	F	Sig.
Corrected Model	1.282[a]	10	.128	31.041	.000
Intercept	10.729	1	10.729	2597.739	.000
Curing	.662	2	.331	80.134	.000
Fly ash	.620	8	.078	18.768	.000
Error	.066	16	.004		
Total	12.077	27			
Corrected Total	1.348	26			
a. R^2= .951 (Adjusted R^2= .920)					

Regression: Regression analysis is performed between UCS and flexural strength, and the results are tabulated in Table 5.4. A correlation of 0.946 ($p<0.0005$) confirms a strong positive relationship between UCS and flexural strength. While $R^2 = 0.895$ indicates that 89.5% of the variance in flexural strength can be explained by UCS. From ANOVA, it can be concluded that the model is statistically significant ($p<0.0005$). From the coefficient table, for every 1 MPa increase in UCS, the model predicts an increase of 0.171 MPa flexural strength. BC soil stabilized at an SS/SH ratio of 1.5 has the same influence on both strength parameters. Also, the t-test confirms the statistical significance of the model.

Table 5. 4 Regression analysis of UCS and flexural strength for alkali-activated BC soil with 0–50% fly ash at modified Proctor density

Correlations

		Flexural strength (MPa)	UCS (MPa)
Pearson Correlation	Flexural strength (MPa)	1.000	.946
	UCS (MPa)	.946	1.000
Sig. (1-tailed)	Flexural strength (MPa)	.	.000
	UCS (MPa)	.000	.
N	Flexural strength (MPa)	27	27
	UCS (MPa)	27	27

Model Summary[b]

Model	R	R Square	Adjusted R Square	Std. Error of the Estimate
1	.946[a]	.895	.890	.07539

a. Predictors: (Constant), UCS (MPa)

b. Dependent Variable: Flexural strength (MPa)

ANOVA[a]

Model		Sum of Squares	df	Mean Square	F	Sig.
1	Regression	1.206	1	1.206	212.184	.000[b]
	Residual	.142	25	.006		
	Total	1.348	26			

a. Dependent Variable: Flexural strength (MPa)

b. Predictors: (Constant), UCS (MPa)

Coefficients[a]

Model		Unstandardized Coefficients		Standardized Coefficients	t	Sig.	95.0% Confidence Interval for B	
		B	Std. Error	Beta			Lower Bound	Upper Bound
1	(Constant)	-.568	.084		-6.797	.000	-.740	-.396

	UCS (MPa)	.171	.012	.946	14.567	.000	.147	.195
a. Dependent Variable: Flexural strength (MPa)								

5.2.4 California Bearing Ratio

Figure 5.5 depicts the CBR of 28 days cured alkali-activated BC soil with various fly ash dosages stabilized using 8 molar NaOH solution at an SS/SH ratio of 1.5. The specimens showed excellent resistance to the plunger penetration with increased fly ash dosages under dry conditions. Specimens with more than 20% replacement exhibited an unsoaked CBR of >100%. When soaked for 4 days in water, the specimens softened due to mineral constituents leaching and delectation of geopolymer structure. The softened soil (100% saturation) offered the least resistance to plunger penetration. Therefore, a considerable reduction in the soaked CBR values was observed, along with considerable swelling like natural soil after submerging in water.

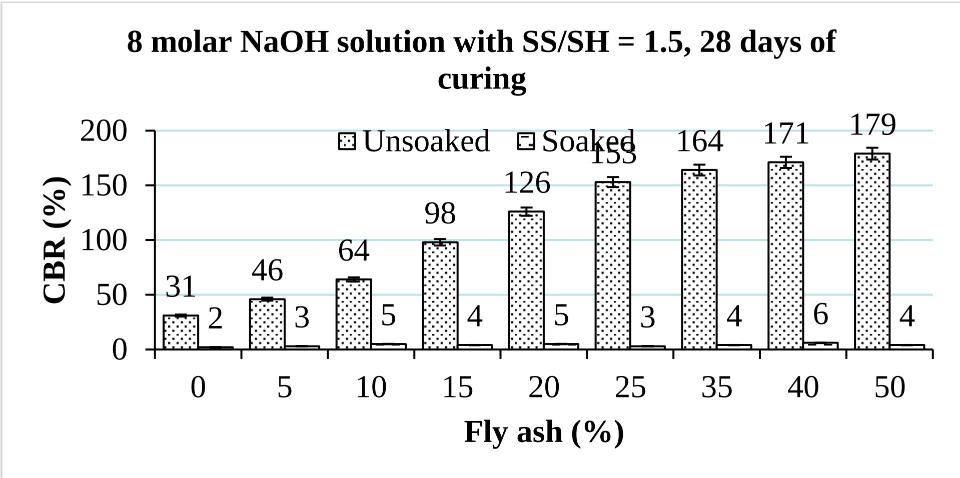

Figure 5. 5 CBR of alkali-activated BC soil with 0–50% fly ash at 1.5 SS/SH ratio after 28 days of curing

5.3 ALKALI-ACTIVATED BC SOIL WITH 5% LIMESTONE POWDER AND CLASS F FLY ASH

5.3.1 Compaction

The precursor fly ash has a negligible amount of calcium content. To enhance the calcium content in the mixes, a constant 5% limestone powder is added to the soil, which increases the pH of the mix. The soil is replaced with a maximum of 5% limestone powder and 45% fly ash.

Figure 5.4 shows the modified Proctor compaction test results of BC soil stabilized with a constant 5% limestone powder and various fly ash dosages. The MDD of 1.91 g/cc at 15.8% OMC was obtained for 5% limestone powder and 5 % fly ash, as depicted in Figure 5.6. Limestone powder replacement of 5% was kept constant for all the samples, and only fly ash dosage was changed. Therefore, all combined percentage indicates the presence of only 5% limestone powder. Initially, OMC was reduced up to 15% replacement and thereafter increased at higher dosages. No significant variations were observed in OMC and MDD values as the quantity of limestone powder used for these mixes is only 5% when compared to mixes with fly ash alone.

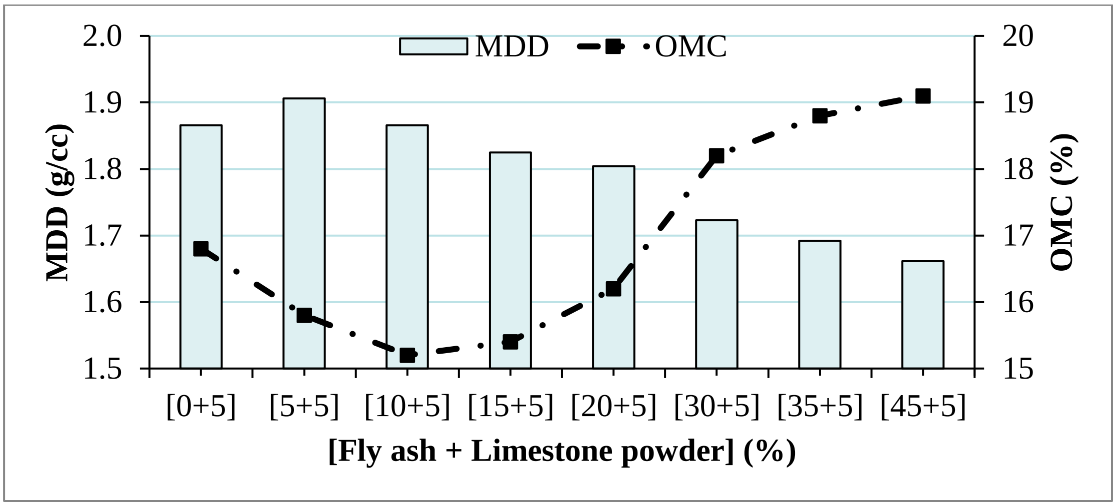

Figure 5. 6 Modified Proctor results for 5% limestone powder and 0–45% fly ash treated BC soil

5.3.2 Unconfined Compressive Strength

The replacement of limestone powder along with fly ash has enhanced the calcium content of the mix. According to Cwirzen et al. 2014, the presence of limestone powder enhances the dissolved Ca along with Si and Al from BC soil and fly ash. A considerable improvement in UCS values was observed at various fly ash dosages for stabilized BC soil at 8 molar NaOH solution and SS/SH ratio of 0.5, depicted in Figure 5.7(a–c). However, at higher SS/SH ratios of 1.0 and 1.5, the UCS values of BC soil replaced with 5% limestone powder along with different percentages of fly ash are lower than the UCS values of BC soil with only fly ash. The strength improvement after 7 to 28 days of curing is marginal. The addition of limestone powder has resulted in quick strength gain on 3 days of curing, and thereafter it was marginal. No cracks were observed on the surface of stabilized specimens. The UCS of 8.4 MPa was attained on 28 days curing for soil replaced with 5% limestone powder and 45% fly ash.

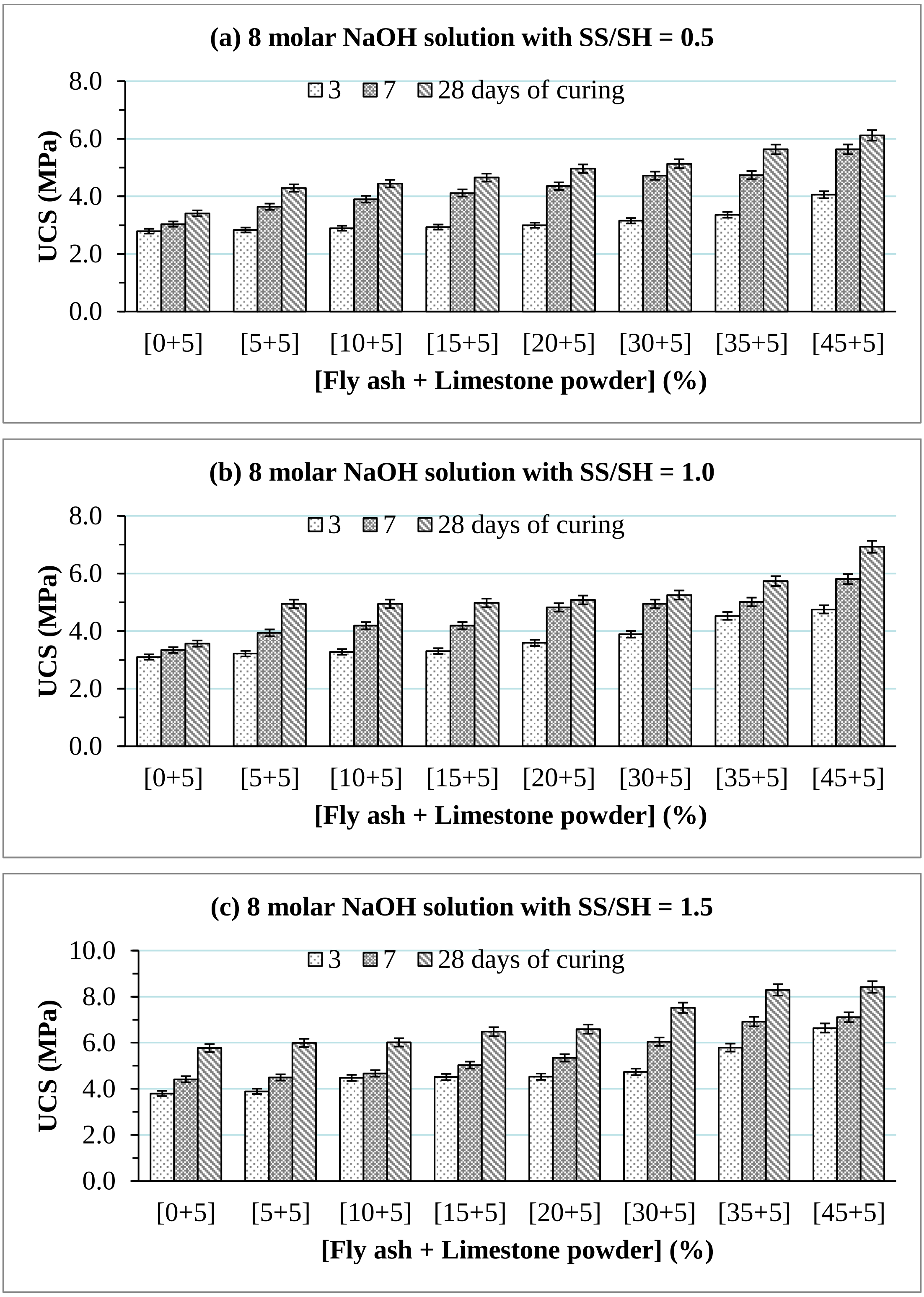

Figure 5. 7 UCS of alkali-activated BC soil with 5% limestone powder and 0–45% fly ash at (a) 0.5, (b) 1.0, and (c) 1.5 SS/SH ratios

ANOVA: Univariate analysis of variance performed indicates that the UCS values are significantly (i.e., $p<0.05$) influenced by the dosage of fly ash, SS/SH ratio, and curing period. $R^2 = 0.942$ indicates that 94.2% of the variance in UCS values can be explained by the dosage of fly ash, SS/SH ratio, and curing period. However, the dosage of limestone power of 5% is the same in all mixes; therefore, its influence remains the same. The ANOVA results are tabulated in Table 5.5.

Table 5. 5 ANOVA of UCS of alkali-activated BC soil with the dosage of fly ash, 5% limestone powder, SS/SH ratio, and curing period at modified Proctor density

Tests of Between-Subjects Effects					
Dependent Variable: UCS (MPa)					
Source	Type III Sum of Squares	df	Mean Square	F	Sig.
Corrected Model	112.709[a]	11	10.246	88.450	.000
Intercept	1626.401	1	1626.401	14039.746	.000
Curing	36.750	2	18.375	158.622	.000
Ratio	35.617	2	17.808	153.730	.000
Fly ash	40.342	7	5.763	49.749	.000
Limestone powder	.000	0	.	.	.
Error	6.951	60	.116		
Total	1746.060	72			
Corrected Total	119.659	71			
a. R^2= .942 (Adjusted R^2= .931)					

E values:- The 'm' values for mixes with 5% limestone powder, various fly ash replacements are depicted in Figure 5.8. The variation of UCS versus E for different curing periods for different mixes is tabulated in Table 5.6.

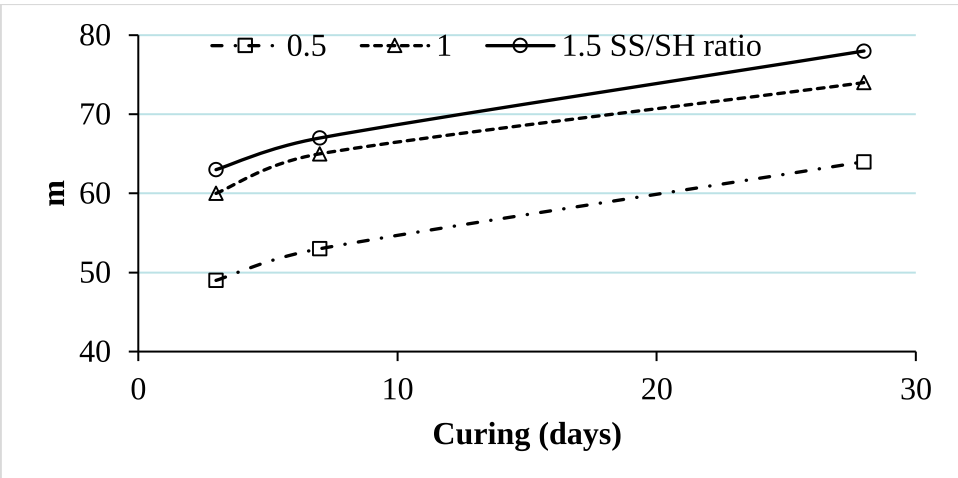

Figure 5. 8 'm' values for alkali-activated BC soil with 5% limestone powder and 0–45% fly ash at modified Proctor density

Table 5. 6 'E' values for alkali-activated BC soil with 5% limestone powder and 0–45% fly ash at modified Proctor density

SS/SH ratio	Curing (days)	UCS (MPa)	m	E (MPa)
0.5	3	2.8–4.1	49	137–201
	7	3.0–5.6	53	159–297
	28	3.4–6.1	64	218–390
1.0	3	3.1–4.8	60	186–288
	7	3.3–5.8	65	215–377
	28	3.6–6.9	74	266–511
1.5	3	3.8–6.6	63	239–416
	7	4.4–7.1	67	295–476
	28	5.8–8.4	78	452–655

5.3.3 Flexural Strength

When the limestone power was added to the mix, due to the enhanced reaction of calcium within the alkali environment, the strength gain at the initial stages was more and thereafter marginal. Maximum flexural strength of 0.92 MPa was attained for the soil mix with 45% fly ash and 5% limestone powder after 28 days of curing, as depicted in Figure 5.9.

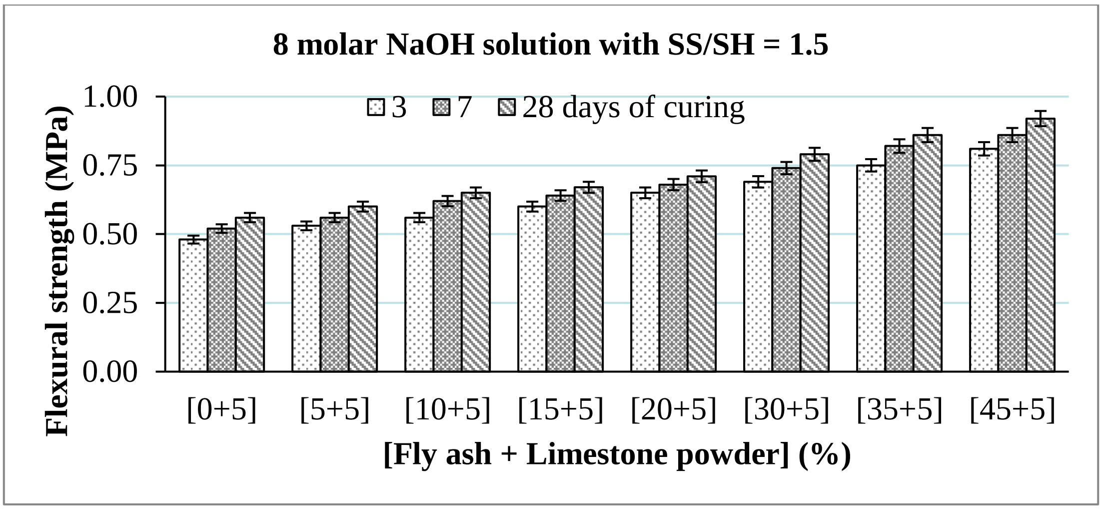

Figure 5. 9 Flexural strength of alkali-activated BC soil with 5% limestone powder and 0–45% fly ash at 1.5 SS/SH ratio

ANOVA: Univariate analysis of variance performed indicates that the flexural strength values are significantly (i.e., $p<0.05$) influenced by the dosage of fly ash, SS/SH ratio, and curing period. $R^2 = 0.995$ indicates that 99.5% of the variance in flexural strength values can be explained by the dosage of fly ash, SS/SH ratio, and curing period. However, the dosage of limestone power of 5%, and SS/SH ratio = 1.5, are the same for all the mixes; therefore, its influence remains the same. The ANOVA results are tabulated in Table 5.7.

Table 5. 7 ANOVA of UCS with the dosage of fly ash, 5% limestone powder, SS/SH ratio, and curing period at modified Proctor density

Tests of Between-Subjects Effects					
Dependent Variable: Flexural strength (MPa)					
Source	Type III Sum of Squares	df	Mean Square	F	Sig.
Corrected Model	.330[a]	9	.037	322.517	.000
Intercept	11.030	1	11.030	97015.199	.000
Curing	.030	2	.015	131.094	.000
Ratio	.000	0	.	.	.
Flyash	.300	7	.043	377.209	.000
Limestone powder	.000	0	.	.	.
Error	.002	14	.000		
Total	11.361	24			
Corrected Total	.332	23			
a. R^2= .995 (Adjusted R^2= .992)					

Regression: Regression analysis is performed between UCS and flexural strength, and the results are tabulated in Table 5.8. A correlation of 0.879 ($p<0.0005$) confirms a strong positive relationship between UCS and flexural strength. R^2 = 0.772 indicates that 77.2% of the variance in flexural strength can be explained by UCS. From ANOVA, it can be concluded that the model is statistically significant ($p<0.0005$). From the coefficient table, for every 1 MPa increase in UCS, the model predicts an increase of 0.080 MPa flexural strength. Also, the t-test confirms the statistical significance of the model.

Table 5. 8 Regression analysis of UCS and flexural strength for alkali-activated BC soil with 5% limestone powder and 0–45% fly ash at modified Proctor density

Correlations			
		Flexural strength (MPa)	UCS (MPa)
Pearson Correlation	Flexural strength (MPa)	1.000	.879
	UCS (MPa)	.879	1.000
Sig. (1-tailed)	Flexural strength (MPa)	.	.000
	UCS (MPa)	.000	.
N	Flexural strength (MPa)	24	24
	UCS (MPa)	24	24
Model Summary[b]			

Model	R	R Square	Adjusted R Square	Std. Error of the Estimate
1	.879[a]	.772	.762	.05863
a. Predictors: (Constant), UCS (MPa)				
b. Dependent Variable: Flexural strength (MPa)				

ANOVA[a]

Model		Sum of Squares	df	Mean Square	F	Sig.
1	Regression	.256	1	.256	74.474	.000[b]
	Residual	.076	22	.003		
	Total	.332	23			
a. Dependent Variable: Flexural strength (MPa)						
b. Predictors: (Constant), UCS (MPa)						

Coefficients[a]

Model		Unstandardized Coefficients		Standardized Coefficients	t	Sig.	95.0% Confidence Interval for B	
		B	Std. Error	Beta			Lower Bound	Upper Bound
1	(Constant)	.221	.054		4.079	.000	.109	.334
	UCS (MPa)	.080	.009	.879	8.630	.000	.061	.099
a. Dependent Variable: Flexural strength (MPa)								

5.3.4 California Bearing Ratio

The addition of 5% limestone powder along with varying fly ash content improved the CBR values after 28 days of curing. The test results are depicted in Figure 5.10. There were no cracks on cured specimens. When these specimens were immersed in water, the leaching of minerals constituents and delectation of set soil could not be controlled. The weakened soil led to a drastic reduction in CBR and considerable swelling of more than 20%, and softening of the mix. This softened soil has shown the least resistance to plunger penetration, thereby exhibiting low soaked CBR values.

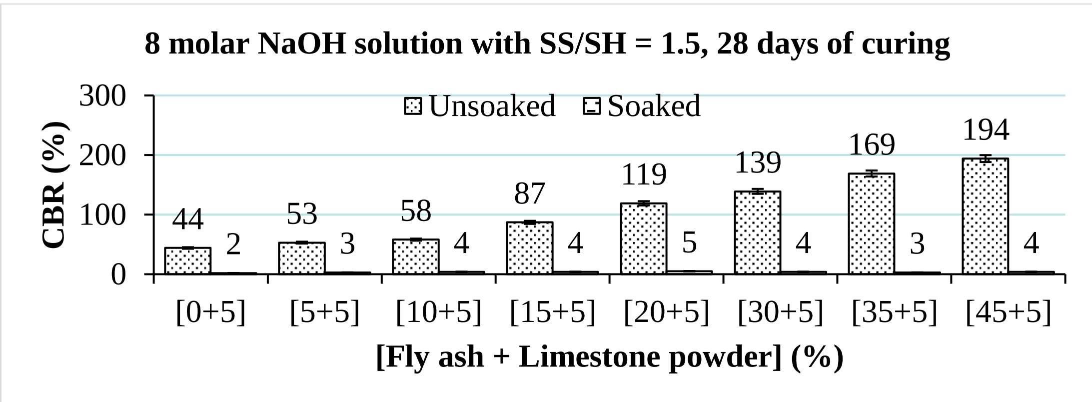

Figure 5. 10 CBR of alkali-activated BC soil with 5% limestone powder and 0–45% fly ash at 1.5 SS/SH ratio after 28 days of curing

5.4 ALKALI-ACTIVATED BC SOIL WITH LIMESTONE POWDER, CLASS F FLY ASH, AND ARECANUT FIBERS

5.4.1 Compaction

The BC soil mixed with precursor materials fly ash, limestone powder, and activated with 8 molar NaOH solution at the SS/SH ratio of 1.5 has attained significant strength gain. To strengthen further, arecanut fibers are used in these mixes and activated using the alkali solution prepared at an SS/SH ratio of 1.5. The trial mixes were conducted with 0.25, 0.5, 0.75, and 1.0% arecanut fibers (by weight of mix) of length 25 mm and diameter of 0.35mm. The mix is workable at a dosage of 0.5%, and fibers are distributed uniformly and beyond; there was the balling effect, and difficult to mix and make it homogenous. Therefore, 0.5% arecanut fibers are fixed in all the mixes. The BC soil achieved an MDD of 1.85 g/cc at 16.8% moisture content when stabilized with 0.5% arecanut fibers. The marginal decrease in MDD of mixes is observed due to the low specific gravity of fibers. Compact packing of the mix at 10% fly ash with 0.5% arecanut fibers resulted in the maximum density of 1.89 g/cc. Even though arecanut fibers exhibit higher water affinity, a small dosage did not cause a significant change in the OMC of mixes. The results are depicted in Figure 5.11. Similarly, soil-fly ash-5% limestone powder mixes with 0.5% arecanut fibers resulted in marginal variation in the OMC and MDD values at modified Proctor, and it is evident from Figure 5.12.

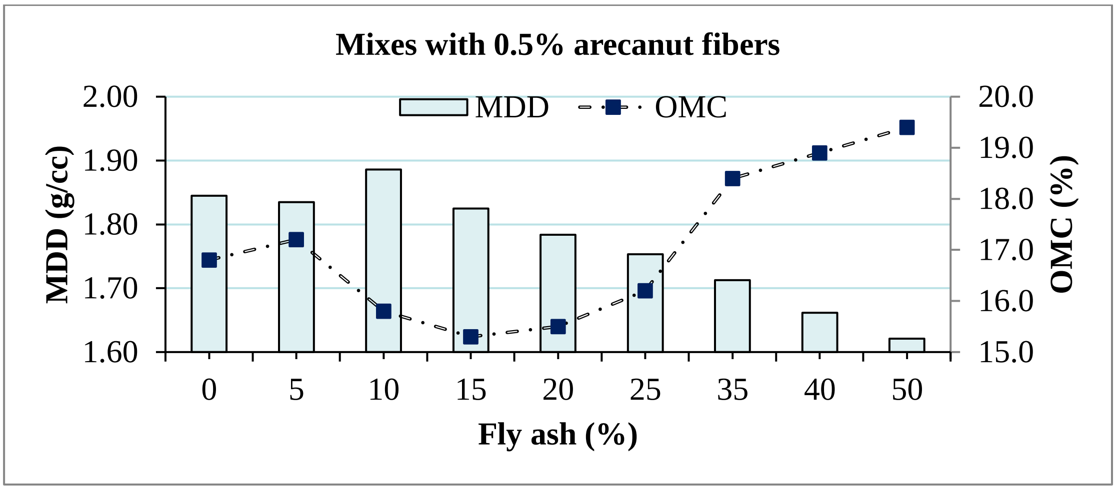

Figure 5. 11 Modified Proctor results for 0–50% fly ash and 0.5% arecanut fiber treated BC soil

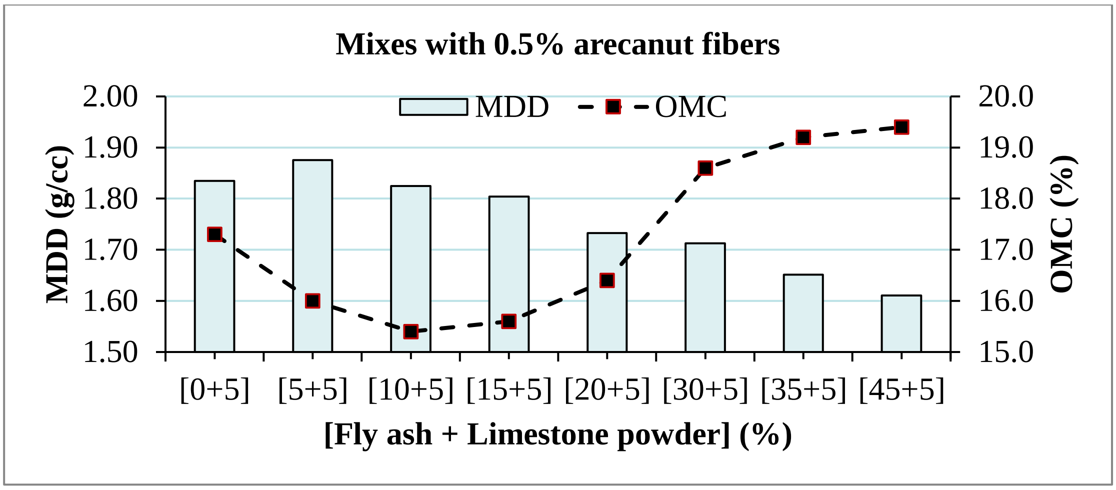

Figure 5. 12 Modified Proctor results for 5% limestone powder, 0–45% fly ash, and 0.5% arecanut fiber treated BC soil

5.4.2 Unconfined Compressive Strength

It is observed that the alkali activation of soil with fly ash and 0.5% arecanut fibers significantly improved UCS strength. The low dissolution of aluminosilicate precursor and polymerization on 3 days of curing period exhibited low UCS. The UCS significantly improved on 7 days of curing, and with further increase in the curing period, a marginal improvement was observed. Higher UCS values were observed at the 50% fly ash replacement due to the presence of a high quantity of precursor material. The alkali-activated soil with 50% fly ash and 0.5% arecanut fibers has exhibited a maximum UCS of 7.1 MPa at alkali solution content of 19.4% on 28 days of curing, and it is evident from Figure 5.13.

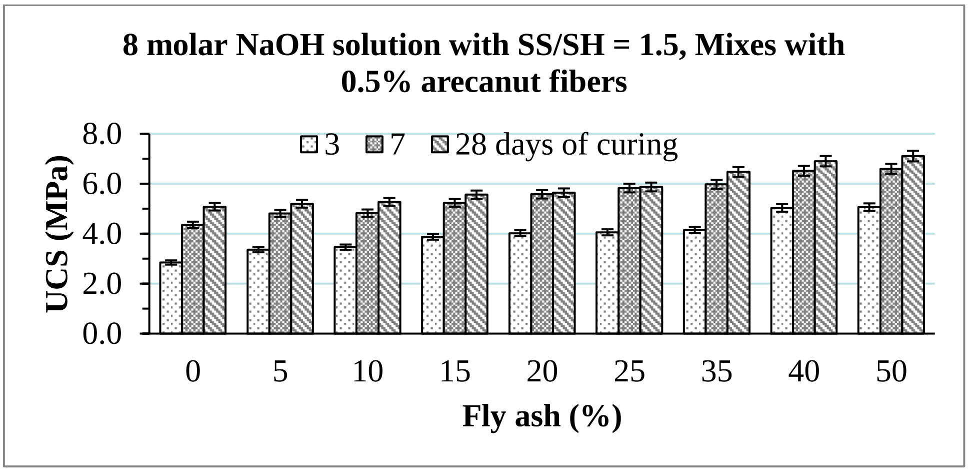

Figure 5. 13 UCS of alkali-activated BC soil with 0–50% fly ash and 0.5% arecanut fibers at 1.5 SS/SH ratio

ANOVA: Univariate analysis of variance performed indicates that the UCS values are significantly (i.e., $p<0.05$) influenced by the dosage of fly ash and curing period. R^2= 0.987 indicates that 98.7% of the variance in UCS values can be explained by the dosage of fly ash and the curing period. However, arecanut fiber dosage of 0.5% and SS/SH ratio of 1.5 are constant in all the mixes; therefore, its influence remains the same. The ANOVA results are tabulated in Table 5.9.

Table 5. 9 ANOVA of UCS of alkali-activated BC soil with the dosage of fly ash, 0.5% arecanut fibers, 1.5 SS/SH ratio, and curing period at modified Proctor density

Tests of Between-Subjects Effects					
Dependent Variable: UCS (MPa)					
Source	Type III Sum of Squares	df	Mean Square	F	Sig.
Corrected Model	31.770[a]	10	3.177	122.543	.000
Intercept	713.535	1	713.535	27522.057	.000
Curing	18.592	2	9.296	358.557	.000
Fly ash	13.179	8	1.647	63.539	.000
Arecanut fiber	.000	0	.	.	.
Error	.415	16	.026		
Total	745.720	27			
Corrected Total	32.185	26			
a. R^2= .987 (Adjusted R^2= .979)					

The improvement in strength was very quick after 3 days of curing for alkali-activated soil with fly ash, 5% limestone powder, and 0.5% arecanut fibers. The quick reaction of limestone powder in the alkaline environment results in initial strength gain. Further, as the curing period increased, a marginal enhancement of strength was observed. The crack propagation was restricted due to the strong bond developed with activated soil. The sample with 45% fly ash, 5% limestone powder, and 0.5% arecanut fibers has achieved the maximum UCS of 6.7 MPa on 28 days of curing, and it is evident from Figure 5.14. There was a marginal decrease in UCS due to the inclusion of light fibers.

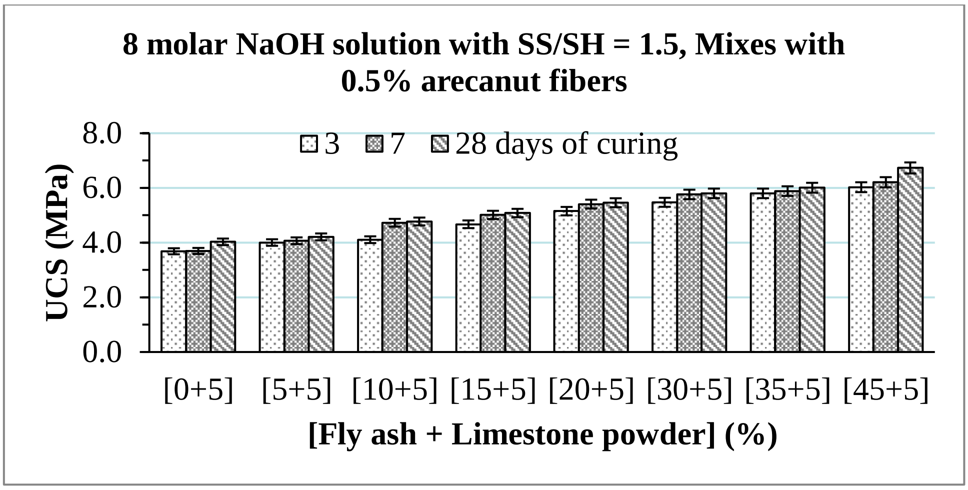

Figure 5. 14 UCS of alkali-activated BC soil with 5% limestone powder, 0–45% fly ash, and 0.5% arecanut fibers at 1.5 SS/SH ratio

ANOVA: Univariate analysis of variance performed indicates that the UCS values are significantly (i.e., $p<0.05$) influenced by the dosage of fly ash and curing period. $R^2 = 0.987$ indicates that 98.7% of the variance in UCS values can be explained by the dosage of fly ash and the curing period. However, limestone powder dosage of 5%, arecanut fiber dosage of 0.5%, and SS/SH ratio of 1.5 are constant in all the mixes; therefore, its influence remains the same. The ANOVA results are tabulated in Table 5.10.

Table 5. 10 ANOVA of UCS of alkali-activated BC soil with the dosage of fly ash, 5% limestone powder, 0.5% arecanut fibers, 1.5 SS/SH ratio, and curing period at modified Proctor density

Tests of Between-Subjects Effects					
Dependent Variable: UCS (MPa)					
Source	Type III Sum of Squares	df	Mean Square	F	Sig.
Corrected Model	17.245[a]	9	1.916	114.560	.000
Intercept	619.150	1	619.150	37016.822	.000
Curing	.606	2	.303	18.110	.000
Ratio	.000	0	.	.	.
Fly ash	16.640	7	2.377	142.117	.000
Limestone powder	.000	0	.	.	.
Arecanut fiber	.000	0	.	.	.
Error	.234	14	.017		
Total	636.630	24			
Corrected Total	17.480	23			
a. R^2= .987 (Adjusted R^2= .978)					

E values:- From equation 3.1, the 'm' values for mixes with 5% limestone powder, various fly ash replacements, and 0.5% arecanut fibers are depicted in Figure 5.15.

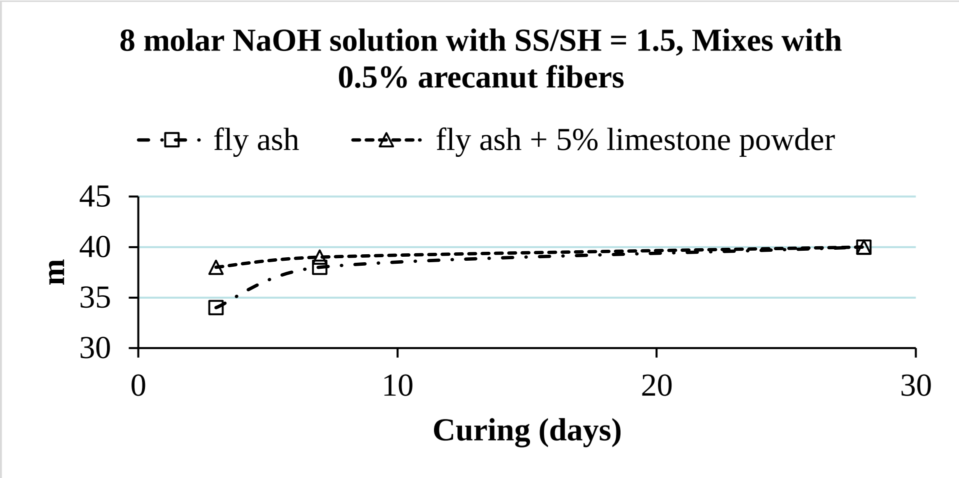

Figure 5. 15 'm' values for alkali-activated BC soil with 5% limestone powder, 0–45% fly ash, and 0.5% arecanut fibers at modified Proctor density

The UCS and E values for different mixes with different curing periods are tabulated in Table 5.11. There was a marginal decrease of E values due to the inclusion of lighter fibers, as shown in Table 5.12.

Table 5. 11 'E' values for alkali-activated BC soil with 5% limestone powder, 0–45% fly ash, and 0.5% arecanut fibers at modified Proctor density

Precursor	Curing (days)	UCS (MPa)	m	E (MPa)
Fly ash	3	2.8–5.1	34	95–173
	7	4.4–6.6	38	167–251
	28	5.1–7.1	40	204–184
Fly ash + 5% limestone powder	3	3.7–6.0	38	141–228
	7	3.7–6.2	39	144–242
	28	4.0–6.7	40	160–268

Table 5. 12 Comparision of 'E' values for alkali-activated BC soil with 5% limestone powder, 0–45% fly ash, with and without 0.5% arecanut fibers at modified Proctor density

Precursor	SS/SH ratio	Curing (Days)	Without arecanut fibers			With 0.5% arecanut fibers		
			UCS (MPa)	m	E (MPa)	UCS (MPa)	m	E (MPa)
Fly ash	1.5	3	4.6–7.4	57	262–422	2.8–5.1	34	95–173
		7	5.0–8.6	60	300–516	4.4–6.6	38	167–251
		28	6.5–9.7	66	429–640	5.1–7.1	40	204–184

Fly ash + 5% limestone powder	1.5	3	3.8–6.6	63	239–416	3.7–6.0	38	141–228
		7	4.4–7.1	67	295–476	3.7–6.2	39	144–242
		28	5.8–8.4	78	452–655	4.0–6.7	40	160–268

5.4.3 Flexural Strength

The BC soil exhibited low flexural strength of 0.02 MPa at modified Proctor density. Significant improvement in flexural strength was observed for the alkali-activated specimens with varying fly ash dosages and 0.5% arecanut fibers cured for 3, 7, and 28 days. The flexural strength of 1.47 MPa was attained with a replacement of 50% fly ash and fibers after 28 days of curing. And it is evident from Figure 5.16. There was a marginal improvement in strength after 7 days of curing for all the mixes. On curing, the addition of arecanut fibers reduced shrinkage cracks as the fibers strongly bonded the stabilized soil. Interfacial friction between fibers and bonded soil restricted the pullout of fibers from the set soil.

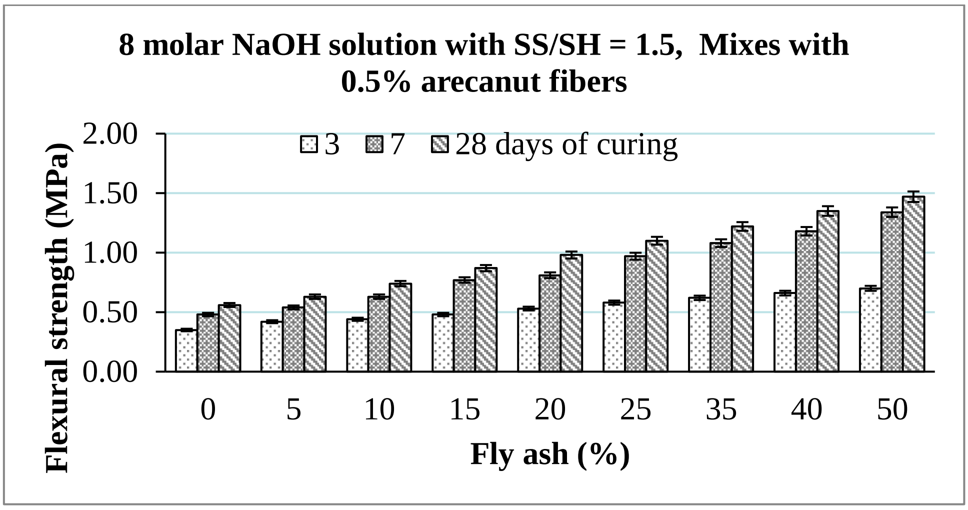

Figure 5. 16 Flexural strength of alkali-activated BC soil with 0–50% fly ash and 0.5% arecanut fibers at 1.5 SS/SH ratio

ANOVA: Univariate analysis of variance performed indicates that the flexural strength values are significantly (i.e., $p<0.05$) influenced by the dosage of fly ash and curing period. R^2 = 0.925 indicates that 92.5% of the variance in flexural strength values can be explained by UCS values. However, arecanut fiber dosage of 0.5% and SS/SH ratio of 1.5 are the same in all the stabilized mixes, which has the same influence on strength. The ANOVA results are tabulated in Table 5.13.

Table 5. 13 ANOVA of flexural strength with the dosage of fly ash, 0.5% arecanut fibers, 1.5 SS/SH ratio, and curing period at modified Proctor density

Tests of Between-Subjects Effects					
Dependent Variable: Flexural strength (MPa)					
Source	Type III Sum of Squares	df	Mean Square	F	Sig.
Corrected Model	2.451[a]	10	.245	19.728	.000
Intercept	17.120	1	17.120	1377.794	.000
Curing	1.019	2	.510	41.005	.000
Fly ash	1.432	8	.179	14.409	.000
Arecanut fiber	.000	0	.	.	.
Error	.199	16	.012		
Total	19.771	27			
Corrected Total	2.650	26			
a. R^2= .925 (Adjusted R^2= .878)					

Regression: Regression analysis is performed between UCS and flexural strength, and the results are tabulated in Table 5.14. A correlation of 0.940 ($p<0.0005$) confirms a strong positive relationship between flexural strength and UCS. R^2= 0.883 indicates that 88.3% of the variance in flexural strength can be explained by UCS. From ANOVA, it can be concluded that the model is statistically significant ($p<0.0005$). From the coefficient table, for every 1 MPa increase in UCS, the model predicts an increase of 0.270 MPa in flexural strength. Also, the t-test confirms the statistical significance of the model.

Table 5. 14 Regression analysis of UCS and flexural strength for alkali-activated BC soil with 0–50% fly ash and 0.5% arecanut fibers at 1.5 SS/SH ratio at modified Proctor density

Correlations			
		Flexural strength (MPa)	UCS (MPa)
Pearson Correlation	Flexural strength (MPa)	1.000	.940
	UCS (MPa)	.940	1.000
Sig. (1-tailed)	Flexural strength (MPa)	.	.000
	UCS (MPa)	.000	.
N	Flexural strength (MPa)	27	27
	UCS (MPa)	27	27

Model Summary[b]				
Model	R	R Square	Adjusted R Square	Std. Error of the Estimate
1	.940[a]	.883	.878	.11142
a. Predictors: (Constant), UCS (MPa)				
b. Dependent Variable: Flexural strength (MPa)				

ANOVA[a]						
Model		Sum of Squares	df	Mean Square	F	Sig.
1	Regression	2.340	1	2.340	188.477	.000[b]
	Residual	.310	25	.012		
	Total	2.650	26			
a. Dependent Variable: Flexural strength (MPa)						
b. Predictors: (Constant), UCS (MPa)						

Coefficients[a]								
Model		Unstandardized Coefficients		Standardized Coefficients	t	Sig.	95.0% Confidence Interval for B	
		B	Std. Error	Beta			Lower Bound	Upper Bound
1	(Constant)	-.590	.103		-5.714	.000	-.802	-.377
	UCS (MPa)	.270	.020	.940	13.729	.000	.229	.310
a. Dependent Variable: Flexural strength (MPa)								

There was a significant improvement in the strength of alkali-activated soil with fly ash, limestone powder mixes along fibers. There was considerable strength gain after 3 days of curing for all the mixes, and this may be due to the quick reaction of limestone powder with alkali solution. The further curing period could not help to enhance the strength. The test results are depicted in Figure 5.17. The mix of 45% fly ash, 5% limestone powder, and 0.5% arecanut fibers attained a flexural strength of 1.2 MPa on 28 days of curing. Therefore, at a higher dosage of fly ash (45%) with limestone powder, a higher amount of dissolvable silica, alumina, calcium, and other reactive elements are formulated to enhance the strength.

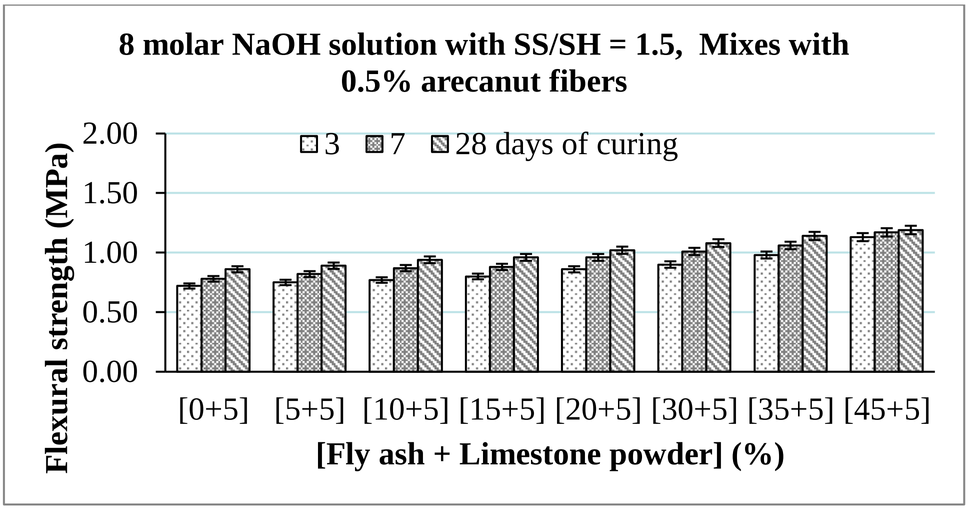

Figure 5. 17 Flexural strength of alkali-activated BC soil with 5% limestone powder, 0–45% fly ash, and 0.5% arecanut fibers at 1.5 SS/SH ratio

ANOVA: Univariate analysis of variance performed indicates that the flexural strength values are significantly (i.e., $p<0.05$) influenced by the dosage of fly ash and curing period. $R^2 = 0.988$ indicates that 98.8% of the variance in flexural strength values can be explained by the dosage of fly ash and curing period. However, arecanut fiber dosage of 0.5%, limestone powder dosage of 5%, and SS/SH ratio of 1.5 are the same for all mixes. The ANOVA results are tabulated in Table 5.15.

Table 5. 15 ANOVA of flexural strength of alkali-activated BC soil with the dosage of fly ash, 5% limestone powder, 0.5% arecanut fibers, 1.5 SS/SH ratio, and curing period at modified Proctor density

Tests of Between-Subjects Effects					
Dependent Variable: Flexural strength (MPa)					
Source	Type III Sum of Squares	df	Mean Square	F	Sig.
Corrected Model	.432[a]	9	.048	123.150	.000
Intercept	21.169	1	21.169	54295.591	.000
Curing	.086	2	.043	110.044	.000
Ratio	.000	0	.	.	.
Fly ash	.346	7	.049	126.895	.000
Limestone powder	.000	0	.	.	.
Arecanut fiber	.000	0	.	.	.
Error	.005	14	.000		
Total	21.606	24			
Corrected Total	.438	23			
a. R^2= .988 (Adjusted R^2= .980)					

Regression: Regression analysis is performed between UCS and flexural strength, and the results are tabulated in Table 5.16. A correlation of 0.919 ($p<0.0005$) confirms a strong positive relationship between flexural strength and UCS. $R^2 = 0.845$ indicates that 84.5% of the variance in flexural strength can be explained by UCS. From ANOVA, it can be concluded that the model is statistically significant ($p<0.0005$). From the coefficient table, for every 1 MPa increase in UCS, the model predicts an increase of 0.145 MPa in flexural strength. Also, the t-test confirms the statistical significance of the model.

Table 5. 16 Regression analysis of UCS and flexural strength for alkali-activated BC soil with 5% limestone powder, 0–45% fly ash, and 0.5% arecanut fibers, 1.5 SS/SH ratio at modified Proctor density

Correlations

		Flexural strength (MPa)	UCS (MPa)
Pearson Correlation	Flexural strength (MPa)	1.000	.919
	UCS (MPa)	.919	1.000
Sig. (1-tailed)	Flexural strength (MPa)	.	.000
	UCS (MPa)	.000	.
N	Flexural strength (MPa)	24	24
	UCS (MPa)	24	24

Model Summary[b]

Model	R	R Square	Adjusted R Square	Std. Error of the Estimate
1	.919[a]	.845	.838	.05549

a. Predictors: (Constant), UCS (MPa)

b. Dependent Variable: Flexural strength (MPa)

ANOVA[a]

Model		Sum of Squares	df	Mean Square	F	Sig.
1	Regression	.370	1	.370	120.117	.000[b]
	Residual	.068	22	.003		
	Total	.438	23			

a. Dependent Variable: Flexural strength (MPa)

b. Predictors: (Constant), UCS (MPa)

Coefficients[a]

Model		Unstandardized Coefficients		Standardized Coefficients	t	Sig.	95.0% Confidence Interval for B	
		B	Std. Error	Beta			Lower Bound	Upper Bound
1	(Constant)	.200	.068		2.931	.008	.059	.342
	UCS (MPa)	.145	.013	.919	10.960	.000	.118	.173

a. Dependent Variable: Flexural strength (MPa)

5.4.4 California Bearing Ratio

The CBR tests are not recommended for stabilized soil. The recent code IRC 37: 2018 recommends the pavement based on UCS values. In the present investigation, the UCS values obtained after 28 days of curing are on the higher side. Therefore, CBR tests are conducted after 28 days of curing. After 28 days of curing the alkali-activated soil with different fly ash dosages, limestone powder and fibers becomes stiff and hard, and thereby CBR values attained are more than 100% at unsoaked condition. Arecanut fibers formed a strong matrix, due to which resistance to the plunger penetration was increased. When immersed in water, due to the delectation of structure by minerals leaching from the set mix, the samples lost most of their strength, exhibited low CBR values. Also, high expansion was observed due to the higher water affinity of the mixes. The results are depicted in Figures 5.18 and 5.19.

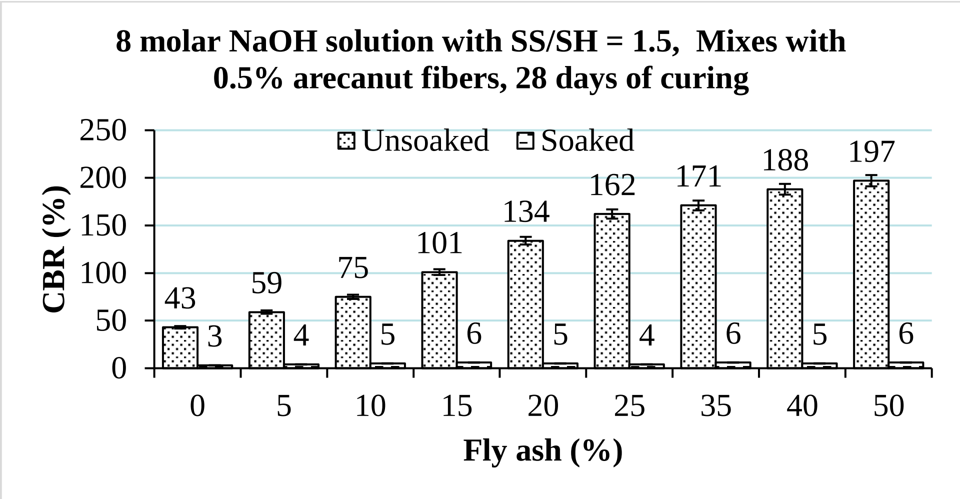

Figure 5. 18 CBR of alkali-activated BC soil with 0–50% fly ash and 0.5% arecanut fibers at 1.5 SS/SH ratio after 28 days of curing

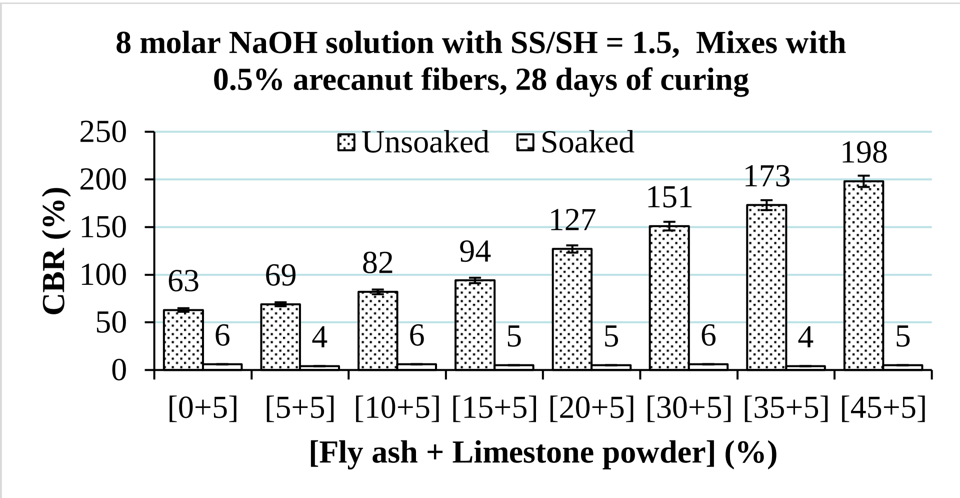

Figure 5. 19 CBR of alkali-activated BC soil with 5% limestone powder, 0–45% fly ash, and 0.5% arecanut fibers at 1.5 SS/SH ratio after 28 days of curing

5.5 ALKALI-ACTIVATED BC SOIL WITH CONSTRUCTION DEMOLITION WASTE

5.5.1 Compaction

Locally available selected CDW was replaced from 10–50% as a precursor material for alkali-activated BC soil. The mixes with higher CDW content exhibited higher modified Proctor density. Due to the inclusion of CDW, the workability of the mix improved, which resulted in easy compaction. Due to the low water affinity of CDW, the OMC decreased at higher replacement levels. A maximum density of 1.97 g/cc was observed at 13.6% OMC for 50% replacement of CDW, which is evident from Figure 5.20.

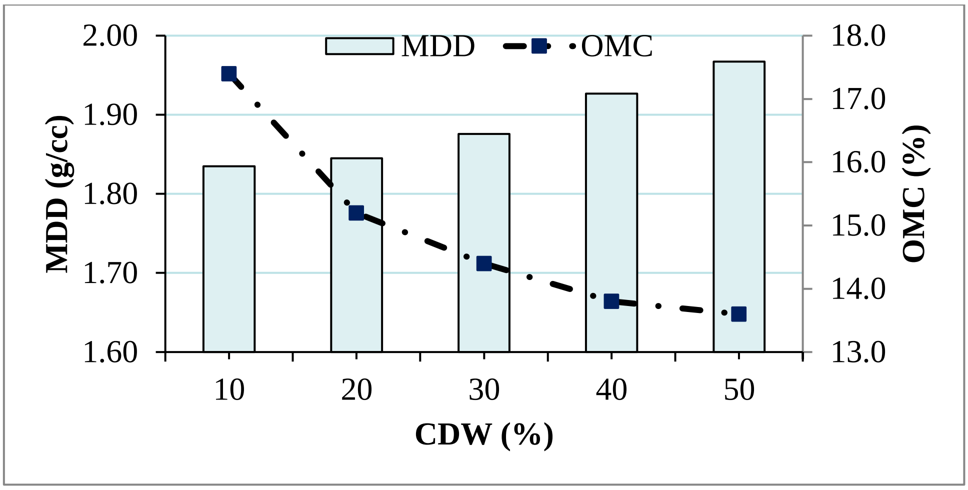

Figure 5. 20 Modified Proctor results for 0–50% CDW treated BC soil

5.5.2 Unconfined Compressive Strength

The UCS tests are conducted for alkali-activated BC soil with varying dosages of CDW with 8 molar NaOH concentration and SS/SH ratios of 0.5, 1.0, and 1.5. The test results are depicted in Figure 5.21(a–c). Only at SS/SH ratio of 1.5, the significant improvement in strength observed due to the solubility/ dissolution of precursor material. The CDW contains cementitious material, which includes set cement and sand that has undergone the hydration process once. At higher replacement of CDW, the specimens exhibited a significant improvement in UCS.

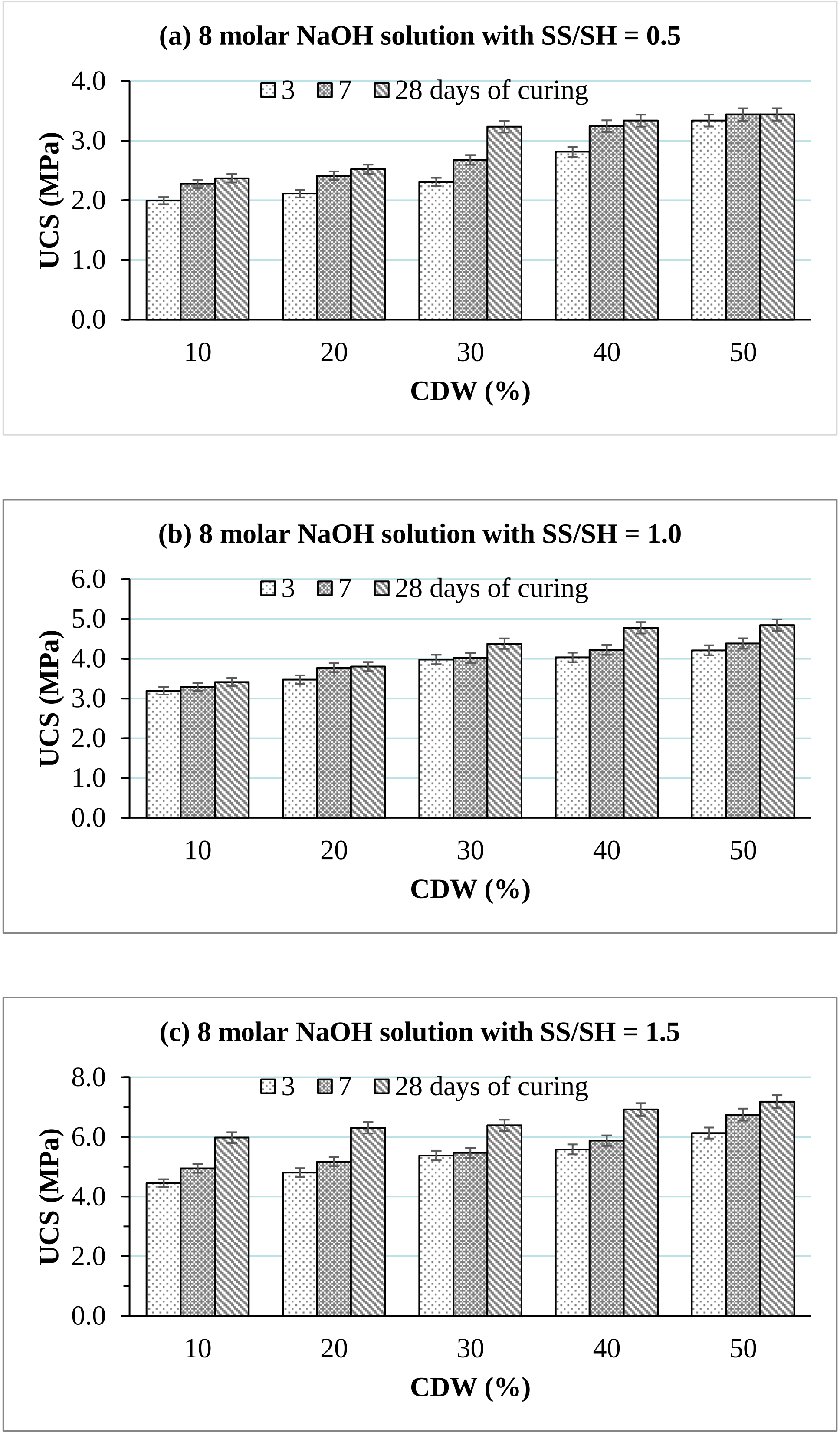

Figure 5. 21 UCS of alkali-activated BC soil with 0–50% CDW at (a) 0.5 (b) 1.0 (c) 1.5 SS/SH ratios

ANOVA: Univariate analysis of variance performed indicates that the UCS values are significantly (i.e., $p<0.05$) influenced by the dosage of CDW, SS/SH ratio, and curing period. $R^2 = 0.974$ indicates that 97.4% of the variance in UCS values can be explained by the dosage of CDW, SS/SH ratio, and curing period. The ANOVA results are tabulated in Table 5.17.

Table 5. 17 ANOVA of UCS of alkali-activated BC soil with the dosage of CDW, SS/SH ratio, and curing period at modified Proctor density

Tests of Between-Subjects Effects					
Dependent Variable: UCS (MPa)					
Source	Type III Sum of Squares	df	Mean Square	F	Sig.
Corrected Model	85.311[a]	8	10.664	165.411	.000
Intercept	788.768	1	788.768	12234.816	.000
CDW	9.690	4	2.422	37.575	.000
Curing	4.188	2	2.094	32.481	.000
Ratio	71.433	2	35.717	554.012	.000
Error	2.321	36	.064		
Total	876.400	45			
Corrected Total	87.632	44			
a. R^2= .974 (Adjusted R^2= .968)					

E values:- From Equation 3.1, the 'm' value obtained for mixes with various CDW replacements is depicted in Figure 5.22. The UCS and E for different mixes with different curing periods are tabulated in Table 5.18. The shear resistance offered by sand particles has contributed to improvement in E values. But, due to less reactivation of CDW with alkali solution, the E values are marginally reduced than mixes with fly ash.

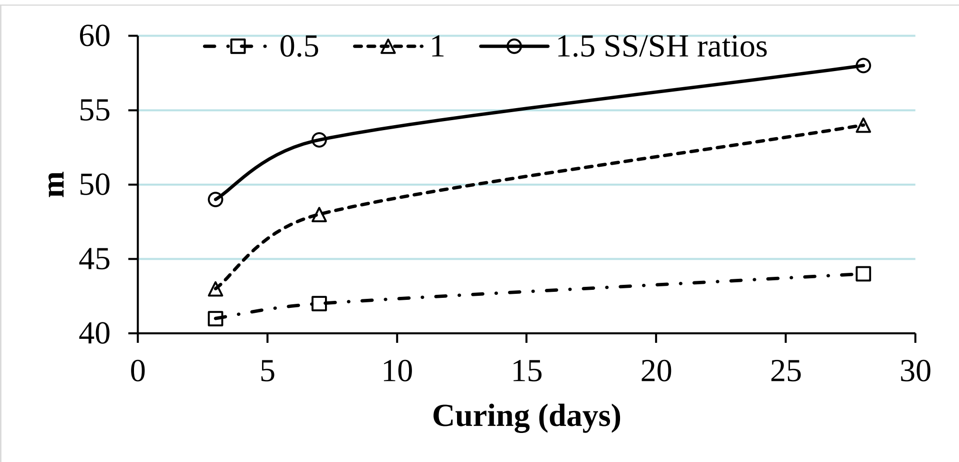

Figure 5. 22 'm' values for alkali-activated BC soil with 0–50% CDW at modified Proctor density

Table 5. 18 'E' values for alkali-activated BC soil with 0–50% CDW at modified Proctor density

SS/SH ratio	Curing (days)	UCS (MPa)	m	E (MPa)
0.5	3	2–3.3	41	82–135
	7	2.3–3.4	42	97–143
	28	2.4–3.4	44	106–150
1.0	3	3.2–4.2	43	138–181
	7	3.3–4.4	48	158–211
	28	3.4–4.8	54	184–259
1.5	3	4.4–6.1	49	216–299
	7	4.9–6.7	53	260–355
	28	6.0–7.2	58	348–418

5.5.3 Flexural strength

The BC soil is replaced with CDW with a varying percentage up to 50% and alkali-activated with a SS/SH ratio solution of 1.5. Due to the formation of hydration products when alkali-activated, the mixes compacted at modified Proctor density created a strong bonding, and there was no volumetric shrinkage with curing. Hence, solid prisms were obtained without the signs of any shrinkage cracks. These specimens exhibited significant improvement in strength. Stabilized specimens replaced with 50% CDW at an SS/SH ratio of 1.5 exhibited a maximum flexural strength of 0.75 MPa after 28 days of curing. The test results are depicted in Figure 5.23.

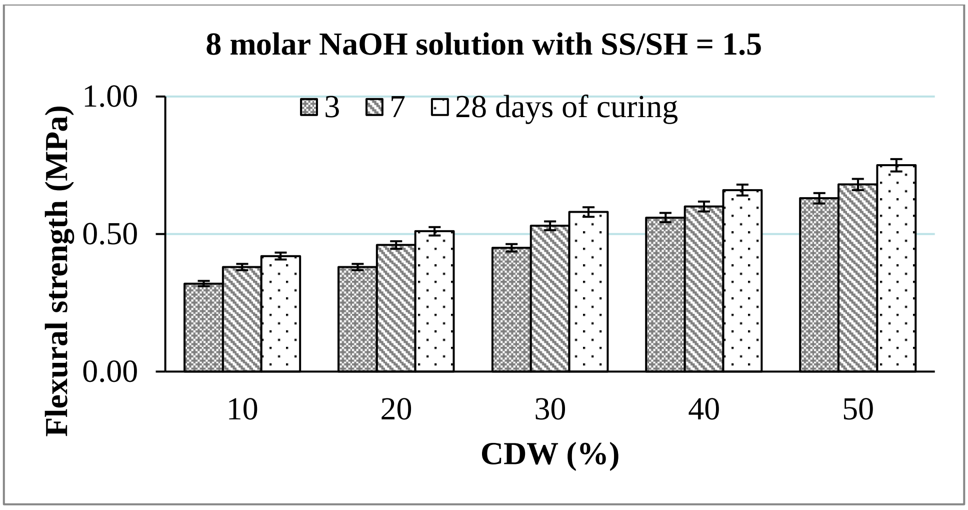

Figure 5. 23 Flexural strength of alkali-activated BC soil with 0–50% CDW at 1.5 SS/SH ratio

ANOVA: Univariate analysis of variance performed indicates that the flexural strength values are significantly (i.e., $p<0.05$) influenced by the dosage of CDW and curing period. $R^2 = 0.996$ indicates that 99.6% of the variance in flexural strength values can be explained by the dosage of CDW and the curing period. However, SS/SH ratio is 1.5 for all the stabilized mixes. The ANOVA results are tabulated in Table 5.19.

Table 5. 19 ANOVA of flexural strength with the dosage of CDW, SS/SH ratio of 1.5, and curing period at modified Proctor density

Tests of Between-Subjects Effects					
Dependent Variable: Flexural strength (MPa)					
Source	Type III Sum of Squares	df	Mean Square	F	Sig.
Corrected Model	.218[a]	6	.036	320.569	.000
Intercept	4.171	1	4.171	36804.765	.000
CDW	.184	4	.046	406.529	.000
Curing	.034	2	.017	148.647	.000
Error	.001	8	.000		
Total	4.390	15			
Corrected Total	.219	14			
a. R^2= .996 (Adjusted R^2= .993)					

Regression: Regression analysis is performed between UCS and flexural strength, and the results are tabulated in Table 5.20. A correlation of 0.897 ($p<0.0005$) confirms a strong positive relationship between UCS and flexural strength. R^2= 0.804 indicates that 80.4% of the variance in flexural strength can be explained by UCS. From ANOVA, it can be concluded that the model is statistically significant ($p<0.0005$). From the coefficient table, for every 1 MPa increase in UCS, the model predicts an increase of 0.139 MPa in flexural strength. Also, the t-test confirms the statistical significance of the model.

Table 5. 20 Regression analysis of UCS and flexural strength for alkali-activated BC soil with 0–50% CDW at modified Proctor density

Correlations			
		Flexural strength (MPa)	UCS (MPa)
Pearson Correlation	Flexural strength (MPa)	1.000	.897
	UCS (MPa)	.897	1.000
Sig. (1-tailed)	Flexural strength (MPa)	.	.000
	UCS (MPa)	.000	.
N	Flexural strength (MPa)	15	15
	UCS (MPa)	15	15
Model Summary[b]			

Model	R	R Square	Adjusted R Square	Std. Error of the Estimate
1	.897[a]	.804	.789	.05740
a. Predictors: (Constant), UCS (MPa)				
b. Dependent Variable: Flexural strength (MPa)				

ANOVA[a]

Model		Sum of Squares	df	Mean Square	F	Sig.
1	Regression	.176	1	.176	53.428	.000[b]
	Residual	.043	13	.003		
	Total	.219	14			
a. Dependent Variable: Flexural strength (MPa)						
b. Predictors: (Constant), UCS (MPa)						

Coefficients[a]

Model		Unstandardized Coefficients		Standardized Coefficients	t	Sig.	95.0% Confidence Interval for B	
		B	Std. Error	Beta			Lower Bound	Upper Bound
1	(Constant)	-.280	.111		-2.514	.026	-.521	-.039
	UCS (MPa)	.139	.019	.897	7.309	.000	.098	.180
a. Dependent Variable: Flexural strength (MPa)								

5.5.4 California Bearing Ratio

The activated BC soil with CDW with curing period has significantly improved unsoaked CBR values. The increase of sand-size particles at 50% replacement of CDW has contributed to higher CBR values due to improved soil friction. After soaking, due to the delectation of bonded soil structure resulting from mineral constituents leaching, the specimens could not retain the strength. Thereby, low soaked CBR values were observed, and the test results are depicted in Figure 5.24. These specimens exhibited high expansion on soaking. Therefore, the selection of CDW for BC soil stabilization lost significance.

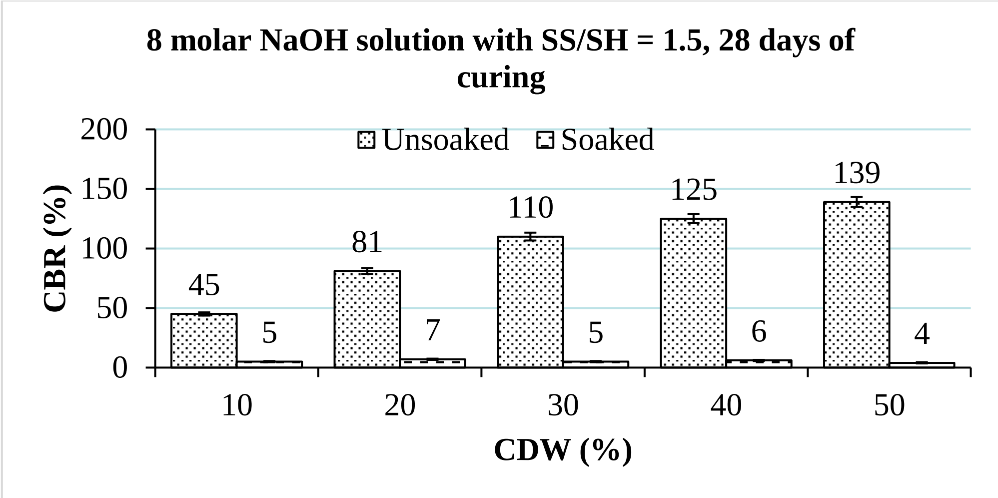

Figure 5. 24 CBR of alkali-activated BC soil with 0–50% CDW at 1.5 SS/SH ratio after 28 days of curing

5.6 FATIGUE PERFORMANCE

The fatigue tests are performed for 1) BC soil + fly ash 2) BC soil + fly ash + limestone powder 3) BC soil + fly ash + arecanut fibres 4) BC soil + fly ash + limestone powder + arcanut fibers, and 5) BC soil + CDW mixes.

Alkali-activated specimens with different precursor materials were subjected to repeated load application under various loads corresponding to 28 days UCS value. The specimens with fly ash sustained more repetitions due to the good bonding created by hydrated gels. The addition of 5% limestone powder resulted in a slight decrease in fatigue life. The addition of fibers was found to be effective in improving fatigue life. The results are tabulated in Table 5.21. But, the bonding developed at the soil-fiber interface for alkali-activated mixes was less than soil-cement-fiber bonding. Due to this, under repeated loads, the separation of fibers from alkali-activated soil was observed. The specimens with CDW sustained comparatively less repeated loads. Cracks developed and propagated at the interface between soil and unreacted particles of CDW. The samples tested at an applied load of 0.2 times UCS sustained more than $1.0\times10^{\wedge 5}$ repetitions.

Table 5. 21 Fatigue life of alkali-activated BC soil with marginal materials

Mix ID	Ingredients (%)	28 days UCS (MPa)	Stress level					
			0.65		0.5		0.35	
			Load (N)	N	Load (N)	N	Load (N)	N
S-Fa	100-0	6.5	4816	36	3705	485	2593	31791
	95-5	6.8		125		3366		37910
	75-25	8.7		2486		27047		70805
	50-50	9.7		12331		41611		86375
S-Fa-L	95-0-5	5.8	4252	46	3271	588	2290	28020
	75-20-5	6.6		656		9307		42820
	50-45-5	8.4		8405		32355		69508
S-Fa-Af	100-0-0.5	5.1	3746	143	2881	823	2017	47481
	95-5-0.5	5.2		193		2878		52053
	75-25-0.5	5.9		287		17832		76365
	50-50-0.5	7.1		9867		49950		115321
S-Fa-L-Af	95-0-5-0.5	4.0	2969	172	2284	769	1599	42587
	75-20-5-0.5	5.5		4666		37849		94906
	50-45-5-0.5	6.7		31964		74228		132548
S-CDW	90-10	6.0	4405	48	3388	396	2372	23609
	70-30	6.4		103		3826		31539
	50-50	7.2		261		12732		45930

Note:- S = BC soil, Fa = class F fly ash, L = Limestone powder, Af = Arecanut fiber, CDW = Construction demolition waste.

5.7 DURABILITY

5.7.1.1 Wetting-Drying

Alkali-activated BC soil with different marginal materials after 7 days of ambient temperature curing was subjected to durability tests. During the wetting cycle, the specimens exhibited more absorption of water with sudden failure. The specimens could not retain the bonding developed by the alkali solution due to the leaching of mineral constituents. Some more trial specimens prepared with high (10 and 12 molar) and low (1 and 2 molar) NaOH concentrations with different SS/SH ratios could not sustain the wetting cycle. Therefore, alkali activation is not suitable for BC soil stabilization with the marginal materials for heavy rainfall areas.

5.7.1.2 Freezing-Thawing

Alkali-activated BC soil with different marginal materials after the specified curing period, when subjected to freezing, exhibited a considerable increase in volume due to water absorption from felt pads. After completing the 1st freezing cycle, these specimens showed a rapid increase in volume due to moisture absorption and softened when thawed. The softened specimens could not resist brushing, and even the unbrushed specimens failed. Therefore, alkali-activated BC soil with selected marginal materials can not sustain in the low-temperature regions.

Failure mechanism:- Each grain of pulverized BC soil contains a clumped group of microparticles. All these BC soil grains are bonded with polymer gel formed. But, when moisture comes in contact with each soil grain, the hydrophilic clay minerals readily absorb it. Attracted water increases the space between clay minerals due to diffused double layer formation. The moisture absorption continues and spreads from grain to grain, which exerts enormous swell pressure on the surrounding particles. As a result, the quick expansion, debonding, and cracking of stabilized soil will progress. The depolymerization of the aluminosilicate matrix results in strength loss of stabilized material in extreme temperature or due to water absorption on soaking. Alkali-activated materials release water during curing to enhance the strength, whereas, water absorption results in strength loss which results in further deterioration. The failure of alkali-activated specimens is depicted in Figure 5.25.

It is mentioned that the presence of water may reduce the concentration of the alkali ions in the gel, changing its properties and its ability to harden (Rios et al. 2019). The failure of the specimens is due to the leaching of metals such as Na, Al, Si, Ca, Fe present in the raw material and alkaline content that is capable of forming (N-A-S-H) gel and (C-(N)-A-S-H) gel. It may hinder the pozzolanic activity in the mix can lead to a further decrease in strength or even total disintegration of the sample.

In a previous study by Tigue et al. 2018, leaching tests conducted on soil-fly ash geopolymer cement depicted that a considerable amount of Al, Ca, Fe, Na, and Si exhibits high leachability. A less amount leaching of heavy metals such as As, Cd, Cr, and Pb was reported. The high concentration of Al, Na, and Si is attributed to the high initial content of Al, Na, and Si in the raw material and alkali activator. The incorporation of the Fe in the geopolymer matrix may reduce its leaching. Ca leaching may support the presence of gypsum in the geopolymer matrix. The leached out Ca may come from the unreacted Ca in the matrix due to the insufficient amount of reactive silica and alumina available for gel formation (Tigue et al. 2018).

(a) Alkali-activated BC soil specimen

(b) Soaked specimens were bulged and exhibited deterioration during the drying cycle

(c) Failure of alkali-activated soil with fly ash during soaking cycle

(d) Water turned into a blackish colour with the softened alkali-activated soil

Figure 5. 25 Alkali-activated BC soil during different stages of durability test

5.8 MICROSTRUCTURAL ANALYSIS

5.8.1 SEM Analysis

At the initial stage, due to the presence of moisture in the stabilized mix, Van der Waals' force, Brownian motion, and electrostatic repulsion exist between the particles. The chemical reaction between reactive aluminosilicates present in the precursor materials in an alkaline environment leads to the formation of amorphous gels of C-(A)-S-H or N-(A)-S-H. Due to the availability of a high amount of Na ions at an early age, N-(A)-S-H gel formation dominates. As time elapses, Ca^{2+} ions dominate over Na^{+} ions forming more C-(A)-S-H gels. If the dissolution rate of Ca^{2+} ions decreases, it might reduce gel formation and strength gain. The interlayer repulsive forces will be dominant if high Ca^{2+} ion concentration and high ionic radius are found in alkali-activated precursors silicate chain. Inserted Al^{3+} ions in C-(A)-S-H gels result in a higher interlayer spacing than CSH and N-(A)-S-H gels. Therefore, the water binding ability of C-(A)-S-H gel is more. According to Zhang et al. 2021, the formation of more C-(A)-S-H gel leads to a less porous structure with time.

The BC soil without any treatment developed many shrinkage cracks on drying, as depicted in Figure 5.26a. If BC soil is used for subgrade, these cracks may propagate to the upper pavement layers during load application, leading to pavement failure at low-stress values due to reflection cracks. Drying shrinkage of the BC soil can be expected during the summer season due to loss of moisture. Figure 5.26b depicts the discontinuous and loose structure of the dry BC soil with more pores. Darker areas represent the air voids. The shrinkage cracks developed due to dehydration of soil are clearly visible. Due to shrinkage, the debonding of arecanut fibers from soil was observed. As observed from different tests, montmorillonite clay mineral is responsible for swell-shrink behaviour, moisture variations, and strength loss. The addition of 5% fly ash to the BC soil has formed a flake-like structure, as depicted in Figure 5.26c. Spherical particles in the mix are the unreacted fly ash, indicating its inertness.

The effect on the morphology of the stabilized mix using fly ash precursor for improving soil properties using alkali solution is depicted in Figure 5.26d. Due to polymerization compound formations by alkali-activated fly ash precursor, the pore spaces were sealed; therefore, no cracks and discontinuities are observed. Dense packing of soil particles due to continuous geopolymer matrix sealed the void spaces.

Also, the polymerization compounds deposited on the rougher fiber surface exhibited excellent bonding of the stabilized mix. Therefore, the stabilized soil interlocked by the fibers is responsible for improving the flexural strength and plunger penetration resistance during the unsoaked CBR test. Figure 5.26e depicts the change in morphology of stabilized soil due to geopolymer product formations.

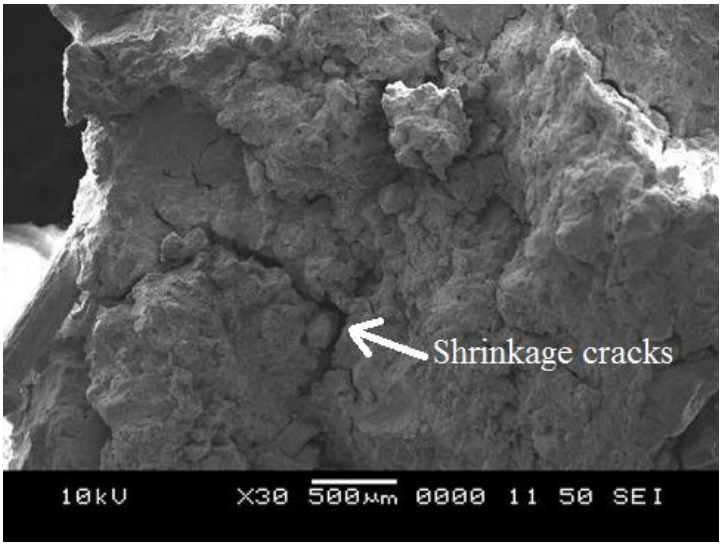

(a) Dry BC soil with shrinkage cracks

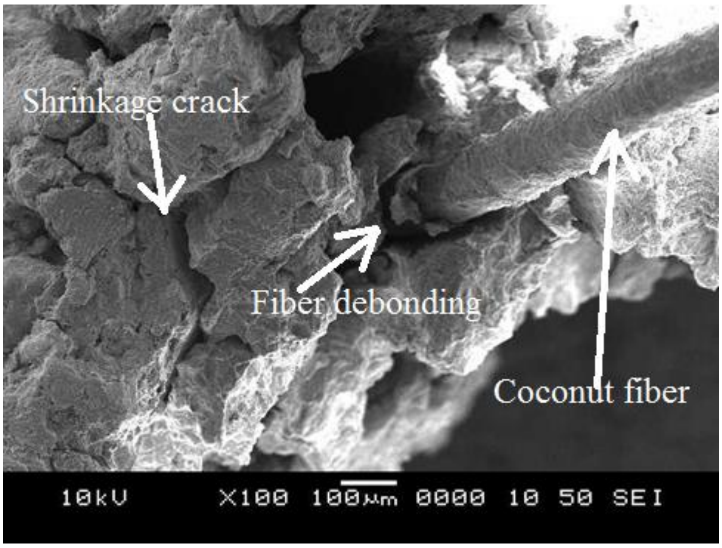

(b) BC soil exhibiting shrinkage cracks and debonded arecanut fiber

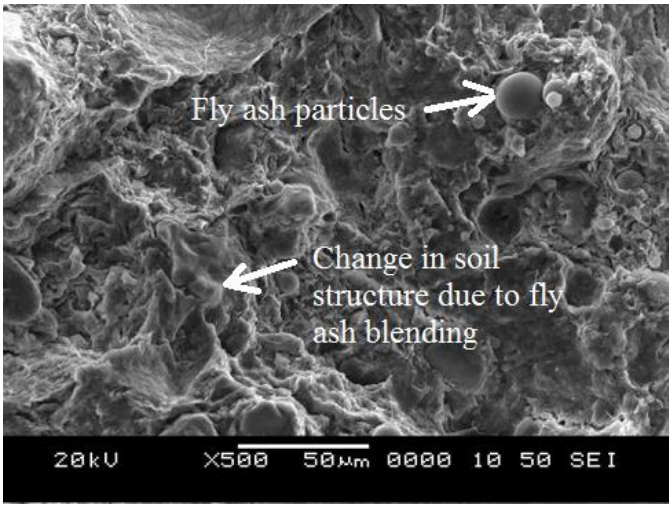

(c) BC soil with 5% fly ash

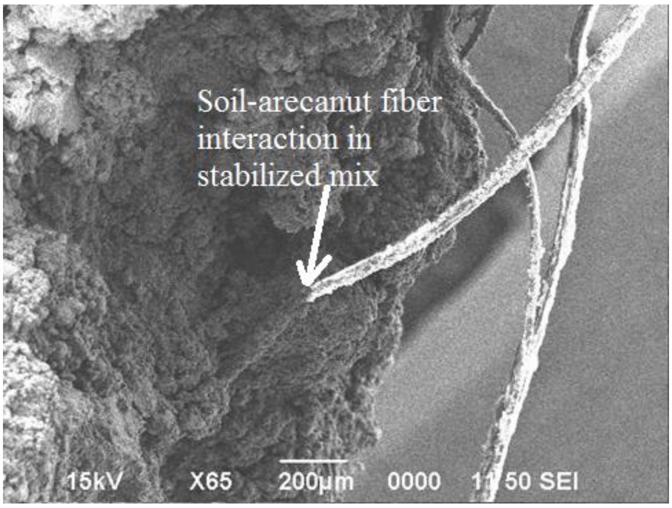

(d) Arecanut fibers bonded in alkali-activated BC soil with fly ash

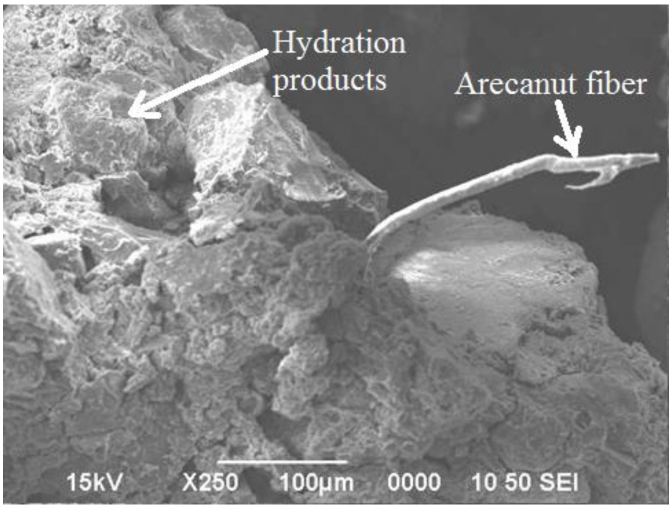

(e) Hydration products of alkali-activated BC soil with fly ash

Figure 5. 26 SEM images of alkali-activated fly ash

Arecanut fibers were strongly bonded in the alkali-activated set soil with precursors fly ash and limestone powder. Interfacial friction between treated soil and fiber was enhanced due to hydration product deposition, as depicted in Figure 5.27. During strength tests, the treated samples failed at higher stress values due to the improved friction with the pullout of fibers. An enlarged view shows the deposits of hydrated gels on the fiber surface, which is depicted in Figure 5.28. The alkali treatment could make the improved soil a compact mass with reduced void spaces. Also, shrinkage cracks were disappeared due to strong fiber bonding and hydration gels.

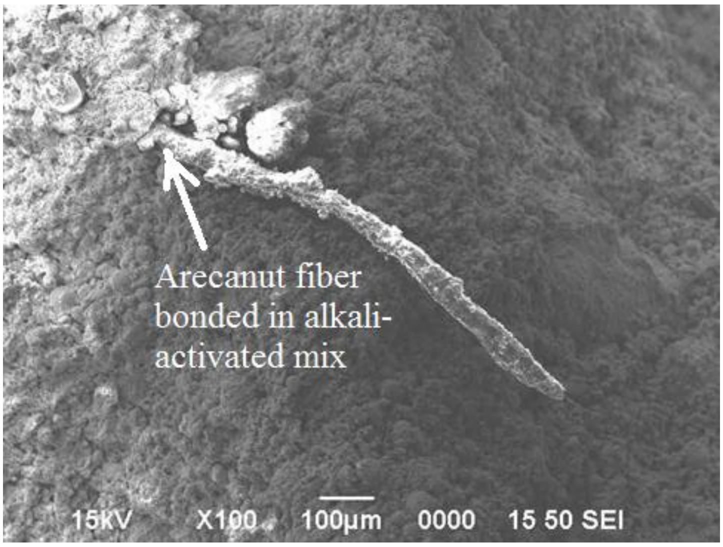

Figure 5. 27 Arecanut fiber firmly bound in alkali-activated BC soil with class F fly ash, and limestone powder

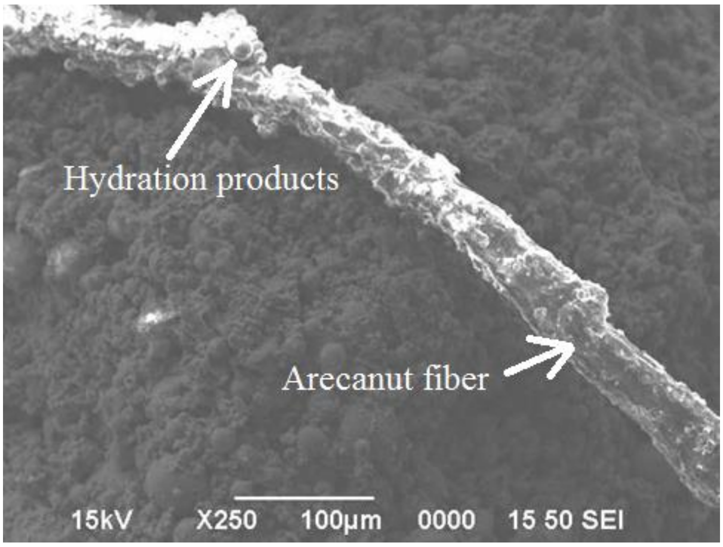

Figure 5. 28 Enlarged view of alkali hydration product deposition on the arecanut fiber surface

In the CDW precursor, the fine particles of set cement were involved in the alkali reaction. When set mortar waste was mixed with the BC soil and stabilized using the alkali solution, the particles of the sand did not show involvement in the reaction. In the presence of a high concentration alkali solution, the inert sand particles with rich silica content were not dissolved. Therefore, available dissolvable silica from sand particles is minimum. But, these non-reactive particles bound in geopolymer gel acts as matrix reinforcement (Bassani et al. 2019). Also, the dissolvable alumina and silica available from BC soil, and other fine particles of CDW, resulted in strength improvement of the activated mix. Spherical particles observed in set soil were from cement. The entire bonded cluster was formed due to the gelation of dissolvable silica, alumina, and other elements from all the mixed ingredients, as depicted in Figure 5.29. Even the inert sand particles contributed to the improvement in frictional resistance of the stabilized soil.

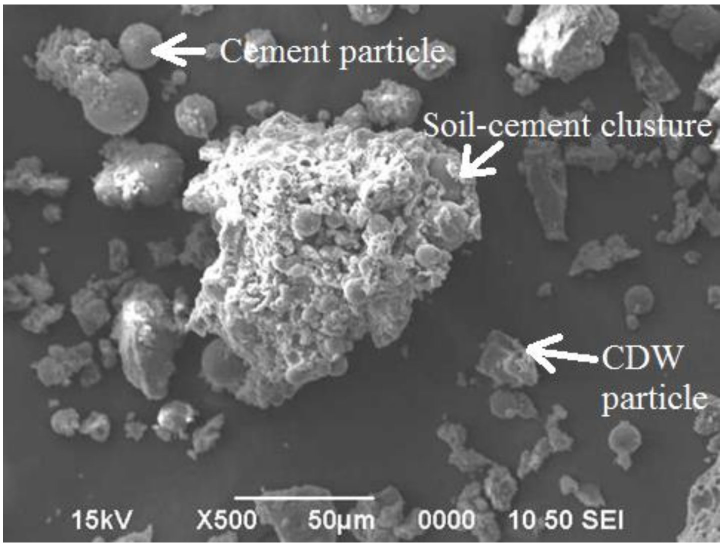

Figure 5. 29 Alkali-activated BC soil with CDW

5.8.2 XRD Analysis

The change in crystalline phases of alkali-activated BC soil with various precursors was identified using XRD analysis. XRD patterns justified the strength improvement by the formation of many geopolymer products. It can be observed that these formations include dissolved silica, alumina, calcium, sulfate, potassium, etc., either obtained from alkali solution or soil and precursor materials. Micrograms depicted show the formation of various products at the highest intensity; however, they spread over multiple 2θ angles. These geopolymer compounds are highly capable of retaining the bond between particles of the stabilized mix in the dry state.

The addition of limestone powder enhanced the formation of calcium-based compounds, resulted in higher intensity peaks. Whereas, mixes stabilized with fly ash alone exhibited less intense peaks, but the compounds formed are spread over many 2θ angles. When CDW was used, the fines present in the waste mortar were reactivated due to their dissolution in a high alkaline environment, resulting in comparatively intermittent intensity peaks.

The common phases observed in the set stabilized mix with fly ash as depicted in Figure 5.30 are:- [G] Gismondine ($CaAl_2Si_2O_8 \cdot 4H_2O$), [M] Millosevichite ($Al_2(SO_4)_3$), [F] Foshagite ($Ca_4(SiO_3)_3(OH)_2$), [X] Xonotlite ($Ca_6Si_6O_{17}(OH)_2$), [N] Nordstrandite ($Al(OH)_3$), [L] Liottite ($(Ca, Na)_4(Si, Al)_6O_{12}(SO_4, OH, Cl, CO_3)_2 \cdot xH_2O$), [C] Calcium Sulfate Hydrate ($CaSO_4 \cdot 0.15H_2O$), [S] Sodium Hydrogen Sulfate ($NaHSO_4$), etc. Along with this, Quartz low (SiO_2) and Pigeonite ($((Ca, Mg, Fe)(Mg, Fe)Si_2O_6)$, which is a mineral of the clinopyroxene subgroup of the pyroxene group, were also found in this stabilized mix.

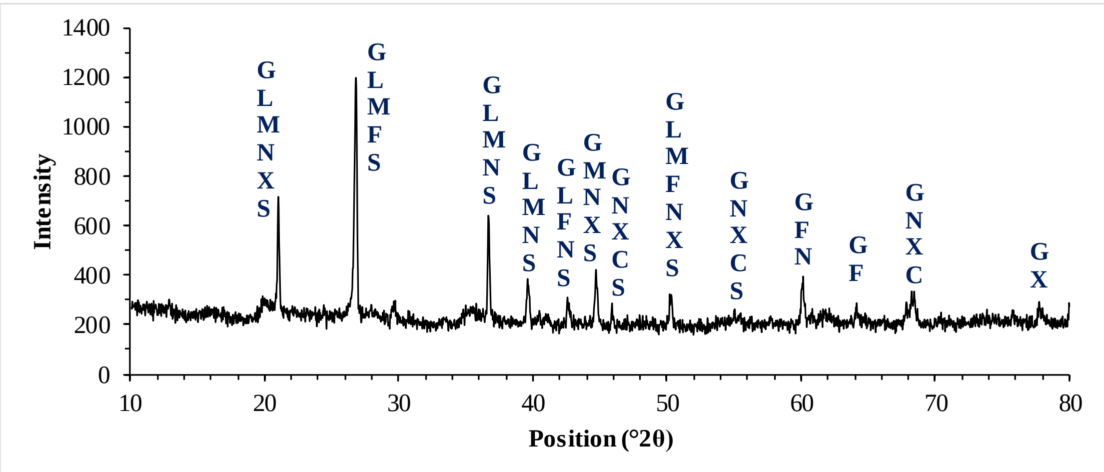

Figure 5. 30 XRD diffractogram of alkali-activated BC soil with class F fly ash

The common phases observed in the set stabilized mix with fly ash and limestone powder as depicted in Figure 5.31 are:- [Gi] Gismondine ($CaAl_2Si_2O_8 \cdot 4H_2O$), [Ca] Calcite ($CaCO_3$), [Al] Aluminum Oxide ($Al_2O_3$), [CSH] Calcium Sulfate Hydrate ($CaSO_4 \cdot 0.15H_2O$), [Mi] Millosevichite ($Al_2(SO_4)_3$), [Gi] Gibbsite ($Al(OH)_3$), [Ma] Magnesite ($MgCO_3$), [Gy] Gypsum ($CaSO_4 \cdot 2H_2O$), [CS] Calcium Sulfate ($CaSO_4$), [Go] Gorgeyite ($K_2Ca_5(SO_4)_6 \cdot H_2O$), [Fo] Foshagite ($Ca_4(SiO_3)_3(OH)_2$), [SHS] Sodium

Hydrogen Sulfate ($NaHSO_4$), [Sp] Spurrite ($Ca_5(SiO_4)_2CO_3$), [Xo] Xonotlite ($Ca_6Si_6O_{17}(OH)_2$), etc.

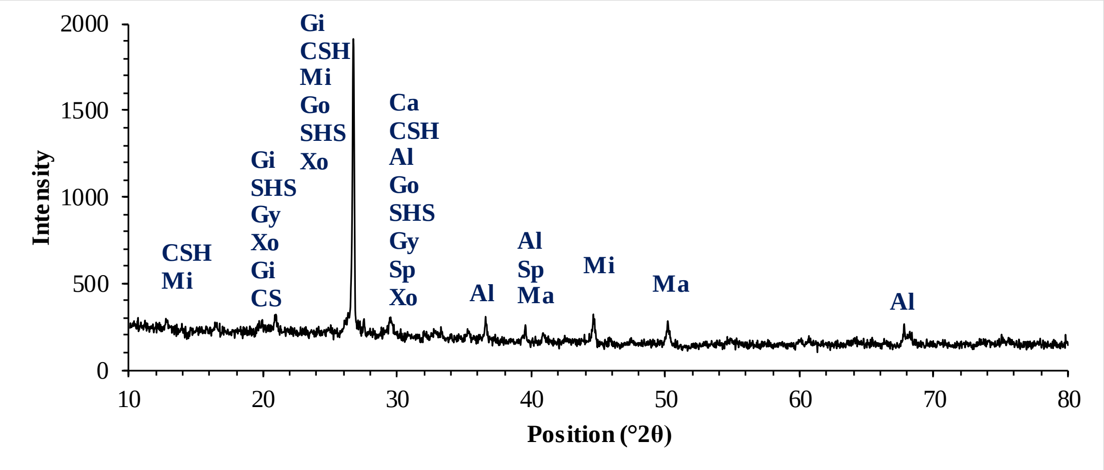

Figure 5. 31 XRD diffractogram of alkali-activated BC soil with limestone powder and class F fly ash

The alkali-activated BC soil with CDW includes the products as depicted in Figure 5.32: [Gi] Gismondine ($CaAl_2Si_2O_8 \cdot 4H_2O$), [L] Liottite ($(Ca, Na)_4(Si, Al)6O_{12}(SO_4, OH, Cl, CO_3)_2 \cdot xH2O$), [S] Sodium Hydrogen Sulfate ($NaHSO_4$), [M] Millosevichite ($Al_2(SO_4)_3$), [C] Calcite ($CaCO_3$), etc.

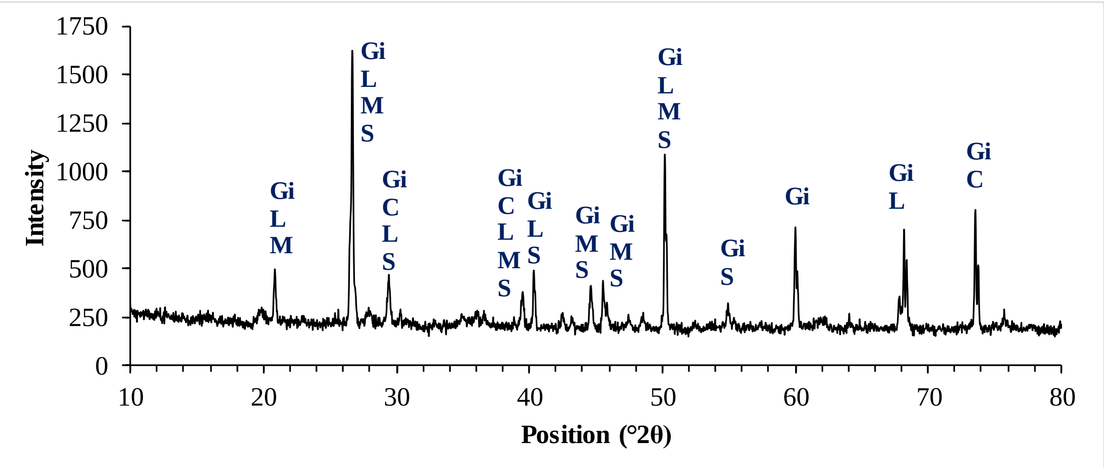

Figure 5. 32 XRD diffractogram of alkali-activated BC soil with CDW

5.9 SUMMARY

At a high SS/SH ratio of 1.5, the BC soil replaced with a higher dosage of marginal materials contributed to significant improvement in UCS strength. The improvement of UCS for stabilized mixes was more than 8 MPa under ambient temperature curing. The lower dissolution of aluminosilicate materials at a low SS/SH ratio of 0.5 has resulted in the low strength of mixes. CBR of many unsoaked stabilized samples was > 100% and acts like a semirigid material. Low CBR(soaked) values (i.e., < 8%) are obtained due to mix softening, delectation of structure, and high moisture absorption of soil. Leaching of the weak mineral constituents such as Al, Ca, Fe, Na, Si, etc., as mentioned by earlier investigations, could be the reason for the loss of strength on soaking. The stabilized mixes failed in both WD and FT tests. The fiber inclusion has improved flexural and fatigue life. These mixes exhibited swelling on soaking, therefore can not sustain under moist conditions. Therefore, the alkali activation technique for stabilizing BC soil with class F fly ash, limestone powder, CDW, and arecanut fiber addition can not be used in the construction of roads (failed in durability tests).

CHAPTER 6
PAVEMENT DESIGN AND COST ANALYSIS

6.1 GENERAL

The economic construction depends on the type of material used and the pavement thickness. A proper soil modification technique can be adopted to achieve this objective. If a stable pavement is to be built over the weak BC soil, its properties should be suitably enhanced by stabilizing with marginal materials and efficient binders. Otherwise, there will be distress in the pavement due to swelling during monsoon and cracks in summer due to moisture variation. The BC soil considered in this investigation could improve the strength and withstand durability tests when mixed with class F fly ash and cement.

During the 1920s, the pavements were designed based on the empirical method. Later it was designed based on the mechanistic-empirical method. The traffic, wheel load, number of axles, tyre pressure, properties of materials, subgrade strength, etc., are the main parameters to be considered for the pavement design. The contact area depends on wheel load, tyre pressure, and wheel load configuration. The tensile strain at the bottom of the asphalt layer and compressive strain on the subgrade is very important to design a pavement. Therefore, for better pavement performance, the strains at the top of the subgrade and bottom of the asphalt layer should be within specified values.

Numerical, analytical, empirical, FEM methods were used for analyzing the flexible pavements. IRC 37: 2018 suggests IITPAVE software to analyze the flexible pavements and it is based on the mechanistic-empirical method. Due to the repeated application of loads, the stresses and strains will accumulate to cause the failure of the pavement. The number of repetitions and magnitude of the wheel load governs the pavement performance and its service life.

6.2 FLEXIBLE PAVEMENT

Pavements are divided into two major categories, flexible and rigid. These days cement-treated/ chemically stabilized sub-base and base courses are recommended for flexible pavements (IRC SP-72: 2015 and IRC 37: 2018). On worn-out flexible pavement, either the flexible or rigid overlay is recommended. Flexible pavement consists of many layers, and the wheel load stress is distributed to subgrade due to grain-to-grain interlocking. Flexible pavements are designed to distribute or transfer the stresses, which depend on the strength properties of each layer. The flexural strength of this pavement is low. Compressive stresses are maximum at the surface during wheel load transmission, which is equal to the contact pressure. With the increase in depth, these stresses will reduce and distributes to a broader area on the subgrade. Hence, the top layer of the pavement should be highly resistant to compressive stresses. The lower layers are designed to sustain lesser compressive loads. The stabilized soil may find its application in lower layers.

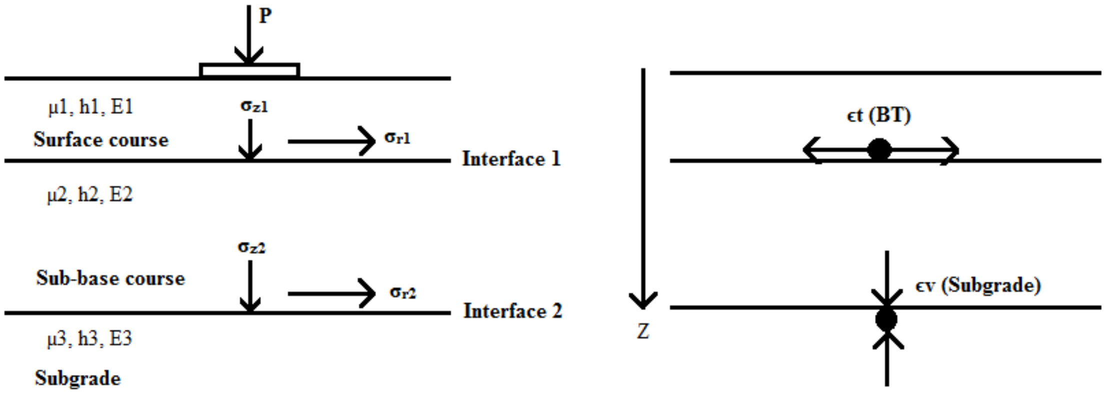

Figure 6. 1 Three-layer pavement system and critical stains at pavement interface

To analyze the flexible pavement, the KENPAVE program was developed at Kentucky University (Huang 1993). It analyses the pavement loaded under a circular area, assuming that the multilayer system is elastic. Linear elastic, nonlinear elastic, or viscoelastic responses under the single or dual wheel assembly can be studied for the multilayer system. It also performs damage analysis. IITPAVE is simple software used in India to analyze pavement. The stress distribution concepts of Boussinesq are taken as the basis for evaluation. It is assumed that all layers are homogeneous, isotropic, the subgrade is semi-infinite, and total interface friction is mobilized.

6.3 STABILIZED MATERIAL PROPERTIES

The cement, fly ash stabilized BC soil passing the durability tests are checked for their suitability in low and high-volume pavements. The design and analysis of low-volume pavements are carried out as per IRC SP-72: 2015 by considering the properties of stabilized soil compacted to standard Proctor density. For the design of high-volume pavements as per IRC 37: 2018, the stabilized soil properties at modified Proctor density are considered. Tables 6.1 and 6.2 show the properties of mixes obtained from the experimental investigation.

Table 6. 1 Properties stabilized BC soil with cement and fly ash

(Cement + Fly ash) (%)	Standard Proctor compaction			Modified Proctor compaction		
	UCS (MPa)		Soaked CBR (%)	UCS (MPa)		Soaked CBR (%)
	7 day	28 day	28 day	7 day	28 day	28 day
(10 + 30)	2.8	3.7	16	2.9	3.7	19
(10 + 35)	2.9	3.8	18	2.9	3.8	22
(10 + 40)	3.0	4.0	22	3.1	4.0	27
(12 + 30)	2.9	3.8	25	3.0	3.9	29
(12 + 34)	2.9	3.9	31	3.1	4.0	35
(12 + 38)	3.0	3.9	40	3.2	4.2	44
(14 + 25)	2.7	3.7	35	3.2	4.2	39
(14 + 30)	3.0	3.8	44	3.4	4.4	48
(14 + 36)	3.1	4.2	54	3.5	4.6	57

Table 6. 2 Properties of stabilized BC soil with cement, fly ash, and 0.5% coconut fibers

(Cement + Fly ash) (%)	Standard Proctor compaction			Modified Proctor compaction		
	UCS (MPa)		Soaked CBR (%)	UCS (MPa)		Soaked CBR (%)
	7 day	28 day	28 day	7 day	28 day	28 day
(10 + 30)	1.3	1.6	27	1.6	3.4	32
(10 + 35)	1.6	1.7	57	2.0	3.8	64
(10 + 40)	1.8	2.0	62	2.3	4.2	68
(12 + 30)	1.3	1.9	105	1.9	3.4	111
(12 + 34)	1.6	2.0	128	2.5	4.1	136
(12 + 38)	2.0	2.5	144	3.2	4.3	151
(14 + 25)	1.4	2.0	129	3.0	3.9	137
(14 + 30)	1.9	2.1	161	3.1	4.1	170
(14 + 36)	2.3	3.0	172	3.3	5.4	185

6.4 LOW-VOLUME ROADS

Traffic:- IRC SP-72: 2015 provides guidelines for designing the flexible pavement when the cumulative standard axles are < 2 msa. For selected rural through routes, traffic of 1–2 msa is included in the revised code. Traffic is categorized as T1–T9, based on cumulative ESAL application for a design period of 10 years. Design catalogues developed are based on both subgrade strength CBR and cumulative ESAL applications. Provisions are made for the usage of gravel/ granular base and sub-bases, along with a modified subgrade. Also, provisions are made for the usage of cement-treated base (CTB) and cement-treated sub-bases (CTSB) over the subgrade.

Table 6. 3 Traffic categories for low-volume roads

Traffic Category	Cumulative ESAL application (msa)
T1	0.01–0.03
T2	>0.03–0.06
T3	>0.06–0.1
T4	>0.1–0.2
T5	>0.2–0.3
T6	>0.3–0.6
T7	>0.6–1.0
T8	>1.0–1.5
T9	>1.5–2.0

Subgrade:- The BC soil classified as MH (Highly plastic silt) as per IS soil classification has a low soaked CBR value of 2%, as mentioned in IRC SP-72: 2015 (Table 6.4). Its free swelling index is 58%. The recommended compaction of expansive soil to 95% standard Proctor density at OMC + (1 or 2)% can be considered for the construction purpose. If BC soil is compacted to a higher density on the dry side of OMC, it may undergo heavy volumetric expansion due to water absorption during the monsoon or flooding. The pavement crust design suggested based on the soaked CBR of improved BC soil with 0.3 m thickness may be a suitable choice. However, the cost of improvement needs to be evaluated. A minimum soaked subgrade CBR of 5% (at least fair) is recommended, with all designed roads to be finished with bituminous surface treatment. The subgrade CBR can be improved with proper stabilization. If economical, a suitable borrow material of 0.3 m thickness can also be considered.

Table 6. 4 Classification of quality of subgrade soil

Class	Soaked CBR range (%)	Quality
S1	2	Very poor
S2	3–4	Poor
S3	5–6	Fair
S4	7–9	Good
S5	10–15	Very good

Sub-base course:- Natural and processed materials like gravel, natural sand, crushed stone, crushed slag, brick metal, kankar, moorum, or combinations thereof are commonly used for sub-bases. When the quicklime does not suit BC soil treatment, the use of cement stabilization can be considered. The treated soil should develop a 7-day minimum UCS of 1.7 MPa. A minimum 100 mm thick CTSB should be provided from practical considerations.

Base course:- MoRD: 2014 recommends the plasticity reduction of BC soil (if PI >30%) by using lime and then treating it with 8–15% cement. The achieved laboratory UCS should be >3 MPa on 7 days of curing. For field application, care should be taken for proper pulverization of the soil by breaking soil clods into fine fractions. Otherwise, the soil clods on the absorption of water may exert swell pressure on surrounding cemented soil, thereby leading to damage. The minimum thickness of CTSB should be 100 mm.

Bituminous surfacing:- The surface dressing is famous in many countries due to its suitability and low cost. For traffic, more than 1×10^5 cumulative ESAL applications, either 2-coat surface dressing or 20 mm Premix Carpet is recommended.

6.5 DESIGN OF LOW-VOLUME ROADS

6.5.1 BC soil as Subgrade

A layer of 0.3 m modified subgrade laid on existing BC soil results in a minimum equivalent CBR value of 8% for most of the mix combinations at standard Proctor density, which passed the durability criteria. The details of individual pavement layers for subgrade class S1 for various traffic categories are as follows.

BC soil stabilized with cement, fly ash, and fibers exhibited soaked CBR of >16% (Table 6.1 and 6.2). Therefore, this mix can be used as modified soil or improved subgrade with granular sub-base and granular base course for various traffic categories, designed for BC soil subgrade CBR of 2%, as depicted in Figure 6.2.

Traffic category	T1	T2	T3	T4	T5	T6	T7	T8	T9
OGPC	0	0	0	0	0	20	20	20	20
Surface Dressing	0	20	20	20	20	0	0	0	0
Bituminous Macadam	0	0	0	0	0	0	0	0	50
WBM Grade-3	0	75	75	75	75	75	75	75	0
WBM/CRMB	0	0	75	75	75	75	150	150	225
Gravel Base	200	150	0	0	0	0	0	0	0
Granular Subbase	0	0	125	125	175	250	200	225	250
Modified Soil	100	100	100	150	150	150	225	200	200

Layer thickness (mm)

Figure 6. 2 Pavement composition for BC soil subgrade with soaked CBR of 2% as per IRC SP-72: 2015

Note:- where, Modified soil/ Improved subgrade (CBR not <10), Granular sub-base (CBR not <20) in an exceptional case can be 15, Gravel base (CBR not <80), in lower base course shall not be <50 as per clause 2.3.5 (in an exceptional case may be relaxed suitably), Base of Grave/ CRMB/ WBM (CBR not <100), where 100 mm thickness is recommended it can be modified to 75 mm for WBM with a corresponding increase of 25 mm in sub-base.

6.5.2 Stabilized BC soil as Subgrade

If the pavement is designed based on soaked CBR (>16% for all combinations) of BC soil treated with cement, fly ash, and coconut fiber as a modified subgrade, the resulting pavement composition is shown in Figure 6.3. In this case, the soaked CBR of the improved subgrade is classified under the S5 (very good) category. Here the thickness of compacted subgrade should not be less than 300 mm.

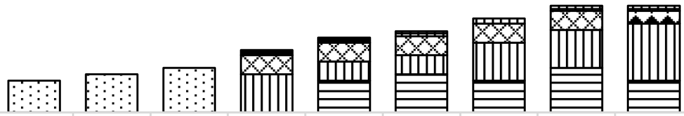

Traffic category	T1	T2	T3	T4	T5	T6	T7	T8	T9
OGPC	0	0	0	0	0	20	20	20	20
Surface Dressing	0	0	0	20	20	0	0	0	0
Bituminous Macadam	0	0	0	0	0	0	0	0	50
WBM Grade-3	0	0	0	75	75	75	75	75	0
WBM/CRMB	0	0	0	150	75	75	150	150	225
Gravel Base	125	150	175	0	0	0	0	0	0
Granular Subbase	0	0	0	0	125	150	125	175	125

Layer thickness (mm)

Figure 6. 3 Pavement composition for improved BC soil subgrade exhibiting soaked CBR of 10–15% as per IRC SP-72: 2015

6.5.3 Stabilized BC soil as Sub-base

The code suggests using lime for modification of BC soil for plasticity reduction. But in this investigation, the plasticity index of BC soil was initially brought down by adding with low calcium fly ash. Only durable mixes with weight loss of < 14% are proposed for use. Treatment with cement was suggested for waterlogged areas, as with the formation of more cementitious products, the strength increases. The stabilized mixes should attain a 7-day UCS of >1.7 MPa. A minimum thickness of 100 mm shall be used.

For the granular sub-base course, the soaked CBR of >20% is required. Under economic constraints, a CBR of >15% may be permitted. However, the concept of CBR is not considered for soil-cement sub-base and base courses.

The cement, fly ash stabilized mixes exhibited a 7-day UCS of >1.7 MPa (Table 6.1). Whereas, (10 + 40), (12 + 38), (14 + 30), and (14 + 36)% (cement + fly ash) stabilized mixes with 0.5% coconut fibers exhibited 7-day UCS of >1.7 MPa (Table 6.2). Therefore, only these mix combinations are suitable for soil-cement sub-base courses laid over the existing BC soil subgrade. The pavement composition using the stabilized BC soil as a sub-base course for various traffic categories is depicted in Figure 6.4. Other mix combinations with fibers did not attain minimum UCS requirement criteria.

6.5.4 Stabilized BC soil as Base

For traffic >1 msa repetitions, a soil-cement base with the blacktopped surface can be used. It is applicable when the hard stones are not available within economical leads. The soil-cement mix should achieve a 7-day UCS of >3.0 MPa. Also, lime treatment was suggested before stabilizing with cement. For field application, thorough pulverization of soil clods is essential. Otherwise, each BC soil clod can exorbitantly absorb moisture and exert swell pressure on surrounding cemented soil, leading to crack formation. A minimum thickness of 100 mm shall be used.

The (10 + 40), (12 + 38), (14 + 30), and (14 + 36)% (cement + fly ash) stabilized mixes exhibited 7-day UCS of >3.0 MPa (Table 6.1). Whereas, (cement + fly ash) stabilized mixes with 0.5% coconut fibers failed to achieve this criterion (Table 6.2). The pavement composition considering soaked CBR of BC soil and cement, fly ash treated BC soil as subgrade is depicted in figures 6.4 and 6.5, respectively. A minimum thickness of 300 mm of cement, fly ash treated BC soil should be provided as the subgrade for pavement composition depicted in figure 6.5. The improved mixes are not preferred as a base layer due to the following reasons:

1. During summer, shrinkage of soil may lead to cracks, which may reflect in the upper layers due to repeated wheel loads.
2. If soil clods are not properly broken/pulverized, it may exert exorbitant swell pressure to the surrounding cemented soil and may also affect the above layers.
3. The water affinity of treated BC soil may be dangerous to the bituminous layers as they are sensitive to water and likely to cause damage.
4. There may not be proper adhesion between stabilized soil and bituminous layer, leading to debonding due to loss of friction at the interface.

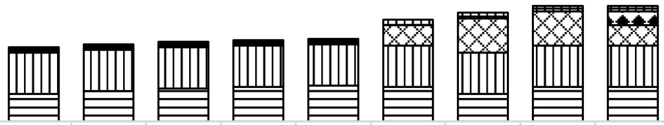

Traffic category	T1	T2	T3	T4	T5	T6	T7	T8	T9
OGPC	0	0	0	0	0	20	20	20	20
Surface Dressing	20	20	20	20	20	0	0	0	0
Bituminous Macadam	0	0	0	0	0	0	0	0	50
Crack Relief Layer	0	0	0	0	0	75	125	125	75
Cement Treated Base	150	150	150	150	150	150	150	150	150
Cement Treated Subbase	100	110	120	125	130	125	100	125	125

Layer thickness (mm)

Figure 6. 4 Pavement composition with CTB and CTSB (stabilized soil) designed for subgrade CBR of 2% as per IRC SP-72: 2015

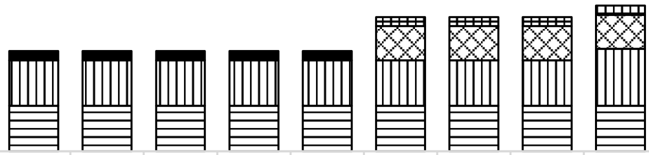

Traffic category	T1	T2	T3	T4	T5	T6	T7	T8	T9
OGPC	0	0	0	0	0	20	20	20	20
Surface Dressing	20	20	20	20	20	0	0	0	0
Bituminous Macadam	0	0	0	0	0	0	0	0	0
Crack Relief Layer	0	0	0	0	0	75	75	75	75
Cement Treated Base	100	100	100	100	100	100	100	100	125
Cement Treated Subbase	100	100	100	100	100	100	100	100	100

Layer thickness (mm)

Figure 6. 5 Pavement composition with CTB and CTSB for cement, fly ash stabilized BC soil subgrade of CBR 10–15% as per IRC SP-72: 2015

6.6 DESIGN OF HIGH-VOLUME ROADS

6.6.1 Design Recommendations as per IRC 37: 2018

As per IRC 37: 2018, the stabilized soil mixes passing both durability test and strength criteria can cater for high-volume traffic from 5–50 msa ESAL applications. A minimum of 500 mm thick subgrade prepared using in-situ soil, or borrow material, or stabilized soil at the field should achieve >97% modified Proctor density. The elastic or resilient component of strain is taken as an input parameter for flexible pavement analysis. The dynamic triaxial test equipment is costlier and is available in limited organizations/ academic institutions. Therefore, the resilient modulus (M_{RS}) can be determined by using equations 6.1 and 6.2 suggested by IRC 37: 2018.

M_{RS} of the subgrade in MPa

for soaked CBR ≤5 %, $M_{RS} = 10.0(CBR)$……………..(6.1)

for soaked CBR >5 %, $M_{RS} = 17.6(CBR)^{0.64}$…………(6.2)

If there is a sufficient difference between the CBR of insitu soil and subgrade, then the design should be based on the equivalent modulus or CBR value of the two materials. Initially, using IITPAVE software, the maximum deflection (δ) under a single wheel load is determined for the considered contact pressure (p) and a two or three-layer system. By using equation 6.3, the effective modulus can be estimated.

$$M_{RS} = [2(1-\mu^2)]/\delta \quad \text{…………(6.3)}$$

The estimated M_{RS} used for the design shall be limited to 100 MPa.

Further, the equivalent CBR value (but not used for the design) can be estimated using the estimated effective M_{RS} in equations 6.2 or 6.3. The effective CBR should be > 5% for 2-way roads catering 450 CVPD during the construction year.

The resilient/elastic modulus of the granular sub-base layer is calculated using equation 6.4. It depends on the effective/ resilient modulus of the supporting layer ($M_{RSupport}$) and the thickness of the granular sub-base (h).

$$M_{RGRAN} = 0.2(h^{0.45})\, M_{RSupport} \quad \text{…(6.4)}$$

For analysis, granular sub-base and granular base are considered as a single layer. However, if a cement-treated base is used over a granular sub-base, both are considered individual layers.

For the CTSB layer using in-situ soil as a drainage cum filtration/ separation layer, commercial geocomposites can be used. The minimum recommended CTSB thickness is 200 mm. The CTSB should attain a 7-day UCS of 1.5–3.0 MPa as per IRC SP:89-Part 2: 2018. Flexural modulus (E_{CGSB}) from third point loading on 28 days of curing can be calculated using equation 6.5. For CTSB, E_{CGSB} may vary from 2000–6000 MPa, but due to 30–35 tonne construction traffic, a design value of 600 MPa can be adopted by considering the susceptibility of crack propagation.

$$E_{CGSB} = 1000(UCS) \quad \text{…………..(6.5)}$$

The CTB should attain a 7/28-day UCS of 4.5/7.0 MPa as per IRC SP: 89-Part 2: 2018. For CTB, the flexural strength of modulus of rupture (M_{RUP}) can be calculated using equation 6.5. Also, M_{RUP} may take a value of approximately 20% of 28 days UCS. For soil cements, M_{RUP} of 0.7 MPa is the limiting or maximum value. Also, the soil loss under 12 WD and FT cycles should not exceed 14% weight loss. To avoid the reflection crack propagation from CTB to bituminous layer, a crack relief layer of 100 mm thickness prepared using crushed aggregates is essential. The crack relief layer should confirm to WMM specifications of MoRTH. If stress absorbing membrane layer (SAMI) is used for this purpose, it should not be considered for pavement analysis as suggested by the code.

For frost susceptible areas, the minimum depth of pavement recommended is 450 mm. The ingress of water should be avoided by providing a proper surface, camber, and drainage. Also, the subgrade can be constructed well above the water table.

Table 6. 5 Design inputs used for high-volume roads

Type of bitumen	VG30	VG40
CSAL	5–20 msa	30–50 msa
Reliability	80%	90%
Reliability factor	1 for CSAL ≥10 msa, & 2 for CSAL <10 msa,	
Bituminous layer	M_{RB} = 2000 MPa	M_{RB} = 3000 MPa
Granular base/ sub-base	M_{RGRAN}, μ = 0.35	
Granular crack relief layer/ AIL	E_{CRL} = 450 MPa, μ = 0.35	
For RAP/ aggregate stabilized with emulsion or foam bitumen	E_{RAP} = 800 MPa, μ = 0.35	
For WMM over CTSB (crushed rock)	E_{WMM} = 350 MPa, μ = 0.35	
CTB	E_{CTB} = 5000 MPa, μ = 0.25	
CTSB	E_{CTSB} = 600 MPa, μ = 0.25	
Subgrade	μ = 0.35	

For the estimation of effective subgrade modulus/ CBR, consider a 2-layer elastic system, μ = 0.35 for both layers, upper layer thickness = 500 mm, single load P = 40000 N, contact pressure p = 0.56 MPa. Therefore, radius of contact area $a = [P/(\pi p)]^{0.5}$ = 150.8 mm. Number of analysis points = 1, depth = 0, radial distance = 0. From equation 6.1, M_{RS} = 20 MPa for BC soil soaked CBR = 2 %. The equivalent CBR of stabilized

BC soil when placed over the BC soil are estimated using equations 6.1, 6.2 and 6.3 (Table 6.6). The sample calculations are given in appendix 1.

Table 6. 6 Estimated effective subgrade modulus and CBR

For cement stabilized BC soil with fly ash				
Soaked CBR (%)	**M_{RS} (MPa)**	**δ (mm)**	**Effective modulus (resilient modulus) of equivalent single layer**	**Effective CBR (%)**
19	116	2.158	69	8
22	127	2.042	73	9
27	145	1.893	78	10
29	152	1.845	80	10
35	171	1.725	86	11
44	198	1.593	93	13
39	184	1.661	89	12
48	210	1.546	96	14
57	234	1.459	102	15
For cement stabilized BC soil with fly ash and coconut fibers				
32	162	1.781	83	11
64	252	1.404	106	16
68	262	1.376	108	17
111	359	1.176	126	21
136	408	1.105	134	23
151	437	1.07	139	25
137	410	1.102	134	24
170	471	1.033	143	26
185	497	1.007	147	27

A minimum effective CBR of 8% was obtained when treated soil is used as a modified subgrade. The pavement composition for various traffic categories is depicted in figures 6.6 to 6.10. For a dual wheel assembly, P = 20000 N, tyre pressure of 0.56 MPa, the pavement compositions, critical strain values are presented for various pavement combinations. The input details for IITPAVE are tabulated in Table 6.5. When stabilized soil passing durability tests is considered for CTSB, then the stabilized BC of minimum soaked CBR 19% should be used as a subgrade to obtain an effective CBR of 8%. None of the stabilized BC soil mixes satisfy the minimum UCS requirement of the CTB layer, therefore, can not be used. The stabilized mixes are highly resistant to frost action; thus, water presence will not affect the pavement. Horizontal tensile strains (ε_t) at the bottom of bituminous and CTB layers and the vertical compressive strain (ε_z)

at the top of the subgrade are critical. Estimated strains at radial distances of 0 and 155 mm are recorded.

6.6.2 Pavement Composition for High-Volume Roads using Cement, Fly ash, and Coconut Fibers Stabilized BC soil in Different Layers

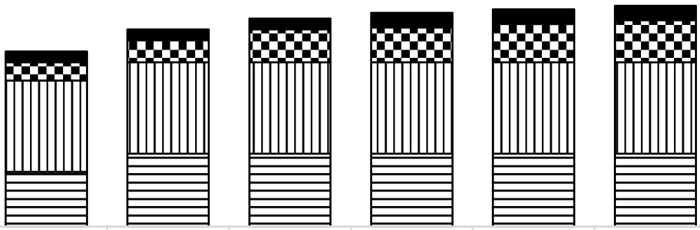

Traffic (msa)	5	10	20	30	40	50
Surface course	30	30	30	40	40	40
Base/Binder course	50	60	90	95	105	115
WMM	250	250	250	250	250	250
GSB	150	200	200	200	200	200

Layer thickness (mm)

Figure 6. 6 Pavement catalogue for stabilized BC soil as modified subgrade of 8% effective CBR with granular base and sub-base above natural BC soil

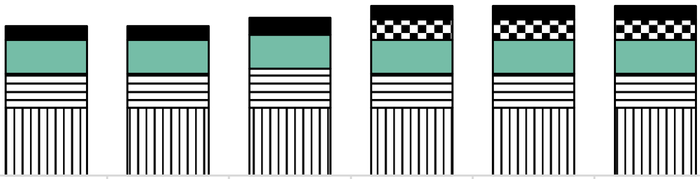

Traffic (msa)	5	10	20	30	40	50
Surface course	40	40	50	40	40	40
Base/Binder course	0	0	0	60	60	60
AIL	100	100	100	100	100	100
CTB	100	100	115	100	100	100
CTSB	200	200	200	200	200	200

Layer thickness (mm)

Figure 6. 7 Pavement catalogue for stabilized durability passed BC soil as CTSB with granular crack relief layer, CTB above soil subgrade of 8% effective CBR

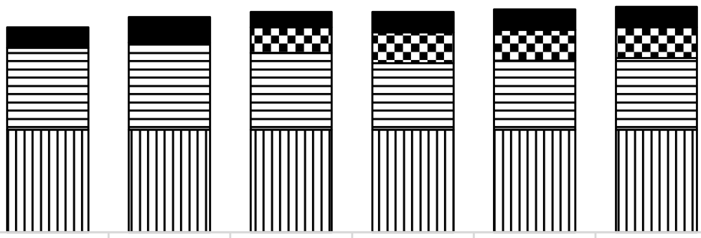

Traffic (msa)	5	10	20	30	40	50
Surface course	40	50	30	40	40	40
Base/Binder course	0	0	50	60	60	60
CTB	160	170	150	130	135	140
CTSB	200	200	200	200	200	200

Layer thickness (mm)

Figure 6. 8 Pavement catalogue for stabilized durability passed BC soil as CTSB with SAMI layer, CTB above soil subgrade of 8% effective CBR

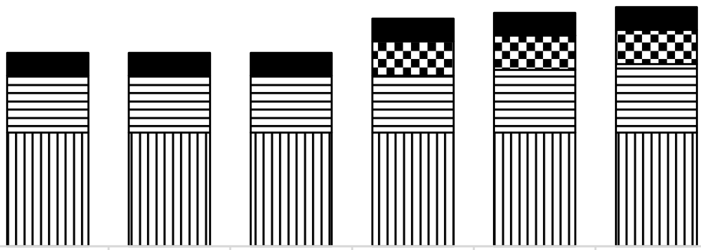

Traffic (msa)	5	10	20	30	40	50
Surface course	40	40	40	40	40	40
Base/Binder course	0	0	0	60	60	60
RAP	100	100	100	100	110	120
CTSB	200	200	200	200	200	200

Layer thickness (mm)

Figure 6. 9 Pavement catalogue for stabilized durability passed BC soil as CTSB with emulsion/foam based bitumen stabilized RAP/virgin aggregate, CTB above soil subgrade of 8% effective CBR

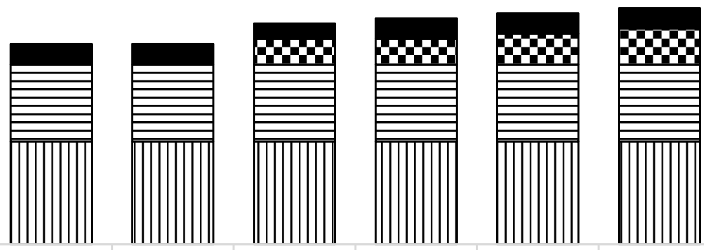

Traffic (msa)	5	10	20	30	40	50
■ Surface course	40	40	30	40	40	40
Base/Binder course	0	0	50	50	60	70
WMM	150	150	150	150	150	150
CTSB	200	200	200	200	200	200

Layer thickness (mm)

Figure 6. 10 Pavement catalogue for stabilized durability passed BC soil as CTSB with granular base above soil subgrade of 8% effective CBR

Table 6. 7 Critical and allowable strains for stabilized BC soil used for high-volume roads

Stabilized BC soil as modified subgrade of 8% effective CBR with granular base and sub-base above natural BC soil						
Traffic (msa)	5	10	20	30	40	50
M_{RGRAN}	197.45	208.19	208.19	208.19	208.19	208.19
ε_t (BT)	3.60E-04	3.27E-04	2.71E-04	2.01E-04	1.88E-04	1.77E-04
ε_v (Subgrade)	-5.46E-04	-4.42E-04	-3.81E-04	-3.29E-04	-3.12E-04	-2.96E-04
ε_t (BT)a	1.36E-02	1.14E-02	9.50E-03	7.08E-03	6.58E-03	6.21E-03
ε_v (Subgrade)a	7.84E-04	6.73E-04	5.78E-04	4.16E-04	3.90E-04	3.72E-04
Stabilized durability passed BC soil as CTSB with granular crack relief layer, CTB above soil subgrade of 8% effective CBR						
ε_t (BT)	1.15E-04	1.15E-04	1.45E-04	1.31E-04	1.31E-04	1.31E-04
ε_t (CTB)	8.07E-05	8.07E-05	7.38E-05	5.92E-05	5.92E-05	5.92E-05
ε_v (Subgrade)	-3.55E-04	-3.55E-04	-3.14E-04	-2.66E-04	-2.66E-04	-2.66E-04
ε_t (BT)a	1.64E-02	1.37E-02	1.15E-02	7.08E-03	6.58E-03	6.21E-03
ε_t (CTB)a	8.60E-05	8.12E-05	7.66E-05	7.41E-05	7.23E-05	7.10E-05
ε_v (Subgrade)a	7.84E-04	6.73E-04	5.78E-04	4.16E-04	3.90E-04	3.72E-04

Stabilized durability passed BC soil as CTSB with SAMI layer, CTB above soil subgrade of 8% effective CBR						
ε_t (CTB)	8.26E-05	7.58E-05	7.39E-05	7.21E-05	7.05E-05	6.88E-05
ε_v (Subgrade)	-3.16E-04	-2.86E-04	-2.83E-04	-2.67E-04	-2.60E-04	-2.53E-04
ε_t (BT)a	1.64E-02	1.37E-02	1.15E-02	7.08E-03	6.58E-03	6.21E-03
ε_t (CTB)a	8.60E-05	8.12E-05	7.66E-05	7.41E-05	7.23E-05	7.10E-05
ε_v (Subgrade)a	7.84E-04	6.73E-04	5.78E-04	4.16E-04	3.90E-04	3.72E-04
Stabilized durability passed BC soil as CTSB with emulsion/foam based bitumen stabilized RAP/virgin aggregate, CTB above soil subgrade of 8% effective CBR						
ε_t (BT)	2.33E-05	2.33E-05	2.33E-05	1.11E-04	1.10E-04	1.09E-04
ε_v (Subgrade)	-5.25E-04	-5.25E-04	-5.25E-04	-3.68E-04	-3.54E-04	-3.42E-04
ε_t (BT)a	1.36E-02	1.14E-02	9.50E-03	7.08E-03	6.58E-03	6.21E-03
ε_v (Subgrade)a	7.84E-04	6.73E-04	5.78E-04	4.16E-04	3.90E-04	3.72E-04
Stabilized durability passed BC soil as CTSB with granular base above soil subgrade of 8% effective CBR						
ε_t (BT)	1.79E-04	1.79E-04	2.26E-04	1.93E-04	1.83E-04	1.73E-04
ε_v (Subgrade)	-5.33E-04	-5.33E-04	-4.46E-04	-4.07E-04	-3.87E-04	-3.67E-04
ε_t (BT)a	1.36E-02	1.14E-02	9.50E-03	7.08E-03	6.58E-03	6.21E-03
ε_v (Subgrade)a	7.84E-04	6.73E-04	5.78E-04	4.16E-04	3.90E-04	3.72E-04

The calculated tensile strains at the bottom of the bituminous layer ε_t (BT), at the bottom of the cement-treated base ε_t (CTB), and vertical compressive strain at the top of the subgrade ε_v (Subgrade), are within allowable stresses ε_t (BT)a, ε_t (CTB)a, and ε_v (Subgrade)a, respectively. The results are tabulated in Table 6.7. The strains for different combinations of wheel load repetitions are calculated using IITPAVE software. The allowable strain values were calculated using equation 6.1 as suggested by IRC 37-2018. The strains for the different wheel load repetitions are calculated using IITPAVE software, and they are within permissible limits.

6.7 COST ANALYSIS

The cost of durability test passed stabilized BC soil mixes suggested for modified soil, improved subgrade, CTSB of low and high-volume roads is tabulated Tables 6.8 and 6.9. Due to the higher cement contents (10, 12, and 14%), the stabilized materials cost is more than the commonly used GSB (Rs. 940/m^3). If the good quality of GSB materials is not abundantly available at the construction site, in such cases, cement-fly ash stabilization of BC soil is economical, provided the marginal materials like fly ash, and coconut fibers are available abundantly. This stabilization technique is effective over time due to the continued reaction of cement; the constructed layer can gain more strength. In the case of submerged embankments, this method is more suitable and stable.

Also, the cost of alkali-treated BC soil with various marginal materials is tabulated in Tables 6.10 to 6.14. The alkali treatment method is costlier and also not useful, as observed from the durability tests. The cost of NaOH flakes and Na_2SiO_3 solutions is higher, and the quantity of these materials required for alkali solution preparation is more. The process involved in the preparation of alkali solutions requires skilled labourers. More precautions are needed during the preparation of alkali solution, as it may cause skin burns, irritation, etc. The storage of alkali solutions requires proper care. Also, the cost of alkali treatment for soil is almost 1.5 to 2 times that of cement, and therefore, it is slightly uneconomical.

The material cost is taken from the schedule of rates 2018, Public Works Department Mangalore, and from suppliers.

Cost of class F fly ash = Rs. 0.3/kg

Cost of OPC = Rs. 5.875/kg

Cost of coconut fibers = Rs. 17/kg

Cost of limestone powder = Rs. 1.5/kg

Cost of CDW = Rs. 0.3/kg

Cost of arecanut fibers = Rs. 17/kg

Cost of NaOH flakes = Rs. 27/kg

Cost of Na_2SiO_3 solution = Rs. 13/kg

The quantity of materials per cubic meter of stabilized BC soil is calculated on a weight basis considering the corresponding dry density of the mixes obtained from Proctor compaction tests. The cost of the alkali solution ingredients is calculated for the corresponding OMC. These quantities are multiplied with the corresponding material cost to obtain the total cost of the mix as specified in the following tables.

Table 6. 8 Cost of BC soil treated with cement and fly ash

Mix ID	Quantity (kg/m^3)			Cost (Rs/m^3)			Quantity (kg/m^3)			Cost (Rs/m^3)		
S-C-Fa	Soil	Fly ash	OPC	Fly ash	OPC	Total	Soil	Fly ash	OPC	Fly ash	OPC	Total
At standard Proctor density							At modified Proctor density					
60-10-30	954	477	159	143	934	1077	1044	522	174	157	1022	1179
55-10-35	869	553	158	166	928	1094	952	606	173	182	1016	1198
50-10-40	775	620	155	186	911	1097	855	684	171	205	1005	1210
58-12-30	916	474	190	142	1114	1256	1003	519	208	156	1220	1375
54-12-34	842	530	187	159	1100	1259	923	581	205	174	1206	1380
50-12-38	775	589	186	177	1093	1269	850	646	204	194	1199	1392
61-14-25	976	400	224	120	1316	1436	1049	430	241	129	1415	1544
56-14-30	885	474	221	142	1300	1442	952	510	238	153	1398	1551
50-14-36	780	562	218	168	1283	1452	845	608	237	183	1390	1573

Table 6. 9 Cost of BC soil treated with cement, fly ash, and coconut fibers

Mix ID	Quantity (kg/m^3)				Cost (Rs/m^3)				Quantity (kg/m^3)				Cost (Rs/m^3)			
S-C-Fa-Cf	Soil	Fly ash	OPC	Coconut fibers	Fly ash	OPC	Coconut fibers	Total	Soil	Fly ash	OPC	Coconut fibers	Fly ash	OPC	Coconut fibers	Total
At standard Proctor density									At modified Proctor density							
60-10-30-0.5	936	468	156	7.8	140	917	133	1190	1690	1014	507	169	152	993	144	1289
55-10-35-0.5	853	543	155	7.8	163	911	132	1205	1680	924	588	168	176	987	143	1306
50-10-40-0.5	760	608	152	7.6	182	893	129	1205	1650	825	660	165	198	969	140	1308
58-12-30-0.5	899	465	186	7.8	140	1093	132	1364	1680	974	504	202	151	1184	143	1478
54-12-34-0.5	832	524	185	7.7	157	1086	131	1374	1660	896	564	199	169	1170	141	1481
50-12-38-0.5	755	574	181	7.6	172	1065	128	1365	1640	820	623	197	187	1156	139	1483
61-14-25-0.5	958	393	220	7.9	118	1291	133	1543	1670	1019	418	234	125	1374	142	1641
56-14-30-0.5	868	465	217	7.8	140	1275	132	1546	1650	924	495	231	149	1357	140	1646
50-14-36-0.5	765	551	214	7.7	165	1258	130	1554	1630	815	587	228	176	1341	139	1655

Table 6. 10 Cost of alkali-activated BC soil with fly ash

Mix ID	SS/SH	Quantity (kg/m^3)				Cost (Rs/m^3)			
S-Fa		Soil	Fly ash	NaOH flakes	Na_2SiO_3 solution	Fly ash	NaOH flakes	Na_2SiO_3 solution	Total
100-0	0.5	1900	0	66.5	103.9	0	1795	1350	3145
100-0	1.0	1900	0	49.9	155.8	0	1346	2025	3372
100-0	1.5	1900	0	39.9	187.0	0	1077	2430	3507
95-5	0.5	1796	95	67.3	105.2	28	1818	1368	3214
95-5	1.0	1796	95	50.5	157.8	28	1364	2052	3443
95-5	1.5	1796	95	40.4	189.4	28	1091	2462	3581
50-50	0.5	825	825	66.9	104.5	248	1806	1359	3412
50-50	1.0	825	825	50.2	156.8	248	1354	2038	3640
50-50	1.5	825	825	40.1	188.1	248	1083	2445	3776

Table 6. 11 Cost of alkali-activated BC soil with fly ash and limestone powder

Mix ID	SS/SH	Quantity (kg/m^3)					Cost (Rs/m^3)				
S-Fa-L		Soil	Fly ash	Limestone powder	NaOH flakes	Na_2SiO_3 solution	Fly ash	Limestone powder	NaOH flakes	Na_2SiO_3 solution	Total
95-0-5	0.5	1777	0	94	67.0	104.7	0	140	1810	1361	3311
95-0-5	1.0	1777	0	94	50.3	157.1	0	140	1357	2042	3539
95-0-5	1.5	1777	0	94	40.2	188.5	0	140	1086	2450	3676
75-20-5	0.5	1350	360	90	62.2	97.2	108	135	1680	1264	3186
75-20-5	1.0	1350	360	90	46.7	145.8	108	135	1260	1895	3398
75-20-5	1.5	1350	360	90	37.3	175.0	108	135	1008	2274	3525
50-45-5	0.5	830	747	83	67.6	105.7	224	125	1826	1374	3549
50-45-5	1.0	830	747	83	50.7	158.5	224	125	1370	2061	3779
50-45-5	1.5	830	747	83	40.6	190.2	224	125	1096	2473	3917

Table 6. 12 Cost of alkali-activated BC soil with fly ash and arecanut fibers

Mix ID	SS/SH	Quantity (kg/m^3)					Cost (Rs/m^3)				
S-Fa-Af		Soil	Fly ash	Arecanut fibers	NaOH flakes	Na_2SiO_3 solution	Fly ash	Arecanut fibers	NaOH flakes	Na_2SiO_3 solution	Total
100-0-0.5	0.5	1900	0	9.5	66.5	103.9	0	162	1795	1350	3307
100-0-0.5	1.0	1900	0	9.5	49.9	155.8	0	162	1346	2025	3533
100-0-0.5	1.5	1900	0	9.5	39.9	187.0	0	162	1077	2430	3669
95-5-0.5	0.5	1796	95	9.5	67.3	105.2	28	161	1818	1368	3375
95-5-0.5	1.0	1796	95	9.5	50.5	157.8	28	161	1364	2052	3604
95-5-0.5	1.5	1796	95	9.5	40.4	189.4	28	161	1091	2462	3742
50-50-0.5	0.5	825	825	8.3	66.9	104.5	248	140	1806	1359	3552
50-50-0.5	1.0	825	825	8.3	50.2	156.8	248	140	1354	2038	3780
50-500.5	1.5	825	825	8.3	40.1	188.1	248	140	1083	2445	3917

Table 6. 13 Cost of alkali-activated BC soil with fly ash, limestone powder, and arecanut fibers

Mix ID	SS/SH	Quantity (kg/m^3)						Cost (Rs/m^3)					
S-Fa-L-Af		Soil	Fly ash	Limestone powder	Arecanut fibers	NaOH flakes	Na_2SiO_3 solution	Fly ash	Limestone powder	Arecanut fibers	NaOH flakes	Na_2SiO_3 solution	Total
95-0-5-0.5	0.5	1743	0	92	9.2	67.7	105.8	0	138	156	1829	1376	3498
95-0-5-0.5	1.0	1743	0	92	9.2	50.8	158.7	0	138	156	1371	2063	3728
95-0-5-0.5	1.5	1743	0	92	9.2	40.6	190.5	0	138	156	1097	2476	3867
75-20-5-0.5	0.5	1300	347	87	8.7	60.6	94.7	104	130	147	1637	1232	3250
75-20-5-0.5	1.0	1300	347	87	8.7	45.5	142.1	104	130	147	1228	1847	3456
75-20-5-0.5	1.5	1300	347	87	8.7	36.4	170.5	104	130	147	982	2217	3580
50-45-5-0.5	0.5	806	725	81	8.1	66.7	104.2	217	121	137	1800	1354	3630
50-45-5-0.5	1.0	806	725	81	8.1	50.0	156.3	217	121	137	1350	2031	3857
50-45-5-0.5	1.5	806	725	81	8.1	40.0	187.5	217	121	137	1080	2438	3993

Table 6. 14 Cost of alkali-activated BC soil with CDW

Mix ID	SS/SH	Quantity (kg/m^3)				Cost (Rs/m^3)			
S-CDW		Soil	CDW	NaOH flakes	Na_2SiO_3 solution	CDW	NaOH flakes	Na_2SiO_3 solution	Total
90-10	0.5	1652	184	68.1	106.4	55	1839	1384	3278
90-10	1.0	1652	184	51.1	159.6	55	1379	2075	3510
90-10	1.5	1652	184	40.9	191.6	55	1103	2490	3649
70-30	0.5	1313	563	57.6	90.0	169	1556	1171	2895
70-30	1.0	1313	563	43.2	135.1	169	1167	1756	3092
70-30	1.5	1313	563	34.6	162.1	169	934	2107	3210
50-50	0.5	984	984	57.1	89.2	295	1541	1159	2995
50-50	1.0	984	984	42.8	133.8	295	1156	1739	3190
50-50	1.5	984	984	34.2	160.5	295	925	2087	3306

The cost comparison of the low-volume pavement is made to check the feasibility of the use of modified soil in construction. The pavement composition's total cost by considering BC soil as subgrade of 2% soaked CBR (Figure 6.2) with gravel/ granular bases and sub-bases for traffic category 6 is Rs. 703 per m^2 area. Whereas, for the pavement with the same soaked subgrade CBR and traffic category, but with cement-treated bases and sub-bases (Figure 6.4), the estimated cost is only Rs. 629 per m^2 area. Therefore, the use of stabilized soil mixes can reduce the construction cost of pavement. The details of the estimated cost are given in Table 6.15.

Table 6. 15 Cost comparison of low-volume roads considering granular base, sub-bases, and cement-stabilized base and sub-bases

Low-volume roads:- Cost estimation for the pavement with gravel/ granular bases and sub-bases					
BC soil as subgrade with 2% soaked CBR, very poor (S1) subgrade, traffic category T6					
Layer	Thickness (mm)	As per SOR		Calculations per m^2 area of pavement	
		Unit	Unit price	Quantity of material required	Cost (Rs.)
OGPC	20	m^2	97	1	97
WBM Grade-3	75	m^3	1260	0.075	95
WBM/CRMB	75	m^3	1050	0.075	79
Granular sub-base	250	m^3	940	0.25	235
Modified soil (S-C-Fa of 50-14-36 mix)	150	m^3	1452	0.15	218
Total cost of materials per m^2 area of pavement in Rs.					703
Low-volume roads:- Cost estimation for the pavement with cement-treated bases and sub-bases					
BC soil as subgrade with 2% soaked CBR, very poor (S1) subgrade, traffic category T6					
Layer	Thickness (mm)	As per SOR		Calculations per m^2 area of pavement	
		Unit	Unit price	Quantity of material required	Cost (Rs.)
OGPC	20	m^2	97	1	97
Crack relief layer	75	m^3	1483	0.075	111
Cement-treated base	150	m^3	1593	0.15	239
Cement-treated sub-base (S-C-Fa of 50-14-36 mix)	125	m^3	1452	0.125	182
Total cost of materials per m^2 area of pavement in Rs.					629

6.8 SUMMARY

In this chapter, the stabilized BC soil mixes, which passed the durability tests and strength criteria as per IRC SP-72: 2015 and IRC 37: 2018, are recommended for use in low and high-volume roads, respectively. The critical strain values determined using the IITPAVE software are within allowable limits. Therefore, if cement-treated mixes are used as improved/ modified subgrade layers or as CTSB, the pavement can perform satisfactorily without undergoing any deformation or failure. Due to continued cementation in submerged conditions, the cement-fly ash stabilized BC soil can gain strength and perform better. The cost of the stabilized materials is worked out and presented. The use of cement-treated soil in the base layer reduces the thickness of the pavement. The cost of pavement constructed with conventional GSB material is higher than pavement constructed with cement-treated soil. If a good quality GSB material is not available on the construction site; these stabilized mixes can be better alternatives, provided that the fly ash and coconut fibers are available abundantly. The alkali treatment method is slightly expensive and unsuitable for stabilized pavement layers under submerged conditions; therefore, it can not be adopted or recommended.

CHAPTER 7

CONCLUSIONS

The following conclusions were drawn from the laboratory investigations of stabilized BC soil with marginal materials and activators.

A. CEMENT STABILIZED BC SOIL WITH MARGINAL MATERIALS

1 The use of class F fly ash has controlled the plasticity characteristics of BC soil. Highest MDD (1.73 g/cc for standard Proctor) was obtained at 10% replacement of fly ash due to the compact packing of voids. As fly ash content increases beyond 15% due to the high specific surface area, the OMC increases.

2 The improvement in UCS values was proportional to the increase in cement and fly ash dosages. The shrinkage cracks were reduced at a higher percentage of fly ash (>20%). As the curing period increases, there is an improvement in UCS strength.

3 The BC soil stabilized with 36% fly ash and 14% cement has attained a UCS value of 3.5 MPa to 7.3 MPa after curing from 7 to 90 days due to the formation of hydration products.

4 The specimens with 10, 12% cement with ≥30% fly ash, and 14% cement with ≥25% fly ash could withstand 12 cycles of the WD test (with weight loss of less than 14 %). Whereas, the specimens with ≤8% cement could not withstand the WD test.

5 Specimens treated with cement-fly ash exhibited better resistance to FT cycles, with soil loss much lower than that observed in WD cycles. The formation of ice crystals on freezing was restricted due to the compact matrix of soil; thus, crack development was restricted. Thawing of soil did not damage the specimens.

6 Negligible volume changes were observed under wetting, freezing, and thawing cycles. However, a slight reduction in volume was observed during the drying cycle due to shrinkage. The retained UCS values were better for the specimens prepared with high cement and fly ash content.

7 The CBR values of these samples are significant (>14%) due to cement hydration. The inclusion of fibers improved CBR, flexural strength, and fatigue life of cement-fly ash blended soil. Also, due to the high tensile strength of fibers, the

crack propagation during the test is restricted. The soaking of specimens in water may further contribute to strength gain due to favoured hydration.

B. ALKALI-ACTIVATED BC SOIL WITH MARGINAL MATERIALS

1 All alkali-activated specimens treated with different precursors exhibited an improvement in UCS at 8 molar NaOH concentration and SS/SH ratio of 1.5. Lower SS/SH concentrations are not effective due to less dissolution of mineral constituents. Increasing stabilizer dosages led to a considerable increase in UCS.

2 The flexural strength and fatigue performance of the mixes were improved, and the specimens did not exhibit any shrinkage cracks on curing.

3 The soaked CBR values of these mixes are very low (5–8%), whereas the unsoaked values are high (>31%). These samples lost strength on soaking and could not withstand durability tests, and can not be used for pavement layers.

4 All alkali-activated specimens collapsed during the wetting cycle of the WD test. In the FT test, a drastic increase in volume and subsequent failure of samples was observed due to softening by water absorption. The leaching of mineral constituents such as Al, Ca, Fe, Na, Si, etc., might be the reason for the collapse of specimens. In addition, the alkali solution cannot retain the bonding due to the high water affinity of BC soil.

C. PAVEMENT DESIGN AND COST ANALYSIS

1 Cement-fly ash stabilized mixes with and without coconut fibers passing the durability criteria are used for low and high-volume pavements in the subgrade, modified soil, CTSB layers as per IRC SP-72: 2015 and IRC 37: 2018.

2 The strains calculated by IIT PAVE considering the stabilized soil in various layers are within allowable limits as per the fatigue and rutting criteria specified in IRC 37: 2018.

3 BC Soil (Stabilized) can be avoided in Base layers due to the development of wide cracks during summer. It may reflect to the top layers.

4 The BC Soil Stabilized with cement-fly ash and after passing durability tests with and without coconut fibers is cheaper in cost than GSB. If GSB material is not available near the construction site, then if the marginal materials class F fly ash and coconut fibers are available abundantly at the site, then this stabilization method is economical.

SCOPE FOR THE FUTURE RESEARCH

1 A test track can be constructed with the soil-cement mixes with class F fly ash and fibers, and the performance can be monitored in different traffic and weather conditions.

2 Tests can be conducted to find the constituents in leached water from alkali-activated soil with marginal materials to understand the reasons for failure.

APPENDIX I

Estimation of effective subgrade modulus/CBR

For BC soil of soaked CBR 2 %, which is ≤5 %,

M_{RS} = 10.0×CBR = 10×2 = 20 MPa

For cement stabilized BC soil with fly ash of soaked CBR of 19%, which is >5%,

$M_{RS} = 17.6\times(CBR)^{0.64} = 17.6\times(19)^{0.64} = 116$ MPa

Consider a 2-layer elastic system,

μ = 0.35 for both layers,

Upper layer thickness = 500 mm,

Single load P = 40000 N,

Contact pressure p = 0.56 MPa.

Therefore, radius of contact area $a = [P/(\pi p)]^{0.5} = 150.8$ mm.

Number of analysis points = 1, depth = 0, radial distance = 0.

For these inputs, using IITPAVE software, the maximum deflection (δ) = 2.158 mm.

For an equivalent single layer system, the M_{RS} value to produce 2.158 mm deflection at the same load for μ = 0.35 is

$M_{RS} = [2(1-\mu^2)]/\delta = [2\times(1-0.35^2)\times0.56\times150.8]/2.158 = 69$ MPa.

The equivalent CBR = $(69/17.6)^{(1/0.64)}$ = 8%.

APPENDIX II

Estimation of weight gain and weight loss during durability test

$$Weight\ gain\ or\ wight\ loss = \frac{Final\ weight - Initial\ wight}{Initial\ weight}$$

Initial weight of FT specimen = 178.8 g

Weight of specimen after 12 FT cycles = 182.4 g

Weight gain = ((182.4-178.8)/178.8)×100 = 2.01%

Initial weight of WD specimen = 179.2 g

Weight of specimen after 12 WD cycles = 172.8 g

Weight loss = ((172.8-179.2)/179.2)×100 = -3.57%

PUBLICATIONS

Journals

1) Chethan, B. A. and Shankar, A. R. (2021). "Strength and Durability Characteristics of Cement and Class F Fly Ash-Treated Black Cotton Soil". *Indian Geotechnical Journal*, 1-13. https://doi.org/10.1007/s40098-020-00488-2
2) Chethan, B. A. and Shankar, A. U. (2021). Effect of Flash Flood and Weather Changes on Unconfined Compressive Strength of Cement-and Fly Ash-Stabilized Black Cotton Soil Used as Road Materials. *International Journal of Pavement Research and Technology*, 1-17. https://doi.org/10.1007/s42947-021-00125-y

Conferences

1) Chethan, B, A., Ravi Shankar, A. U., Raghuram K Chinnabhandar. and Avinash H T. (2020). "Strength and Durability Characteristics of Fly Ash Admixed Black Cotton Soil" *Second ASCE India Conference on "Challenges of Resilient and Sustainable Infrastructure Development in Emerging Economies" (CRSIDE2020),* March 2-4, 2020, Novotel Kolkata. ***(Under printing process).***
2) Chethan, B. A., Ravi Shankar A. U., Bhagyalakshmi, P. and Amulya S. (2020). "Stabilization of Black Cotton Soil with Alkali Solution, GGBS and Arecanut Fiber" *Civil Engineering Trends and Challenges for Sustainability (CTCS 2020),* December 22-23, 2020. NITTE Karkala. ***(Presented).***
3) Chethan, B. A., Ravi Shankar, A. U., Raghuram K Chinnabhandar. and Doma Hemanth Kumar. (2021). "Alkali Activated Black Cotton Soil with Partial Replacement of Class F Fly Ash and Arecanut Fiber Reinforcement" *Advances in Construction Technology and Management (ACTM-2021),* March 11-12, 2021, Department of Civil Engineering College of Engineering Pune (COEP). ***(Presented and being considered for publication).***
4) Chethan, B, A. and Ravi Shankar, A. U. (2021). "Areca Fiber Reinforced Alkali Activated Black Cotton Soil using Class F Fly ash and Limestone powder for Pavements", *at 12th International Conference on Road and Airfield Pavement Technology 2021 (ICPT 2021),* July 14-15, 2021, Transportation Engineering Division, Department of Civil Engineering, University of Moratuwa Sri Lanka. ***(Under publication process).***

Research Conclave

1) Chethan, B. A. and Ravi Shankar, A. U. (2020). “Laboratory investigation on black cotton soil stabilized with alkali solution along with partial replacement of construction and demolition waste”, *"RESEARCH CONCLAVE -2020"* September 15-17, 2020, Department of Civil Engineering, St Joseph Engineering College, Mangaluru. Best paper presentation award. ***(Presented).***

REFERENCES

Abe, S. S., Masunaga, T., Honna, T. and Wakatsuki, T. (2006). "Comprehensive assessment of the clay mineralogical composition of lowland soils in West Africa." *Soil Sci. Plant Nutr.*, 52(4), 479–488.

Ackroyd, L. W. and Husain, R. (1986). "Residual and lacustrine black cotton soils of north-east Nigeria." *Geotechnique*, 36(1).

Ahmed, A. and Ugai, K. (2011). "Environmental effects on durability of soil stabilized with recycled gypsum." *Cold Reg. Sci. Technol.*, 66(2–3), 84–92.

Akhtar, A. and Sarmah, A. K. (2018). "Construction and demolition waste generation and properties of recycled aggregate concrete: a global perspective." *J. Clean. Prod.*, 186, 262–281.

Almakhadmeh, M. and Soliman, A. M. (2021). "Effects of mixing water temperatures on properties of one-part alkali-activated slag paste." *Constr. Build. Mater.*, 266, 121030.

Amadi, A. A. (2014). "Enhancing durability of quarry fines modified black cotton soil subgrade with cement kiln dust stabilization." *Transp. Geotech.*, 1(1), 55–61.

Amulya, S., Ravi Shankar, A. U. and Praveen, M. (2020). "Stabilisation of lithomargic clay using alkali activated fly ash and ground granulated blast furnace slag." *Int. J. Pavement Eng.*, 21(9), 1114–1121.

Arora, S. and Aydilek, A. H. (2005). "Class F fly-ash-amended soils as highway base materials." *J. Mater. Civ. Eng.*, 17(6), 640–649.

Arulrajah, A., Piratheepan, J., Disfani, M. M. and Bo, M. W. (2013). "Geotechnical and geoenvironmental properties of recycled construction and demolition materials in pavement subbase applications." *J. Mater. Civ. Eng.*, 25(8), 1077–1088.

ASTM C618-19: (2019). "Standard specification for coal fly ash and raw or calcined natural pozzolan for use in concrete." *ASTM Int. West Conshohocken, PA.*

ASTM D1635/D1635M-19: (2012). "Standard test method for flexural strength of soil-cement using simple beam with third-point loading." *ASTM Int. West Conshohocken, PA.*

ASTM D4609-08: (2008). "Standard guide for evaluating effectiveness of admixtures for soil stabilization." *ASTM Int. West Conshohocken, PA.*

ASTM D559/D559M-15: (2015). “Standard test methods for wetting and drying compacted soil-cement mixtures.” *ASTM Int. West Conshohocken, PA.*

ASTM D560/D560M-16: (2016). “Standard test methods for freezing and thawing compacted soil-cement mixtures.” *ASTM Int. West Conshohocken, PA.*

Autef, A., Joussein, E., Gasgnier, G. and Rossignol, S. (2012). “Role of the silica source on the geopolymerization rate.” *J. Non. Cryst. Solids,* 358(21), 2886–2893.

Bagewadi, S. V and Rakaraddi, P. G. (2015). “Effect of geopolymer on the strength of black cotton soil.” *Int. J. Res. Eng. Technol.*, 4(August), 229–231.

Bahar, R., Benazzoug, M. and Kenai, S. (2004). “Performance of compacted cement-stabilised soil.” *Cem. Concr. Compos.*, 26(7), 811–820.

Balan, K. (1995). “Studies on engineering behaviour and uses of geotextiles with natural fibres.”

Barbosa, V. F. F. and MacKenzie, K. J. D. (2003). “Thermal behaviour of inorganic geopolymers and composites derived from sodium polysialate.” *Mater. Res. Bull.*, 38(2), 319–331.

Bassani, M., Tefa, L., Coppola, B. and Palmero, P. (2019). “Alkali-activation of aggregate fines from construction and demolition waste: Valorisation in view of road pavement subbase applications.” *J. Clean. Prod.*, 234, 71–84.

Belviso, C., Cavalcante, F., Niceforo, G. and Lettino, A. (2017). “Sodalite, faujasite and A-type zeolite from 2: 1dioctahedral and 2: 1: 1 trioctahedral clay minerals. A singular review of synthesis methods through laboratory trials at a low incubation temperature.” *Powder Technol.*, 320, 483–497.

Bergado, D. T., Anderson, L. R., Miura, N. and Balasubramaniam, A. S. (1996). “Soft ground improvement in lowland and other environments.” AsCE.

Bernal, S. A., Rodríguez, E. D., Gutiérrez, R. M. de, Gordillo, M. and Provis, J. L. (2011). “Mechanical and thermal characterisation of geopolymers based on silicate-activated metakaolin/slag blends.” *J. Mater. Sci.*, 46(16), 5477–5486.

Blankenagel, B. J. and Guthrie, W. S. (2006). “Laboratory characterization of recycled concrete for use as pavement base material.” *Transp. Res. Rec.*, 1952(1), 21–27.

Boardman, D. I., Glendinning, S. and Rogers, C. D. F. (2001). “Development of stabilisation and solidification in lime–clay mixes.” *Geotechnique*, 51(6), 533–543.

Bowles, J. E. (1992). *Engineering properties of soils and their measurement.* McGraw-

Hill, Inc.
Buchwald, A., Kaps, C. and Hohmann, M. (2003). "Alkali-activated binders and pozzolan cement binders–complete binder reaction or two sides of the same story." *Proc. 11th Int. Congr. Chem. Cem. (ICCC), Durban, South Africa*, 1238–1246.
Buchwald, A., Zellmann, H.-D. and Kaps, C. (2011). "Condensation of aluminosilicate gels—model system for geopolymer binders." *J. Non. Cryst. Solids*, 357(5), 1376–1382.
Cabalar, A. F. and Karabash, Z. (2014). "California bearing ratio of a sub-base material modified with tire buffings and cement addition." *J. Test. Eval.*, 43(6), 1279–1287.
Cabalar, A. F., Karabash, Z. and Mustafa, W. S. (2014). "Stabilising a clay using tyre buffings and lime." *Road Mater. Pavement Des.*, 15(4), 872–891.
Cabrera, J. G. and Woolley, G. R. (1994). "Fly ash utilisation in civil engineering." *Stud. Environ. Sci.*, Elsevier, 345–356.
Cai, Y., Shi, B., Ng, C. W. W. and Tang, C. (2006a). "Effect of polypropylene fibre and lime admixture on engineering properties of clayey soil." *Eng. Geol.*, 87(3–4), 230–240.
Cai, Y., Shi, B., Ng, C. W. W. and Tang, C. sheng. (2006b). "Effect of polypropylene fibre and lime admixture on engineering properties of clayey soil." *Eng. Geol.*, 87(3–4), 230–240.
Chauhan, M. S., Mittal, S. and Mohanty, B. (2008). "Performance evaluation of silty sand subgrade reinforced with fly ash and fibre." *Geotext. Geomembranes*, 26(5), 429–435.
Chen, F. H. (2012). *Foundations on expansive soils*. Elsevier.
Collivignarelli, M. C., Abbà, A., Miino, M. C., Cillari, G. and Ricciardi, P. (2021). "A review on alternative binders, admixtures and water for the production of sustainable concrete." *J. Clean. Prod.*, 295, 126408.
Coudert, E., Paris, M., Deneele, D., Russo, G. and Tarantino, A. (2019). "Use of alkali activated high-calcium fly ash binder for kaolin clay soil stabilisation: Physicochemical evolution." *Constr. Build. Mater.*, 201, 539–552.
Criado, M., Fernández-Jiménez, A. and Palomo, A. (2007). "Alkali activation of fly ash: Effect of the SiO2/Na2O ratio: Part I: FTIR study." *Microporous mesoporous Mater.*, 106(1–3), 180–191.

Cristelo, N., Cunha, V. M. C. F., Dias, M., Gomes, A. T., Miranda, T. and Araújo, N. (2015). "Influence of discrete fibre reinforcement on the uniaxial compression response and seismic wave velocity of a cement-stabilised sandy-clay." *Geotext. Geomembranes*, 43(1), 1–13.

Cristelo, N., Cunha, V. M. C. F., Gomes, A. T., Araújo, N., Miranda, T. and Lurdes Lopes, M. de. (2017). "Influence of fibre reinforcement on the post-cracking behaviour of a cement-stabilised sandy-clay subjected to indirect tensile stress." *Constr. Build. Mater.*, 138, 163–173.

Cristelo, N., Glendinning, S., Fernandes, L. and Pinto, A. T. (2012). "Effect of calcium content on soil stabilisation with alkaline activation." *Constr. Build. Mater.*, 29, 167–174.

Cristelo, N., Glendinning, S., Fernandes, L. and Pinto, A. T. (2013). "Effects of alkaline-activated fly ash and Portland cement on soft soil stabilisation." *Acta Geotech.*, 8(4), 395–405.

Cristelo, N., Glendinning, S. and Teixeira Pinto, A. (2011). "Deep soft soil improvement by alkaline activation." *Proc. Inst. Civ. Eng. Improv.*, 164(2), 73–82.

Cwirzen, A., Provis, J. L., Penttala, V. and Habermehl-Cwirzen, K. (2014). "The effect of limestone on sodium hydroxide-activated metakaolin-based geopolymers." *Constr. Build. Mater.*, 66, 53–62.

Dang, L. C., Fatahi, B. and Khabbaz, H. (2016). "Behaviour of expansive soils stabilized with hydrated lime and bagasse fibres." *Procedia Eng.*

Daraei, A., Herki, B. M. A., Sherwani, A. F. H. and Zare, S. (2018). "Slope stability in swelling soils using cement grout: a case study." *Int. J. Geosynth. Gr. Eng.*, 4(1), 10.

Das, A. and Pandey, B. B. (1999). "Mechanistic-empirical design of bituminous roads: an Indian perspective." *J. Transp. Eng.*, 125(5), 463–471.

Davidovits, J. (1991). "Geopolymers: inorganic polymeric new materials." *J. Therm. Anal. Calorim.*, 37(8), 1633–1656.

Davidovits, J. (2002). "Environmentally driven geopolymer cement applications." *Proc. 2002 Geopolymer Conf. Melbourne. Aust.*

Dempsey, B. J. and Thompson, M. R. (1967). *cDurability properties of lime-soil mixtures. (No. Hpr-1/3/), Bureau of Public Roads /US.*

Diop, M. B. and Grutzeck, M. W. (2008). "Low temperature process to create brick."

Constr. Build. Mater., 22(6), 1114–1121.
Dixon, J. B., Weed, S. B. and Parpitt, R. L. (1990). "Minerals in soil environments." *Soil Sci.*, 150(2), 562.
Durante Ingunza, M. P., Pereira, K. L. de A. and Francisco dos Santos Junior, O. (2015). "Use of sludge ash as a stabilizing additive in soil-cement mixtures for use in road pavements." *J. Mater. Civ. Eng.*, 27(7), 6014027.
Duxson, P., Fernández-Jiménez, A., Provis, J. L., Lukey, G. C., Palomo, A. and Deventer, J. S. J. van. (2007a). "Geopolymer technology: the current state of the art." *J. Mater. Sci.*, 42(9), 2917–2933.
Duxson, P., Mallicoat, S. W., Lukey, G. C., Kriven, W. M. and Deventer, J. S. J. van. (2007b). "The effect of alkali and Si/Al ratio on the development of mechanical properties of metakaolin-based geopolymers." *Colloids Surfaces A Physicochem. Eng. Asp.*, 292(1), 8–20.
Duxson, P., Provis, J. L., Lukey, G. C. and Deventer, J. S. J. Van. (2007c). "The role of inorganic polymer technology in the development of 'green concrete.'" *Cem. Concr. Res.*, 37(12), 1590–1597.
Duxson, P., Provis, J. L., Lukey, G. C., Mallicoat, S. W., Kriven, W. M. and Deventer, J. S. J. Van. (2005). "Understanding the relationship between geopolymer composition, microstructure and mechanical properties." *Colloids Surfaces A Physicochem. Eng. Asp.*, 269(1–3), 47–58.
Dwivedi, A. and Jain, M. K. (2014). "Fly ash–waste management and overview: A Review." *Recent Res. Sci. Technol.*, 6(1).
Estabragh, A. R., Khatibi, M. and Javadi, A. A. (2016). "Effect of cement on treatment of a clay soil contaminated with glycerol." *J. Mater. Civ. Eng.*, 28(4), 4015157.
Estabragh, A. R., Moghadas, M. and Javadi, A. A. (2013). "Effect of different types of wetting fluids on the behaviour of expansive soil during wetting and drying." *Soils Found.*, 53(5), 617–627.
Estabragh, A. R., Namdar, P. and Javadi, A. A. (2012). "Behavior of cement-stabilized clay reinforced with nylon fiber." *Geosynth. Int.*, 19(1), 85–92.
Etim, R. K., Eberemu, A. O. and Osinubi, K. J. (2017). "Stabilization of black cotton soil with lime and iron ore tailings admixture." *Transp. Geotech.*, 10, 85–95.
Fatehi, H., Abtahi, S. M., Hashemolhosseini, H. and Hejazi, S. M. (2018). "A novel

study on using protein based biopolymers in soil strengthening." *Constr. Build. Mater.*, 167, 813–821.

Fernández-Jiménez, A. and Palomo, A. (2005). "Composition and microstructure of alkali activated fly ash binder: Effect of the activator." *Cem. Concr. Res.*, 35(10), 1984–1992.

Fernández-Jiménez, A., Palomo, A. and Criado, M. (2005). "Microstructure development of alkali-activated fly ash cement: a descriptive model." *Cem. Concr. Res.*, 35(6), 1204–1209.

Firoozi, A. A., Olgun, C. G., Firoozi, A. A. and Baghini, M. S. (2017). "Fundamentals of soil stabilization." *Int. J. Geo-Engineering*, 8(1), 1–16.

Gadre, A. D. and Chandrasekaran, V. S. (1994). "Swelling of black cotton soil using centrifuge modeling." *J. Geotech. Eng.*, 120(5), 914–919.

Garcia-Lodeiro, I., Palomo, A., Fernández-Jiménez, A. and Macphee, D. E. (2011). "Compatibility studies between NASH and CASH gels. Study in the ternary diagram Na2O–CaO–Al2O3–SiO2–H2O." *Cem. Concr. Res.*, 41(9), 923–931.

Ghafoori, N. and Cai, Y. (1998). "Laboratory-made roller compacted concretes containing dry bottom ash: Part ii—long-term durability." *Mater. J.*, 95(3), 244–251.

Gosavi, M. and Patil, K. (2004). "Improvement of properties of black cotton soil subgrade through synthetic reinforcement." *J. Inst. Eng. Part CV, Civ. Eng. Div.*, 84, 257–262.

Guidobaldi, G., Cambi, C., Cecconi, M., Comodi, P., Deneele, D., Paris, M., Russo, G., Vitale, E. and Zucchini, A. (2018). "Chemo-mineralogical evolution and microstructural modifications of a lime treated pyroclastic soil." *Eng. Geol.*, 245, 333–343.

Guzman, E. M. B. De, Stafford, D., Alfaro, M. C., Doré, G. and Arenson, L. U. (2018). "Large-scale direct shear testing of compacted frozen soil under freezing and thawing conditions." *Cold Reg. Sci. Technol.*, 151, 138–147.

Hafid, K. El and Hajjaji, M. (2015). "Effects of the experimental factors on the microstructure and the properties of cured alkali-activated heated clay." *Appl. Clay Sci.*, 116, 202–210.

Halsted, G. E., Adaska, W. S. and McConnell, W. T. (2008). "Guide to cement-modified soil (CMS)."

Hardjito, D., Wallah, S. E., Sumajouw, D. M. J. and Rangan, B. V. (2004). "On the development of fly ash-based geopolymer concrete." *Mater. J.*, 101(6), 467–472.

Ho, H.-J., Iizuka, A. and Shibata, E. (2020). "Chemical recycling and use of various types of concrete waste: a review." *J. Clean. Prod.*, 124785.

Hollanders, S., Adriaens, R., Skibsted, J., Cizer, Ö. and Elsen, J. (2016). "Pozzolanic reactivity of pure calcined clays." *Appl. Clay Sci.*, 132, 552–560.

Horpibulsuk, S., Rachan, R., Chinkulkijniwat, A., Raksachon, Y. and Suddeepong, A. (2010). "Analysis of strength development in cement-stabilized silty clay from microstructural considerations." *Constr. Build. Mater.*, 24(10), 2011–2021.

https://www.mapsofindia.com. (2020). "major-soil-types-map."

https://www.statista.com/. (2021). "statistics/219343/cement-production-worldwide/."

Huang, Y. H. (1993). *Pavement analysis and design*.

Ibrahaim, M. A., Moafaq, A. A. and Abdulrahman, H. A. (2011). "Long Term Strength and Durability of Clayey Soil Stabilized With Lime." *Eng. Tech. Jl*, 29(4).

IRC 37: (2018). "Guidelines for design of flexible pavements." *Indian Roads Congr. New Delhi*.

IRC SP-72: (2015). "Guidelines for the design of flexible pavements for low volume rural roads." *Indian Roads Congr. New Delhi*.

IRC SP:89-Part 2: (2018). "Guidelines for the design of stabilized pavements."

IS 1498: (2016). "Classification and identification of soils for general engineering purposes." *Bur. Indian Stand. New Delhi*.

IS 269: (2020). "Ordinary Portland cement - specification (sixth revision)." *Bur. Indian Stand. New Delhi*.

IS 2720-Part 10: (2015). "Methods of test for soils: Determination of unconfined compressive strength." *Bur. Indian Stand. New Delhi*.

IS 2720-Part 16: (2016). "Methods of test for soil: Laboratory determination of CBR." *Bur. Indian Stand. New Delhi*.

IS 2720-Part 3/Section-1: (2016). "Methods of test for soils: Determination of specific gravity - fine grained soils." *Bur. Indian Stand. New Delhi*.

IS 2720-Part 4: (2015). "Methods of test for soils - Grain size analysis." *Bur. Indian Stand. New Delhi*.

IS 2720-Part 40: (2016). "Methods of test for soils: Determination of free swell index of soils.” *Bur. Indian Stand. New Delhi*.

IS 2720-Part 5: (2015). “Method of test for soils: Determination of liquid and plastic limit.” *Bur. Indian Stand. New Delhi*.

IS 2720-Part 6: (2016). “Methods of test for soils: Determination of shrinkage factors.” *Bur. Indian Stand. New Delhi*.

IS 2720-Part 7: (2016). “Methods of test for soils: Determination of water content-dry density relation using light compaction.” *Bur. Indian Stand. New Delhi*.

IS 2720-Part 8: (2015). “Methods of test for soils: Determination of water content-dry density relation using heavy compaction.” *Bur. Indian Stand. New Delhi*.

IS 2720 Part-25: (1982). “Methods of test for soils: Determination of silica sesqioxide ratio.” *Bur. Indian Stand. New Delhi*.

IS 383: (2016). “Coarse and fine aggregate for concrete - Specification.” *Bur. Indian Stand.*

Iyengar, S. R., Masad, E., Rodriguez, A. K., Bazzi, H. S., Little, D. and Hanley, H. J. M. (2013). “Pavement subgrade stabilization using polymers: Characterization and performance.” *J. Mater. Civ. Eng.*, 25(4), 472–483.

Jafar, B., Stuart, P. and Steiner, R. (1996). “STABILIZATION / SOLIDIFICATION OF HAZARDOUS WASTES USING FLY ASH.” 122(OCTOBER), 935–940.

Jain, S., Singhal, S. and Pandey, S. (2020). “Environmental life cycle assessment of construction and demolition waste recycling: a case of urban India.” *Resour. Conserv. Recycl.*, 155, 104642.

Jayasree, P. K., Balan, K., Peter, L. and Nisha, K. K. (2014). “Volume change behavior of expansive soil stabilized with coir waste.” *J. Mater. Civ. Eng.*, 27(6), 4014195.

Jerod, G. and Wayne, A. (2020). “Cement-Stabilized Subgrade Soils.” undefined-64.

Jiménez, J. R., Ayuso, J., Galvín, A. P., López, M. and Agrela, F. (2012). “Use of mixed recycled aggregates with a low embodied energy from non-selected CDW in unpaved rural roads.” *Constr. Build. Mater.*, 34, 34–43.

Kalkan, E. (2009). “Effects of silica fume on the geotechnical properties of fine-grained soils exposed to freeze and thaw.” *Cold Reg. Sci. Technol.*, 58(3), 130–135.

Kang, X., Ge, L. and Liao, W.-C. (2016). “Cement hydration–based micromechanics modeling of the time-dependent small-strain stiffness of fly ash–stabilized soils.” *Int. J. Geomech.*, 16(3), 4015071.

Khattab, S. A., Al-Mukhtar, M. and Fleureau, J.-M. (2007). “Long-term stability characteristics of a lime-treated plastic soil.” *J. Mater. Civ. Eng.*, 19(4), 358–366.

Kien, T. T., Thanh, L. T. and Lu, P. V. (2013). “Recycling construction demolition waste in the world and in Vietnam.” *Int. Conf. Sustain. Built Environ. Now Futur. Hanoi*, 27.

Kim, Y., Dang, M. Q. and Do, T. M. (2016). “Studies on compressive strength of sand stabilized by alkali-activated ground bottom ash and cured at the ambient conditions.” *Int. J. Geo-Engineering*, 7(1), 15.

Kogbara, R. B. (2014). “A review of the mechanical and leaching performance of stabilized/solidified contaminated soils.” *Environ. Rev.*, 22(1), 66–86.

Komnitsas, K., Zaharaki, D., Vlachou, A., Bartzas, G. and Galetakis, M. (2015). “Effect of synthesis parameters on the quality of construction and demolition wastes (CDW) geopolymers.” *Adv. Powder Technol.*, 26(2), 368–376.

Kumar, A. and Gupta, D. (2016). “Behavior of cement-stabilized fiber-reinforced pond ash, rice husk ash-soil mixtures.” *Geotext. Geomembranes*, 44(3), 466–474.

Kumar, A., Walia, B. S. and Bajaj, A. (2007). “Influence of fly ash, lime, and polyester fibers on compaction and strength properties of expansive soil.” *J. Mater. Civ. Eng.*, 19(3), 242–248.

Kumar, P. and Singh, S. P. (2008). “Fiber-reinforced fly ash subbases in rural roads.” *J. Transp. Eng.*, 134(4), 171–180.

Kværnø, S. H. and Øygarden, L. (2006). “The influence of freeze–thaw cycles and soil moisture on aggregate stability of three soils in Norway.” *Catena*, 67(3), 175–182.

Leelavathamma, B., Mini, K. M. and Pandian, N. S. (2005). “California bearing ratio behavior of soil-stabilized class F fly ash systems.” *J. Test. Eval.*, 33(6), 406–410.

Lekha, B. M., Goutham, S. and Shankar, A. U. R. (2015). “Evaluation of lateritic soil stabilized with Arecanut coir for low volume pavements.” *Transp. Geotech.*, 2, 20–29.

Lemaire, K., Deneele, D., Bonnet, S. and Legret, M. (2013). “Effects of lime and cement treatment on the physicochemical, microstructural and mechanical characteristics of a plastic silt.” *Eng. Geol.*, 166, 255–261.

Lemougna, P. N., Madi, A. B., Kamseu, E., Melo, U. C., Delplancke, M.-P. and Rahier, H. (2014). “Influence of the processing temperature on the compressive strength of Na activated lateritic soil for building applications.” *Constr. Build. Mater.*, 65, 60–66.

Li, J., Tang, C., Wang, D., Pei, X. and Shi, B. (2014). "Effect of discrete fibre reinforcement on soil tensile strength." *J. Rock Mech. Geotech. Eng.*, 6(2), 133–137.

Liew, Y.-M., Heah, C.-Y. and Kamarudin, H. (2016). "Structure and properties of clay-based geopolymer cements: A review." *Prog. Mater. Sci.*, 83, 595–629.

Lin, D.-F., Lin, K.-L., Hung, M.-J. and Luo, H.-L. (2007). "Sludge ash/hydrated lime on the geotechnical properties of soft soil." *J. Hazard. Mater.*, 145(1–2), 58–64.

Llatas, C. (2011). "A model for quantifying construction waste in projects according to the European waste list." *Waste Manag.*, 31(6), 1261–1276.

MacKenzie, K. J. D. (2009). "Utilisation of non-thermally activated clays in the production of geopolymers." *Geopolymers*, Elsevier, 294–314.

Maneli, A., Kupolati, W. K., Abiola, O. S. and Ndambuki, J. M. (2016). "Influence of fly ash, ground-granulated blast furnace slag and lime on unconfined compressive strength of black cotton soil." *Road Mater. Pavement Des.*, 17(1), 252–260.

Marandi, S. M., Bagheripour, M. H., Rahgozar, R. and Zare, H. (2008). "Strength and ductility of randomly distributed palm fibers reinforced silty-sand soils." *Am. J. Appl. Sci.*, 5(3), 209–220.

Martin, J. P., Collins, R. A., Browning, J. S. and Biehl, F. J. (1990). "Properties and use of fly ashes for embankments." *J. energy Eng.*, 116(2), 71–86.

Maubec, N., Deneele, D. and Ouvrard, G. (2017). "Influence of the clay type on the strength evolution of lime treated material." *Appl. Clay Sci.*, 137, 107–114.

McDowell, C. (1959). "Stabilization of soils with lime, lime-flyash, and other lime reactive materials." *Highw. Res. Board Bull.*, 231(1), 60–66.

McGown, A., Andrawes, K. Z. and Al-Hasani, M. M. (1978). "Effect of inclusion properties on the behaviour of sand." *Geotechnique*, 28(3), 327–346.

McKeen, R. G. (1988). "Soil characterization using suction measurements." *Proc. 25th Paving Transp. Conf.*, University of New Mexico, Albuquerque.

Mehta, K. S., Sonecha, R. J., Daxini, P. D., Ratanpara, P. B. and Gaikwad, K. S. (2014). "Analysis of engineering properties of black cotton soil & stabilization using by lime." *J. Eng. Res. Appl.*, 4(5), 25–32.

Miao, S., Shen, Z., Wang, X., Luo, F., Huang, X. and Wei, C. (2017). "Stabilization of highly expansive black cotton soils by means of geopolymerization." *J. Mater. Civ. Eng.*, 29(10), 4017170.

Mirzaii, A. and Negahban, M. (2016). “California bearing ratio of an unsaturated deformable pavement material along drying and wetting paths.” *Road Mater. Pavement Des.*, 17(1), 261–269.

Misra, A., Biswas, D. and Upadhyaya, S. (2005). “Physico-mechanical behavior of self-cementing class C fly ash–clay mixtures.” *Fuel*, 84(11), 1410–1422.

Miura, N., Horpibulsuk, S. and Nagaraj, T. S. (2001). “Engineering behavior of cement stabilized clay at high water content.” *Soils Found.*, 41(5), 33–45.

Moghal, A. A. B., Chittoori, B. C. S. and Basha, B. M. (2018). “Effect of fibre reinforcement on CBR behaviour of lime-blended expansive soils: reliability approach.” *Road Mater. Pavement Des.*, 19(3), 690–709.

Mohamed, A. M. O. (2002). “Hydro-mechanical evaluation of soil stabilized with cement-kiln dust in arid lands.” *Environ. Geol.*, 42(8), 910–921.

MoRD: (2014). “Specifications for rural roads.” *Indian Roads Congr. New Delhi*.

MoRT&H: (2021). “Annual Report.” *Minist. Road Transp. Highw. New Delhi, India.*

Murmu, A. L., Jain, A. and Patel, A. (2019). “Mechanical properties of alkali activated fly ash geopolymer stabilized expansive clay.” *KSCE J. Civ. Eng.*, 23(9), 3875–3888.

Nalbantoğlu, Z. (2004). “Effectiveness of class C fly ash as an expansive soil stabilizer.” *Constr. Build. Mater.*, 18(6), 377–381.

Nelson, J. and Miller, D. J. (1997). *Expansive soils: problems and practice in foundation and pavement engineering*. John Wiley & Sons.

Nevels James B, J. (2001). “Longitudinal cracking of a bicycle trail due to drying shrinkage.” *Expans. Clay Soils Veg. Influ. Shallow Found.*, 132–157.

Nickovic, S., Vukovic, A., Vujadinovic, M., Djurdjevic, V. and Pejanovic, G. (2012). “High-resolution mineralogical database of dust-productive soils for atmospheric dust modeling.” *Atmos. Chem. Phys.*, 12(2), 845–855.

Oh, D.-Y., Noguchi, T., Kitagaki, R. and Park, W.-J. (2014). “CO2 emission reduction by reuse of building material waste in the Japanese cement industry.” *Renew. Sustain. Energy Rev.*, 38, 796–810.

Ola, S. A. (1978). “The geology and geotechnical properties of the black cotton soils of northeastern Nigeria.” *Eng. Geol.*, 12, 375–391.

Osinubi, K. (2000). “Stabilisation of tropical black clay with cement and pulverised coal bottom ash admixture.” *Adv. unsaturated Geotech.*, 289–302.

Osinubi, K. J., Oyelakin, M. A. and Eberemu, A. O. (2011). “Improvement of black cotton soil with ordinary Portland cement-locust bean waste ash blend.” *Electron. J. Geotech. Eng.*, 16(F), 619–627.
Ossa, A., García, J. L. and Botero, E. (2016). “Use of recycled construction and demolition waste (CDW) aggregates: A sustainable alternative for the pavement construction industry.” *J. Clean. Prod.*, 135, 379–386.
Osula, D. O. A. (1996). “A comparative evaluation of cement and lime modification of laterite.” *Eng. Geol.*, 42(1), 71–81.
Oza, J. B. and Gundaliya, P. J. (2013). “Study of black cotton soil characteristics with cement waste dust and lime.” *Procedia Eng.*, 51, 110–118.
Palomo, A., Grutzeck, M. W. and Blanco, M. T. (1999). “Alkali-activated fly ashes: A cement for the future.” *Cem. Concr. Res.*, 29(8), 1323–1329.
Pandian, N. S. (2013). “Fly ash characterization with reference to geotechnical applications.” *J. Indian Inst. Sci.*, 84(6), 189.
Pandian, N. S. and Krishna, K. C. (2003). “The pozzolanic effect of fly ash on the California bearing ratio behavior of black cotton soil.” *J. Test. Eval.*, 31(6), 479–485.
Patel, S. and Shahu, J. T. (2015). “Engineering properties of black cotton soil-dolime mix for its use as subbase material in pavements.” *Int. J. Geomate*, 8(1), 1159–1166.
Payá, J., Monzó, J., Borrachero, M. V, Mellado, A. and Ordoñez, L. M. (2001). “Determination of amorphous silica in rice husk ash by a rapid analytical method.” *Cem. Concr. Res.*, 31(2), 227–231.
PCA. (1979). *Soil-cement construction handbook*. Portland Cement Association.
Phani Kumar, B. R. and Sharma, R. S. (2004). “Effect of fly ash on engineering properties of expansive soils.” *J. Geotech. Geoenvironmental Eng.*, 130(7), 764–767.
Phummiphan, I., Horpibulsuk, S., Sukmak, P., Chinkulkijniwat, A., Arulrajah, A. and Shen, S.-L. (2016). “Stabilisation of marginal lateritic soil using high calcium fly ash-based geopolymer.” *Road Mater. Pavement Des.*, 17(4), 877–891.
Pradhan, P. K., Kar, R. K. and Naik, A. (2012). “Effect of random inclusion of polypropylene fibers on strength characteristics of cohesive soil.” *Geotech. Geol. Eng.*, 30(1), 15–25.
Priyadarshee, A., Gupta, D., Kumar, V. and Sharma, V. (2015). “Comparative study on performance of tire crumbles with fly ash and kaolin clay.” *Int. J. Geosynth. Gr. Eng.*,

1(4), 38.
Provis, J. L. (2014). “Geopolymers and other alkali activated materials: why, how, and what?” *Mater. Struct.*, 47(1–2), 11–25.
Provis, J. L. and Deventer, J. S. J. Van. (2013). *Alkali activated materials: state-of-the-art report, RILEM TC 224-AAM*. Springer Science & Business Media.
Prusinski, J. R. and Bhattacharja, S. (1999). “Effectiveness of Portland cement and lime in stabilizing clay soils.” *Transp. Res. Rec.*, 1652(1), 215–227.
Puppala, A. J. and Musenda, C. (2000). “Effects of fiber reinforcement on strength and volume change in expansive soils.” *Transp. Res. Rec.*, 1736(1), 134–140.
Puppala, A. J., Pedarla, A., Hoyos, L. R., Zapata, C. and Bheemasetti, T. V. (2016). “A semi-empirical swell prediction model formulated from ‘clay mineralogy and unsaturated soil’properties.” *Eng. Geol.*, 200, 114–121.
Rao, S. M. and Acharya, I. P. (2013). “Synthesis and characterization of fly ash geopolymer sand.” *J. Mater. Civ. Eng.*, 26(5), 912–917.
Ravishankar, U. and Raghavan, S. (2004). “Coir stabilised lateritic soil for pavements.” *Proc. Indian Geotech. Conf. Ahmedabad, India*, 45–52.
Reddy, N. G., Tahasildar, J. and Rao, B. H. (2015). “Evaluating the influence of additives on swelling characteristics of expansive soils.” *Int. J. Geosynth. Gr. Eng.*, 1(1), 7.
Reeves, G. M., Sims, I. and Cripps, J. C. (2006). “Clay materials used in construction.” Geological Society of London.
Reis, G. S. dos, Quattrone, M., Ambrós, W. M., Grigore Cazacliu, B. and Hoffmann Sampaio, C. (2021). “Current Applications of Recycled Aggregates from Construction and Demolition: A Review.” *Materials (Basel).*, 14(7), 1700.
Ren, X. and Hu, K. (2014). “Effect of nanosilica on the physical and mechanical properties of silty clay.” *Nanosci. Nanotechnol. Lett.*, 6(11), 1010–1013.
Richardson, C. K., Markuszewski, R., Durham, K. S. and Bluhm, D. D. (1986). “Effect of caustic and microwave treatment on clay minerals associated with coal.” *Miner. Matter Ash Coal, Amer. Chem. Soc*, 513–523.
Rios, S., Cristelo, N., Miranda, T., Araújo, N., Oliveira, J. and Lucas, E. (2018). “Increasing the reaction kinetics of alkali-activated fly ash binders for stabilisation of a silty sand pavement sub-base.” *Road Mater. Pavement Des.*, 19(1), 201–222.

Rios, S., Cristelo, N., Viana da Fonseca, A. and Ferreira, C. (2015). "Structural performance of alkali-activated soil ash versus soil cement." *J. Mater. Civ. Eng.*, 28(2), 4015125.

Rios, S., Ramos, C., Viana da Fonseca, A., Cruz, N. and Rodrigues, C. (2019). "Mechanical and durability properties of a soil stabilised with an alkali-activated cement." *Eur. J. Environ. Civ. Eng.*, 23(2), 245–267.

Robnett, Q. L. (1980). "Use of marginal materials in highway construction." *Proc. 66th Annu. Road Sch. Purdue Univ. West Lafayette, Indiana, US.*

Rollings, M. P. (1996). *Geotechnical materials in construction*. McGraw-Hill Professional Publishing.

Saberian, M. and Li, J. (2020). "Effect of freeze–thaw cycles on the resilient moduli and unconfined compressive strength of rubberized recycled concrete aggregate as pavement base/subbase." *Transp. Geotech.*, 27, 100477.

Sahu, V., Srivastava, A., Misra, A. K. and Sharma, A. K. (2017). "Stabilization of fly ash and lime sludge composites: Assessment of its performance as base course material." *Arch. Civ. Mech. Eng.*, 17(3), 475–485.

Salahudeen, A. B., Eberemu, A. O. and Osinubi, K. J. (2014). "Assessment of cement kiln dust-treated expansive soil for the construction of flexible pavements." *Geotech. Geol. Eng.*, 32(4), 923–931.

Sarbaz, H., Ghiassian, H. and Heshmati, A. A. (2014). "CBR strength of reinforced soil with natural fibres and considering environmental conditions." *Int. J. Pavement Eng.*, Taylor & Francis.

Sargent, P., Hughes, P. N. and Rouainia, M. (2016). "A new low carbon cementitious binder for stabilising weak ground conditions through deep soil mixing." *Soils Found.*, 56(6), 1021–1034.

Sargent, P., Hughes, P. N., Rouainia, M. and White, M. L. (2013). "The use of alkali activated waste binders in enhancing the mechanical properties and durability of soft alluvial soils." *Eng. Geol.*, 152(1), 96–108.

Scheuermann Filho, H. C., Beck Saldanha, R., Gravina da Rocha, C. and Cesar Consoli, N. (2021). "Sustainable Binders Stabilizing Dispersive Clay." *J. Mater. Civ. Eng.*, 33(3), 6020026.

Schuhmacher, M., Domingo, J. L. and Garreta, J. (2004). "Pollutants emitted by a

cement plant: health risks for the population living in the neighborhood." *Environ. Res.*, 95(2), 198–206.
Scrivener, K. L. and Kirkpatrick, R. J. (2008). "Innovation in use and research on cementitious material." *Cem. Concr. Res.*, 38(2), 128–136.
Seiffarth, T., Hohmann, M., Posern, K. and Kaps, C. (2013). "Effect of thermal pre-treatment conditions of common clays on the performance of clay-based geopolymeric binders." *Appl. Clay Sci.*, 73, 35–41.
Sekkel, A., Kara, E. M., Klouche, F. and Bireche, S. (2020). "Valorization of concrete waste in swelling clay's treatment." *Innov. Infrastruct. Solut.*, 6(1), 1–10.
Şenol, A. (2012). "Effect of fly ash and polypropylene fibres content on the soft soils." *Bull. Eng. Geol. Environ.*, 71(2), 379–387.
Sharma, A. K. and Sivapullaiah, P. V. (2016). "Ground granulated blast furnace slag amended fly ash as an expansive soil stabilizer." *Soils Found.*, 56(2), 205–212.
Shi, B., Chen, S. and Zheng, C. (2014). "Expansive soil crack depth under cumulative damage." *Soil Behav. Geomech.*, 1–14.
Shi, X. S., Collins, F. G., Zhao, X. L. and Wang, Q. Y. (2012). "Mechanical properties and microstructure analysis of fly ash geopolymeric recycled concrete." *J. Hazard. Mater.*, 237, 20–29.
Show, K.-Y., Tay, J.-H. and Goh, A. T. C. (2003). "Reuse of incinerator fly ash in soft soil stabilization." *J. Mater. Civ. Eng.*, 15(4), 335–343.
Silva, R. A., Oliveira, D. V, Miranda, T., Cristelo, N., Escobar, M. C. and Soares, E. (2013). "Rammed earth construction with granitic residual soils: The case study of northern Portugal." *Constr. Build. Mater.*, 47, 181–191.
Singhi, B., Laskar, A. I. and Ahmed, M. A. (2016). "Investigation on soil–geopolymer with slag, fly ash and their blending." *Arab. J. Sci. Eng.*, 41(2), 393–400.
Sivakumar Babu, G. L., Vasudevan, A. K. and Sayida, M. K. (2008). "Use of coir fibers for improving the engineering properties of expansive soils." *J. Nat. Fibers*, 5(1), 61–75.
Sivakumar, V., McKinley, J. D. and Ferguson, D. (2004). "Reuse of construction waste: performance under repeated loading." *Proc. Inst. Civ. Eng. Eng.*, 157(2), 91–96.
Snellings, R., Mertens, G. and Elsen, J. (2012). "Supplementary cementitious materials." *Rev. Mineral. Geochemistry*, 74(1), 211–278.

Sobhan, K. (2008). “Improving the tensile strength and toughness of a soil-cement-fly ash pavement subgrade with recycled HDPE strips.” *GeoCongress 2008 Geosustainability Geohazard Mitig.*, 1065–1072.

Solanki, P. and Zaman, M. (2012). “Microstructural and mineralogical characterization of clay stabilized using calcium-based stabilizers.” *Scan. Electron Microsc.*, IntechOpen.

Sore, S. O., Messan, A., Prud’Homme, E., Escadeillas, G. and Tsobnang, F. (2018). “Stabilization of compressed earth blocks (CEBs) by geopolymer binder based on local materials from Burkina Faso.” *Constr. Build. Mater.*, 165, 333–345.

Sperberga, I., Sedmale, G., Stinkulis, G., Zeila, K. and Ulme, D. (2011). “Comparative study of illite clay and illite-based geopolymer products.” *IOP Conf. Ser. Mater. Sci. Eng.*, IOP Publishing, 222027.

Steinberg, M. (1998). *Geomembranes and the control of expansive soils in construction, McGraw-Hill, New York.*

Sudhakaran Pillai, M. and Vasudev, R. (2001). “Applications of coir in agriculturaltextiles.” *Int. Semin. Tech. Text.*, 1–5.

Sudhakaran, S. P., Sharma, A. K. and Kolathayar, S. (2018). “Soil Stabilization Using Bottom Ash and Areca Fiber: Experimental Investigations and Reliability Analysis.” *J. Mater. Civ. Eng.*, 30(8), 04018169.

Sukmak, P., Horpibulsuk, S., Shen, S.-L., Chindaprasirt, P. and Suksiripattanapong, C. (2013). “Factors influencing strength development in clay–fly ash geopolymer.” *Constr. Build. Mater.*, 47, 1125–1136.

Sukmak, P., Silva, P. De, Horpibulsuk, S. and Chindaprasirt, P. (2014). “Sulfate resistance of clay-portland cement and clay high-calcium fly ash geopolymer.” *J. Mater. Civ. Eng.*, 27(5), 4014158.

Taher, S. A., Alyousify, S. and Hassan, H. J. A. (2020). “COMPARATIVE STUDY OF USING FLEXIBLE AND RIGID PAVEMENTS FOR ROADS: A REVIEW STUDY.” *J. Duhok Univ.*, 23(2), 222–234.

Tan, T., Huat, B. B. K., Anggraini, V., Shukla, S. K. and Nahazanan, H. (2019). “Strength behavior of fly ash-stabilized soil reinforced with coir fibers in Alkaline environment.” *J. Nat. Fibers*, 1–14.

Tang, C.-S., Wang, D.-Y., Cui, Y.-J., Shi, B. and Li, J. (2016). “Tensile strength of

fiber-reinforced soil.” *J. Mater. Civ. Eng.*, 28(7), 4016031.
Tang, C., Shi, B., Gao, W., Chen, F. and Cai, Y. (2007). “Strength and mechanical behavior of short polypropylene fiber reinforced and cement stabilized clayey soil.” *Geotext. Geomembranes*, 25(3), 194–202.
Tchakoute, H. K., Rüscher, C. H., Djobo, J. N. Y., Kenne, B. B. D. and Njopwouo, D. (2015). “Influence of gibbsite and quartz in kaolin on the properties of metakaolin-based geopolymer cements.” *Appl. Clay Sci.*, 107, 188–194.
Tigue, A. A. S., Malenab, R. A. J., Dungca, J. R., Yu, D. E. C. and Promentilla, M. A. B. (2018). “Chemical stability and leaching behavior of one-part geopolymer from soil and coal fly ash mixtures.” *Minerals*, 8(9), 411.
Tironi, A., Trezza, M. A., Scian, A. N. and Irassar, E. F. (2013). “Assessment of pozzolanic activity of different calcined clays.” *Cem. Concr. Compos.*, 37, 319–327.
Türköz, M. and Tosun, H. (2011). “A GIS model for preliminary hazard assessment of swelling clays, a case study in Harran plain (SE Turkey).” *Environ. Earth Sci.*, 63(6), 1343–1353.
Uddin, K., Balasubramaniam, A. S. and Bergado, D. T. (1997). “Engineering behavior of cement-treated Bangkok soft clay.” *Geotech. Eng.*, 28, 89–119.
Verdolotti, L., Iannace, S., Lavorgna, M. and Lamanna, R. (2008). “Geopolymerization reaction to consolidate incoherent pozzolanic soil.” *J. Mater. Sci.*, 43(3), 865–873.
Vidal, H. (1969). “The principle of reinforced earth.” *Highw. Res. Rec.*, (282).
Viswanadham, B. V. S., Phanikumar, B. R. and Mukherjee, R. V. (2009). “Swelling behaviour of a geofiber-reinforced expansive soil.” *Geotext. Geomembranes*, 27(1), 73–76.
Vitale, E., Deneele, D., Russo, G., Sarno, D. De, Nicotera, M. V, Papa, R. and Urciuoli, G. (2019a). “Chemo-mechanical behaviour of lightweight cemented soils.” *Acta Geotech.*, 1–13.
Vitale, E., Russo, G., Dell’Agli, G., Ferone, C. and Bartolomeo, C. (2017). “Mechanical behaviour of soil improved by alkali activated binders.” *Environments*, 4(4), 80.
Vitale, E., Russo, G. and Deneele, D. (2019b). “Use of Alkali-Activated Fly Ashes for Soil Treatment.” *Natl. Conf. Res. Geotech. Eng.*, Springer, 723–733.
Walsh, K. D., Houston, W. N. and Houston, S. L. (1993). “Evaluation of in-place wetting using soil suction measurements.” *J. Geotech. Eng.*, 119(5), 862–873.

Wang, D., Ma, W., Niu, Y., Chang, X. and Wen, Z. (2007). "Effects of cyclic freezing and thawing on mechanical properties of Qinghai–Tibet clay." *Cold Reg. Sci. Technol.*, 48(1), 34–43.

Wang, D., Zentar, R. and Abriak, N. E. (2018). "Durability and swelling of solidified/stabilized dredged marine soils with class-F fly ash, cement, and lime." *J. Mater. Civ. Eng.*, 30(3), 4018013.

Weng, L. and Sagoe-Crentsil, K. (2007). "Dissolution processes, hydrolysis and condensation reactions during geopolymer synthesis: Part I—Low Si/Al ratio systems." *J. Mater. Sci.*, 42(9), 2997–3006.

Wilkinson, A., Haque, A. and Kodikara, J. (2010). "Stabilisation of clayey soils with industrial by-products: part A." *Proc. Inst. Civ. Eng. Improv.*, 163(3), 149–163.

Wu, J. Y., Huang, K. and Sungkar, M. (2017). "Remediation of slope failure by compacted soil-cement fill." *J. Perform. Constr. Facil.*, 31(4), 4017022.

Wu, Z., Deng, Y., Liu, S., Liu, Q., Chen, Y. and Zha, F. (2016). "Strength and micro-structure evolution of compacted soils modified by admixtures of cement and metakaolin." *Appl. Clay Sci.*, 127, 44–51.

Xiao, H., Wang, W. and Goh, S. H. (2017). "Effectiveness study for fly ash cement improved marine clay." *Constr. Build. Mater.*, 157, 1053–1064.

Xu, H. and Deventer, J. S. J. Van. (2000). "The geopolymerisation of alumino-silicate minerals." *Int. J. Miner. Process.*, 59(3), 247–266.

Yang, Z., Zhang, F., Na, X. and Yu, H. (2020). "Thaw settlement and mechanical properties of admixture-stabilized frozen soil." *J. Cold Reg. Eng.*, 34(2), 4020005.

Yilmaz, I. (2009). "Swell potential and shear strength estimation of clays." *Appl. Clay Sci.*, 46(4), 376–384.

Yousuf, A., Manzoor, S. O., Youssouf, M., Malik, Z. A. and Khawaja, K. S. (2020). "Fly ash: production and utilization in India-an overview." *J Mater Env. Sci*, 11(6), 911–921.

Yunsheng, Z., Wei, S., Qianli, C. and Lin, C. (2007). "Synthesis and heavy metal immobilization behaviors of slag based geopolymer." *J. Hazard. Mater.*, 143(1–2), 206–213.

Zaimoglu, A. S. (2010). "Freezing–thawing behavior of fine-grained soils reinforced with polypropylene fibers." *Cold Reg. Sci. Technol.*, 60(1), 63–65.

Zhang, D.-W., Zhao, K., Wang, D. and Li, H. (2021). "Relationship of amorphous gel-microstructure-elastoviscosity properties of alkali-activated materials fresh pastes with different Ms waterglass." *Constr. Build. Mater.*, 287, 123023.

Zhang, M., Guo, H., El-Korchi, T., Zhang, G. and Tao, M. (2013). "Experimental feasibility study of geopolymer as the next-generation soil stabilizer." *Constr. Build. Mater.*, 47, 1468–1478.

Zografou, A. (2015). "The use of china clay waste as a construction material using alkali-activated cement technology." University of Bath.

Zumrawi, M. M. E., Abdelmarouf, A. O. and Gameil, A. E. A. (2017). "Damages of buildings on expansive soils: diagnosis and avoidance." *Int. J. Multidiscip. Sci. Emerg. Res.*, 6(2), 108–116.

BIODATA

1	Name	Mr. CHETHAN B A
2	Date of Birth	11-02-1985
3	Qualification	B.E in Civil Engineering
		M.E in Highway Engineering
4	Experience	10 years of teaching experience as Assistant Professor in Government Engineering College Hassan, Karnataka.
		2 years of experience as a Highway Engineer in AICE India Pvt Ltd., Bangalore.
5	Permanent Address	S/o Achutha Prabhu B # 1-1057/1 Mukrampady House, Kemminje Village, Puttur Taluk, Dakshina Kannada, Karnataka -574202
6	Email ID:	chethanba@gmail.com
7	Ph. No.:	9686847540

Academic Details:

Degree	**Major**	**Institute**	**Duration**	**Percentage/ CGPA**
Ph.D. under QIP	Laboratory Investigations on Black Cotton Soil Stabilized with Inorganic Additives and Marginal Materials	National Institute of Technology Karnataka, Surathkal	2018 – 2021	8.15
M.E	Highway Engineering	UVCE, Bangalore	2006 – 2008	81.46
B.E	Civil Engineering	K.V.G College of Engineering, Sullia, D.K., Karnataka	2002 – 2006	75.19

Subjects studied during Ph.D. course work

- Pavement Design
- Urban Transport Planning
- Road Materials, Construction Methods, and Quality Control
- Statistical Methods
- Research Methodology

Subjects taught for UG/PG students

- Elements of Civil Engineering
- Geotechnical Engineering I
- Geotechnical Engineering II
- Highway Geometric Design
- Pavement Design
- Statistical and Numerical Methods

Professional Body Membership

1. Life member of Indian Society for Technical Education (ISTE)
2. Life member of Indian Roads Congress (IRC)

Publications

Journals Papers

1) Chethan, B. A. and Shankar, A. R. (2021). "Strength and Durability Characteristics of Cement and Class F Fly Ash-Treated Black Cotton Soil." *Indian Geotechnical Journal*, 1-13. https://doi.org/10.1007/s40098-020-00488-2.
2) Chethan, B. A. and Shankar, A. U. (2021). Effect of Flash Flood and Weather Changes on Unconfined Compressive Strength of Cement-and Fly Ash-Stabilized Black Cotton Soil Used as Road Materials. *International Journal of Pavement Research and Technology*, 1-17. https://doi.org/10.1007/s42947-021-00125-y

Conference Papers

1) Chethan B. A., Das S., Amulya S. and Shankar A.U.R. (2021). "Experimental Investigations on RBI Grade 81 Stabilized Lateritic Soil." *In Recent Trends in Civil Engineering. Lecture Notes in Civil Engineering*, vol 105. Springer, Singapore. https://doi.org/10.1007/978-981-15-8293-6_27

Papers presented at the conference:

1) Chethan B.A., Das S., Amulya S., and Shankar A.U.R. (2019). "Experimental Investigations on RBI Grade 81 Stabilized Lateritic Soil," *International Conference "Trending Moments & Steer Forces – Civil Engineering Today (TMSF – 2019)"* October 31-November 1, 2019, DBCE, Fatroda Goa.
2) Amulya S., Kumar H Pammar., Aditya Singh., Chethan B.A., Das S., and Shankar A.U.R. (2019). "Durability Studies of Black Cotton Soil Stabilized with Ground Granulated Blast Furnace Slag and Alkali Solution," *International Conference "Trending Moments & Steer Forces – Civil Engineering Today (TMSF – 2019),"* October 31-November 1, 2019, DBCE, Fatroda Goa. ***(Presented).***
3) Chethan, B. A., Ravi Shankar, A. U., Raghuram K C. and Avinash H T. (2020). "Strength and Durability Characteristics of Fly Ash Admixed Black Cotton Soil," *Second ASCE India Conference on "Challenges of Resilient and Sustainable Infrastructure Development in Emerging Economies" (CRSIDE2020),* March 2-4, 2020, Novotel Kolkata. ***(Under printing process)***.
4) Avinash, H. T., Ravi Shankar, A. U., Chethan, B. A., Raghuram K. C., and Amulya, S. (2020). "Development of Alkali Activated Slag Concrete by Partial Replacement of Sand with Granulated Blast Furnace Slag," *Second ASCE India Conference on "Challenges of Resilient and Sustainable Infrastructure Development in Emerging Economies" (CRSIDE2020),* March 2-4, 2020, Novotel Kolkata. ***(Under printing process)***.
5) Amulya, S., Ravi Shankar, A. U., Avinash, H. T. and Chethan, B. A. (2020). "Utilization of Black Cotton Soil Stabilized with Ground Granulated Blast Furnace Slag and Alkali Solution in Pavement Construction," *Second ASCE India Conference on "Challenges of Resilient and Sustainable Infrastructure Development in Emerging Economies" (CRSIDE2020),* March 2-4, 2020, Novotel Kolkata. ***(Under printing process)***.
6) Raghuram K C., Ravi Shankar, A. U., Chethan, B. A. and Avinash H T. (2020). "Comparision of Performance of Stone Matrix Asphalt (SMA) using VIATOP Pellets and Sisal Fibers," *Second ASCE India Conference on "Challenges of Resilient and Sustainable Infrastructure Development in Emerging Economies" (CRSIDE2020)*, March 2-4, 2020, Novotel Kolkata. ***(Under printing process)***.

7) Chethan, B. A., Ravi Shankar A. U., Bhagyalakshmi, P. and Amulya S. (2020). "Stabilization of Black Cotton Soil with Alkali Solution, GGBS and Arecanut Fiber," *Civil Engineering Trends and Challenges for Sustainability (CTCS 2020)*, December 22-23, 2020. NITTE Karkala. ***(Presented)***.

8) Chethan, B. A., Ravi Shankar, A. U., Raghuram K C. and Doma Hemanth Kumar. (2021). "Alkali Activated Black Cotton Soil with Partial Replacement of Class F Fly Ash and Arecanut Fiber Reinforcement" *Advances in Construction Technology and Management (ACTM-2021),* March 11-12, 2021, College of Engineering Pune (COEP). ***(Under publication process)***.

9) Chethan B. A., Lekha B. M. and A. U. Ravi Shankar, "Laboratory Investigation of Lateritic Soil Stabilized with Arecanut Coir along with Cement and its Suitability as a Modified Subgrade," *Advances in Construction Technology and Management (ACTM-2021)*, March 11-12, 2021, College of Engineering Pune (COEP). ***(Under publication process)***.

10) Chethan, B, A. and Ravi Shankar, A. U. (2021). "Areca Fiber Reinforced Alkali Activated Black Cotton Soil using Class F Fly ash and Limestone powder for Pavements." *12th International Conference on Road and Airfield Pavement Technology 2021 (ICPT 2021),* July 14-15, 2021, Transportation Engineering Division, Department of Civil Engineering, University of Moratuwa Sri Lanka. ***(Under publication process)***.

11) Chethan, B, A. and Ravi Shankar, A. U. (2021). "Laboratory Investigations on Lateritic Soil Stabilized with RBI Grade 81, Coconut Fiber and Aggregates," *12th International Conference on Road and Airfield Pavement Technology 2021 (ICPT 2021),* July 14-15, 2021, Transportation Engineering Division, Department of Civil Engineering, University of Moratuwa Sri Lanka. ***(Under publication process)***.

12) Chethan, B. A. and Ravi Shankar, A. U. (2020). "Laboratory investigation on black cotton soil stabilized with alkali solution along with partial replacement of construction and demolition waste," *"RESEARCH CONCLAVE -2020"* September 15-17, 2020, Department of Civil Engineering, St Joseph Engineering College, Mangaluru. Best paper presenter award. ***(Presented)***.